Vol. 130 No. 1, September 1, 1981 ISSN 0003-2670

ANALYTICA CHIMICA ACTA

International journal devoted to all branches of analytical chemistry

ELSEVIER SCIENTIFIC PUBLISHING COMPANY

ANALYTICA CHIMICA ACTA

International journal devoted to all branches of analytical chemistry
Revue internationale consacrée à tous les domaines de la chimie analytique
Internationale Zeitschrift fur alle Gebiete der analytischen Chemie

PUBLICATION SCHEDULE FOR 1981 (incorporating the section on Computer Techniques and Optimization)

	J	F	M	A	M	J	J	A	S	O	N	D
Analytica Chimica Acta	123	124/1	124/2	125	126	127	128	129	130/1	130/2	131	132
Section on Computer Techniques and Optimization		133/1			133/2			133/3			133/4	

Scope. *Analytica Chimica Acta* publishes original papers, short communications, and reviews dealing with eve aspect of modern chemical analysis, both fundamental and applied. The section on *Computer Techniques a Optimization* is devoted to new developments in chemical analysis by the application of computer techniques and l interdisciplinary approaches, including statistics, systems theory and operation research. The section deals with tl following topics: Computerized acquisition, processing and evaluation of data. Computerized methods for tl interpretation of analytical data including chemometrics, cluster analysis, and pattern recognition. Storage and retriev systems. Optimization procedures and their application. Automated analysis for industrial processes and quali control. Organizational problems.

Submission of Papers. Manuscripts (three copies) should be submitted as designated below for rapid and efficie handling:

Papers from the Americas to: Professor Harry L. Pardue, Department of Chemistry, Purdue University, West Lafayett IN 47907, U.S.A.

Papers from all other countries to: Dr. A. M. G. Macdonald, Department of Chemistry, The University, P.O. Box 36 Birmingham B15 2TT, England.

For the section on *Computer Techniques and Optimization:* Dr. J. T. Clerc, Universität Bern, Pharmazeutisches Institu Sahlistrasse 10, CH-3012 Bern, Switzerland.

American authors are recommended to send manuscripts and proofs by INTERNATIONAL AIRMAIL.

Submission of an article is understood to imply that the article is original and unpublished and is not being consider for publication elsewhere. Upon acceptance of an article by the journal, the author(s) resident in the U.S.A. will b asked to transfer the copyright of the article to the publisher. This transfer will ensure the widest dissemination information under the U.S. Copyright Law.

Information for Authors. Papers in English, French and German are published. There are no page charge Manuscripts should conform in layout and style to the papers published in this Volume. Authors should consu Vol. 121, p. 353 for detailed information. Reprints of this information are available from the Editors or from: Elsevi Editorial Services Ltd., Mayfield House, 256 Banbury Road, Oxford OX2 7DE (Great Britain).

Reprints. Fifty reprints will be supplied free of charge. Additional reprints (minimum 100) can be ordered. An ord form containing price quotations will be sent to the authors together with the proofs of their article.

Advertisements. Advertisement rates are available from the publisher.

Subscriptions. Subscriptions should be sent to: Elsevier Scientific Publishing Company, P.O. Box 211, 1000 A Amsterdam, The Netherlands. The section on *Computer Techniques and Optimization* can be subscribed to separatel

Publication. *Analytica Chimica Acta* (including the section on *Computer Techniques and Optimization*) appears 11 volumes in 1981. The subscription for 1981 (Vols. 123–133) is Dfl. 1639.00 plus Dfl. 198.000 (postage) (tot approx. U.S. $942.00). The subscription for the *Computer Techniques and Optimization* section only (Vol. 133) is D 149.00 plus Dfl. 18.00 (postage) (total approx. U.S. $86.00). Journals are sent automatically by airmail to the U.S. and Canada at no extra cost and to Japan, Australia and New Zealand for a small additional postal charge. All earli volumes (Vols. 1–121) except Vols. 23 and 28 are available at Dfl. 164.00 (U.S. $84.00), plus Dfl. 13.00 (U.S. $6.5 postage and handling, per volume.

Claims for issues not received should be made within three months of publication of the issue, otherwise they cann be honoured free of charge.

Customers in the U.S.A. and Canada who wish to obtain additional bibliographic information on this and oth Elsevier journals should contact Elsevier/North Holland Inc., Journal Information Center, 52 Vanderbilt Avenue, Ne York, NY 10017. Tel: (212) 867-9040.

ELECTROANALYSIS IN HYGIENE ENVIRONMENTAL, CLINICAL and PHARMACEUTICAL CHEMISTRY

Proceedings of a Conference organised by th Electroanalytical Group of the Chemical Societ London, held at Chelsea College, University c London, U.K., 17-20 April, 1979.

edited by W. FRANKLIN SMYTH, Chelse College, University of London, U.K.

ANALYTICAL CHEMISTRY SYMPOSIA SERIES 2

The proceedings of this international conference comprise 39 papers, principally concerned wit how potentiometric and voltammetric methods of electroanalysis are used to solve a wide rang of analytical problems in the fields of clinical chemistry, hygiene, pharmacy, pharmacology an environmental chemistry.

Although the papers reflect the many topics under discussion certain themes predominate. Thes include investigation of the actual electrochemical techniques and instrumentation, the importanc of the mechanism of the electrochemical reaction at the chosen indicator electrode in optimisin the electroanalytical 'finish', and direct, rapid and sensitive measurement in complex biologic matrices. The results on the determination of inorganic, organic and organometallic substance in complex matrices such as body fluids, factory air and the aqueous environment are also di cussed. On-line analysis with and without a prior separation process, speciation studies by th application of 'cold' electroanalytical methods and details of novel electrode construction, instru mental design and analytical methods complete the discussion.

SELECTED CONTENTS: **Plenary Lectures.** New Ion Selective Electrodes and Their Clinical and Biological Application *(D. Amman, H.-B. Jenny, P. C. Meier and W. Simon)*. Polarographic Analysis of Nucleic Acids *(E. Palaček)*. Electrochemical Gas Monitors in Occupational Hygiene *(I. Bergman)*. Electroanalytical Applications in Pharmacy and Pharmacology *(G. J. Patriarche and J.-C. Vire)*. Stripping Voltammetry of Molecules of Pharmaceutical Importance *(W. Franklin Smyth)*. A Critical Assessment of the Voltammetric Approach for the Study of Toxic Trace Metals in Biological Specimens *(H. W. Nürnberg)*. Polarographic Analysis of Pesticides in Food Products *(J. Davidék)*. **Keynote Lectures.** Design Principles and Behaviour of Sensitive Calcium Ion-Selective Electrodes *(G. J. Moody and J. D. R. Thomas)*. The Determination of Radiation Damages in Native DNA by Single Sweep Voltammetry *(J. M. Sequaris and P. Valenta)*. The Importance of Measuring Oxidation-Reduction Systems in Clinical Research *(J. Chayen)*. Determination of Mercury in Urine by Potentiometric Stripping Analysis *(D. Jagner and K. Årén)*. Differential Pulse Polarographic Determination of Drugs in Pharmaceutical Formulations *(E. Jacobsen)*. Trace Level Polarographic Analysis of Drugs in Body Fluids *(M. A. Brooks)*. Electrochemical Approaches to Environmental Pollution Control *(S. das Gupta, B. Fleet and I. F. T. Kennedy)*. Electroanalysis of Economic Poisons *(J. Osteryoung, J. W. Whittaker and M. R. Smyth)*.

CONTRIBUTORS OF OTHER PAPERS:

A. Apoteker, C. H. P. Bruins, K. Brunt, J. S. Burmicz, A. Catterall, I. E. Davidson, D. A. Doombos, N. M. Fayad, Zs. Feher, A. G. Fogg, J. P. Hart, A. Ivaska, V. J. Jennings, D. B. Kell, V. R. Krishnan, H. P. van Leeuwen, K. Ohzeki, E. Pungor, S. Jayarama Reddy, R. C. Rooney, T. Rydström, R. Samuelsson, E. Schumacher, W. James Scott, R. J. Simpson, R. Sternberg, G. Svehla, Y. M. Temerk, D. R. Thévenot, K. Toth, F. Umland, Y. Vaneesorn, A. Watson, P. D. J. Weitzman.

1979 xii + 464 pages US $ 70.75/Dfl. 145.00 ISBN 0-444-41850-4

ELSEVIER

P.O. Box 211, Amsterdam
The Netherlands
52 Vanderbilt Ave
New York, N.Y. 10017

The Dutch guilder price is definitive. US $ prices are subject to exchange rate fluctuations.

More and more primary literature?
Less and less time to read it?

take TrAC

trends in analytical chemistry

A monthly publication of short, critical reviews and news on trends and developments in analytical chemistry

How much better informed you could be if only you had the time to keep up with the latest developments.

Time we cannot give you, but we can give you concise, critical information on what is going on in the analytical sciences. Every month, as it happens.

It's all in TrAC – Trends in Analytical Chemistry – new for the 1980's from Elsevier and yours now at a low introductory rate.

Introductory Offer
SIXTEEN ISSUES FOR
THE PRICE OF TWELVE!

Volume 1 – 1981/82 – of **Trends in Analytical Chemistry** will have sixteen issues: March 1981 and monthly from October 1981 to December 1982. Order the **Personal Edition** before December 1981 and receive all sixteen issues for US $42.50 (USA and Canada), £20.00 (UK), 91.50 Dutch guilders Europe), 95.50 Dutch guilders (elsewhere). Or order the **Library Edition** for US $133.25 or 260.00 Dutch guilders throughout the world.

All issues of both editions are sent by air worldwide.

The Dutch guilder price is definitive.

Take just a minute to order either edition now – you will enjoy the time it saves you later.

ELSEVIER

TrAC is your opportunity to learn from researchers in related fields, to get first-hand, detailed reports on important developments in methodology and instrumentation. **TrAC** brings you current information on trends and techniques from laboratories all over the world.

Lab managers will find in **TrAC** evaluations of new methods and techniques which will enable them to make better-informed purchasing decisions. As a training aid **TrAC** is more up-to-date than any textbook.

TrAC is written in clear, jargon-free language, avoiding highly specialized terminology and provides you with a working knowledge of related methodology and techniques.

In every issue you will find:
- short critical reviews written for an interdisciplinary audience
- feature articles
- insights into the function, organization and operation of industrial, government or research laboratories
- news on topics of general interest
- teaching aids – TrAC is more up-to-date than any textbook
- articles on the history of analytical chemistry
- reports on meetings and book reviews

Trends in Analytical Chemistry comes in either the monthly **Personal Edition** or the special **Library Edition** which includes the monthly issues plus a hardbound volume containing all the review articles published over the year and indexed for easy retrieval.

Order Form

Special Introductory Offer for the Personal Edition valid until December 31, 1981

To **ELSEVIER Dept. TrAC. AP**
P.O. Box 330, 1000 AH Amsterdam, The Netherlands
52 Vanderbilt Avenue, New York, NY 10017

US residents may call (212) 867-9040 and charge their American Express, Master Charge or Visa/Bankamericard account.

Yes! Please enter my subscription now – Volume 1 – 1981/82
☐ Personal Edition ☐ Library Edition
I enclose my ☐ personal cheque ☐ bankcheque
Orders from individual subscribers must be prepaid.
☐ Please send me a free sample copy first.

Name: _____ Position: _____ Date: _____
Address: _____
_____
City: _____ State: _____ Postal Code _____

7198

New Horizons in Catalysis

Proceedings of the 7th International Congress on Catalysis, Tokyo, Japan, 30 June – 4 July, 1980

edited by T. SEIYAMA, *Kyushu University and* K. TANABE, *Hokkaido University, Japan*

STUDIES IN SURFACE SCIENCE AND CATALYSIS 7

Unparalleled interest in the science and technology of catalysis has arisen largely due to the essential role of catalysts in pollution control, the use of natural resources and the problems of energy conservation. This quadrennial conference attracted over 1000 delegates from 38 countries and during the course of the meeting 5 plenary lectures, 101 contributed papers and 63 communications were presented with the result that the range of topics covered was as wide as the science of catalysis itself.

In two volumes the text comprises the complete manuscripts, comments and responses, emerging as an invaluable guide to the results of much illuminating research leading directly to developments not only in fundamental theory and understanding of heterogeneous catalysts, but also in the application of catalysis in industry. At a time when catalysis is so vitally important, these proceedings provide a most thorough and comprehensive survey of, for example, catalyst design and preparation, and the development of new catalytic processes of technological importance. The studies encompass a broad variety of adsorption and catalysis by metals, alloys, metal oxides, zeolites and supported catalysts, with many examples of various surface science techniques which have been successfully applied to energy related subjects. Arguably the world's foremost conference on catalysis, these volumes will be essential in libraries and all research laboratories seriou ly concerned with catalysis research.

CONTENTS: **Plenary Lectu** Molecular Shape Selective Catalysis *(P. B. Weisz)*. Surface Science and Catalysis *(G. Ertl)* Coordination Chemistry of Me Surfaces and Metal Complexe *(E. L. Muetterties)*. Recent Proc ress in Elucidating the Mecha nism of Heterogeneous Catal *(K. Tamaru)*. Anchored Comple in Fundamental Catalytic Research *(Y. I. Yermakov)*.

1981 1586 pages (in 2 volumes) US $170.75 / Dfl. 350.00 D-444-99750-4

P.O. Box 211,
1000 AE Amsterdam,
The Netherlands.

52 Vanderbilt Ave.,
New York, N.Y. 10017.

The Dutch guilder price is definitive US $ p are subject to exchange rate fluctuations.

ELSEVIER

ANALYTICA CHIMICA ACTA
VOL. 130 (1981)

ANALYTICA CHIMICA ACTA

International journal devoted to all branches of analytical chemistry

ELSEVIER SCIENTIFIC PUBLISHING COMPANY

Anal. Chim. Acta, Vol. 130 (1981)

Analytica Chimica Acta, 130 (1981) 1—8
Elsevier Scientific Publishing Company, Amsterdam — Printed in The Netherlands

FAST DETERMINATION OF ANIONS BY COMPUTERIZED ION CHROMATOGRAPHY COUPLED WITH SELECTIVE DETECTORS

J. SLANINA*, F. P. BAKKER, P. A. C. JONGEJAN, L. VAN LAMOEN and J. J. MÖLS
Netherlands Energy Research Foundation (ECN), Petten, N.H. (The Netherlands)
(Received 17th February 1981)

SUMMARY

Up to 18 samples per hour can be analyzed for chloride, nitrate and sulfate by ion chromatography if the columns are thermostated (at ca. 40°C) and dead volume is minimized by the use of very small suppressor columns and minimal tubing. Accurate results are obtained from simple samples such as rain-water but nitrite, phosphate and bromide can interfere. These interferences can be avoided by the use of multiple detectors, such as a u.v. monitor at 220 nm and ion-selective electrodes (for fluoride and bromide). For samples containing more than 0.5 ppm of the ions of interest, a sample loop is used directly; the accuracy is typically 2—5%. For lower concentrations, a concentrator column is used with sample volumes up to 4 ml; this results in detection limits of 1—6 ppb for bromide, chloride, nitrate and sulfate. The computerized system is capable of analyzing large series of samples unattended.

The introduction of ion chromatography by Small et al. [1] has provided a very potent tool for wet analytical chemistry. Two advantages of ion chromatography were clear from the beginning: the detection limit is very low, especially if a concentrator column is applied [2], and some anions, e.g. sulfate, can be measured very selectively [3] whereas many other methods can give erroneous results.

Initially, ion chromatography was employed in this laboratory as a trace technique and as a reference method. The results of a number of round-robins for, e.g., rain-water made it clear that the analytical techniques employed here for sulfate were not always accurate, with the exception of isotope dilution [4]. In view of the number of analyses that have to be done, isotope dilution is somewhat time-consuming; but ion chromatography is also not very fast, the time needed for one sample being 16 min or more under standard conditions.

Attempts were therefore made to speed up the ion-chromatographic method. The requirements for fast chromatographic analysis are straightforward: short retention times and sharp peaks. Short retention times are obtained by using short columns, optimum eluant and high pumping speed. At a flow rate of 3 ml min^{-1}, with a solution containing 0.002 M Na_2CO_3 and 0.001 M $NaHClO_3$ as eluant, sulfate is eluted in 3—4 min from a standard 250 × 3-mm Dionex anion-exchanger column. However, the separation of

0003—2670/81/0000—0000/$02.50

species with shorter retention times is not very good when a standard Dionex column is used because of peak dispersion.

Several parameters influence peak dispersion; dead volume and mass transfer kinetics are very important. The dead volume in the original Dionex 10 apparatus is quite large, the suppressor column contributing substantially. The original 250 × 6-mm suppressor column was therefore replaced by two 250 × 3, or 100 × 3 or even 100 × 1.5-mm columns in parallel (see Fig. 1); one column was used, while the other was regenerated. The positions of valves and columns in the Dionex apparatus are such that at least 4 m of connecting tube is necessary. Even so, relatively fast determinations are feasible (up to 10 determinations per hour), but it was decided to build a new apparatus with less than 0.5 m of tubing. Previous investigations [3] indicated that thermostatting the separator columns at temperatures between 35 and 60°C resulted in better separation, presumably because of better mass transfer kinetics. The pressure drop over the column was about 30% less at 50°C. The stability of the Dionex ion exchanger was good at 50°C (the lifetime of columns was 3 months or better if the samples were not too dirty). However, the big negative water peak observed at the beginning of the chromatogram when sample volumes larger than 500 μl were injected, influenced the results for species with short retention times. Accordingly, either a 500-μl sample loop or a concentrator column was used. A Dionex concentrator column was used initially, but fluoride and chloride were not sufficiently retained when more than 10 ppm sulfate was present in the sample. Zipax SAX pellicular exchanger (Dupont) has a higher capacity and was found to retain all ions except fluoride. To obtain a better signal—noise ratio, a pulse dampener was employed. A Dionex conductivity cell was employed as a detector. The noise was less than 4 μmho when the coil of 0.2-mm stainless steel tubing which acts as heat exchanger was thermostatted within 0.01°C.

This system is capable of performing 15—20 analyses per hour. Chloride, nitrate and sulfate are well separated in the concentration range 0.02—20 ppm. The separations between chloride and nitrite, bromide and nitrate, and sulfite and sulfate, are not complete but 1 ppm nitrite, bromide and sulfite do not interfere in the proposed system, which can therefore be used for simple matrices such as rain-water and surface waters. The accuracy is typically 3% or better and the results obtained in several round-robins on rain-water were very satisfactory.

In the ECN rain chemistry program, all chloride, nitrate and sulfate determinations (more than 3000 per year) are now done by the high-speed ion-chromatographic system. The detection limits are excellent (20 ppb or better if a concentrator column is employed), and so the method is also used in the analysis of samples from low-volume impactors.

For more complex mixtures a better separation is necessary, but then one sample will take 16—30 min. Another approach would be the parallel application of several detectors, e.g., conductivity in combination with u.v.

spectrometry and ion-selective electrodes. Even under optimal conditions for separations, the determination of fluoride is problematic because of the overlap between the fluoride, hydroxide and carbonate peaks [3]. Because of the preceding separation in the ion-chromatographic system, the selectivity of the detectors can be less important in this case than in other applications. For example, both nitrite and nitrate are detected at 210 nm, but they are well separated in the fast ion-chromatographic system. For different problems, the following combinations of detectors can be used successfully: conductivity plus fluoride-selective electrode, conductivity plus chloride-selective electrode, conductivity plus determination of chloride by the well-known mercury(II)—thiocyanate flow injection method, conductivity plus u.v. spectrometry plus bromide-selective electrode, and conductivity plus u.v. spectrometry and fluoride-selective electrode. The results of the latter combinations are reported below.

EXPERIMENTAL

Apparatus

Figure 1 gives the general layout of the ion-chromatographic system. The components of the system are listed in Table 1. A three-way valve (1) connects the sample loop (100—4000 μl) either with a six-way valve which selects

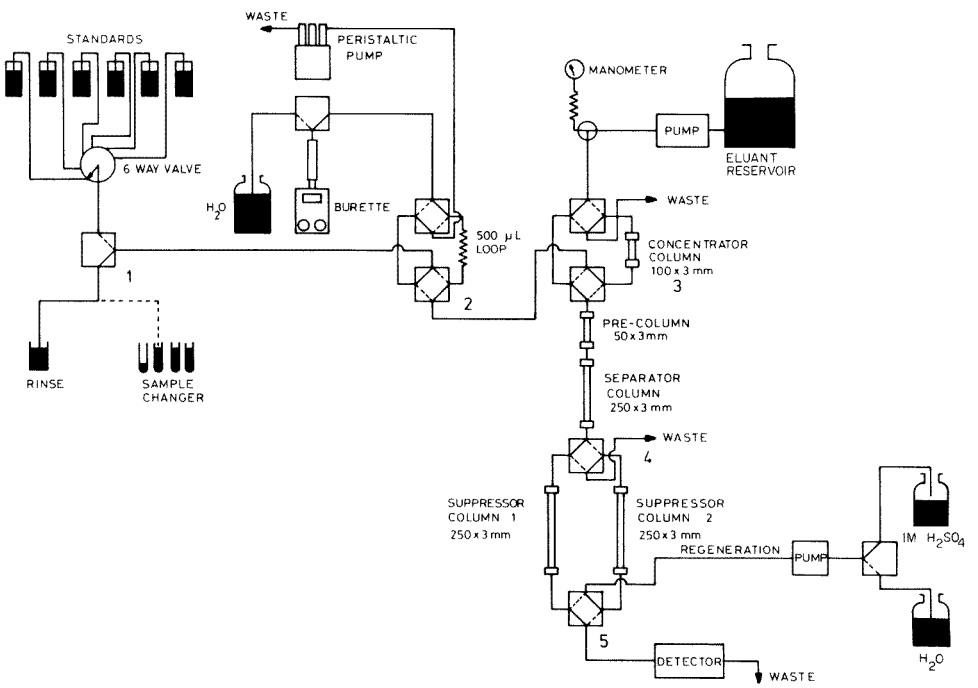

Fig. 1. Schematic diagram of the ion-chromatographic system.

TABLE 1

Components for the ion-chromatographic system

Pumps	Eluant pump, Leroy Somer HS 56 R; regenerating pump, CFG A 2001
Connectors	Flair-Fit (U.S.) and Cheminert (U.K.)
Tubing	0.3-mm i.d., 1-mm o.d. (Eriks, The Netherlands)
Valves	Pneumatic 3-way, 4-way (Flair-Fit) and six-way (Cheminert) valves. They are actuated by Kunke 3-way electric valves
Peristaltic pump	Gilson Minipuls 2
Sample changer	Gilson SC6, 300 samples capacity
Sample transfer	ECN design
Conductivity cell	Dionex
Conductivity meter	ECN design, equipped with 4.5 digit read out and automatic ranging. Ranges in combination with the ECN cell: 0--2.000, 0—20.000 and 0—200.000 μmho [3]
Buret	Metrohm E415
Separation columns	Dionex anion separator (250 × 3 mm)
Concentration column	Zipax SAX (100 × 3 mm)
Columns	Omnifit (U.K.) and 1.5-mm teflon tubing equipped with flare-fit connectors
Suppressor resin	Biorad AG50W-X16 200—400-mesh cation exchanger
Pre-column	Dionex anion exchanger or Zipax SAX, 50 × 3 mm
U.v. detector	Zeiss PM 2 ALC
Electrodes	F^- electrode (Metrohm), Br^- electrode, Hg_2Br_2 type (Ionel, Mount Hope, Canada)
Amplifier system	2 high impedance inputs (10^{13} Ω), ECN design [5, 6]
Computer system	PDP 11-03 LSI with 32K memory. This system is described elsewhere [5, 7]

standards, or with the sample changer as previously described [5]. Samples up to 500 μl are introduced directly by means of a sample loop. For sample volumes between 0.5 and 4 ml, a concentrator column is necessary. The sample is pumped through the concentrator column by means of a 5-ml motor buret.

The concentrator column is brought into the eluant stream by means of valve 3. The eluant is 0.002 M Na_2CO_3—0.001 M $NaHClO_3$ [1]. Valves 4 and 5 are operated simultaneously. One of the suppressor columns is actually used in the system, while the other is regenerated by pumping 1 M HNO_3 for 5 min followed by washing with demineralized water for 15 min. The suppressor columns break through after 30 min.

The detectors are placed in series and connected by 0.3-mm tubing in the following order: conductivity cell, u.v. monitor and ion-selective electrodes. The electrodes are mounted in an electrode holder with a built-in reference electrode, as described earlier [6]. In this system the distance between the flat surfaces of the reference electrode and of the measuring electrodes is 0.1—0.2 mm. For fluoride measurements, the eluant is mixed (1 + 1) with a solution containing 0.1 M acetic acid, 0.1 M sodium acetate, 0.1 M potassium chloride, and 300 ppb fluoride.

A simple peak-height procedure is applied. The operator specifies the time interval for measuring the background and the top of the peak [3].

Procedures

The standardization and quality-control procedures are the same as described elsewhere [6, 7]. Six standards are measured and a calibration curve is computed. The standardization is repeated and if the results agree within preset limits, samples are analyzed. After 18 samples a standard is injected and the system is recalibrated if the result is unsatisfactory.

A substantial number of standards is necessary, even if only the conductivity detector is employed. The calibration graphs are not straight at low concentrations, notwithstanding the linear response of the conductivity detector. This is caused by displacement of the equilibrium $H^+ + HCO_3^- \rightleftharpoons CO_2 + H_2O$, to the right by H^+ ions, originating from hydrochloric acid, nitric acid, etc. formed in the suppressor column. The effect of this phenomenon can easily be calculated. Assuming that the K_1 value for H_2CO_3 is 4×10^{-7}, the resulting HCO_3^- concentration is about 3×10^{-5} M, and this was confirmed by the measured conductivity. The maximum amount (originating from the measured acids) of hydrogen ion that is bound by HCO_3^- is 3×10^{-5} M. If the peaks are assumed to have triangular shape, the concentration can be calculated, above which a straight calibration curve is obtained. In the case of nitrate ions, this calculated value is 10 ppm; experimentally, the calibration graph is straight for nitrate concentrations exceeding 8 ppm. Linear regression of the results in the range 8—20 ppm nitrate indicates a blank of 1.7 ppm. The maximum amount of hydrogen ion that is bound by HCO_3^- corresponds to 1.5 ppm nitrate.

RESULTS

The results of two configurations of ion chromatography are reported. In the first, the 25-cm Dionex anion-exchanger column was used with a 500-μl sample loop, and the detection was accomplished by conductivity, u.v. at 220 nm and a fluoride-selective electrode. In the second configuration, again with the 25-cm Dionex anion-exchanger column, sampling was done with a 4.0-ml loop and a 10-cm concentrator column (Zipax SAX) was used; here detection was accomplished by conductivity, u.v. at 220 nm and a bromide-selective electrode (Hg_2Br_2 type).

The first configuration is applicable for samples in the concentration range 0.5—100 ppm. The selectivity is very good: bromide and phosphate do not interfere in the measurement of nitrate by u.v., and any interference of nitrate on chloride is detected easily because a nitrite peak is recorded by the u.v. detector. The results are given in Table 2. For calibration, six standards are used, in the range 1—20 ppm for chloride, nitrate and sulfate, and 10—200 ppb for fluoride. Generally, the precision of the results is better than the accuracy. The calibration curves are sigmoidal in the case of chloride and

TABLE 2

Results obtained for 0.5-ml samples with the first configuration and the conductivity detector (except where specified)

Taken	Found														
	Fluoride[a]			Nitrate[b]			Chloride			Nitrate			Sulfate		
	n[c]	$\bar{x}$	s(%)	n	$\bar{x}$	s(%)	n	$\bar{x}$	s(%)	n	$\bar{x}$	s(%)	n	$\bar{x}$	s(%)
Demineralized water	10	1.5	52	10	0.007	50	10	−0.002	260	10	0.007	90	10	0.011	70
10 ppb F^- 1 ppm Cl^-, NO_3^-, SO_4^{2-}	10	10.2	10.3	10	1.01	0.63	10	1.04	1.57	10	1.02	1.07	10	1.05	3.1
50 ppb F^- 5 ppm Cl^-, NO_3^-, SO_4^{2-}	20	48.19	7.0	20	5.02	0.81	20	5.03	1.6	20	5.04	0.74	20	5.10	2.6
100 ppb F^- 10 ppm Cl^-, NO_3^-, SO_4^{2-}	20	92.8	0.91	20	10.11	0.50	20	10.27	0.92	20	10.16	0.48	20	10.36	0.63
150 ppb F^- 15 ppm Cl^-, NO_3^-, SO_4^{2-}	10	150	1.1	10	15.3	0.3	10	15.3	1.0	10	15.14	0.4	10	15.1	0.4

[a]Fluoride-selective electrode. [b]U.v. detector. [c]n = Number of determinations, $\bar{x}$ = mean value found, s(%) = relative standard deviation.

TABLE 3

Measurement of low concentrations of chloride, nitrate, sulfate and bromide
(Conductivity detector, unless specified otherwise)

Amount of ion added (ppb)	Found (ppb)														
	Bromide[a]			Nitrate[b]			Chloride			Nitrate			Sulfate		
	n[c]	$\bar{x}$	s(%)	n	$\bar{x}$	s(%)	n	$\bar{x}$	s(%)	n	$\bar{x}$	s(%)	n	$\bar{x}$	s(%)
—[d]	10	0.86	18	10	1.8	56	10	0.97	144	10	1.09	91	10	3.08	70
50	10	37.1	2.36	10	50.4	1.33	10	37.5	6.9	10	61.9	3.9	10	44.4	10.0
100	10	109	1.16	10	98.5	2.6	10	94.1	4.6	10	134	3.4	10	93.4	9.8
200	10	200.4	0.7	10	208.6	2.3	10	190.3	3.3	10	277.8	1.9	10	194.3	5.7

[a]Bromide-selective electrode. [b]U.v. monitor. [c]Abbreviations as in Table 2. [d]Demineralized water.

sulfate, which means that the deviations depend on the number of standards. For the work concerned here, a fairly large concentration range (0.5—20 ppm) was required and so a maximum deviation of 3% had to be accepted. The deviation could be made less if the standards were chosen in a narrower range. The two suppressor columns gave slightly different results but the difference was less than 2%. The standard deviation when only one suppressor column was used was less than 0.8% for a 10 ppm standard.

The detection limits defined as three times the standard deviation found for blank measurements, can be derived from the results obtained with demineralized water. Thus the detection limit is 2.5 ppb for fluoride (i.s.e.), 10 ppb for nitrate (u.v.), and with the conductivity detector, 20 ppb for nitrate, 15 ppb for chloride and 25 ppb for sulfate.

The interference of cations on the fluoride measurements with the fluoride-selective electrode can be eliminated in the combined system (see Table 2). For example, in checks on the effects of calcium and aluminum ions on the determination of 100 ppb fluoride, concentrations of 80—200 ppm of calcium or aluminum ions caused a positive error of only 2—3% with no significant trends in the results; the relative standard deviations were 2—3% in all cases.

With this first configuration, calibration required 45 min. The rate of analysis was 18 samples per hour, consisting of 72 individual results.

For samples containing less than 1 ppm of the ions of interest, the second instrumental configuration is preferable. This involves larger (up to 4 ml) volumes of sample and a concentrator column. The Zipax SAX exchanger used in the concentrator column is not stable at the pH of the eluant (ca. 9) or at elevated temperatures and must be renewed after 14 days. In real life, most concentrator columns are poisoned long before that time.

In rain-water samples, the problem of the determination of bromide was encountered. If a bromide-selective electrode is used, the interference of chloride is disastrous if a preliminary separation is not done; further the separation between very low bromide and high nitrate concentrations is impossible by ion chromatography. To overcome this problem, a bromide-selective electrode, a u.v. monitor and the conductivity detector were used. The bromide-selective electrode gives two peaks per sample, the first corresponding to chloride and the second to bromide. The system was calibrated by six standards, containing, respectively, 100—2000 ppb Cl^-, NO_3^- and SO_4^{2-} and 20—400 ppb Br^-. The results are given in Table 3.

The detection limits, defined as above, can be derived from the results obtained with demineralized water. Thus the detection limits with this configuration are 0.5 ppb for bromide (i.s.e.), 3 ppb for nitrate (u.v.), and with the conductivity detector, 3 ppb for nitrate, 4 ppb for chloride and 6 ppb for sulfate.

Especially in the cases of bromide and chloride, the precision of the results is much better than the accuracy. There are two main reasons for this: the calibration curves for bromide and chloride exhibit very marked curva-

ture, and the stability of the standards is a problem at very low concentrations. Better results can be obtained if the standards can be chosen to cover a narrow range, but the wide calibration range was needed for the rain-water studies here. The results of the nitrate conductivity measurements are clearly influenced by bromide, as was to be expected.

The calibration procedure takes about 75 min, and 12 samples can be analyzed per hour with the second configuration.

It can be concluded that rapid determinations by ion chromatography are feasible. The selectivity of the method can be a problem but this can be solved rather easily by applying different detector systems. The automatic system is able to function for 24 h per day, mainly because of the automated frequent check by standards followed by recalibration if necessary.

REFERENCES

1 M. Small, T. S. Stevens and W. C. Bauman, Anal. Chem., 47 (1975) 1801.
2 M. A. Fulmer, J. Penkrot and R. J. Nadalin, in J. D. Mulik and E. Sawicki (Eds.), Ion Chromatographic Analysis of Environmental Pollutants, Vol. 2, Ann Arbor, Ann Arbor, MI, 1979, pp. 381—400.
3 J. Slanina, W. A. Lingerak, J. E. Ordelman, P. Borst and F. P. Bakker, in J. D. Mulik and E. Sawicki (Eds.), Ion Chromatographic Analysis of Environmental Pollutants, Vol. 2, Ann Arbor, Ann Arbor, MI, 1979, pp. 305—317.
4 D. Klockow, J. Teckentrup and W. Merz, Mikrochim. Acta, (1978) 535.
5 J. Slanina, F. P. Bakker, A. Bruyn-Hes and J. J. Möls, Anal. Chim. Acta, 113 (1980) 331.
6 J. Slanina, W. Lingerak and F. Bakker, Anal. Chim. Acta, 117 (1980) 91.
7 J. Slanina, F. P. Bakker, J. J. Möls, J. E. Ordelman and A. Bruyn-Hes, Anal. Chim. Acta, 112 (1979) 45.

Analytica Chimica Acta, 130 (1981) 9—22
Elsevier Scientific Publishing Company, Amsterdam — Printed in The Netherlands

AN ELECTROCHEMICAL REACTIVATION METHOD FOR SOLID ELECTRODES USED IN ELECTROCHEMICAL DETECTORS FOR HIGH-PERFORMANCE LIQUID CHROMATOGRAPHY AND FLOW INJECTION ANALYSIS

H. W. VAN ROOIJEN and H. POPPE

Laboratory for Analytical Chemistry, University of Amsterdam, Nieuwe Achtergracht 166, 1018 WV Amsterdam (The Netherlands)

(Received 24th March 1981)

SUMMARY

An electrochemical reactivation method for solid electrodes used in electrochemical detectors is optimized for glassy carbon electrodes. Application of a voltage pulse train for 5 min is effective in restoring the response of the electrode after deactivation by organic compounds. Potassium hexacyanoferrate(II) and DL-synephrine were used to test the reactivation of electrodes; 2,6-dihydroxybenzoic acid and urine served to deactivate them. The effects of the amplitude, d.c. level, and frequency of the applied voltage pulse train, as well as the mode of termination, are discussed.

The increasing complexity of mixtures to be separated by high-performance liquid chromatography (h.p.l.c.) has intensified the need for detection systems with high sensitivity and selectivity. The introduction of electrochemical detection with solid electrodes has been a valuable contribution. Selectivity, sensitivity, high anodic working ranges and simplicity of operation and cell construction are the main features of electrochemical detectors with solid electrodes. Accordingly, the application of solid electrode materials [1] like platinum, gold, graphite and other carbon-containing substances has become popular in amperometric [2, 3] and coulometric [4, 5] detection systems. Unfortunately, solid electrodes show a decrease in the activity of the surface with use, and this usually leads to a gradual decrease in detection limits and sensitivity. Understanding of the deactivating processes at solid electrodes requires an insight into the surface reactions involved in the electrochemical conversion of the analyte as well as into other processes and reactions occurring at the electrode surface. However, little is known about general surface chemistry and the field of electrochemistry at solid electrodes is no exception, although a substantial amount of knowledge about some specific phenomena at solid electrodes has been gathered [1, 6—11].

Adsorption of the analyte or reaction products after oxidation or reduction, possibly forming polymeric films [6], may be responsible for some of the problems encountered. In the case of glassy carbons and other carbon-

containing compounds, however, the presence or the formation of carbonyl or hydroxyl groups [7—11] on the electrode surface may be involved. When these processes affect the accuracy in analytical applications, an electrode-cleaning procedure becomes essential. The cell has to be dismounted and the electrode is cleaned by mechanical [7, 12, 13], chemical [7, 14] or electrochemical means [7, 15] or by a combination of these methods [1, 7, 14, 15]. After reassembly, a time-consuming conditioning procedure [1, 3] is usually necessary before background current and noise level are reduced to acceptable levels.

In static electroanalytical chemistry, procedures for cleaning and conditioning the electrodes in situ have been proposed. Such procedures would be even more valuable in electrochemical l.c. detection because the necessity of dismounting the cell interferes seriously with the continuity which is inherent to this technique. The feasibility of cleaning solid electrodes using voltage pulse-train programs was therefore investigated. A measure of the effectiveness of these procedures was needed. It is of course impossible to monitor the performance of electrodes after various treatments for all kinds of electrochemical reactions for which the detector might be used. In order to obtain such a measure, the behaviour of the electrode in the oxidation of potassium hexacyanoferrate(II) in a solution buffered at pH 2.8 was studied. The selection of this compound is arbitrary and may be criticised because a reaction involving a one-electron transfer in an inorganic species might not be representative of the much more complicated reactions involved in the electrochemical detection of organic molecules. However, it has been found by other workers, and confirmed here, that electrodes which are "active" towards hexacyanoferrate(II) are active in other reactions as well. Further, the hexacyanoferrate couple has the advantage that its behaviour under reversible conditions is well established.

A similar, more or less arbitrary, standardisation was necessary for the deactivation of the electrode. Oxidation of phenolic compounds can deactivate carbon electrodes severely [1, 7]; again, this was confirmed. 2,6-Dihydroxybenzoic acid was therefore adopted as a standard to deactivate the electrode before the application of the voltage pulse-train program.

THEORY

The current—voltage curves observed for potassium hexacyanoferrate(II) provide useful information concerning the reversibility of the reaction $Fe(CN)_6^{4-} \rightleftharpoons Fe(CN)_6^{3-} + e^-$ taking place at an electrode surface in aqueous solutions. Data are available to calculate the formal potential of the $Fe(CN)_6^{4-}$/$Fe(CN)_6^{3-}$ couple. If the reaction is electrochemically reversible, the measured half-wave potential, $E_{1/2}$, will be virtually the same as the formal potential, E_0', and the theoretical and measured current—voltage curves will have the same shape. Irreversible behaviour normally results in changes of the shape of the measured current—voltage curve and shifts of the half-wave potential to higher values [1, 3].

In the present investigations, a silver—silver chloride reference electrode without a salt bridge was used. As the chloride concentration was 10^{-2} M and the standard potential of the Ag/AgCl electrode was +0.2223 V [16], a potential of +0.340 V vs. the normal hydrogen electrode was calculated for this reference electrode, with corrections for ionic strength. For the hexacyanoferrate couple, additional corrections for the protonation of the hexacyanoferrate(II) complexes must be included. The values $K_1 = 10^{4.28}$ and $K_{1,2} = 10^{2.3}$ were taken for the protonation constants [17], +0.358 V [16] was used for the standard potential of the couple, and a formal potential of +0.114 V vs. the Ag/AgCl reference electrode was thus calculated for pH 2.8.

For the application of amperometric or coulometric detection in h.p.l.c., the exact shape and $E_{1/2}$ values of current—voltage curves are not of vital importance, as the potential of the working electrode is usually set on the limiting current plateau. For selectivity reasons, however, it is often convenient to choose a potential as low as possible. For the reversible anodic case, the following relationship between current and voltage is valid

$$i = i_{l,a} \times 10^{\Delta E/59}/(1 + 10^{\Delta E/59})$$

where $\Delta E = E - E_0'$, E is the potential of the working electrode (mV), E_0' is the formal potential of the couple (mV), $i_{l,a}$ is the anodic limiting current, and i is the current measured at potential E. From this equation it can be seen that, at a potential of +200 mV vs. the Ag/AgCl reference electrode, the current amounts to 97% of the limiting current.

As deactivation results in a shift of the value of $E_{1/2}$ to higher potentials, the value of the current produced by oxidation of potassium hexacyanoferrate(II) at 200 mV will decrease rapidly on deactivation. The performance of the electrode can be characterized by comparing the limiting current measured, for instance, at +700 mV with the current measured at +200 mV. By calculating $i_{200}/0.97\ i_{700} = \rho$ from the measured currents, an expression is found to characterize the electrode performance: ρ will have values between 0 and 1, where $\rho = 1$ indicates reversible behaviour. Deactivation will cause a decrease of ρ. In the hydrodynamic applications of amperometry and coulometry, the time integral $\int_0^t i(t)\mathrm{d}t$ for the whole peak is measured. The relationship between $\int_0^t i(t)\mathrm{d}t$ and E will be called the coulomb—voltage curve. The integral is proportional to the bulk concentration of the analyte. The coulomb—voltage curves have similar shape and similar $E_{1/2}$ values as current—voltage curves measured in electrochemistry in stirred solutions and so characterization of the electrode by ρ can be applied to flow-through detection as well.

EXPERIMENTAL

Instrumentation

The coulometric detection cell (Kipp Analytica, Emmen, The Netherlands) was of similar design as described earlier [4]. The three-electrode system

consisted of two flat glassy carbon plates serving as the working and auxiliary electrodes and a silver tube of 0.5 mm i.d. covered on the inside with silver chloride, serving the dual purpose of reference electrode and outlet. The surface area of the working auxiliary electrode was 3 cm^2 and the spacer thickness was 100 μm.

Figure 1 shows a schematic diagram of the measuring equipment. All liquid flow lines consisted of teflon and nylon tubings. A background electrolyte storage vessel (E) was pressurized with nitrogen by means of a pressure regulator (P_R, P) which was custom-made. The background electrolyte was forced through two pneumatically actuated six-way rotary valves K_I and K_{II} (Chromatronix HPSV-20, U.S.A.) with sample loops of 500 and 32 μl, which were placed in series. The connection between the two valves was made as short as possible. The loops of the valves were fed by hydrostatic syphoning from two sample containers (H_I and H_{II}) which contained deactivating agent and potassium hexacyanoferrate(II) solutions, respectively. The samples were purged with nitrogen and stirred continuously. The valve K_{II} was connected directly with the cell by 25 cm of teflon tubing (0.25 mm i.d.). The cell was kept under pressure by means of a restrictor (R), (10 m of teflon tubing, 0.25 mm i.d.) in order to avoid air bubbles. The flow was measured with a modified millilitre pipet (FM).

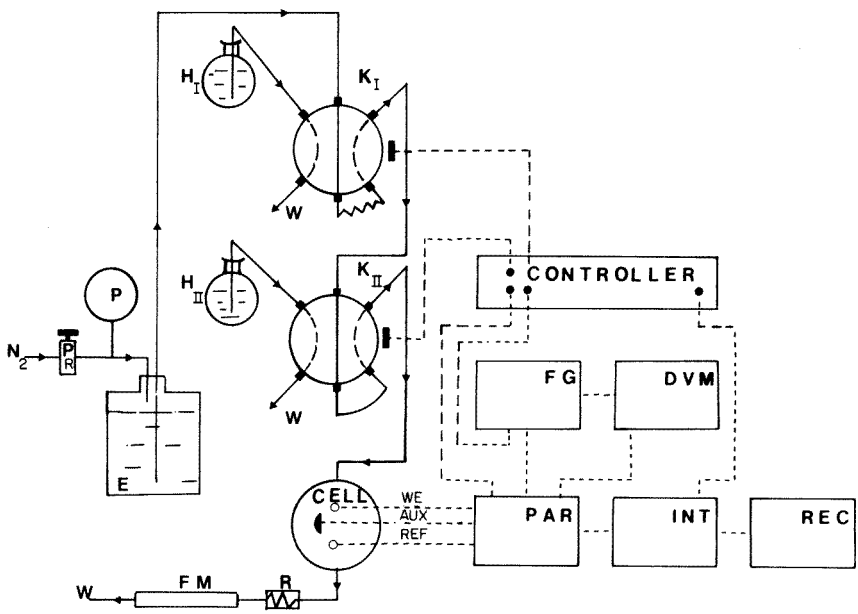

Fig. 1. Schematic diagram of the measuring equipment. Gas system: N_2, nitrogen supply; PR, pressure regulator; P, Bourdon-type manometer. Liquid system: E, background electrolyte storage vessel; K_I, K_{II}, six-way rotary valves; H_I, H_{II}, sample containers; W, waste; CELL, coulometric flow-through cell; R, resistor; FM, flow meter. Electronic system: CONTROLLER, timing unit; FG, function generator; DVM, voltmeter; PAR, double potentiostat; INT, integrator; REC, recorder.

The equipment could be operated automatically. A custom-made timing unit controlled the following functions: (1) switching of the potential from 200 mV to 700 mV and back, the potential being controlled by a double potentiostat (Princeton Applied Research, Model 173-179); (2) activation of the pneumatic actuators of the six-way rotary valves; (3) connection of the signal of the function generator (Pulse Generator 8012 B, Hewlett-Packard) to the potentiostat; and (4) the run/stop commands of the integrator (Autolab system I computing integrator, Spectra Physics, Santa Clara, CA). The signal was displayed on a stripchart recorder (type RE647, Goerz Electro, Wien, Austria). Steady-state potentials could be read on a multimeter (DM2, Sinclair Radionics Ltd., Huntingdon, Gt. Britain).

Chemicals

Anhydrous acetic acid (99.5%), potassium hexacyanoferrate(II) and 2,6-dihydroxybenzoic acid were of analytical grade (Baker Chemicals, Merck, and Fluka, respectively). Potassium chloride was of Suprapur quality (Merck); DL-synephrine was from Sigma Chemicals.

All chemicals were dissolved in double-distilled water and the solutions were filtered through 0.8-μm Millipore filters. The background electrolyte was 0.1 M in acetic acid and 0.01 M in potassium chloride; the pH was 2.8. Deactivating solutions and hexacyanoferrate(II) solutions were prepared in the background electrolyte. The standard deactivating solution was made by diluting 15 ml of a filtered saturated solution of 2,6-dihydroxybenzoic acid to 400 ml; this contained approximately 400 μg ml^{-1}. The test solution was 10^{-4} M $K_4Fe(CN)_6$.

Urine samples were filtered through paper and then 0.8-μm Millipore filters.

Electrodes

Two types of glassy carbon electrode (grade GC-10, Tokai Electrode Manufacturing Co., Tokyo; and V25, Le Carbone Lorraine, Paris) and a carbon paste electrode (EA267c Metrohm) were examined. The glassy carbon electrodes were ground with Amaril 303 until a flat surface (± 2 μm) with a dull appearance was obtained, after which the electrodes were scoured with self-adhesive flint paper 600 and finally polished with Diaplast 0.7 SS diamond paste until a shiny surface was obtained. The gold and platinum electrodes were of high purity and were carefully polished with alumina.

One of the glassy carbon electrodes was not polished and was later covered with carbon paste by rubbing the surface over a layer of carbon paste on a computer card; the excess of paste was removed by rubbing on new cards. This method provided a nice thin layer of carbon paste on the glassy carbon electrode.

The electrodes tested are abbreviated in the subsequent discussion as follows:

GCL I and GCL III:	glassy carbon, Lorraine, polished
GCL II:	glassy carbon, Lorraine, scoured
GCL II-CP:	GCL II covered with carbon paste

GCT: glassy carbon, Tokai, polished
Au I and Au II: gold, polished
Pt I and Pt II: platinum, polished.
After the surface treatment all electrodes excepted GCL II-CP were cleaned with acetone before the cell was assembled.

Procedures

All potentials mentioned in the subsequent paragraphs are referred to the Ag/AgCl reference electrode. Before a set of measurements was started, this electrode was stabilized by passing an anodic current of about 30 μA for 15 min.

Programs executed by the timing unit consisted mainly of the following subroutines. In the regeneration step, the voltage pulse train applied had a square potential wave of variable amplitude and d.c. level with a frequency of 0.5 Hz (unless indicated otherwise) and an application time of 300 s. In the deactivation step, 500 μl of the deactivating agent was injected, and this was oxidized at +700 mV vs. Ag/AgCl. In the activity tests, the responses at +200 mV were measured for five injections of the hexacyanoferrate(II) solution; the potential was then changed to +700 mV and after a stabilization time of 200 s, the responses for a further five injections were measured. The mean values of the peak areas at 200 mV and 700 mV were used to calculate the value of ρ. In the final subroutine, hydrodynamic coulomb—voltage curves were produced by plotting the peak areas (μC) against the corresponding potential.

RESULTS AND DISCUSSION

Hydrodynamic coulomb—voltage curves for potassium hexacyanoferrate-(II) were determined for all electrodes with the exception of GCL II-CP. No additional information concerning the previous history of deactivation of the electrodes was available, except for the fact that several organic substances (e.g., catecholamines, ascorbic acid, phenolic compounds) had been oxidized at the electrode surface. The shapes of the hydrodynamic coulomb—voltage curves and the values of the half-wave potentials suggested a more or less severe state of deactivation for the electrodes (Fig. 2). However, the Au II electrode did not show too much deviation from the theoretical curve, probably because it had been less frequently applied in previous work. A first pilot experiment showed that switching of the potential of the working electrode between +1.5 V and —1.5 V and vice versa for some time improved the electrode performance considerably.

A second pilot experiment was done to examine the influence of the magnitude of the amplitude and the length of time of the reactivation treatment. At a d.c. level of 0 V, amplitudes of 0.8 and 2.0 V (at 0.5 Hz frequency) and also self-recovery (referred to as "0 V amplitude") were used to reactivate the electrode after an injection of the deactivating agent. The recovery was

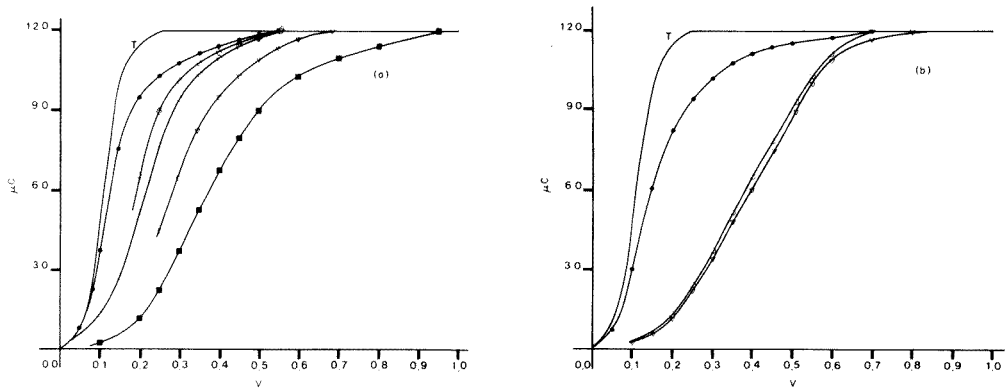

Fig. 2. Hydrodynamic coulomb—voltage curves of $K_4Fe(CN)_6$ at various electrodes. The vertical axis is the peak integral $\int_0^t i(t)dt$ (μC); the horizontal axis is the potential (V) vs. the Ag/AgCl electrode. In (a): (T) theoretical curve; (•) Au II; (◇) Pt I; (○) Au I; (▽) Pt II; (▪) GCL III. In (b): (T) theoretical curve; (•) GCL II; (○) GCL I; (▽) GCT.

measured as a function of the application time by interrupting the voltage pulse train after a certain period and testing the activity. The activity test was repeated after further applications of the pulse train for varying times, t; each new pulse train added its contribution to the reactivation process. The experiments were carried out with the GCL II-CP and the GCT electrodes. Directly after deactivation ρ was practically zero. A pulse train with 2.0-V amplitude reactivated these electrodes, giving ρ values 0.86 for GCT and 0.95 for GCL II-CP after an application time of 250 s. A pulse train with 0.8-V amplitude was not effective, and indeed was no improvement on self-recovery of the electrode (0 V amplitude). Figure 3 shows a typical picture of the reactivation process as a function of time and amplitude. These results indicated that optimization of the voltage pulse train with respect to amplitude, d.c. level and frequency was necessary. The application time was chosen as 300 s.

Frequency optimization

The frequency was optimized for the GCL II-CP and GCT electrodes. The electrode was first deactivated and then a voltage pulse-train was applied, followed by an activity test. The voltage pulse train had the following characteristics: 0-V d.c. level, 2-V amplitude, 300-s application time, with variable frequency.

The best results were found when the frequency was 0.5 Hz. Higher frequencies resulted in lower values of ρ. Lower frequencies gave less reproducible behaviour. If the potential was set at +2.0 V or −2.0 V for 300 s, ρ exceeded its theoretical value of $\rho = 1$ and the reproducibility was extremely bad. A purely anodic or cathodic treatment was therefore expected to be not feasible. A frequency of 0.5 Hz was used in all further experiments.

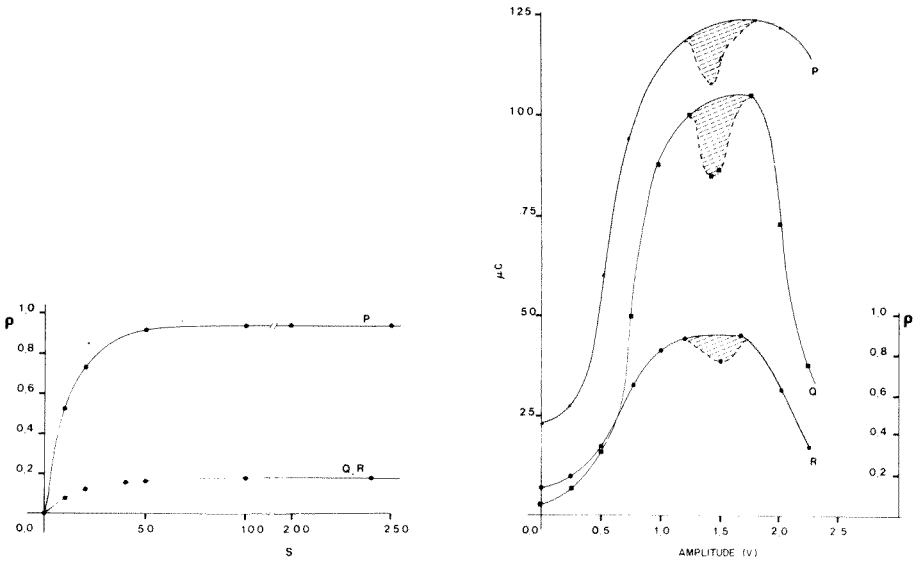

Fig. 3. Value of ρ as a function of the amplitude and pulse-train application time. The horizontal axis is the application time (s). Amplitudes: (P) 2 V; (Q) 0.8 V; (R) "0 V".

Fig. 4. Response and ratio curves for $K_4Fe(CN)_6$ and the GCT electrode as a function of the amplitude. The horizontal axis is the amplitude of the voltage pulse train at a d.c. level of 0 V. The vertical axis for the P and Q curves is response (μC) towards $K_4Fe(CN)_6$, and is dimensionless for the R curve. (P) Response towards $K_4Fe(CN)_6$ at 700 mV; (Q) response towards $K_4Fe(CN)_6$ at 200 mV; (R) value of ρ. The hatched areas indicate uncertainties in the measurement.

Amplitude optimization

The electrodes GCL II-CP and GCT were used to optimize the amplitude of the voltage pulse train. The electrodes were first reactivated with a cleaning voltage pulse train of sufficiently high amplitude (1.8 V) at a d.c. level of 0 V with a frequency of 0.5 Hz and an application time of 300 s so as to ensure that the activity of the electrode was restored before deactivation when the preceding test voltage pulse train was not capable of reactivating the electrode sufficiently. Thus the test cycle was: cleaning voltage pulse train → deactivation → test voltage pulse train → activity test → cleaning voltage pulse train, etc.

The test voltage pulse train had the same characteristics as the cleaning voltage pulse train except for the amplitude which was varied. The response curves of hexacyanoferrate(II) at 200 and 700 mV are presented in Fig. 4 as a function of the amplitude of the test voltage pulse train; the value of ρ is also plotted. The response curves are of similar shape for both electrodes. Maximum response is found for amplitudes of 1.25 V and between 1.8 and 2 V, resulting in values of ρ = 0.88 for the GCT electrode and ρ = 0.82 for the GCL II-CP electrode. Surprisingly, during these experiments, a minimum for the response curves was found at amplitudes between 1.50 and 1.75 V.

The minimum showed variable values and sometimes vanished completely; its cause is not understood.

D.c. level optimization

The d.c. level was optimized in the same way as the amplitude. The cleaning voltage pulse train had an amplitude of 1.8 V for the GCT electrode and 2.0 V for the GCL II-CP electrode for a d.c. level of 0 V. All other characteristics were the same. The test voltage pulse train had the same characteristics as the cleaning voltage pulse train, except for the variable d.c. level.

From Fig. 5, it can be seen that the optimum d.c. level lay between —0.6 V and —0.4 V. Again the curves were of similar shape for the GCL II-CP and the GCT electrode. The ratio ρ reached values of ρ = 0.93 for the GCT electrode and ρ = 0.88 for the GCL II-CP electrode.

The influence of the end potential of the voltage pulse train

In experiments with DL-synephrine, it was found that the final potential of the pulse train affected the response considerably (Fig. 6). In previous experiments the voltage pulse train was randomly interrupted after the 300-s application time. For DL-synephrine, peak areas appeared to be 25—30% larger when the pulse train was terminated at negative potentials (cathodic termination) than those obtained after termination at positive potentials (anodic termination). This phenomenon was not found for the hexacyanoferrate(II) solution. The chemical properties of the electrode probably change in the

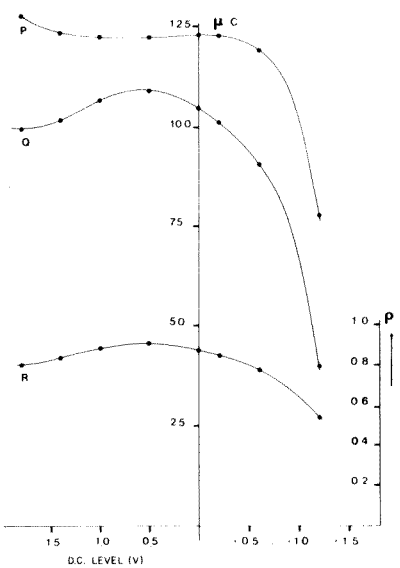

Fig. 5. Response and ratio curves for $K_4Fe(CN)_6$ at the GCT electrode as a function of the d.c. level of the voltage pulse train at an amplitude of 1.8 V. The vertical axes and the meanings of P, Q and R are the same as in Fig. 4.

anodic and cathodic parts of the pulse train, causing differences in the electrode response.

These results indicated the need to control the end potential of the voltage pulse train. Additional experiments showed that when the voltage pulse train was dampened out exponentially with a time constant of 10 s towards the potential which was used to monitor DL-synephrine (700 mV), the response was 80% of the response when the voltage pulse train was terminated cathodically (Fig. 7). Similar results were found for the response to 4,6-dihydroxybenzoic acid. The precision was better than 4% for this method.

The stabilization process after application of a voltage pulse train for cleaning purposes is unfortunately nearly as time-consuming as it is after cell dismounting. An attempt was made to obtain shorter stabilization times by applying voltage pulse trains which decayed exponentially, but the rate of the stabilization process was not affected. Unless indicated otherwise, voltage pulse trains were terminated cathodically in all further experiments.

In summary, the optimal conditions for the GCT and GCL II-CP electrodes are: a frequency of 0.5 Hz, a d.c. level of −0.6 to −0.4 V and an application time of 300 s, with an amplitude of 1.8 V for the GCT electrode or of 2.0 V for the GCL II-CP electrode.

Physical effects

Reactivation of glassy carbon and carbon paste electrodes using optimized voltage pulse-train cleaning leads to some visible roughening of the electrode surface. Extended application even leads to gradual etching. These effects, however, appear to have no effect on the noise level and the background current.

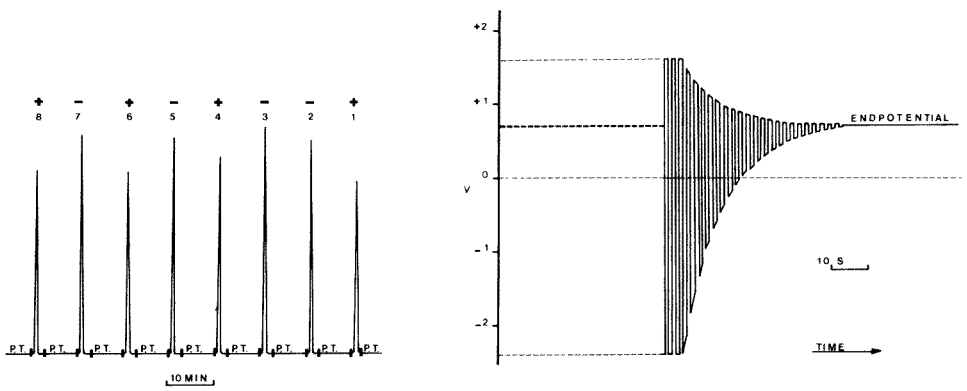

Fig. 6. Eight injections of DL-synephrine with randomly terminated intermediate voltage pulse-train cleaning: peaks 1, 4, 6 and 8 were obtained after anodically terminated voltage pulse train, and peaks 2, 3, 5 and 7 after cathodically terminated voltage pulse train.

Fig. 7. Exponentially dampened voltage pulse-train termination with a time constant of 10 s. The end potential is +700 mV vs. Ag/AgCl electrode.

APPLICATIONS

The efficiency of reactivation by voltage pulse trains was investigated for several deactivating solutions.

Reproducibility test for injections of 2,6-dihydroxybenzoic acid

2,6-Dihydroxybenzoic acid is oxidized at the GCT electrode. When 10 injections (32 μl) of the standard solution of 2,6-dihydroxybenzoic acid were made successively without intermediate voltage pulse-train cleaning, the response decreased with each following peak (Fig. 8a). When an optimal voltage pulse train was used between each injection the response was constant, the precision being better than 2% (Fig. 8b).

Response and hydrodynamic coulomb—voltage curve of DL-synephrine at the GCT electrode

This catecholamine was used to prepare hydrodynamic coulomb—voltage curves measured in various ways (Fig. 9). Curve (a) shows the results of 8 successive injections at a fixed potential without intermediate voltage pulse-train reactivation. Peak areas decreased with each subsequent injection to a somewhat steady level, indicating deactivation of the electrode surface. For the results shown by curve (b) a randomly terminated voltage pulse train was applied before each injection. This curve gives some indication that two successive oxidation steps are involved. Curve c shows the response of the cell towards injections of the DL-synephrine solution, preceded by a cathodically terminated voltage pulse train. Responses are higher for this method, compared with curve b, and the two oxidation steps are more pronounced. The precision of the points of curve c was better than 2%.

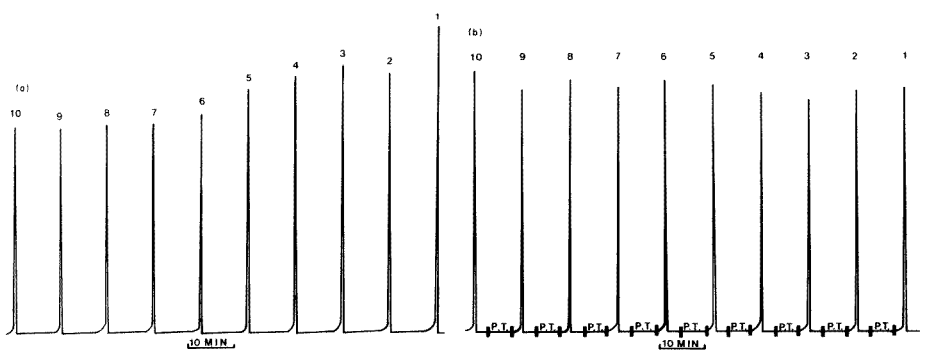

Fig. 8. Response of the GCT electrode to 10 successive injections of 2,6-dihydroxybenzoic acid: (a) without intermediate voltage pulse-train cleaning; (b) with intermediate cathodically terminated voltage pulse-train cleaning.

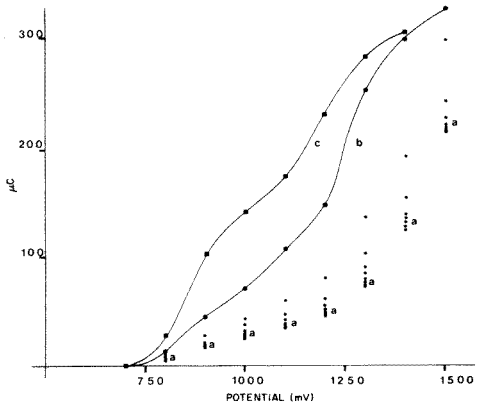

Fig. 9. Hydrodynamic coulomb—voltage curves for DL-synephrine measured by different methods at the GCT electrode. (a) 8 successive injections at a fixed potential without intermediate voltage pulse-train cleaning; (b) with randomly terminated voltage pulse-train cleaning; (c) with cathodically terminated voltage pulse-train cleaning.

Reactivation of a GCT electrode deactivated with unpurified urine

In view of the widespread application of electrochemical detection in biomedical analysis, it seemed worthwhile to determine the effectiveness of the proposed method in cases where the electrode is deactivated by a complex mixture of biomedical origin.

Urine from normal adults was used, and about 500 μl was injected in each run. Table 1 gives the results of 8 successive runs; deactivation brought the ratio ρ down to 0.10. The voltage pulse train was capable of restoring the activity of the electrode (ρ = 0.82); the precision was better than 3%.

Conclusions

Deactivated solid electrodes can be reactivated to a reproducible level by applying a voltage pulse train. Cleaning by this procedure leads to some roughening of the electrode surface, but no influence on the background current and the noise level is to be expected. Deactivating organic compounds can be measured with good precision if a voltage pulse train is applied between measurements.

To obtain the optimum effect, voltage pulse trains should be terminated exponentially, anodically or cathodically, depending on the substance to be measured. Optimal conditions at pH 2.8 in the case of 2,6-dihydroxybenzoic acid appear to be: frequency 0.5 Hz, amplitude 1.25 V or 1.8—2 V, d.c. level —0.4 V to —0.6 V and application time 300 s.

Voltage pulse-train cleaning is easy to build in as an option for electrochemical flow-through detectors for h.p.l.c. and flow injection analysis using solid electrodes, and facilitates electrode maintenance. The stabilization time after the treatment is of the same order of magnitude as for all other electrode cleaning methods. However, reactivation could be done automatically overnight.

TABLE 1

Results obtained on 8 successive experiments with urine and potassium hexacyanoferrate(II) at the GCT electrode[a]

Run	0	1	2	3	4	5	6	7	8	Mean value
R_p 700	26735	27333	27430	27694	28143	28179	28279	28579	28041	27819
σ_p 700	0.7	0.9	0.6	0.6	0.7	0.5	0.5	1.3	1.0	2.1%
R_p 200	21734	22102	21561	20945	22292	21791	21802	21707	22056	21776
σ_p 200	0.7	0.3	0.8	0.7	0.5	1.0	0.6	0.6	0.7	1.8%
ρ_p	0.83	0.83	0.81	0.78	0.82	0.80	0.79	0.78	0.81	0.81
X	6.62 $\times 10^6$	6.48 $\times 10^6$	6.53 $\times 10^6$	6.61 $\times 10^6$	7.09 $\times 10^6$	6.88 $\times 10^6$	6.89 $\times 10^6$	6.81 $\times 10^6$	6.72 $\times 10^6$	6.74 $\times 10^6$
R_d 700	19266	17029	16468	16224	16890	17653	17684	16978	—	16989
σ_d 700	1.9	1.2	2.0	1.6	2.2	2.9	1.9	1.7	—	3.2%
R_d 200	4108	2169	1732	1608	1884	2205	2237	2159	—	2064
σ_d 200	4.8	4.3	5.8	4.8	4.5	3.9	4.6	5.1	—	9.9%
ρ_d	0.23	0.13	0.11	0.10	0.12	0.13	0.12	0.12	—	0.12

[a] R_p 700, response to $K_4Fe(CN)_6$ at 700 mV after the voltage pulse train; R_p 200, the same at 200 mV; σ_p 700, relative standard deviation of R_p 700; σ_p 200, relative standard deviation of R_p 200; ρ_p, ratio after the voltage pulse train; X, response to urine injection; R_d 700, response to $K_4Fe(CN)_6$ at 700 mV after deactivation; R_d 200, the same at 200 mV; σ_d 700, relative standard deviation of R_d 700; σ_d 200, relative standard deviation of R_d 200; ρ_d, ratio after deactivation.

This work would not have been possible without the skill and inventiveness of Messrs. K. Camstra and J. Kuysten who solved the mechanical and electronic problems, respectively. Mr. P. Bierman devised and built the timing unit. Mr. M. Groeneveld was responsible for polishing the electrodes. Prof. Dr. G. den Boef was so kind as to review the manuscript with care.

REFERENCES

1 R. N. Adams, Electrochemistry at Solid Electrodes, M. Dekker, New York, 1969.
2 P. T. Kissinger, C. J. Refshauge, R. Dreiling and R. N. Adams, Anal. Lett., 6 (1973) 465.
3 P. T. Kissinger, Anal. Chem., 49 (1977) 447 A.
4 J. Lankelma and H. Poppe, J. Chromatogr., 125 (1976) 375.
5 H. Poppe, in J. F. K. Huber (Ed.), Instrumentation for HPLC, Elsevier, Amsterdam, 1978.
6 R. C. Kolle and D. C. Johnson, Anal. Chem., 51 (1979) 741.
7 W. E. van der Linden and J. W. Dieker, Anal. Chim. Acta, 119 (1980) 1.
8 D. Laser and M. Ariel, J. Electroanal. Chem., 52 (1974) 291.
9 B. D. Epstein, E. Dolle Malle and J. S. Matson, Carbon, 9 (1971) 609.
10 J. W. Dieker, W. E. van der Linden and H. Poppe, Talanta, 25 (1978) 151.
11 L. Dunsch and R. Nauman, Z. Chem., 14 (1974) 31.
12 R. M. Wightman, E. C. Palk, S. Borman and M. A. Dayton, Anal. Chem., 50 (1978) 1410.
13 B. Fleet and C. J. Little, J. Chromatogr. Sci., 12 (1974) 747.
14 I. M. Kolthoff and N. Tanaka, Anal. Chem., 26 (1954) 632.
15 H. E. Zittel and F. J. Miller, Anal. Chem., 37 (1965) 200.
16 G. Milazzo and S. Caroli, Tables of Standard Electrode Potentials, J. Wiley, New York, 1978.
17 L. G. Sillén and A. E. Martell, Stability Constants of Metal-Ion Complexes, Chem. Soc. Spec. Publ., London, 1964; Supplement, 1971.

Analytica Chimica Acta, 130 (1981) 23—30
Elsevier Scientific Publishing Company, Amsterdam — Printed in The Netherlands

A SENSITIVE HIGH-PERFORMANCE LIQUID CHROMATOGRAPHIC METHOD FOR DETERMINATION OF THE ANTI-NEOPLASTIC AGENTS VP 16-213 AND VM 26 IN BIOLOGICAL FLUIDS

J. J. M. HOLTHUIS and W. J. VAN OORT*

Department of Analytical Pharmacy, Subfaculty of Pharmacy, State University of Utrecht, Catharijnesingel 60, 3511 GH Utrecht (The Netherlands)

H. M. PINEDO

Netherlands Cancer Institute and Department of Oncology, Academic Hospital of the Free University of Amsterdam, De Boelelaan 1117, 1007 MB Amsterdam (The Netherlands)

(Received 2nd April 1981)

SUMMARY

A rapid and sensitive high-performance liquid chromatographic assay of the two anti-neoplastic podophyllotoxin analogs VP 16-213 and VM 26 in plasma and urine is described. The drugs are extracted, after adding an internal standard (ethyl ester of *p*-hydroxybenzoic acid) with an optimum amount of chloroform. After evaporation of the organic layer, the extracts are redissolved in the eluent and chromatographed on a Lichrosorb reversed-phase C_{18} column, with u.v. detection at 280 nm. Quantification is based on peak height ratios. The combination of an improved sample treatment and proper selection of chromatographic conditions results in a limit of determination of 30 ng of VP 16-213 or 50 ng of VM 26 per ml of plasma. Preliminary clinical pharmacokinetic results show that the sensitivity and selectivity of the assay are adequate for drug monitoring in clinical research.

VP 16-213 and VM 26 are promising new anti-neoplastic agents, active against small-cell anaplastic bronchial carcinoma, larger-cell bronchial carcinoma, acute and chronic leukemias, lymphomas, testicular teratomas and central nervous system malignancies [1, 2]. The compounds are synthesized by modification of the natural product podophyllotoxin [3], which is obtained by extraction from the roots of *Podophyllum peltatum*, and

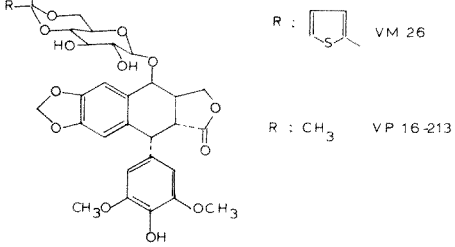

epimerized to yield epipodophyllotoxin. Epipodophyllotoxin is demethylated at the 4′-position and provided with a glucopyranoside group at the 4-position by an ether linkage. The presence of a thiophene group (VM 26) instead of a methyl group (VP 16-213), attached to the sugar, results in differences in membrane permeability, lipophilicity, protein-binding properties, and extent of metabolism [4]. Both compounds are potent and less toxic than the parent compound [3]. Especially for VP 16-213, which is presently being used extensively in clinical trials, a method of determination is necessary for the optimization of therapeutic schedules, clinical pharmacological studies, investigations on bio-availability, pharmacokinetics and metabolism.

Particularly for single-dose pharmacokinetic investigations, a sensitive assay is needed: at the end of 3—6 half-lives of the elimination phase, the expected concentration of the drugs is in the range of 20—100 ng ml^{-1} of plasma. Furthermore, lower doses (50 mg m^{-2}) are administered in currently used combination therapies with VP 16-213, rather than in single-agent therapy (300 mg m^{-2}). VM 26 is administered in even lower doses because of its higher toxicity [1]. Both drugs are excreted by the kidneys. Experiments with labeled compounds have shown that about 15% of the dose of VP 16-213 and about 35% of that of VM 26 are excreted as metabolites [4, 5]. Possible metabolites are hydroxy acids (ring-opened lactones) [6], and aglycones.

Recently, Strife et al. [6], Farina et al. [7] and Allen [8] published high-performance liquid chromatographic (h.p.l.c.) methods for the determination of VP 16-213 and VM 26 in plasma with a quantification limit of 0.5 μg ml^{-1} of plasma. Despite the reportedly higher sensitivity which can be obtained with methanolic solutions of pure VP 16-213, i.e., 50—100 ng ml^{-1} [6, 8], this sensitivity was unattainable in analyses of serum, plasma and urine.

The present paper describes improved clean-up procedures and chromatographic conditions for the determination of VP 16-213 and VM 26 in plasma and urine. The methods are sensitive enough to allow drug monitoring during 6 half-lives of the elimination phase.

EXPERIMENTAL

Materials and apparatus

VP 16-213 and VM 26 were kindly supplied by Bristol Myers, Nederland BV. The ethyl ester of *p*-hydroxybenzoic acid (Merck, p.a.) was used. Chloroform (p.a., Merck) was distilled from glass before use. The other solvents and chemicals were of analytical-grade quality. The chromatographic system consisted of a 6000A solvent delivery system, a U6K septumless injection system or an automatic sample injection device WISP model 710, and a u.v. absorbance detector model 440 with fixed wavelength filters for detection at 254 nm and 280 nm (all from Waters Associates, Milford, MA). A reversed phase RP-18 Lichrosorb column (Chrompack; 30 cm × 4.6 mm i.d.; 10-μm particle size) was used. Centrifuge glass tubes (7 ml) for extraction and evaporation were heated at 400°C for 1 h and washed afterwards with water and pure methanol, to prevent adsorption effects.

Procedures

Sample treatment. Blood samples were collected from patients during the 30—60 min period of intravenous infusion of the drugs (in a 2- or 3-day schedule) and during 1—3 days after the last dose. Immediately after the blood had been sampled in heparin-containing tubes, the samples were centrifuged and the plasma was transferred to a glass tube and stored at −18°C. For quantification of VP 16-213 and VM 26, 1 ml of plasma within the lower range, or 0.5 ml within the higher range and 50 μl of a methanolic solution of the internal standard, the ethyl ester of *p*-hydroxybenzoic acid, were mixed in a glass tube. For the concentration range below 1000 ng of VP 16-213 or VM 26 per ml, the concentration of the internal standard solution was 2.0 μg ml^{-1} of methanol; for the higher range, the concentration of this solution was 20.0 μg ml^{-1} of methanol. The sample was extracted with 1.0 ml of chloroform. After shaking for 1 min and centrifugation at 2500 *g* for 3 min, the aqueous layer was rejected. Subsequently, the organic layer was washed twice with 1 ml of 0.01 M phosphate buffer pH 7.3, each step involving 30 s of shaking and 1 min of centrifugation. The organic layer was transferred to a centrifuge tube and evaporated at 20°C under nitrogen. The residue was dissolved in 50—200 μl of the mobile phase and sonicated for 6 min; 25—50 μl of this solution was injected into the chromatograph. For concentration levels near the lower limit of determination, the residue was dissolved in 50 μl of the mobile phase.

For the determination of the drugs in urine, 1 ml of urine was buffered by adding 100 μl of 0.1 M phosphate buffer pH 7.3. The extraction and subsequent sample treatment of plasma and urine were similar.

Chromatography. For the determination of VP 16-213 and VM 26 in plasma, the mobile phase was methanol—water—acetic acid, 50:49:1 w/w (pH 3.33); for VP 16-213 and VM 26 in urine, the mobile phase was 45:54:1 w/w (pH 3.28). The apparent pH values were measured in methanol—water mixtures, with glass electrodes calibrated in aqueous buffers. For the determination of VM 26 in urine, the flow rate was 1.5 ml min^{-1}; for all other cases it was 1.0 ml min^{-1}. Chromatography was done at ambient temperature.

RESULTS AND DISCUSSION

In Fig. 1 the relation between the capacity factor, k', of VP 16-213, VM 26, the internal standard and caffeine, and the fraction of methanol of the mobile phase is represented. Strife et al. [6] showed that VM 26 can be used as the internal standard in the determination of VP 16-213, and vice versa. However, pure compounds are not yet commercially available. After a consideration of k', blank extracts, u.v. absorption and lipophilicity, the ethyl ester of *p*-hydroxybenzoic acid was selected as an appropriate internal standard. Calibration curves of methanolic solutions fitted a straight line passing through the origin in the studied range of 10 ng—30 μg (absolute amount) of VP 16-213 injected into the chromatographic system; the corre-

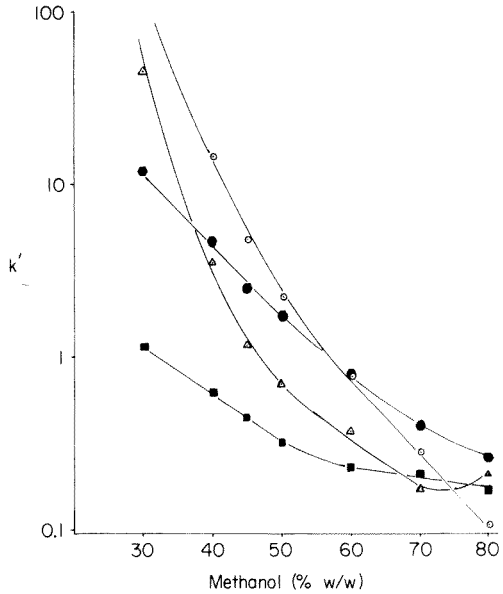

Fig. 1. Relation between the capacity factors of (△) VP 16-213, (○) VM 26, (●) the ethyl ester of *p*-hydroxybenzoic acid, and (■) caffeine and the fraction of methanol in the mobile phase on a Lichrosorb RP-18 column.

lation coefficient was 0.999. For the 15 ng—30 μg linear range of VM 26, the correlation coefficient was 0.999. Standard deviations of repetitive determinations on methanolic solutions of VP 16-213 or VM 26 (n = 6) were 2.3 or 3.0%, respectively, in the higher range, and 4.1 or 2.4% in the lower range of the calibration graphs.

For the selection of a proper liquid—liquid extraction system, the partition coefficients of VP 16-213, VM 26 and the internal standard were determined for several solvents. Chloroform, dichloromethane, ethyl acetate and 1-pentanol were suitable for extraction of VP 16-213 and VM 26, with partition coefficients larger than 25. Chloroform was selected. Glass tubes can be replaced by polypropylene tubes to achieve minimal loss of VP 16-213 and VM 26 by adsorption effects. The mobile phase is acidified with a little acetic acid, which results in some improvement of the reproducibility of the retention volumes of potentially interfering peaks, while decomposition of the drugs by opening of the lactone ring in alkaline media is prevented. The yield of the chloroform extraction of VP 16-213 and of VM 26 approaches 100%.

Evaporation of the chloroform layer and dissolution of the residue in methanol or mobile phase, as in the earlier methods [6—8], gives rise to a number of interfering peaks in the chromatograms, as can be seen in these papers. This results in a rather high detection limit of 0.5 μg ml^{-1} of plasma, compared to the detection limit of 10 ng (absolute amount) for the pure compounds (at 254 nm as well as at 280 nm).

In the work described here, attempts were made to characterize the nature of the compounds causing these interfering peaks and to develop an improved procedure for the analysis. Because of the high partition coefficients, smaller phase-volume ratios can be used (e.g., 1 : 1); this provides reduced evaporation time and fewer interfering impurities from the biological fluids. One of the most pronounced interfering peaks (k' = 0.32 for a mobile phase containing 50% methanol), close to the peak of VP 16-213, proved to be caffeine. The peak was absent in chromatograms from caffeine-free plasma and the peak height increased on addition of pure caffeine to the plasma samples. The u.v.-absorption ratio at 280 nm and 254 nm was similar to the ratio for caffeine. The epipodophyllotoxins and caffeine exhibit little difference in lipophilicity (Table 1) and cannot be separated completely by the liquid—liquid extraction procedure during the sample treatment.

Given the large partition coefficients of VP 16-213, VM 26 and the internal standard in the chloroform—water system, the organic layer could be washed twice with 0.01 M phosphate buffer pH 7.3 to remove some of the interfering compounds. The height of several interfering peaks then decreased markedly. The recoveries of VP 16-213 and VM 26 did not change. The improvement obtained by these washings was more pronounced with detection at 280 nm compared to 254 nm; consequently the detection wavelength of 280 nm was chosen for the procedure. Caffeine, however, could not be removed in this way.

From chromatography on C_{18} μBondapak reversed-phase columns (Waters Associates), it became apparent that the capacity factors of caffeine and VP 16-213 were nearly the same; variation of the composition of the mobile phase did not improve the separation. Better separation was obtained by using Lichrosorb columns, which have a lower surface coverage of chemically-bonded C-18 groups.

From Fig. 1, the optimal composition of the mobile phase can be chosen for maximal separation of the drugs, the internal standard and caffeine. With a proper choice of the mobile phase composition, the limits of determination in biological fluids approach the detection limits for pure samples of these compounds. Statistical evaluation of the results obtained for plasma and urine is given in Table 2. When the pH of the biological samples, the washing solutions and the mobile phase is maintained between 4 and 9.3 [6, 7], solutions of VP 16-213 and VM 26 are stable for at least several months. Automatic injection of a series of samples is easily done.

TABLE 1

Partition coefficients of VP 16-213, VM 26, ethyl ester of *p*-hydroxybenzoic acid and caffeine in a water—chloroform system (1:1 v/v) at 20°C

VP 16-213	55.0	Ethyl-*p*-hydroxybenzoic acid	27.2
VM 26	>100	Caffeine	11.0

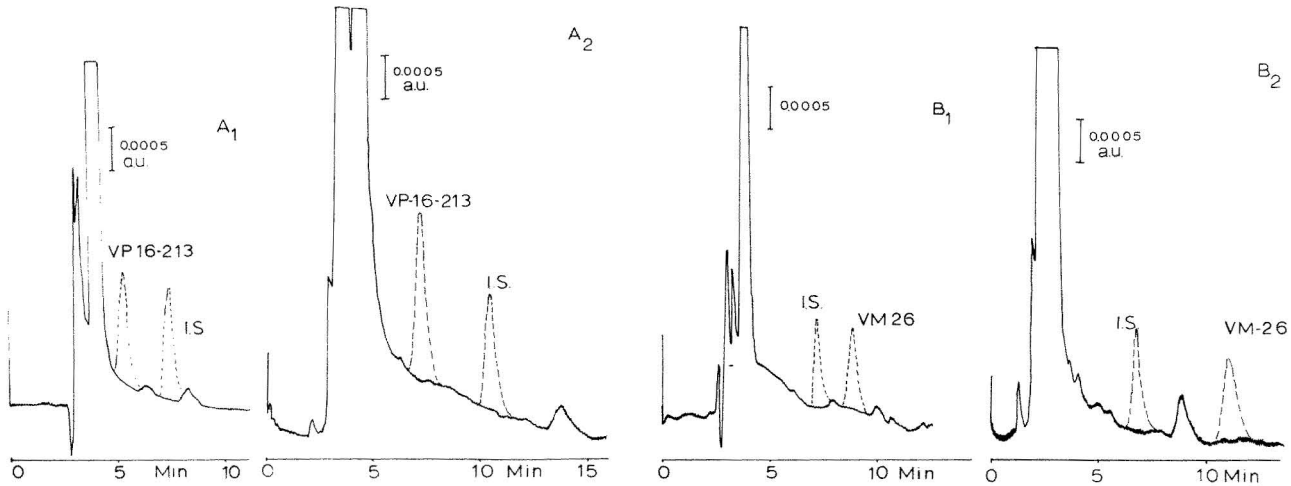

Fig. 2. (A1) Chromatograms of extracts of blank plasma and patient plasma containing 285 ng of VP 16-213 per ml; (A2) chromatograms of extracts of blank urine and urine spiked with 505 ng of VP 16-213 per ml; (B1) chromatograms of extracts of blank plasma and patient plasma containing 690 ng of VM 26 per ml; (B2) chromatograms of extracts of blank urine and urine spiked with 887 ng of VM 26 per ml.

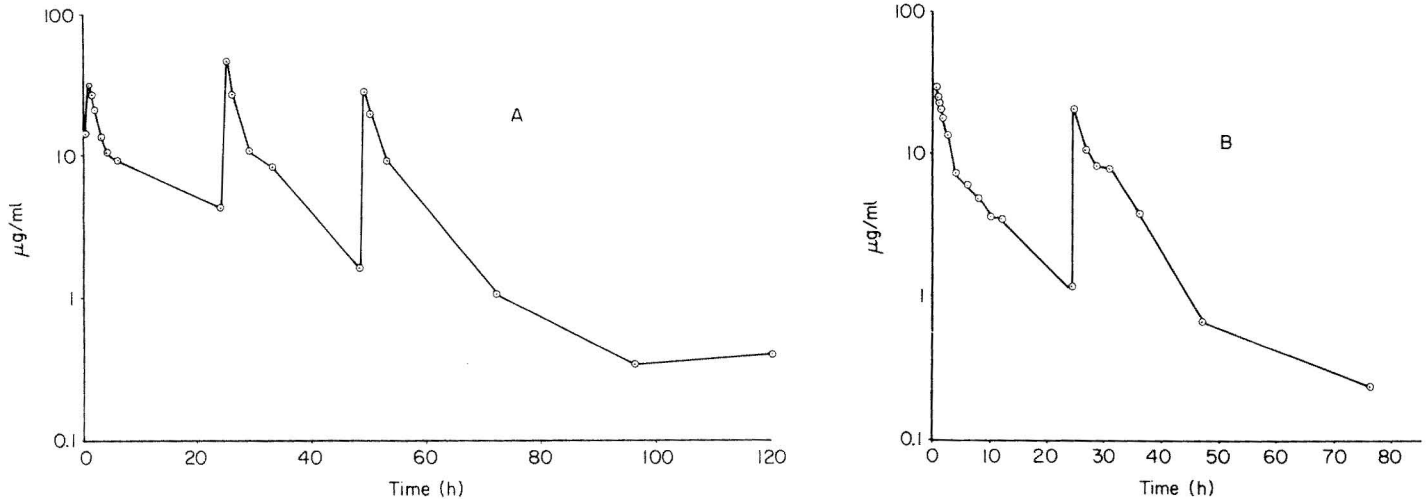

Fig. 3. Concentration of VP 16-213 or VM 26 as a function of time, obtained by analysis of plasma samples of patients: (A) patient received 280 mg of VP 16-213 (190 mg m^{-2}) during a 1-h infusion on a three-day schedule (0, 24 and 48 h); (B) patient received 140 mg of VM 26 (90 mg m^{-2}) during a 30-min infusion on a two-day schedule (0 and 24 h).

TABLE 2

Statistical evaluation

Compound	Concentration range ($\mu g\ ml^{-1}$)	Matrix	Calibration graph			R.s.d.[c] (%)
			Slope	Intercept[a]	r^b	
VP 16-213	1—30	Plasma	0.167	—0.042	0.9996	4.5
	0.03—1.00	Plasma	3.776	0.043	0.9966	2.9
	0.05—1.00	Urine	3.531	—0.009	0.9994	2.9
VM 26	1—30	Plasma	0.074	—	0.9996	5.3
	0.05—1.00	Plasma	1.448	0.006	0.9994	2.3
	0.07—1.00	Urine	0.935	0.007	0.9990	3.1

[a]The intercepts for all calibration curves are not significantly different from zero at $p = 0.05$. [b]Correlation coefficient. [c]For $n = 6$.

It can be concluded that the combination of sample treatment and proper selection of chromatographic conditions results in the limit of determination needed for a sensitive assay in pharmacokinetic investigations. Typical chromatograms obtained in blank, patient and spiked samples are shown in Fig. 2.

Preliminary clinical pharmacokinetic results

The method described was tested on blood samples from patients receiving VP 16-213 or VM 26 during 30—60-min infusions, in a 2—3-day schedule. In Fig. 3, typical log concentration/time curves are presented. The log concentration/time curve of VP 16-213 shown in Fig. 3 (190 mg m^{-2}) fits a two-compartment model with a half-life of the elimination phase of 16.5 h. The log concentration/time curve of VM 26 (90 mg m^{-2}) could fit a three-compartment model with an elimination half-life of 7.4 h. An extensive study on the clinical pharmacokinetics of both drugs is presently being undertaken, in which blood samples are collected over a longer period, to establish the different pharmacokinetic parameters, such as half-lives, distribution volumes and amount of excretion, to obtain more information for the explanation of the remarkable, different elimination rates during the several days of administration, shown in Fig. 3.

REFERENCES

1 M. Rozencweig, D. D. Von Hoff, J. E. Henney and F. M. Muggia, Cancer, 40 (1977) 334.
2 A. M. Arnold, Cancer Chemother. Pharmacol., 3 (1979) 71.
3 C. Keller-Juslén, M. Kuhn, A. von Wartburg and H. Stähelin, J. Med. Chem., 14 (1971) 936.
4 P. J. Creaven and L. M. Allen, Clin. Pharmacol. Ther., 18 (1975) 227.
5 P. J. Creaven and L. M. Allen, Clin. Pharmacol. Ther., 18 (1975) 221.
6 R. J. Strife, I. Jardine and M. Colvin, J. Chromatogr., 182 (1980) 211.
7 P. Farina, G. Marzillo and M. D'Incalci, J. Chromatogr., 222 (1981) 141.
8 L. M. Allen, J. Pharm. Sci., 69 (1980) 1440.

Analytica Chimica Acta, 130 (1981) 31—43
Elsevier Scientific Publishing Company, Amsterdam — Printed in The Netherlands

AN EXAMINATION OF CHEMICALLY-MODIFIED SILICA SURFACES USING FLUORESCENCE SPECTROSCOPY

C. H. LOCHMÜLLER*, DAVID B. MARSHALL and D. R. WILDER
P. M. Gross Chemical Laboratory, Duke University, Durham, NC 27706 (U.S.A.)
(Received 5th March 1981)

SUMMARY

Aminated microparticulate silica gel was derivatized with the fluorescent tag, dansyl chloride, to produce a chemically-modified silica surface that could be examined by fluorescence spectroscopy; also a dansylated silica was further derivatized with various alkyl functionalities. The labelled silicas were introduced into solvents and solvent mixtures of different polarities and the emission spectra obtained were compared with the spectra of a model compound, *n*-propyldansylamide, in the same solvents. It was found that residual amine groups, as well as unreacted silanol groups, produced a polar surface environment that was reflected in the emission maximum of the spectrum of the modified silica. The degree of residual surface polarity also appears to be a function of the aminopropylsilane reagents used.

Chemically-bonded stationary phases for liquid chromatography have been used for over a decade but the mechanism of interaction of these unique sorbents with solute is still not completely understood. It is for this reason that the study of chemically-modified silica surfaces, particularly those prepared on substrates typical of packing materials for liquid chromatography, remains an active area of study. Various methods have been used to attempt a characterization of the immobilized organic layer which constitutes the sorptive medium of these materials. Chromatographic studies correlating changes in solute retention with properties of the bonded phase have been numerous [1—16] and have contributed valuable data to the construction of an improved, physical representation of the chemically-modified surface. In addition, spectroscopic techniques have been employed to probe modified silica surfaces in an attempt to provide information which complements these chromatographic data and thus the formulation of accurate sorption models. In studies using e.s.r. [17], n.m.r. [18, 19], transmission u.v.-visible [20], i.r. [21—23], and photoacoustic [24—30] spectroscopy, such aspects of chemically-modified silica surfaces as the mobility of bound organic functions, accessibility to solvent, and interaction with adjacent surface species, have been investigated.

This report extends the use of spectroscopic studies to include molecular fluorescence spectroscopy. The method is applicable to the study of bonded phases because it is adaptable to opaque or turbid samples requiring only

0003—2670/81/0000—0000/$02.50

minor changes in photon collection geometry. The bonded ligand environment is particularly amenable to fluorescence examination because optical emission is generally more sensitive to environmental factors than is optical absorption. The wavelength and intensity of u.v.-visible emission is not only influenced by solvent polarity, but is also dependent on such properties as solvent viscosity, the presence of quenchers, solvent pH, hydrogen-bonding capability, fluorophore concentration and temperature effects [31, 32].

Dansyl chloride was employed as the fluorescent tag in the fluorimetric characterization of modified silicas undertaken in this study. When reacted with amine groups to form sulfonamide derivatives, it produces a high quantum-yield fluorophore that provides emission spectra in the visible region, well-removed from the excitation spectra of the compound. The dansyl group is widely used in biochemical studies [33—35], and has been used to tag SnO_2 electrodes [36] and polymer films [37] to investigate the surface environment on these solid matrices.

To investigate fully the effect of the nature and extent of surface coverage of bonded ligands on the character of the derivatized silica surface, a variety of aminated silicas of varying surface coverage were prepared. These materials included silicas made using mono-, di-, and tri-ethoxysilane reagents. Such derivatizing reagents provide an assessment of silicas that contain only monomeric surface groups (monoethoxysilane) and silicas on which the potential for surface polymerization exists (di- and tri-ethoxysilane). The dansylated silicas were suspended in solvents spanning a large range in polarity to investigate the influence of different solvents on groups immobilized on silica. The fluorescence spectra of the resulting solvent—silica slurries were compared to true solution spectra of the analogous dansyl amide derivative in the same solvents. The differences manifested by the emission spectra of the bonded and free solution fluorophores allowed an assessment of the accessibility to solvent of the immobilized group. Finally, a series of alkylated (methyl, octyl, and octadecyl) dansyl silicas was prepared with very low dansyl coverages. The fluorescence of these silicas in solvents and aqueous solvent mixtures was studied to evaluate the ability of the fluorescent tag to indicate solvent interactions with nonpolar, modified surfaces.

EXPERIMENTAL

Chemicals and reagents

The silanes used were obtained from Petrarch Systems (Levittown, PA) and were used without further purification (aminopropyltriethoxysilane, aminopropylmethyldiethoxysilane, aminopropyldimethylmonoethoxysilane, trimethylchlorosilane, octyldimethylchlorosilane, octadecyldimethylchlorosilane, and octylmethyldichlorosilane). The silica used was LiChrosorb SI-100 (EM Laboratories, Elmsford, NY) with a mean particle size of 10 ± 1 μm and an average pore diameter of 10 nm. The nominal surface area of the silica was 240 $m^2\ g^{-1}$. Reagent-grade toluene was fractionally distilled from

calcium hydride and stored over sodium metal. The aminopropyl modified silicas were washed with Spectranalyzed-grade benzene, acetone, methanol, and with distilled deionized water. Solvents used for fluorescence measurement were all of spectral-grade quality. All other chemicals were reagent grade except dansyl chloride (5-dimethylaminonaphthalenesulfonyl chloride) (Aldrich Chemical Co., Milwaukee, WI) which was recrystallized prior to use.

Preparation and characterization of chemically modified silicas

All of the aminated substrates were prepared in identical fashion by the following surface modification scheme. Oven-dried silica gel (2 g) was introduced into a three-neck reaction vessel containing a magnetic stir bar and the flask was purged with dry nitrogen gas. Dry toluene (50 ml) was then added. Approximately a two-fold excess (based on the assumption that there are four silanol groups/10 nm^2 and accounting for the surface area of the silica matrix) was added to the reaction mixture with stirring. Both exhaustively (excess of silane, refluxing toluene, and 24-h reaction times), and partially aminated silicas (stoichiometric deficiency of silane, room temperature, and 20-min reaction times) were prepared. The resulting materials were washed and Soxhlet-extracted for 24 h with acetonitrile. The finished materials were dried for 8 h in vacuum and the amine content determined by non-aqueous acid—base titrimetry.

Dansylated silicas were prepared as follows. Approximately 1 g of aminated silica gel was introduced into a three-neck flask containing 30 ml of dry acetonitrile and 2 drops of dry pyridine under dry nitrogen gas. To this suspension was added 0.2 g of dansyl chloride in 10 ml of dry acetonitrile and the mixture was heated at 50°C for 24 h.

After termination of the reaction, the dansylated silica was Soxhlet-extracted with dry acetonitrile for 24 h and dried in vacuum. The surface coverage data for aminated substrates and for the dansylated materials are shown in Table 1. An aliquot of each of the dansyl silicas was left to stand for 12 h in 5 ml of 0.1 M KOH in methanol. The fluorescence spectra of the supernatant hydrolysate solutions and those of the model compound *n*-propyldansyl sulfonamide were observed to be identical [λ_{max} (emission) = 502 nm].

A group of alkyl dansyl silicas was prepared with very sparse dansyl coverages (by using 5 drops of aminating reagent for 2.5 g of silica, reacted for 20 min) via the above procedure. Aliquots of the sparingly dansylated silica were then silylated with trimethylchlorosilane, octyldimethylchlorosilane, and octadecyldimethylchlorosilane by the procedure of Evans et al. [38]. The octylated and octadecylated dansyl silicas were also end-capped with trimethylchlorosilane. The maximum dansyl coverage for the alkylated dansyl silicas was estimated to be 0.02—0.03 mmol of dansyl per g of silica. The ratios of alkyl functionalities to dansyl were roughly 18:1, 12:1, and 14:1 for trimethyl, dimethyloctyl, and dimethyloctadecyl, respectively.

TABLE 1

Coverage data for aminated and dansylated silicas

Substrate	Amine content[a] (mmol g^{-1})	Dansyl content (mmol g^{-1})	Percentage conversion (%)
Aminopropyl (partial)	0.258	0.18	70
Aminopropyl (full)	0.462	0.25	54
Aminopropylmethyl (partial)	0.095	0.07[b]	73
Aminopropylmethyl (full)	0.500	0.25	50
Aminopropyldimethyl (partial)	0.490	0.25	51
Aminopropyldimethyl (full)	0.618	0.31	50
Aminopropyldimethyl-octyl[c]	0.280	0.15	54

[a]Substituents on silane reagents. Reactive groups were triethoxy, diethoxy, and monoethoxy substituents, respectively. [b]Insufficient nitrogen—sulfur content for meaningful elemental determination. Data obtained by photoacoustic quantitative measurement. [c]Substrate was pre-reacted with octylmethyldichlorosilane before amination. The carbon content of the octyl-modified silica prior to amination was 8.0%.

Fluorescence measurements

The fluorescence of surface-bound dansyl groups was studied using a Perkin Elmer MPF-3 spectrophotometer. A quartz cell was used in the acquisition of solution fluorescence spectra. Data from dry bonded phases were obtained by introducing the sample into quartz capillary tubes and mounting these tubes in the center of the sample turret to obtain optimal emission intensity. The location of Rayleigh scattering peaks, Raman peaks, and higher order bands was ascertained and these artifacts were observed to be well removed from the emission envelope of the dansyl fluorophore. A study of fluorescence intensity and stability as a function of time was undertaken with the incident radiation set first at the excitation maximum, then at 200 nm. It was found that the fluorescent probe used was stable, both in the free and surface-bound state, during the 1-h test intervals. All spectra were recorded at ambient temperature.

RESULTS AND DISCUSSION

Surface environmental effects

Fluorescence spectra were obtained for the dansylated silica prepared on the three aminated supports, both in the dry form and with entrained solvents varying in polarity from hexane to water. Solutions of the *n*-propyl dansylamide model compound (at 1×10^{-6} M) were prepared in the same solvents and the fluorescence spectra of these solutions were similarly obtained. The emission maxima for the systems are compiled in Table 2 and representative spectral traces are shown in Fig. 1.

Surface environmental effects provide a plausible explanation for the observed trends in the position of the emission maxima observed for the

TABLE 2

Emission maxima (nm) for dansylated silicas and solutions of the *N*-propyl dansylamide model compound

Solvent	Model compound[a]	Aminated substrates[b]		
		Aminopropyl-dimethyl	Aminopropyl-methyl	Aminopropyl
Hexane	441	475	485	486
Cyclohexane	443	474	486	484
Dioxane	474	482	484	482
Ethyl acetate	482	488	489	487
Acetonitrile	499	500	502	505
Methanol	502	503	505	507
Water (pH 2)	527	507	518	515
Water	538	512	520	522
n-Propylamine	479	—	—	—
Dry	—	478	484	495

[a]*N*-propyl dansylamide. [b]Substituents on silanes. Reactive groups on the silanes were monoethoxy, diethoxy, and triethoxy functions, respectively.

different aminated silicas. Except for the *n*-propylaminodimethylethoxysilane, there exists the definite possibility that unreacted alkoxy groups can hydrolyze during the workup procedure to produce silanol functions. In addition, linear polymers can be formed during reactions using a dialkoxysilane and, in the case of trialkoxy materials, cross-linking is also possible. One would expect then that "surface polarity" might increase with decreasing alkylation at the silicon and this is indeed observed with λ_{max} = 478, 484, and 495 for n = 2, 1, and 0, respectively, in $(CH_3)_nSi$—(Matrix). The aminopropyl silica surface has both *n*-propylamine groups and hydroxyl groups which could interact with an immobilized dansyl group. The λ_{max} for the model compound is 502 nm in methanol and 479 nm in *n*-propylamine. If these values are taken to be roughly representative of the effect that a hydroxyl or an amine environment has, then the intermediate λ_{max} of 495 nm for the dansyl fluorophore on the aminopropyl substrate could represent some intermediate regime. Treatment of this silica with iodomethane resulted in a material with a fluorescence maximum blue-shifted as expected (λ_{max} = 467 nm).

A significant aspect of Table 2 is the relative response of immobilized dansyl groups to solvent. It can be seen that the range of the solvent shifts of the immobilized dansyl groups on all of the aminated substrates is compressed in comparison with the very extensive range shown by the model compound in solution, i.e., 441 nm in hexane to 538 nm in water. The immobilized fluorophore spectra parallel the model compound spectral shifts in general with an indication of increased affinity for the more polar solvents. A plot of the λ_{max} values for two of the silicas in various solvents vs. λ_{max} for the model compound in these same solvents is shown in Fig. 2.

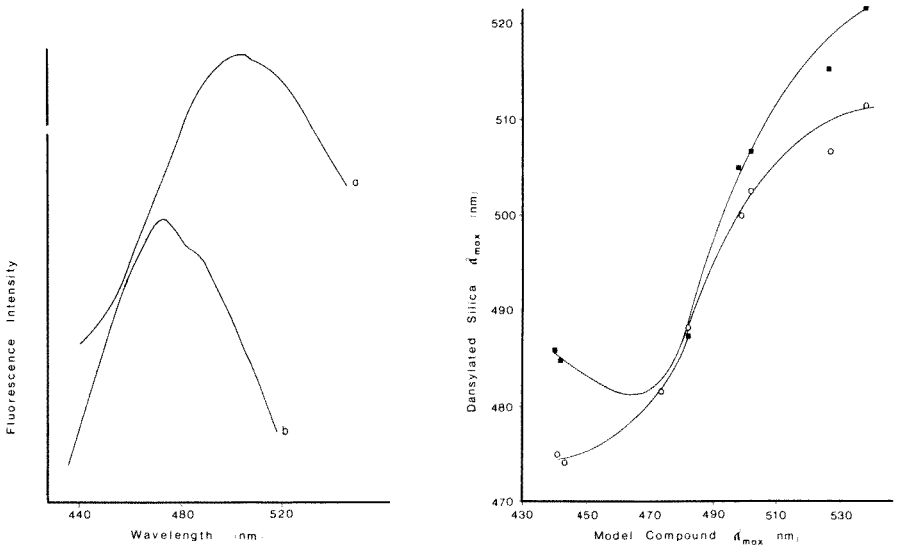

Fig. 1. Fluorescence spectra of the dansyl systems: (a) dansyl amide model compound; (b) dansylated silica, aminopropyldimethyl substrate.

Fig. 2. Emission maxima for dansylated silica vs. emission maxima for model compound (shift data in Table 2): (■) aminopropyl substrate; (○) aminopropyldimethyl substrate.

A comparison of solvent shift data of the model compound was further used to characterize the polarity of the silica surface environments on the three aminated substrates. This was accomplished by plotting spectral shift data as a function of the dielectric constant of the solvents used in the experiment (see Fig. 3). The dielectric constant as used here serves only as a convenient parameter for correlation of general solvent properties and its use should not suggest an attempt at precise physical modelling. Accepting the crude nature of this, and recognizing the appropriate caveats, one sees a reasonable correlation for all solvents except *p*-dioxane and water. The former is much more "polar" than its bulk dielectric constant would suggest. The apparent environmental polarity in terms of "dielectric constant", for the aminated substrates taken from Fig. 1 increases from $D = 4$, to $D = 6$ and finally $D = 14$ as the number of silylmethyl groups varies through 2, 1, 0.

Further information about the surface environment was sought through the preparation of partially-reacted silicas which represent varying degrees of coverage (see Table 1). The fluorescence emission maxima of these materials were obtained and are presented in Table 3. In every case, a red shift is observed for these materials relative to the saturation coverage silica. This may arise from the inherently high polarity of the unreacted silica functionality itself. This effect persists even in the presence of entrained solvent however, and therefore, a degree of caution is required. It is possible that the micro environment of a "partially-covered" surface consists of high density patches and open unreacted regions rather than sparsely scattered

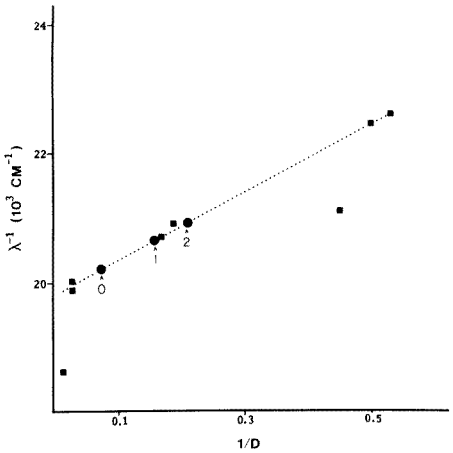

Fig. 3. Emission maxima (cm^{-1}) as a function of bulk dielectric constant: (•) modified silicas (0, 1, 2 = no. of methyl groups on silicon); (▪) model compound.

individual reaction sites. If so, the observed red shift may arise from excimer-based phenomena (see below). Interestingly, a silica prepared by partial reaction first with octylmethyldichlorosilane then with aminopropylmethyl silyl reagent and finally with dansyl chloride, exhibits a relative blue shift which persists even in the presence of entrained solvents.

Additional experiments were performed to establish the relative affinity of the dansyl group for different solvents and the various silica surfaces. Aliquots of oven-dried native silica and an aminopropyldimethyl aminated support were introduced into solutions of the model compound in *n*-hexane. Fluorescence spectra were recorded for these samples and it was found that the λ_{max} for the model compound—native silica suspension had shifted to 510 nm, while that of model compound—aminated silica shifted to 468 nm. Both of these values are in excellent agreement with the expected λ_{max}

TABLE 3

Emission maxima (nm) for partially- and fully-aminated silica supports in the dry state and in hexane or water

Substrate	Dry	*n*-Hexane	Water
Aminopropyl[a]	495	486	522
Aminopropyl[b]	498	490	526
Aminopropylmethyl[a]	484	485	520
Aminopropylmethyl[b]	503	490	526
Aminopropyldimethyl[a]	478	475	512
Aminopropyldimethyl[b]	484	480	519
Octylaminopropylmethyl	470	474	—[c]

[a]Fully-covered. [b]Partially-covered. [c]Material was too hydrophobic to provide a slurry for examination.

for the dansyl group in contact with hydroxylic and aminated environments, respectively. To probe further the relative affinity of the *N*-propyldansylamide model compound for solvent vs. silica, portions of the solutions of the model compound in cyclohexane, water, and dioxane were introduced into vials containing native silica. The shifts in emission maxima for the suspensions were from 443 to 502 nm in cyclohexane, from 538 to 526 nm in water, and no change in the 474 nm λ_{max} in dioxane.

These results demonstrate clearly, then, that changes seen in the dansyl group spectra on the aminated substrates were brought about by surface environmental effects, and that the three supports differ considerably in inherent polarity, a finding that is significant in the chromatographic application of these substrates. It is important that a certain degree of caution be exercised when emission maxima in free solution are compared with maxima on the surface to evaluate the environmental polarity at the surface. It is possible that the dansyl fluorophore forms ground state—excited state complexes (excimers) in either or both free solution and surface-bound states. The wavelength and intensity of excimer fluorescence is known to be much more sensitive to physical adsorption on silica gel than that of the normal monomer fluorescence [39]. Shifts in fluorescence maxima upon going from the free solution to surface-bound forms may reflect changes in the ratio of excimer to monomer excited states as well as actual changes in the polarity of the environment. However, changes in the fluorescence of the surface-bound fluorophore are expected to be reliable indicators of changes in polarity at the surface, as long as comparisons are restricted to data obtained from the same lot of dansylated silica (or silica with identical pore characteristics and dansyl surface coverage).

Selective sorption effects

Fluorescence measurements are of potential use in studies of selective sorption of components from binary and ternary solvent mixtures. Such an experiment was performed in the hope of detecting just such a preferential sorption of one of the constituents of a solvent mixture onto the dansylated silicas. If the equilibrium situation is one in which a multilayer of one solvent component forms on the surface, this could reasonably be expected to result in a fluorescence shift more characteristic of such an environment than that of the homogeneous solution phase; i.e., if there is indeed a preferential sorption of a layer of methanol from the poor *n*-hexane solvent, there should result a corresponding shift in the λ_{max} of the immobilized dansyl group to reflect this alteration in the surface environment. There should be little change in the ethyl acetate—methanol mixtures, however, since both have similar solvating properties for the dansyl group, and the effect of the small fraction of methanol added to the bulk ethyl acetate solvent should produce no measurable change in the λ_{max} for this system unless it is preferentially sorbed. Solvent mixtures of 1:100, 1:200, and 1:1000 parts (by volume) of methanol in both *n*-hexane and ethylacetate

were employed. Aliquots (0.01 g) of dansylated aminopropyl and aminopropyldimethyl silicas were introduced into 5 ml of each of the solvent mixtures and 10^{-5} M solutions of the *N*-propyl dansylamide model compounds were also prepared. The observed fluorescence maxima for each are given in Table 4.

These data show that the methanol—ethyl acetate mixtures cause almost no change in the λ_{max} for the dansylated silicas or solutions of the model compound. This is the anticipated result if one considers the relative sorption strength of these two solvent components. The case of the *n*-hexane—methanol systems is quite different. The λ_{max} values for the dansylated silicas in contact with solvents of higher methanol content manifest red-shifts indicative of a more polar environment. Somewhat unexpectedly, however, this same trend is seen in the behavior of the model compound solution. The reasonable explanation for this is that a preferential aggregation of methanol cosolvent occurs around each free dansyl molecule. This occurs analogously in the bonded case as well.

Dynamic equilibrium effects

A series of alkyl dansyl silicas with low dansyl coverages was synthesized to study the effects of varying the alkyl chain length. The fluorescence maxima of untreated (DS), methylated (MDS), octylated (OCS) and octadecylated (ODDS) dansyl silicas in various pure solvents are listed in Table 5. All alkylations were done with monochlorosilanes to eliminate the possibility of polymerization, thus, they are representative of "brush-type" phases. After the values in Table 5 were recorded (within 2 h of sample preparation), all samples were warmed to 40°C for 10 min, and then cooled back to ambient temperature. All gave the same emission values except MDS in water, which was red-shifted by 5 nm to 474 nm, and DS in acetonitrile, which was red-shifted by 10 nm to 516 nm. The three alkylated silicas also

TABLE 4

Emission maxima for dansylated silicas and the *N*-propyl dansylamide model compound in mixed solvent systems

Solvents	Volume ratio	Emission maxima (nm)			
		Model compound[a]	Dansylated silicas[b]		
			AP	APD	O—APM
Methanol—*n*-hexane	1:100	476	504	497	480
Methanol—*n*-hexane	1:200	462	504	482	476
Methanol—*n*-hexane	1:1000	444	483	476	470
Methanol—ethyl acetate	1:100	484	494	488	482
Methanol—ethyl acetate	1:200	484	492	487	482
Methanol—ethyl acetate	1:1000	484	493	485	484

[a] *N*-propyl dansylamide. [b] AP, aminopropyl substrate: APD, aminopropyldimethyl substrate; O—APM, octylaminopropylmethyl substrate.

TABLE 5

Fluorescence maxima of alkylated dansyl silicas in pure solvents at room temperature

Silica	Wavelength (nm)				
	Dry	Tetrahydrofuran	Acetonitrile	Methanol	H_2O
DS	485	487	506	510	532
MDS	468	480	499	500	469
OCS	468	479	498	498	468
ODDS	470	478	498	496	468

showed slight changes in peak shape upon warming in acetonitrile with shifts too small to be measured reliably. Besides those trends expected for changes in environment polarity, some other interesting trends can be seen in these fluorescence data. Alkylation of the surface results in a blue shift in dry form from dry DS, the magnitude of which is essentially independent of alkyl chain length. The emission maxima of the three alkylated silicas show small decreases with increasing alkyl chain length in contact with the solvents tetrahydrofuran, acetonitrile, and methanol. There is a 4-nm difference in the DS maxima in acetonitrile versus methanol, but this difference disappears for the alkyl silicas. Additional effects are observed when the fluorescence of these silicas is investigated in mixed aqueous organic solvent systems. Table 6 summarizes the data obtained in 50% (by volume) organic solvent—water systems upon both initial sample preparation and after warming to 40°C followed by cooling to ambient temperature. The maxima for all the mixed solvents, regardless of the nature of the organic solvent, are red-shifted with respect to the values obtained in the pure organic solvents with the exception of the octadecylated silica (ODDS). (The 2-nm shift observed for ODDS in aqueous tetrahydrofuran is within experimental error.) This material undergoes a small blue shift in aqueous methanol relative to pure methanol. Differences between the various alkyl silicas for any one solvent—water system are much more pronounced than the analogous differences in the pure solvents. The maxima of all the silicas except ODDS show red shifts upon warming in the aqueous acetonitrile system, whereas no such "kinetic wetting effects" are observed in the aqueous tetrahydrofuran or methanol systems for the methylated and octylated dansyl silicas. A red shift upon warming is observed for the non-alkylated material in all mixed solvents.

The "kinetic wetting effects" observed in the alkylated dansyl silicas in aqueous acetonitrile systems, together with the absence of such effects in the alkyl silicas in pure acetonitrile, indicated that acetonitrile is a poor transporting agent for water. This is not surprising since acetonitrile is a poor hydrogen-bond acceptor compared to either tetrahydrofuran or methanol. Essentially, the lifetime of any acetonitrile—water complex is long compared to the time it takes for acetonitrile to move through the chains. The rate at which it does so, however, is similar to the rates for tetrahydrofuran and

TABLE 6

Fluorescence of alkyl dansyl silicas in 50% organic solvent—water systems: peak maxima after initial mixing and after warming

Silica	Wavelength (nm)					
	Tetrahydrofuran—H_2O		Acetonitrile—H_2O		Methanol—H_2O	
	Initial	After	Initial	After	Initial	After
DS	506	510	520	524	506	522
MDS	495	495	505	510	512	513
OCS	489	489	504	509	507	507
ODDS	484	482	498	498	492	492

methanol. In general, minor "kinetic wetting effects" in pure solvents are apparently magnified in solvent—water mixtures. The presence of "kinetic wetting effects" for the unalkylated dansyl silica in pure solvents may reflect competition between solvent and residual silanols and/or residual adsorbed water for the dansyl groups, and/or solvent association with surface silanols which kinetically inhibits solvent migration.

McCormick and Karger [40] have previously noted extraction of organic modifier into the stationary phase and this is confirmed by the fluorescence data here. They also noted extraction of small amounts (reaching a plateau at 3% by volume) of water. This is also demonstrated by the data in Tables 5 and 6 for the methyl and octyl phases. Given enough heat or enough time, presumably the octadecyl phase might show similar slight red-shifts in solvent—water systems relative to the pure solvents. McCormick and Karger attribute this water extraction to association with residual surface silanols. The mixed solvent data reported here indicate that while there is a certain amount of water present in the stationary phase, that amount varies with the nature of the organic cosolvent; i.e., at least some water may be present simply because of its association with the cosolvent. The marked decrease in emission wavelength of ODDS in aqueous methanol versus pure methanol may reflect a self-association of the octadecyl chains induced by the presence of water [16].

Scott and Simpson [41] have recently advocated the use of polymeric versus brush-type phases because of "self-association of the chains causing solvent equilibration problems". The present study provides complementary evidence to their observation, but in addition, an indication of "solvent equilibration problems" in methyl dansylated silica is also observed. Self-association of the chains contributes to the equilibration problem, but apparently any nonpolar surface additive will inhibit solvent migration.

The fluorescence sample handling methods used in this work present some problems in the reliable extrapolation of the observed kinetic effects to actual equilibration problems in liquid chromatography. A more satisfactory arrangement would be one in which an actual column (e.g., a quartz tube)

is used so that changes in fluorescence maxima with sudden changes in the nature of the solvent flowing over the tagged silica could be followed. Such an arrangement is presently under construction in this laboratory.

Conclusion

Despite the obvious limitation of the necessity of bonding a fluorescent molecule to the silica surface, fluorescence spectroscopy may nevertheless provide a useful and sensitive probe of chemically-modified silicas. Judicious choice of fluorescent tags which emulate molecules that have useful properties for bonded stationary phases can provide valuable information about the behavior of surface-bound ligands. In addition, the use of fluorescent tags at low surface concentrations on nonpolar-phase silicas shows promise for the investigation of solvent-nonpolar bonded phase interactions. The reliability of extrapolating the information obtained in such investigations to actual nonpolar bonded phases as typically used in liquid chromatography depends on the tag molecule behaving as a passive indicator of solvent composition within the bonded phase. In the case of dansylsulfonamide this appears to be the case in the sense that the emission maximum observed seems to be influenced, in the majority, by changes in the average local dielectric field and not by directed interactions localized on the dansyl moiety.

This work was supported by a grant from the National Science Foundation, CHE-781807.

REFERENCES

1 D. C. Lock, J. Chromatogr. Sci., 12 (1974) 433.
2 J. H. Knox and G. Vasvari, J. Chromatogr., 83 (1973) 181.
3 E. J. Kikta, Jr. and E. Grushka, Anal. Chem., 48 (1976) 1098.
4 J. H. Knox and A. Pryde, J. Chromatogr., 112 (1975) 171.
5 R. E. Majors and M. J. Hopper, J. Chromatogr. Sci., 12 (1974) 767.
6 H. Hemetsberger, W. Maasfeld and H. Ricken, Chromatographia, 9 (1976) 303.
7 H. Hemetsberger, M. Kellermann and H. Ricken, Chromatographia, 10 (1977) 726.
8 H. Hemetsberger, P. Behrensmeyer, J. Henning and H. Ricken, Chromatographia, 12 (1979) 71.
9 K. K. Unger, N. Becker and P. Roumeliotis, J. Chromatogr., 125 (1976) 115.
10 K. Karch, I. Sebestian and I. Halasz, J. Chromatogr., 122 (1976) 3.
11 H. Colin and G. Guiochon, J. Chromatogr., 158 (1978) 183.
12 H. Colin and G. Guiochon, J. Chromatogr. Sci., 18 (1980) 54.
13 M. C. Hennion, C. Picard and M. Caude, J. Chromatogr., 166 (1978) 21.
14 W. Melander, D. E. Campbell and C. Horvath, J. Chromatogr., 158 (1978) 215.
15 J. Chmielowiec and H. Sawatzky, J. Chromatogr. Sci., 17 (1979) 245.
16 C. H. Lochmüller and D. R. Wilder, J. Chromatogr. Sci., 17 (1979) 574.
17 N. Sistoraris, W. O. Riede and H. Sillescu, Ber. Bunsen ges. Phys. Chem., 79 (1975) 882.
18 M. F. Burke, 1980, personal communication.
19 J. H. Pickett, C. H. Lochmüller and L. B. Rogers, Sep. Sci., 5 (1970) 23.
20 L. T. Mimms, M. A. McKnight and R. W. Murray, Anal. Chim. Acta., 89 (1977) 355.
21 M. L. Hair and W. Hertl, J. Phys. Chem., 73 (1969) 2372.

22 H. Hertl and M. L. Hair, J. Phys. Chem., 75 (1971) 2181.
23 M. L. Hair and W. Hertl, J. Phys. Chem., 77 (1973) 1965.
24 M. J. D. Low and G. A. Parodi, Spectrosc. Lett., 11 (1978) 581.
25 M. J. D. Low and G. A. Parodi, Appl. Spectrosc., 34 (1980) 76.
26 D. E. Leyden, M. L. Steele, B. B. Jablonski and R. B. Somoano, Anal. Chim. Acta, 100 (1978) 545.
27 A. B. Fischer, J. B. Kinney, R. H. Staley and M. S. Wrighton, J. Am. Chem. Soc., 101 (1979) 6501.
28 C. H. Lochmüller, S. F. Marshall and D. R. Wilder, Anal. Chem., 52 (1980) 19.
29 C. H. Lochmüller and D. R. Wilder, Anal. Chim. Acta, 116 (1980) 19.
30 C. H. Lochmüller and D. R. Wilder, Anal. Chim. Acta, 118 (1980) 101.
31 G. G. Guilbault (Ed.), Fluorescence, M. Dekker, New York, 1967.
32 E. L. Wehry (Ed.), Modern Fluorescence Spectroscopy, Vol. 2, Plenum, New York, 1976.
33 W. R. Gray, in C. H. W. Hirs (Ed.), Methods in Enzymology, Vol. XI, Academic Press, New York, 1967.
34 G. Weber, Biochem. J., 51 (1952) 155.
35 B. S. Hartley, Biochem. J., 119 (1970) 805.
36 H. S. White and R. W. Murray, Anal. Chem., 51 (1979) 236.
37 J. R. Rasmussen, D. E. Bergbreiter and G. M. Whitesides, J. Am. Chem. Soc., 99 (1977) 4746.
38 M. B. Evans, A. D. Dale and C. J. Little, Chromatographia, 13 (1980) 5.
39 L. D. Weis, T. R. Evans and P. A. Leermakers, J. Am. Chem. Soc., 90 (1968) 6109.
40 R. M. McCormick and B. L. Karger, Anal. Chem., 52 (1980) 2249.
41 R. F. W. Scott and C. F. Simpson, J. Chromatogr., 197 (1980) 11.

Analytica Chimica Acta, 130 (1981) 45—53
Elsevier Scientific Publishing Company, Amsterdam — Printed in The Netherlands

FLOW INJECTION ANALYSIS FOR GLUCOSE AND UREA WITH ENZYME REACTORS AND ON-LINE DIALYSIS

L. GORTON and L. ÖGREN
Analytical Chemistry, University of Lund, P.O. Box 740, S-220 07 Lund (Sweden)
(Received 23rd March 1981)

SUMMARY

A flow injection system for glucose and urea determination is described. The glucose determination uses immobilized glucose oxidase in a reactor designed to give 100% substrate conversion. The hydrogen peroxide formed is converted to a coloured complex with 4-aminophenazone and *N,N*-dimethylaniline. The coupling is catalysed by a reactor containing immobilized peroxidase. The coloured complex is measured in a flow-through spectrophotometric cell. Urea is converted to ammonia in a reactor with immobilized urease and detected with an ammonia gas membrane electrode. Proteins and other interfering species from serum samples are removed in an on-line dialyzer. Calibration curves are linear for glucose in the range 1.6×10^{-4}—1.6×10^{-2} M and for urea in the range 10^{-4}—10^{-1} M. The samples are 25 μl for glucose determination and 100 μl for urea determination. Linear ranges can be changed by varying the sample sizes. The effects of the dialyser, enzyme reactors and detectors on dispersion are evaluated.

Continuous flow-injection analysis (f.i.a.) has a number of advantages for enzymatic determinations of substrates as shown by Růžička, Hansen and their coworkers [1—4]. Further advantages would be obtained if the systems were adapted to immobilized enzymes and included some on-line sample pretreatment. A flow-through dialyser should be able to replace the protein precipitation step, but in practice some difficulties have been reported with the dialysis technique [1, 5].

Enzyme reactors have frequently been used with sample injection techniques for determinations of glucose [6, 7] testosterone [7], urea [8, 9] and uric acid [10], and their properties in flow systems have been fully investigated for glucose [11], urea [12] and L-amino acid oxidase [13] as well as for chromatographic peaks [14]. In the present paper, the properties of a combined system including f.i.a. technique, an on-line dialyser, and on-line enzyme reactors are reported. The technique was applied to the determination of glucose and urea with a spectrophotometric and an electrochemical detector, respectively.

EXPERIMENTAL

Flow injection systems

The flow systems for glucose and urea determinations are shown in Fig. 1. The components were a Gilson 4-channel peristaltic pump (Minipuls 2),

0003—2670/81/0000—0000/$02.50

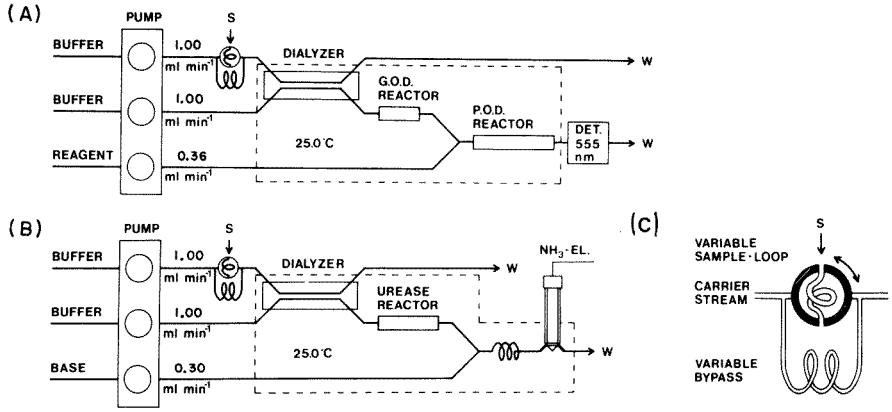

Fig. 1. Flow injection systems for detection of (A) glucose and (B) urea. The injector is shown schematically in C. For a detailed explanation, see text.

a Bifok 54-cm dialyser, an EIL ammonia flow-through electrode, and a McPherson spectrophotometer with a flow-through cuvette. The peak values from the spectrophotometer and from the pH meter were read digitally in addition to the analogue recording. The smallest relative standard deviation (0.12% for 10 measurements) was obtained with an integration time of 100 ms on the spectrophotometer. The total dead volume of the cuvette was 100 μl, 34 μl of which was in the 10-mm light path. The tubings were made of teflon, i.d. 0.3 mm, with Altex fittings. The sample was introduced by a rotating valve with a bypass loop [15] (Fig. 1C). For this study the sample was introduced with a syringe into a sample loop of teflon tubing (0.8 mm i.d.), but for real applications the fourth channel of the pump could have been used. The length of the sample loops was varied to obtain sample volumes of 25, 50, 100, 150 and 200 μl. The dialyser consisted of two plates screwed together with either an 11.5- or 17-μm thick membrane of Cuprophan between them; rectangular grooves (0.1 mm deep, 1.5 mm wide, 540 mm long) were cut in each plate giving a membrane area of 8.1 cm^2. The dialyser and the enzyme reactor were immersed in water thermostatted at 25.0°C.

Phosphate buffer (0.1 M, pH 6.0) was pumped through both the upper channels in Fig. 1A. The reagent solution was 2.9 mM in 4-aminophenazone and 0.1 M in phosphate buffer pH 6.0, and was saturated with *N,N*-dimethylaniline. When phenol was used instead of *N,N*-dimethylaniline, its concentration was 42 mM. The buffer reservoir was kept at 50°C with oxygen bubbling through it for about 5 min before use, to prevent microbubbles of air interfering with the spectrophotometric measurements.

Tris—HCl buffer (50 mM, pH 7.0) was pumped through both buffer channels in Fig. 1B. The base was 0.5 M NaOH.

Enzyme reactors

Glucose oxidase from *Aspergillus niger* (EC.1.1.2.3; Serva 22741) was immobilized on porous glass (Corning CPG-10, 80—120 mesh, pore diameter

72.9 nm) with glutaraldehyde as described before [11]; 60 mg of enzyme were used per gram of glass, 77% of which was actually bound to the glass. The reactor was a teflon tube (i.d. 3 mm, volume 200 μl) with the ends threaded internally to fit the Altex connectors. The enzyme-treated glass was kept in place with circular pieces of polypropylene gauze (8 threads per mm; mesh size 0.02—0.03 mm).

Horse radish peroxidase (EC.1.11.1.7; Sigma P8375) was immobilized in the same way; 60 mg of enzyme was used per gram of glass, and 22% of the enzyme was actually bound. The reactor size was either 200 or 400 μl.

Jack bean urease (EC.3.5.1.5; Sigma U4002) was immobilized as described before [12]; 60 mg of enzyme was used per gram of glass, 55% of the enzyme being bound. The reactor volume was 300 μl.

RESULTS AND DISCUSSION

Optimization of the flow system

The length of the bypass loop of the injector was varied when 150 μl of a 3 mM solution of an inert model substance, catechol, was injected as the sample. The system was as shown in Fig. 1A, except that the detector was placed immediately after the dialyser. The peaks were broadened up to 10% at a loop length of 10 cm, and 3% at 20 cm. A loop length of 60 cm was used in all subsequent tests. Figure 2 shows the effect of the sample size on the signal. The steady-state signal is also shown for comparison (2500 μl). Almost half of the dispersion originates from the dialyser; the remaining contributions come about equally from the detector and injector. A sample volume of 150 μl gave the optimal relation between sensitivity and dispersion. The carry-over was zero if the time between injections was 45 s or more at a flow rate of 1.0 ml min^{-1} in both channels. It was 9% for intervals of 20 s.

The mutual influence between the sample line and the detector line of the dialyser was studied by varying the flow rates one at a time, with the other at 1.0 ml min^{-1}. If only the peak heights were to be considered, the pumping speeds should be 0.3 ml min^{-1} for the sample line and 1.0 ml min^{-1} for the detector line. However, when the effect on peak broadening was also considered, a flow rate of 1.0 ml min^{-1} in both channels seemed to be the most advantageous. The dialysis membrane is sensitive to large differences in pressure between the channels and equal flow rates are therefore to be preferred. The tubing between the dialyser and the detector cell plus the enzyme reactors will cause some overpressure in the detector channel, and this will result in a small liquid flow through the membrane pores towards the sample side. The flow counteracts clogging of the pores by macromolecules on the sample side.

Two membranes were tested, with a flow rate of 1.0 ml min^{-1} in both the sample and detector channels. Transfer was 16% through the 11.5-μm membrane and 13.4% through the 17-μm membrane when a solution of catechol was pumped through the sample line. The concentration dependence was

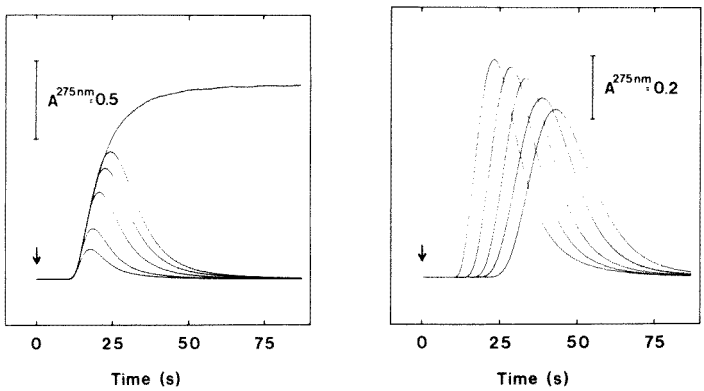

Fig. 2. Response curves obtained by injecting 25, 50, 100, 150, 200 and 2500 μl (steady state) of 3 mM catechol solution. Manifold as in Fig. 1 A, with the detector in place of the GOD reactor.

Fig. 3. The dispersion of 150-μl injections of 3 mM catechol solutions with, from left to right, 0, 100, 200, 300 and 400-μl enzyme reactors in the flow system. Manifold as in Fig. 1 A, but with the detector immediately after the GOD reactor.

tested with injections of various sizes. The calibration curves were strictly linear (r = 0.9999) over the range covered by the spectrophotometer. This is to be expected since the dialysed fraction should be concentration-independent for each solute if the time, temperature and volume are kept constant. There will of course be an appreciable back-diffusion from the detector side when the dialysed fractions are as high as those given above.

Figure 3 shows the dispersion in a flow system containing the dialyser, simulated enzyme reactors of various sizes and the spectrophotometric detector. The reactors were filled with porous silanized glass without any enzyme. It can be seen that the dispersion increases with reactor size. Reactors larger than 300 μl contribute more to the total dispersion of the system than the dialyser. If smaller reactors are used, the largest contribution comes from the dialyser.

Determination of glucose

Most clinical glucose determinations use a colour reaction coupled to the hydrogen peroxide produced by glucose oxidase. The reactions used in this study were

$$\beta\text{-D-glucose} + O_2 + H_2O \xrightarrow[\text{oxidase}]{\text{glucose}} \text{gluconic acid} + H_2O_2$$

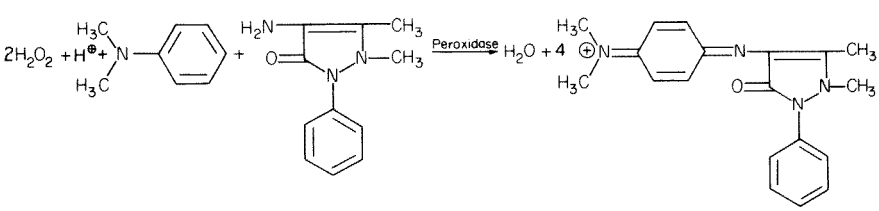

o-Dianisidine is the most used colour reagent but it was ruled out in the present method as it adsorbed strongly to the porous glass. 4-Aminophenazone, which is one of at least 30 compounds reported for glucose determinations, was tested and there was no problem from adsorption. Phenol is most frequently applied as coupling reagent for 4-aminophenazone but *N,N*-diethylaniline has also been recommended [16]. The product formed with *N,N*-dimethylaniline had a higher molar absorptivity, 26×10^3 l mol^{-1} cm^{-1} at 555 nm, than that obtained with phenol which was 11×10^3 l mol^{-1} cm^{-1} at 505 nm. Compounds of this type are considered to be less affected by interferences from other substances in serum than *o*-dianisidine.

The flow dependence of the colour-forming reaction with a 200-μl peroxidase reactor is shown in Fig. 4. Measurements were made with a steady-state supply of hydrogen peroxide (0.074 mM after mixing). The ratio between the sample and the reagent flow rate was 1:0.36 in this experiment as well as in all the following tests. As expected from the molar absorptivities, the absorbance of the coloured complex formed with *N,N*-dimethylaniline under flow conditions is much greater than that formed with phenol. The reaction rate in the reactor is also higher with the aniline, and 100% conversion efficiency can be maintained at higher flow rates. If a reactor volume of 400 μl is selected for the final analytical system, there will be some reserve capacity because the total flow rate will be 1.36 ml min^{-1}.

To test the linearity of the response, hydrogen peroxide samples were injected into a manifold from which the dialyser had been removed. A linear relation was found between the concentration of hydrogen peroxide in 150-μl samples and the peak absorbance in the range 10^{-6}—3×10^{-4} M H_2O_2. The slope of a log—log plot was 1.009, (r = 0.99992), i.e., the reaction was strictly stoichiometric. The calibration curve started to bend just after 3×10^{-4} M H_2O_2, largely because of a decrease in the conversion efficiency of the enzyme reactor. The conversion efficiency could have been increased by increasing either the size of the reactor or the reagent concentration as both were found to contribute to the decrease. This was not done, however, because the spectrophotometer would then impose a limit. The absorbance was 1.3 at 3×10^{-4} M H_2O_2.

Glucose samples were next injected into the manifold shown in Fig. 1 A; i.e., the system contained the dialyser, a 200-μl glucose oxidase reactor and a 400-μl peroxidase reactor. The calibration was tested for two sample sizes (Fig. 5). A comparison was also made with the steady-state level. The method measures the concentration of β-D-glucose but a second scale for total glucose is added for convenience; the latter is based on the assumption that 63.5% of the glucose is β-D-glucose. The reported results were obtained at 45 samples/hour so that the carry-over would be negligible. The glucose (total) range of clinical interest is 2—16 mM for blood; the normal fasting value is 4.2 mM. The range for urine samples is normally 0.1—1 mM; an excess indicates malfunctions. The linear range of the method will thus cover the concentrations of clinical interest if 25-μl samples are taken. The sensitivity

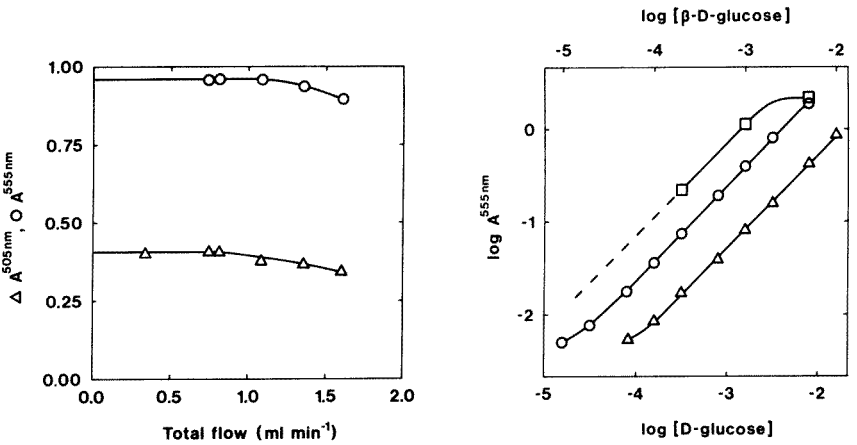

Fig. 4. Flow dependence of the colour-forming reaction with a 200-μl POD reactor. Coupling reagent: (○) *N*,*N*-dimethylaniline or (△) phenol.

Fig. 5. Calibration curves obtained with the flow system in Fig. 1A. Sample volumes: (△) 25 μl and (○) 100 μl. (□) Steady-state measurements.

can be adjusted upward or downward by changing the sample size, the size or thickness of the dialysis membrane and the flow rate. Table 1 shows the results obtained for two reference sera.

Urine samples produced a transient spectrophotometric signal because of differences in ionic strength between the buffer and the sample. The method could be adapted for urine by increasing the ionic strength of the buffer with appropriate additions of phosphate and sodium chloride and normalizing the ionic strength of the sample.

Determination of urea

The ammonia electrode shows a concentration-dependent memory effect [17] which has to be taken into account in addition to carry-over between samples. The memory effect may prevent the determination of a sample of low concentration immediately after a sample of high concentration. If the time is long enough to give separate peaks, the second reading will be correct.

TABLE 1

Analysis of reference sera from a calibration curve or with standard additions

Sample	Concentration of glucose (mM)		
	Nominal	Calibration curve	Standard addition
Pathonorm B serum	1.94[a]	1.73 ± 0.02[c]	1.59[d]
Technicon serum	12.4[b]	11.8 ± 0.08	12.1

[a]Range 1.66—2.22 mM. [b]Mean of the three different methods. [c]Standard deviation for 3 determinations. [d]Single determination.

This is in contrast to the additive effect of the tail when there is real carry-over. Figure 6 illustrates the behaviour of the ammonia electrode when equal samples were injected at varying intervals of time.

Figure 7 shows the calibration graphs for the determination of ammonia and urea with the system shown in Fig. 1B. A comparison between a steady-state system without dialyser and with dialyser shows that 27% of both ammonia and urea is dialysed. The enzyme reactor does not give complete conversion above 0.05 M urea. The levelling off of the upper curve depends on a pH change caused by the large amount of ammonium chloride added. A flow-injection determination of ammonia with 100-μl samples gives a response which is 35% of the dialysed steady-state level. The flow-injection response for urea is 27% of the steady-state level measured after dialysis. There is a slight downward bend for the dynamic curves, caused by the increased response times of the electrode at low concentrations [17]. The difference between the calibration curves for urea and ammonia is caused by different dispersion patterns. Adams and Carr [9] also observed different time courses for urea and ammonia profiles after passage through a urease reactor. The difference in peak shape in the present system was much less than that reported by Adams and Carr; the dialyser may have contributed to a levelling effect.

The range of interest for determination of urea in sera is 3.3—9.7 mM, which lies within the strictly linear part of the calibration curve. The urea concentration in urine is normally 0.33—0.58 M. Optimization of the method for urine would therefore require a reduction in the sensitivity,

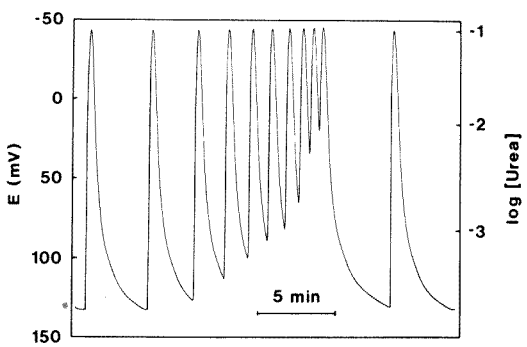

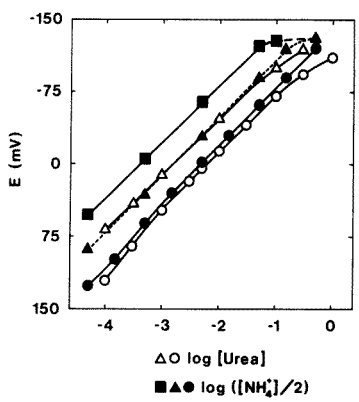

Fig. 6. The negligible influence of electrode memory effect on the result with the urea detection system (Fig. 1B). All samples were 25 μl 100 mM urea. The smallest spacing is 35 s.

Fig. 7. Calibration graphs for urea (open symbols) and ammonium ion (filled symbols) in the urea detection system (Fig. 1B): (○, ●) flow injection for 100-μl samples; (△, ▲) steady-state measurements; (■) steady-state measurements without dialyser.

e.g., by taking smaller samples or by dilution of the samples. Effects on the electrode caused by differences in ionic strength between the sample solution and the internal filling solution [17] appear to be smaller in flow injection runs than in continuous immersion. Changes in ionic strength have less effect in this potentiometric method than in the spectrophotometric method for glucose.

Comparison of systems

The presence of serum proteins or sediments from urine samples interferes more or less with all detection methods. In spectrophotometric methods, pronounced interferences are caused by light scattering, adsorption on the cell windows, and reaction with the reagents to produce coloured compounds. Gas electrode membranes tend to be clogged by precipitates and adsorption to the walls may cause ion-exchange effects. Clogging of the dialysis membrane also occurs with time but it is simpler to clean this single component than the whole analytical system. A proper design with a slightly higher pressure on the detector side of the dialyzer reduces clogging of the pores.

Hansen et al. [1] stated that dialysis was not a very practical approach in flow injection analysis. The improvement reported here on the dialysis step is largely due to using a larger surface area (at least 8 times larger than used before [5]) at the expense of doubling the dead volume. The dialysed fraction becomes an order of magnitude larger and the lack of sensitivity noted earlier [1] is remedied. From a practical point of view, the membrane can be replaced very quickly. The dialyser represents a dispersing element in the flow system but this can be balanced against the dispersion of other components of the system. The results given in Table 1 show differences up to 9% between the two methods of evaluation; ionic strength and viscosity effects are the main factors behind the difference. The procedures required to remove these sources of error will depend on the intended application and the detailed design of the system.

The pros and cons of enzyme reactors versus a flow-injection system with a soluble enzyme can be evaluated correctly only when each of the systems has been optimised for the same application. The reactors used in this work are unnecessarily large for samples containing low substrate concentrations, e.g., glucose in sera or urine. Smaller reactors would result in reduced dispersion and, at least with the spectrophotometric detector, a higher sample through-put. In the urea determinations, the speed of analysis is mainly governed by the electrode properties, but faster electrode constructions are possible [18]. Complete conversion of the substrate is usually not practical with a soluble enzyme in flowing streams, so that stopped-flow and kinetic measurements become necessary [2—4]. Reactors containing immobilized enzymes can be designed so that 100% of the substrate is converted to products. The conversion then becomes independent of small or moderate changes in flow rate, temperature, pH, ionic strength, and inhibitor concen-

tration [19]. The product concentration becomes a strictly linear function of the substrate concentration over a wider range than is available with soluble enzymes.

The authors thank Professor Gillis Johansson for valuable discussions concerning this work. This work was supported by grants from the Swedish Board for Technical Development.

REFERENCES

1 E. H. Hansen, J. Růžička and B. Rietz, Anal. Chim. Acta, 89 (1977) 241.
2 J. Růžička and E. H. Hansen, Anal. Chim. Acta, 99 (1978) 37.
3 J. Růžička and E. H. Hansen, NBS Spec. Publ., 519 (1979) 501.
4 A. Ramsing, J. Růžička and E. H. Hansen, Anal. Chim. Acta, 114 (1980) 165.
5 J. Růžička and E. H. Hansen, Anal. Chim. Acta, 87 (1976) 353.
6 L. Gorton, Proc. Workshop on Flow Injection Analysis, No. 8. Swedish Chemical Society, Uppsala, Sweden, October, 1977.
7 P. Cremonesi and R. Bovara, Biotechnol. Bioeng., 18 (1976) 1487.
8 B. Danielsson, B. Mattiasson and K. Mosbach, Pure & Appl. Chem., 51 (1979) 1443.
9 R. E. Adams and P. W. Carr, Anal. Chem., 50 (1978) 944.
10 A. Iob and H. A. Mottola, Anal. Chem., 52 (1980) 2332.
11 L. Gorton and K. M. Bhatti, Anal. Chim. Acta, 105 (1979) 43.
12 G. Johansson and L. Ögren, Anal. Chim. Acta, 84 (1976) 23.
13 G. Johansson, K. Edström and L. Ögren, Anal. Chim. Acta, 85 (1976) 55.
14 L. Ögren, I. Csiky, L. Risinger, L. G. Nilsson and G. Johansson, Anal. Chim. Acta, 117 (1980) 71.
15 J. Růžička and E. H. Hansen, Anal. Chim. Acta, 114 (1980) 19.
16 P. Kabasakalian, S. Kalliney and A. Westcott, Clin. Chem., 20 (1974) 606.
17 P. L. Bailey and M. Riley, Analyst, 100 (1975) 145.
18 P. L. Bailey, in J. D. R. Thomas (Ed.), Ion-Selective Electrode Reviews, Vol. 1, Pergamon, Oxford, 1980.
19 G. Johansson, Appl. Biochem. Biotechnol., in press.

Analytica Chimica Acta, 130 (1981) 55—63
Elsevier Scientific Publishing Company, Amsterdam — Printed in The Netherlands

A SEMI-AUTOMATIC ALKALINE PEROXODISULPHATE METHOD FOR THE ROUTINE DETERMINATION OF TOTAL DISSOLVED NITROGEN IN SEA WATER

R. J. SHEPHERD[a] and I. M. DAVIES*

Department of Agriculture and Fisheries for Scotland, Marine Laboratory, Victoria Road, Aberdeen AB9 8DB (Gt. Britain)

(Received 13th March 1981)

SUMMARY

Nydahl's method for the determination of dissolved organic nitrogen (DON) in distilled water has been modified for the determination of total dissolved nitrogen (TDN) in sea water. Samples (9 cm^3) are digested batch-wise with alkaline potassium peroxodisulphate solution. An improved buffering system permits the automatic measurement of the nitrate formed, and allows the analysis of 50—80 samples per day. DON may be determined as the difference between TDN and the sum of inorganic nitrogen species. The standard deviation of TDN determinations is 0.7 μg N dm^{-3} at about 15 μg TDN dm^{-3}. The method is applied to a range of samples including tanker ballast water, oil platform production water, and zooplankton.

The quantification of nitrogen in its soluble organic forms has interested marine chemists engaged in hydrographic, primary production and pollution studies [1—3]. The concentrations of particular dissolved organic nitrogen (DON) species in sea water may be low and while methods have been developed for some specific compounds (notably the amino acids) the bulk of the DON remains uncharacterised. Whilst a large portion of the DON in sea water is probably derived from soluble exudates from algae, it will also contain a wide range of other compounds including animal proteins, urea and other excretary products, nucleic acids, etc.

DON is commonly determined in four stages: (a) removal of particulate organic nitrogen by filtering through a 0.45-μm pore membrane or equivalent glass-fibre filter; (b) oxidation of soluble organic nitrogen to inorganic forms of nitrogen; (c) determination of total inorganic nitrogen; and (d) correction for inorganic nitrogen species present before oxidation. Published oxidation techniques for sea water include Kjeldahl digestion [4] which converts organic nitrogen to ammonium salts, ultraviolet irradiation [5] which yields a mixture of nitrate and nitrite, and alkaline peroxodisulphate digestion [6, 7] which yields nitrate only.

---

[a]Present address: Core Laboratories (UK) Ltd., Kirkhill Industrial Estate, Dyce, Aberdeen, Gt. Britain.

0003—2670/81/0000—0000/$02.50

As in the earlier report by Koroleff [7], preliminary experiments carried out here using ultraviolet irradiation gave variable (60—100%) recoveries of organic and inorganic nitrogen compounds added to natural sea water. Also the application of the u.v. method to sea water containing added oily water effluent from a production platform gave results significantly lower than those obtained by peroxodisulphate oxidation. However, for clean open sea water a N:P ratio (approximately 20:1) was obtained using these digestion techniques [8, 9], which was similar to that reported by Butler [2] using u.v. irradiation.

Experiments were carried out on a range of contaminated and clean sea waters using a later version [10] of Koroleff's [6] alkaline peroxodisulphate oxidation technique. These showed that the degree of pH control during nitrate determination was not adequate. Nydahl [11] studied the oxidation of nitrogen compounds by alkaline peroxodisulphate digestion in distilled water and in synthetic sea water media and discussed the capabilities and limitations of total nitrogen determination by this technique. He developed a theoretical basis for the selection of alkali and peroxodisulphate concentrations, and improved the pH control for the nitrate to nitrite reduction stage. The present paper describes some modifications necessary for the application of Nydahl's method in the routine analysis of small samples of natural and polluted sea water, and to samples of contaminated saline effluents.

EXPERIMENTAL

Reagents and their preparation

Glass-distilled water and analytical-grade chemicals were used in the preparation of all reagents. The use of redistilled water for recrystallisation of potassium peroxodisulphate and for preparing the alkaline peroxodisulphate reagent was found to reduce the reagent blank up to 20%, but ordinary glass-distilled was used routinely in the investigations reported here.

Recrystallised potassium peroxodisulphate. Dissolve 70 g of $K_2S_2O_8$ in 500 cm^3 of freshly boiled distilled water which has been cooled to 60°C. Cool the solution to nearly 0°C in a deep freeze and collect the crystals which have formed on a glass-fibre filter. Repeat the procedure with this product and dry the twice-purified crystals in an evacuated desiccator over silica gel. Weigh out suitable portions and store them in sealed vials.

Alkaline peroxodisulphate reagent (0.6 M sodium hydroxide—0.1 M potassium persulphate). Dissolve 2.40 g of sodium hydroxide in approximately 90 cm^3 of freshly boiled distilled water. When the temperature has fallen below 60°C, add and dissolve 2.70 g of recrystallised $K_2S_2O_8$. Dilute to 100 cm^3 when cool.

Tris(hydroxymethyl)aminomethane buffer (Tris-HCl). Pipette 2.7 cm^3 of 1.5 M HCl into 31 cm^3 of 0.45 M Tris base (54.50 g of Tris base in 1 dm^3 of distilled water) and dilute to 1 dm^3.

Nitrate reagents. Prepare the following solutions: (a) 2% (w/v) ammonium

chloride with 1 cm^3 of Brij (wetting agent) per dm^3; (b) 1% (w/v) sulphanilamide in 10% (v/v) hydrochloric acid; (c) 0.1% (w/v) *N*-1-naphthylethylenediamine dihydrochloride.

Reduction column. Thread 2 m of 1-mm diameter cadmium wire into 2.05 m of 2-mm i.d. polythene tubing. Condition by washing successively with 10 cm^3 of 10% (v/v) HCl, 10 cm^3 of distilled water, 10 cm^3 of 2% (w/v) $CuSO_4$, and 10 cm^3 of sea water. Run the Auto-Analyzer for 1 h with ammonium chloride and 40 μg NO_3—N dm^{-3} in sea water, and for 30 min with 0.05 M H_2SO_4 in sea water to condition the column.

Procedure

Pipette 3 cm^3 of alkaline peroxodisulphate reagent and 9 cm^3 of each filtered sea-water sample into 20-cm^3 ampoules using automatic pipettes. Include at least 4 ampoules containing 3 cm^3 of alkaline peroxodisulphate reagent only, with each batch of samples for blank and calibration (see Discussion). Seal the ampoules and place them in a pressure cooker containing about 1 dm^3 of hot water on a hot plate or gas burner. Close the lid of the cooker and, when a free flow of steam is observed, fit the weighted valve and adjust the heating to obtain a steady temperature of 120° C and internal pressure of 207 kN m^{-2} (29 psi) for 15 min at this pressure. Allow the cooker to cool before opening.

Remove and open the ampoules and dissolve the hydroxide precipitate by injecting 1 cm^3 of 1.5 M HCl into each ampoule with a micropipette. Occasionally it may be necessary to leave the samples for 5—10 min for the precipitate to dissolve completely, or to inject the following 1 cm^3 of distilled water. Inject 1 cm^3 of distilled water and then 1 cm^3 of 0.45 M Tris base. Pipette 3 cm^3 of this partially buffered solution into a clean 8.5-cm^3 sample cup and dilute with 5 cm^3 of the Tris—HCl buffer, added from a syringe dispenser.

Determine nitrate in the samples using the manifold shown in Fig. 1 at 20 samples per hour (2:1 sample-to-wash ratio). A 22.5% (equal to the dilution

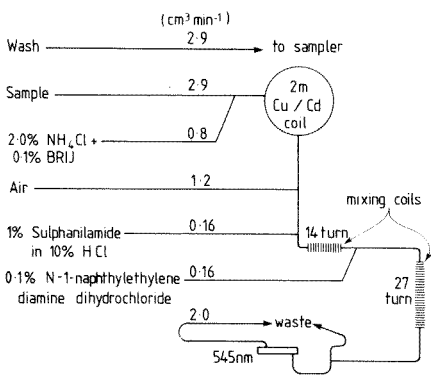

Fig. 1. Manifold for the determination of nitrate in oxidised and natural sea water samples.

of samples following the oxidation and buffering procedures) low-nitrate natural sea water (LSW, <0.1 μg NO_3—N dm^{-3}) adjusted with concentrated sulphuric acid to be 0.05 M in H_2SO_4, is used as the wash solution.

When the method was applied at sea, it was found convenient to use a butane blow torch and tongs for sealing the ampoules, a single ring electric radiant heater, fitted with a regulator, for heating the pressure cooker, and a wire basket (which holds 32 ampoules) to support the ampoules in the cooker.

RESULTS AND DISCUSSION

Modification to Nydahl's procedure

The procedure described allows 50—80 samples per day to be analysed for TDN either in the laboratory or at sea. The modifications to Nydahl's method [11] necessary to achieve this analytical output are: (a) reduction of sample and reagent volume and handling; (b) use of micro- and macro-autopipettes; (c) use of the high-capacity Tris—HCl buffer (suggested by Nydahl); (d) performance of oxidations in sealed ampoules; and (e) the use of the automatic nitrate determination.

It is apparent that while precision can be maintained at small volumes by use of automatic pipettes, use of a buffer of sufficient capacity to cope with variations in the more concentrated, less accurately prepared, reagents is essential. The use of sealed ampoules as reaction vessels eliminates evaporation of samples and reduces the danger of the contamination found with open vessels. Uncleaned ampoules were used throughout this work because preliminary tests with acid-cleaned ampoules did not reveal any random or systematic contamination from ampoules as received from the manufacturer. The ampoules also proved convenient for storage of samples before and after oxidation.

The dilution of samples by reagents is reduced from $\times 10$ to $\times 4.4$ in the modification, which helps to compensate for the limited optical path length normal in flow-through colorimeters.

Automatic nitrate determination has many advantages over manual procedures both in the laboratory and at sea [12, 13]. The method outlined here is a modification of that reported by Armstrong et al. [14] and Stainton [15]; variations of the method are widely used. The method is not tolerant of certain polluted or chemically altered samples in which pH, buffer capacity or oxygen content may differ significantly from oceanic samples [16]. This, combined with the sensitivity of copperized cadmium reduction columns to large changes in chloride content and the inaccuracies caused by refractive index variations in flow-through cells [17], means that samples, blanks, and standards must be matrix-matched. The volume of blank available makes the customary practice of running samples against a (sample and reagent) blank wash impossible and discrete blanks must be run. Standards and samples should be corrected for this blank.

Acidified 22.5% sea water was chosen as wash to avoid differences in

chloride content and refractive index between wash and samples. An acidified wash has been suggested by Nydahl [16] for manually operated reduction columns. Its application in the automatic method also helps to reduce changes in reduction efficiency over a run of samples by minimising the hydroxide formation that occurs at the pH of the buffered samples, which is close to the optimum pH for reduction. The pH of the wash is unsuitable for azo dye formation and an apparent blank of about 4 μg NO_3—N dm^{-3} is introduced for diluted LSW.

Calibration and blanks

Ideally, sea-water blanks and standards should be carried through the entire oxidation procedure together with samples. Natural sea water always contains considerable quantities of organic and/or inorganic nitrogen and is therefore unsuitable as a blank. It was therefore necessary to develop an alternative calibration procedure. Four procedures were investigated: (a) LSW and nitrate standards, prepared in the same water, were oxidised and buffered as described above; (b) 3-cm^3 aliquots of the alkaline peroxodisulphate reagent were digested in sealed ampoules, and 9-cm^3 aliquots of LSW or LSW nitrate standards were then added, followed by 1.5 M HCl, dilution and buffering as described; (c) LSW and LSW nitrate standards were diluted with distilled water to the same degree as samples (i.e., ×4.4); (d) LSW and LSW nitrate standards were diluted ×4.4 with the Tris—HCl buffer to yield the same buffer strength as that present in samples taken through the procedure.

No significant difference (95% level) was observed between the slopes of calibration curves (Fig. 2) prepared by these methods; method (a) resulted in a high blank, as expected. Only method (b) includes complete matrix matching and assessment of the blank arising from all reagents. This procedure

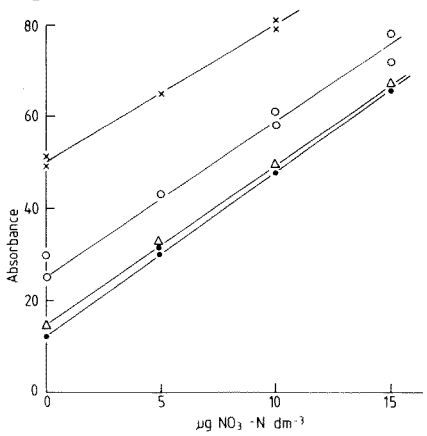

Fig. 2. Calibration curves for nitrate in sea water under various treatments (absorbance in arbitrary units). (×) Nitrate added to sea water prior to oxidation; (○) nitrate in sea water added to reagents after oxidation; (•) nitrate standards prepared in diluted (22.5%) sea water; (△) nitrate in sea-water standards diluted ×4.4 with Tris—HCl buffer.

allows standards of appropriate concentration to be prepared at any time during the nitrate determinations if an adequate number of oxidised blanks have been prepared. While this indicates that method (b) is suitable for calibration, further tests were carried out to ensure that the high reagent concentration in the blanks at oxidation did not adversely affect the kinetics of the decomposition of the peroxodisulphate, and that no interference occurred from unoxidised compounds added to the ampoules after digestion. Increasing the digestion time after 15 min did not significantly alter the blank response, indicating that decomposition was complete. Digestion of 1—9-cm^3 aliquots of sea water and dilution after oxidation to a total volume of 12 cm^3 with LSW prior to acidification and buffering demonstrated that no measurable interference occurred from the diluting water. For a range of 6 dilutions, the mean TDN was 11.3 $\mu g\ dm^{-3}$ (c.v. 10.1%).

Accuracy and precision

The method and calibration procedures assume quantitative oxidation of all nitrogen compounds to nitrate. Because many of the DON compounds in sea water cannot at present be fully characterised, it is impossible to check completely the accuracy of TDN methods, especially the efficiency of the oxidation of individual organic-nitrogen compounds.

Nydahl [11] published a list of 39 compounds which gave oxidation yields over 87% in distilled water compared with the Kjeldahl nitrogen determination. He also included eight compounds which gave poor (<83%) recoveries, and concluded that yields from peroxodisulphate oxidation are low for compounds containing nitrogen—nitrogen bonds and HN=C groups. The determination of TDN at the 10 μg N dm^{-3} level for the compounds listed in Table 1 added as spikes to natural sea water gave recoveries of 88—

TABLE 1

Recovery of inorganic and organic nitrogen compounds added at the 10 μg N dm^{-3} level to natural sea water (LSW)

	TDN (μg N dm^{-3})		Recovery of added N (%)	
Sea water	5.0	5.4	—	—
	5.0	5.4	—	—
Potassium nitrate	15.5	15.2	103	100
Potassium nitrite	16.2	16.2	110	110
Ammonium chloride	14.9	14.9	97	97
Urea	15.2	15.3	100	101
Glycine	14.3	14.0	91	88
2,2'-Bipyridine	16.2	16.5	110	113
Na_2—EDTA	15.5	15.0	103	98
Overall mean TDN (excluding sea water)	= 15.35, s.d. = 0.736, c.v. = 4.8%			
Overall mean recovery	= 101.5%, s.d. = 7.36%, c.v. = 7.2%			

113% at a TDN concentration of 15.3 μg N dm^{-3}. Measurements of a 5 μg N dm^{-3} methyl orange standard in sea water confirmed the low recovery of nitrogen from N=N bonds reported by Nydahl in distilled water media.

The coefficient of variation (c.v.) of the reagent blank, read directly from the wash water line (i.e., not corrected for the pH effect discussed previously) was 1% (Table 2). On correcting sea-water samples for this blank, a c.v. of 4% was routinely obtained. The detection limit of the method, calculated as twice the standard deviation of the blank, was 0.18 μg N dm^{-3}; i.e., 23 ng N per sample.

Calculation of dissolved organic nitrogen

Dissolved organic nitrogen (DON) may be determined by calculating the difference between total dissolved nitrogen and the sum of inorganic (nitrate, nitrite and ammonium ions) concentrations for the same filtered sample. The accuracy of the results for DON depends on the classes of nitrogen compounds present, their relative concentrations, and on the accuracy of the methods used to determine the inorganic forms of nitrogen [11]. It is important to optimise all the methods with regard to accuracy and contamination, and the well-known problems common to inorganic nitrogen determinations must be considered. Organic nitrogen values calculated by difference will obviously reflect the errors of all methods used. Typically, coefficients of variation of 4—7% were obtained for DON, depending on the distribution of nitrogen between the various species.

Applications

The potential problems arising from the application of the method to saline water containing more than 40 mg dm^{-3} organic carbon or 0.62 mM of Group II elements (which would exceed the oxidising capacity or alkalinity, respectively, of the peroxodisulphate reagent) have been pointed out by Nydahl [11]. The method may be extended to these waters by using smaller sample aliquots and dilution, after oxidation, with LSW without significant

TABLE 2

Comparison of the precision of various parts of the TDN procedure

Sample	No. of results	Mean TDN (μg dm^{-3})	Standard deviation	Coefficient of variation (%)
Reagent blank	4	7.7	0.09	1
Sample and reagent blank	9	14.5	0.304	2
Bulked sample[a]	10	14.4	0.164	1
Sample (corrected for blank)	9	6.8	0.304	4

[a]Replicate samples were mixed after the final buffering, and aliquots of this mixture were taken to determine the precision of nitrate determination in presence of TN reagents.

loss of precision. In this way, oil platform production waters and ballast water from segregated-ballast oil tankers have been analysed.

This method is primarily concerned with dissolved nitrogen, but preliminary investigations (Table 3) indicate reasonable agreement between particulate nitrogen measurements by peroxodisulphate oxidation (by subtraction of the results obtained for filtered and unfiltered samples), and by CHN analyser. This peroxodisulphate method may therefore be of use in providing a "first estimate" of particulate nitrogen concentrations in the field laboratory.

More specific application of the sensitivity of the technique has been made in the measurement of total nitrogen in individual, or small groups, of zooplankton (Table 4). These animals are completely dissolved by the peroxodisulphate reagent.

TABLE 3

Comparison of particulate nitrogen measurements (mg m^{-3}) by CHN analyser and alkaline peroxodisulphate digestion for waters from a large experimental ecosystem [18]

Sample	CHN[a]	$K_2S_2O_8$ oxidation[b]	"Recovery" Oxidation/CHN (%)	Sample	CHN[a]	$K_2S_2O_8$ oxidation[b]	"Recovery" Oxidation/CHN (%)
1	90.9	98	108	4	72.6	64	88
2	93.8	83	88	5	72.9	56	77
3	72.8	(36)	(49)	6	185.7	230	124

[a] 1-dm^3 sample volume. [b] Calculated by difference between results for 9-cm^3 aliquots of unfiltered sample and filtered sample (taken from filtrate obtained during separation of particulate material for the CHN analyser).

TABLE 4

Measurements of total nitrogen per individual in eight samples of zooplankton from Loch Ewe, Scotland

Species	No. of individuals in sample	Cephalothorax length (mm)	Total N/ individual (μg)
Acartia clausii	1	0.98	1.29
Acartia clausii	1	0.98	1.24
Acartia clausii	1	0.49	0.16
Acartia clausii	1	0.49	0.19
Pseudocalanus elongatus	2	1.03—1.06	1.52
Pseudocalanus elongatus	10	0.57—0.67	0.21
Temora longicornis	4	0.99—1.06	1.98
Temora longicornis	4	0.99—1.06	2.04

REFERENCES

1 O. Holm-Hansen, J. D. H. Strickland and P. M. Williams, Limnol. Oceanogr., 11 (1966) 548.
2 E. I. Butler, Estuarine Coastal Mar. Sci., 8 (1979) 195.
3 E. I. Butler, S. Knox and M. I. Liddicoat, J. Mar. Biol. Assoc. U.K., 59 (1979) 239.
4 J. D. H. Strickland and T. R. Parsons, A Practical Handbook of Sea Water Analysis, Bulletin 167, Fish. Res. Brd. Canada, 1972, p. 310.
5 F. A. J. Armstrong and S. Tibbitts, J. Mar. Biol. Assoc. U.K., 48 (1968) 143.
6 F. Koroleff, Determination of Total Nitrogen in Natural Waters by Means of Digestion, International Council for the Exploration of the Sea, Hydrography Committee, C.M. 1969/C:8, p. 4.
7 F. Koroleff, in K. Grasshoff (Ed.), Methods of Sea Water Analysis, Verlag Chemie, New York, 1976, p. 116.
8 J. Murphy and J. P. Riley, Anal. Chim. Acta, 27 (1962) 31.
9 D. W. Menzel and N. Corwin, Limnol. Oceanogr., 10 (1965) 280.
10 C. F. D'Elia, P. A. Stendler and N. Corwin, Limnol. Oceanogr., 22 (1977) 760.
11 F. Nydahl, Water Res., 12 (1978) 1123.
12 J. P. Riley, D. E. Robertson, J. W. R. Dutton, N. T. Mitchell and P. J. Le B. Williams, in J. P. Riley and G. Skirrow (Eds.), Chemical Oceanography, Vol. 3, Academic Press, London, 1975, p. 193.
13 K. Grasshoff and M. Ehrhardt, in K. Grasshoff (Ed.), Methods of Sea Water Analysis, Verlag Chemie, New York, 1976, p. 267.
14 F. A. J. Armstrong, C. R. Stearns and J. D. H. Strickland, Deep-Sea Res., 14 (1967) 381.
15 M. P. Stainton, Anal. Chem., 46 (1974) 1616.
16 F. Nydahl, Talanta, 23 (1976) 349.
17 T. C. Loder and P. A. Glibert, Adv. Autom. Anal., 2 (1976) 48.
18 J. C. Gamble, J. M. Davies and J. H. Steele, Bull. Mar. Sci., 27 (1977) 146.

Analytica Chimica Acta, 130 (1981) 65—72
Elsevier Scientific Publishing Company, Amsterdam — Printed in The Netherlands

FLOW INJECTION DETERMINATION OF TRACES OF COBALT BY CATALYSIS OF THE SPADNS—HYDROGEN PEROXIDE REACTION WITH SPECTROPHOTOMETRIC DETECTION

TAKESHI YAMANE

Department of Chemistry, Faculty of Education, Yamanashi University, Takeda-4, Kofu-shi, 400 (Japan)

(Received 20th March 1981)

SUMMARY

A flow injection system is proposed for the rapid sensitive determination of traces of cobalt based on its catalysis of the oxidation of SPADNS [2(4-sulfophenylazo)-1,-8-dihydroxynaphthalene-3,6-disulfonic acid] by hydrogen peroxide in alkaline media. The stopped-flow technique is used to increase the sensitivity, so that 0.05—2 ng of cobalt (5—200 ppb) can be determined in 10—20 μl at a sampling rate of 60 h^{-1}. Relative standard deviations are 2.0% for 100 ppb Co by normal flow injection and 2.5% for 50 ppb Co in the stopped-flow mode.

Kinetic methods of analysis based on catalytic reactions have received considerable attention because of their great sensitivity achieved with inexpensive apparatus. Dynamic measurements, however, are usually required and some additional variables affecting quantitative measurements must be controlled. In particular, it is essential to control the reaction conditions strictly and to measure the change of reactant or product concentration as a function of time as accurately as possible.

Flow injection analysis, developed by Růžička and Hansen [1, 2], is considered to be very suitable for combination with kinetic measurements, because reaction conditions can be controlled by judicious selection of such parameters as pumping rate, length and inner diameter of the tubing, temperature of reaction coils, etc.

The present paper reports a study of a flow injection determination of nanogram levels of cobalt based on catalysis and spectrophotometric detection. Several indicator reactions have been reported for cobalt [3, 4]. Most involve the oxidation of aromatic 1,2-dihydroxy compounds, although the well-known luminol—hydrogen peroxide reaction has been extensively used. Cobalt has been found to catalyze the oxidation of SPADNS {2(4-sulfophenylazo)-1,8-dihydroxynaphthalene-3,6-disulfonic acid} by hydrogen peroxide in alkaline media. This cobalt-catalyzed oxidation has been studied in detail by using a flow injection system, and optimal manifolds were established for determining traces of cobalt.

0003—2670/81/0000—0000/$02.50

EXPERIMENTAL

Reagents

All chemicals used were of analytical grade. A standard cobalt solution (500 μg ml^{-1}) was prepared by dissolving 0.250 g of cobalt (99.99%) in 5 M nitric acid and diluting to 500 ml with 0.5 M nitric acid. More dilute solutions were prepared from this solution. SPADNS solution (3.5 × 10^{-4} M) was prepared by dissolving 0.040 g of SPADNS (trisodium salt; Dotite reagent) in 200 ml of water. This solution could be used for at least 2 weeks after preparation if it was stored in a refrigerator. Before use, 5 ml of this solution was diluted to 50 ml with the addition of 10 ml of buffer solution (pH 9.4; 0.1 M sodium hydrogencarbonate and 0.05 M sodium carbonate mixed in a ratio of 10:3) and water. Hydrogen peroxide solution (0.4%) was prepared by dilution of a 30% solution with water.

Apparatus and manifold

The manifold (Fig. 1) was made from teflon tubing (i.d. 0.5 mm) and all connectors were also made from teflon. The micro-pump (double plunger type), spectrophotometer and recorder were as used earlier [5]. A model HM-5B pH meter (Toa Dempa) was used. The temperature of the reaction coil (R in Fig. 1) was kept constant to within 0.5°C by a model G-51 (Takara) temperature controller with a thermistor detector.

Procedure

The flow system used is shown in Fig. 1. The sample is injected manually at point S with a Hamilton gas-tight syringe via a septum sample injector into the flowing mixed reagent stream. The reagent streams are pumped at the same flow rate in order to achieve effective mixing of both solutions. The reaction is started by injection of sample and proceeds in the reaction coil R. As the sample zone reaches the flow cell, the decrease in the absorbance of SPADNS at 520 nm, owing to its oxidation, is measured and recorded. The peak heights measured can be related to the cobalt concentration. In

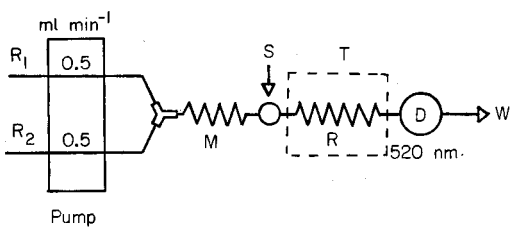

Fig. 1. Schematic diagram of the flow injection system for catalytic spectrophotometric determination of cobalt. (R_1) Hydrogen peroxide (0.4%); (R_2) SPADNS (3.5 × 10^{-5} M); (M) mixing coil (150 cm); (R) reaction coil (300 cm); (S) point of sample injection; (D) detector; (W) waste; (T) temperature-controlled bath.

the stopped-flow technique, the reagent streams are stopped 15 s after sample injection for a suitable period, before pumping and measuring as described above.

RESULTS AND DISCUSSION

SPADNS is decolorized on oxidation by hydrogen peroxide. The analytical signal recorded is a peak with a sharp initial rise. Peak height is considered to correspond to the apparent rate of the catalyzed reaction because it represents the change in absorbance during a fixed reaction time. Preliminary experiments showed that this cobalt-catalyzed oxidation occurs most effectively at pH 9—10. The wavelength of maximum absorption of SPADNS is slightly shifted toward longer wavelengths as the pH is increased, e.g., from 513 nm at pH 9.0 to 520 nm at pH 10.0. Absorbance measurements were made at 520 nm in all subsequent studies, because small shifts in wavelength had less effect at this wavelength, and the maximum rate of oxidation occurs at pH 9.4 (see below).

Effect of pH

The manifold shown in Fig. 1 was used to check the effect of pH on the rate of the catalyzed oxidation; fixed amounts of cobalt were injected (10 μl or 20 μl of 100 ppb solution, corresponding to 1 or 2 ng of cobalt, respectively). The pH was adjusted with carbonate buffer solutions prepared by mixing 0.1 M sodium hydrogencarbonate and 0.05 M sodium carbonate solutions in various ratios, the concentration of sodium hydrogencarbonate being kept constant throughout. Figure 2 shows that the maximal reaction rate occurs at about pH 9.4.

The volume of pH 9.4 buffer solution added to the SPADNS solution also affected the reaction rate (Fig. 3). Maximal peak heights were observed for 8—10 ml of solution. The marked decrease in peak height with smaller volumes of buffer is probably caused by low buffering capacity, because the sample solutions are weakly acidic. In experiments with sample solutions above pH 5, made by addition of small amounts of carbonate buffer (pH 9.4) to the acidic cobalt solution or by dilution of stock solution with water only, an appreciable decrease in the peak height was found compared with sample solutions below pH 4. Therefore, the sample solution was adjusted to about pH 3 by the addition of small amounts of dilute nitric acid, and 10 ml of pH 9.4 buffer was added to the SPADNS solution. It can be seen that small changes in pH values around 9.4 and in buffer volume around 10 ml do not affect the reaction rate significantly, but of course large changes should be avoided.

It is important to note that the catalyzed reaction was retarded by the presence of small amounts of ammonium ions and therefore ammonia buffer could not be used. This retardation is probably due to the formation of stable cobalt ammines.

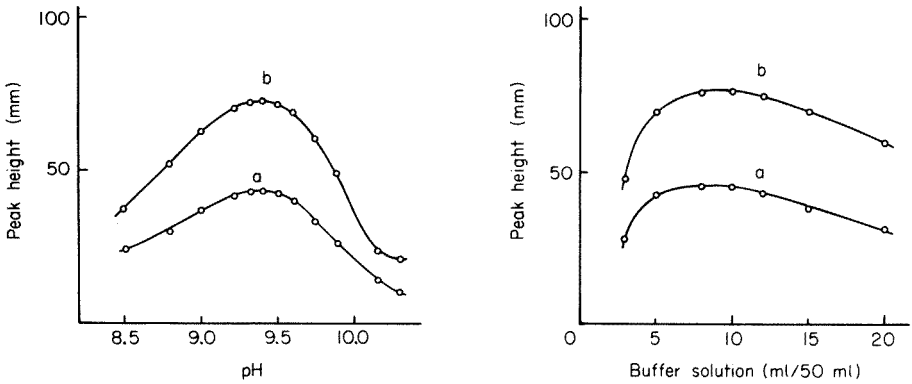

Fig. 2. Effect of pH on the peak height (the rate of cobalt-catalyzed oxidation of SPADNS). Samples of (a) 10 μl and (b) 20 μl of 100 ppb Co solution were injected.

Fig. 3. Effect of the volume of pH 9.4 carbonate buffer on the peak height. Buffer was prepared by mixing 0.1 M sodium hydrogencarbonate and 0.05 M sodium carbonate in the ratio 10:3. (a) and (b) as in Fig. 2.

Reagent concentrations and temperature

The rate of the catalyzed oxidation was measured for different concentrations of hydrogen peroxide and SPADNS. A strong dependence of peak height on hydrogen peroxide concentration was observed at low concentrations (0.01—0.25%) but the peak height became almost independent of the concentration in the range 0.3—1.0%, and a concentration of 0.4% was therefore selected. The peak height increased almost linearly with increasing SPADNS concentration in the range 2.1—4.9 $\times$ 10^{-5} M; the peak height at 4.2 $\times$ 10^{-5} M was about 1.3 times that at 2.8 $\times$ 10^{-5} M SPADNS, when 1 ng of cobalt was injected. Thus, for experimental convenience, 3.5 $\times$ 10^{-5} M SPADNS was chosen for the analytical procedure.

The dependence of the catalyzed reaction on the temperature of the reaction coil was studied by injecting 1 ng of cobalt (10 μl of 100 ppb solution). The peak height increased by 1.4 and 1.7 times as the temperature was increased from 25°C to 30 and to 35°C, respectively. Thus a controlled temperature was needed to achieve reproducible results. Although higher sensitivity could be obtained by raising the temperature of the reaction coil, a controlled reaction temperature in the range 25—30°C is adequate and more convenient.

Interferences

Sample solutions containing 100 ppb or 50 ppb of cobalt and various concentrations of other ions were injected exactly as in the recommended procedure. The results are given in Table 1. Zinc(II) and iron(III) interfered when present above 1 ppm, as did nickel(II) and chromium(III) above 2 ppm. Aluminum(III) could be tolerated up to at least 20 ppm by adding 0.5 M sodium fluoride. The other ions examined had no or only a slight effect

TABLE 1

Effect of diverse ions on recovery of cobalt (100 ppb)

Diverse ion	Conc. (ppm)	Relative error (%)	Diverse ion	Conc. (ppm)	Relative error (%)
Ni	0.5	2.0	Ag	10	0
	2	5.8		20	2.5
Fe(III)	0.5	−2.0	Hg(II)	20	0
	1	−7.3	Se(IV)	20	0
Cu(II)	5	1.6	Pb	10	0
	10	29		20	−4.5
Ca	2	2.6	As(III)	5	0
	10	4.9	Cd	1	0
Mg	2	1.4		2	2.3
	10	4.8	Mn(II)	10	0
V(V)	2	0		20	−2.5
Mo(VI)	20	0	I^-	20	0
W(VI)	10	0		40	−2.3
Zn	0.5	2.5	F^-	400	1.3
	1	7.7	NH_4^+	1.8	0
Al	4	0		3.6	−1.3
	10	−10		18	−13
	10[a]	0	Acetate	400	−2.7
	20[a]	−2.4	Citrate	25	−2.5
Cr(III)	0.5	0	Oxalate	35	0
	1	−2.5		70	−7.0
	2	−10	Phosphate	27	−2.1
Cr(VI)	2	0		54	−5.0
	10	−2.0	EDTA	37	−100

[a]Addition of 1 ml of 0.5 M sodium fluoride solution before dilution of the sample solution to 50 ml.

when present in concentrations 100—200 times that of cobalt. Interference by EDTA and ammonium ions is probably due to complex formation with cobalt.

The effect of ionic strength was also studied, with sodium sulphate added to a 100 ppb cobalt solution. No significant effect was observed up to 0.2 M. When sodium chloride was added, the apparent peak height increased with increasing concentration of sodium chloride. The real peak height, however, was not affected by the addition of sodium chloride up to 0.32 M because the blank peak increased commensurately up to this concentration. However, the presence of sodium chloride above 0.2 M is not desirable because it has a tendency to give a negative peak in the blank signal, which is due to the difference in refractive index between the solutions [6].

Study of the flow system

When the cobalt determination was carried out by flow injection, the sensitivity largely depended on such parameters as the flow rate, line length,

tube diameter and sample volume. The peak height increased as the flow rate decreased (Fig. 4) and with increasing length of reaction coil, because the longer residence time of the sample zone which allowed the catalyzed reaction to proceed further. Peak broadening, however, was observed under these conditions, because of increased dispersion of the sample zone in the coil. Greater peak broadening and some decrease in sensitivity were found when tubing with larger internal diameter was used, e.g., 1.0 mm in place of 0.5 mm (Fig. 4, e), as a result of more significant sample dispersion. Peak height increased with increasing sample volumes injected as was expected, but considerable negative deviation from a linear dependence was observed even in the narrow range of sample volumes of 5—30 μl. Thus, injection of a large sample is not necessarily advantageous because its effect on increasing the sensitivity is not in proportion, it can cause a higher blank signal, it may affect the regularity of the flow, and it would require longer reaction coils for complete mixing.

A typical continuous trace for the catalytic spectrophotometric determination of cobalt is shown in Fig. 5, with the manifold finally selected (Fig. 1). With this manifold, a small blank signal appears when pure water is injected because of the dilution of the colored reagent solution.

In an attempt to further improve the sensitivity, a stopped-flow technique was applied. This technique has the important possibility of increasing the sensitivity especially of kinetic methods [2, 7]. Adequate reaction time for optimal sensitivity is allowed by stopping the flow for a certain period

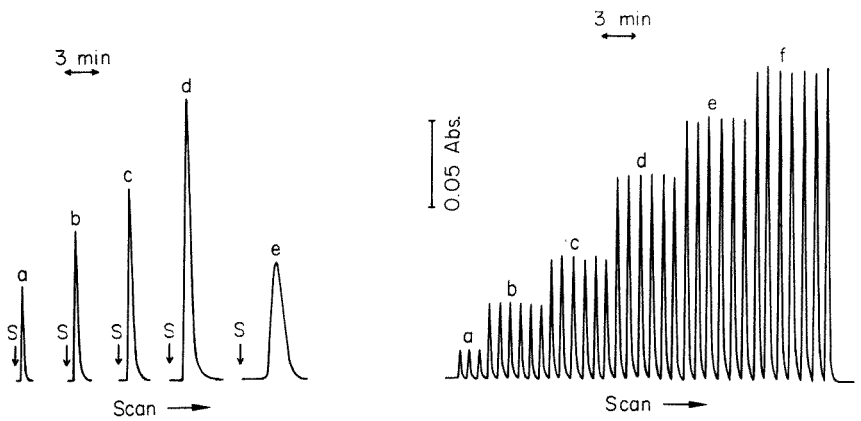

Fig. 4. Effect of the pumping rate and inner diameter of the reaction coil on the peak height and shape for 10-μl injections of 100 ppb Co solution, with equal flow rates for hydrogen peroxide and SPADNS: (a) 0.75; (b) 0.5; (c) 0.35; (d) 0.23; (e) 0.5 ml min^{-1}. Tubing internal diameter: (a)—(d) 0.5 mm; (e) 1.0 mm. Samples are injected at point S; other experimental conditions and manifold as in Fig. 1.

Fig. 5. Typical continuous signal traces for cobalt (0—200 ppb) by continuous flow with 10-μl samples. (a) Blank; (b) 0.25 ng; (c) 0.50 ng; (d) 1.0 ng; (e) 1.5 ng; (f) 2.0 ng of cobalt. Temperature of reaction coil, 30°C.

without further significant dispersion of the sample zone, in contrast to flowing through a longer reaction coil at a low flow rate. Usually, the sample zone is stopped within the measurement cell and a broad signal is observed, in contrast to the sharp signal obtained in the normal continuous flow mode [2, 7—9]. In this work, the sample zone was stopped within the reaction coil, and a sharper, more sensitive peak was obtained, as shown in Fig. 6.

Calibration graphs obtained by this are shown in Fig. 7. Linear graphs up to 100 ppb are obtained by injection of 10-μl samples for the continuous flow and stopped-flow (for 30 s) modes, but under the other conditions linear relationships were not observed. With this method, as little as 0.05 ng (5 ppb) of cobalt can be determined by injection of only a 10-μl sample solution. Satisfactory results for reproducibility with injection of 10-μl samples were obtained: the relative standard deviations were 2.0% (n = 10) for 100 ppb of cobalt by the continuous flow injection method and 2.5% (n = 14) for 50 ppb of cobalt in the stopped-flow mode. The method requires no complicated manipulation. The analytical signal is available within 50 s after sample injection, indicating a rate of analysis of ca. 60 samples per hour.

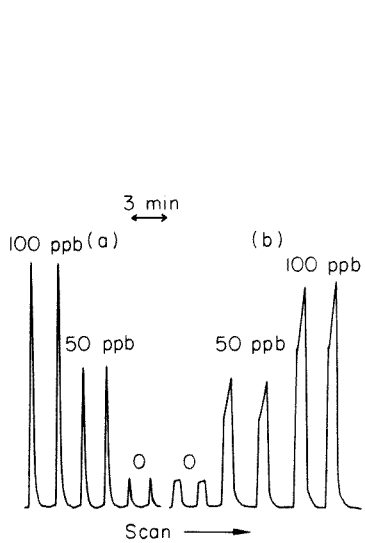

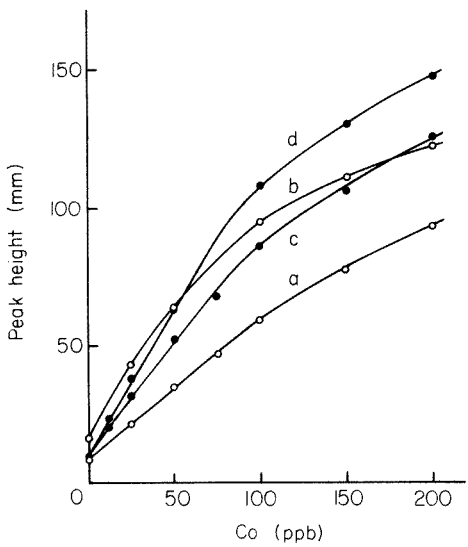

Fig. 6. Peak profile of different stopped-flow modes for injection of 10 μl of 0, 50 and 100 ppb cobalt solutions. Sample zone was stopped (a) in the reaction coil or (b) in the flow cell for 30 s (for details see text). Other experimental conditions and manifold as in Fig. 1.

Fig. 7. Calibration graphs for cobalt by (a, b) continuous and (c, d) stopped-flow techniques. Sample volumes were 10 μl for (a), (c), (d) and 20 μl for (b). The flow was stopped for 30 s for (c) and 60 s for (d). Other experimental conditions and manifold as in Fig. 1. Temperature of reaction coil, 30°C.

The author thanks Mr. K. Yamashita for his assistance in the experimental work.

REFERENCES

1 J. Růžička and E. H. Hansen, Anal. Chim. Acta, 78 (1975) 145.
2 J. Růžička and E. H. Hansen, Anal. Chim. Acta, 99 (1978) 37.
3 K. B. Yatsimirskii, Kinetic Methods of Analysis, Pergamon, Oxford, 1966.
4 H. A. Mottola, CRC Crit. Rev. Anal. Chem., 4 (1975) 229.
5 T. Yamane and T. Fukasawa, Anal. Chim. Acta, 119 (1980) 389.
6 H. Bergamin F°, B. F. Reis and E. A. Zagatto, Anal. Chim. Acta, 97 (1978) 427.
7 J. Růžička and E. H. Hansen, Anal. Chim. Acta, 114 (1980) 19.
8 J. Růžička and E. H. Hansen, Anal. Chim. Acta, 106 (1978) 207.
9 A. Ramsing, J. Růžička and E. H. Hansen, Anal. Chim. Acta, 114 (1980) 165.

Analytica Chimica Acta, 130 (1981) 73—79
Elsevier Scientific Publishing Company, Amsterdam — Printed in The Netherlands

FLUORIMETRIC DETERMINATION OF MAGNESIUM BY TERNARY COMPLEX FORMATION WITH PYRIDOXAL NICOTINYLHYDRAZONE AND AMINES

M. A. CEJAS, A. GOMEZ-HENS and M. VALCARCEL*
Department of Analytical Chemistry, Faculty of Sciences, University of Cordoba (Spain)
(Received 17th March 1981)

SUMMARY

The synthesis, characteristics and analytical applications of pyridoxal nicotinylhydrazone are described. This compound reacts with magnesium(II) in the presence of ammonia, ethylenediamine or pyridine, to produce a 1:1:1 Mg(II)—pyridoxal nicotinylhydrazone—amine fluorescent complex (λ_{ex} 395 nm, λ_{em} 480 nm). A fluorimetric method is proposed for the determination of magnesium(II) (20—100 ng ml^{-1} in the solution measured); isobutanol is used to extract the complex, reducing the number of interferences.

Pyridoxal and its derivatives have been used for biochemical purposes but little is known about their value in inorganic analysis. Some derivatives have been used as photometric reagents: pyridoxal thiosemicarbazone is suitable for determinations of iron(III) and cobalt(II) [1], pyridoxal-2-pyridylhydrazone for the determination of vanadium(V) [2], and pyridoxal salicylylhydrazone for determinations of zirconium(IV), titanium(IV) and aluminium(III) [3]. Pyridoxal azine has been synthesized [4] but is too insoluble for use as a reagent. Pyridoxal nicotinylhydrazone (PNH, I) is proposed here as a new fluorimetric reagent in inorganic analysis, particularly for the determination of magnesium

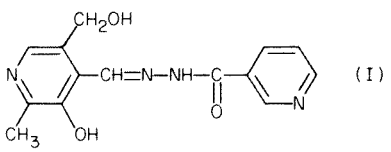

(I)

Many methods have been proposed for the fluorimetric determination of magnesium [5]. Generally, alkaline media are required and a preliminary extraction is often advised. Ethylenediamine or some other amine is frequently used in these methods, although the role of the amine has not been clarified in most cases. For example, in the method with 2,3-bis(salicylindeneamino)-benzofuran [6], a diethylamine—hydrochloric acid buffer solution of pH 10.5 was used, and when preliminary extraction was necessary, diethylamine or pyridine was added to the aqueous phase. In determinations of magnesium(II) with 8-quinolinol [7—9] or its sulfonate [10—13], triethanol-

amine, ammoniacal and Tris buffer solutions have been used. A 1:2:1 ternary complex of magnesium—8-quinolinol—pyridine has been indicated [14].

Several *o,o'*-dihydroxyazo compounds have been described as fluorimetric reagents for magnesium [15]; *o,o'*-dihydroxyazobenzene has been applied for magnesium in water, blood serum, urine [16, 17] and soils [18] and ethylenediamine has been used in these systems. Of course, many other fluorimetric determinations of magnesium do not involve amines [14].

EXPERIMENTAL

Apparatus and reagents

A Perkin-Elmer MPF-43 spectrofluorimeter was used with 1-cm quartz cells and the xenon arc source. The instrument was standardized with a 1 μg ml^{-1} solution of quinine (λ_{ex} 350 nm, λ_{em} 450 nm). Slit widths were 6 nm for all measurements. A Perkin-Elmer Model 599 spectrometer with a temperature programmed cell was used for infrared studies.

Pyridoxal nicotinylhydrazone was used as a 0.05% (w/v) solution in ethanol. A magnesium(II) stock solution (1 mg Mg ml^{-1}) was prepared from magnesium nitrate and standardized by titration with EDTA. Working solutions were prepared daily by suitable dilution. All solvents and reagents were of analytical-reagent grade.

Synthesis of pyridoxal nicotinylhydrazone. Dissolve pyridoxal hydrochloride (1 g) in 120 ml of water and neutralize with 1 M sodium hydroxide solution. Add 0.69 g of nicotinic acid hydrazide in 40 ml of ethanol, reflux for 1 h and cool to 0°C. Filter off the yellow product and recrystallize from aqueous 50% ethanol (yield 81.7%). [Calculated for $C_{14}H_{14}O_3N_3 \cdot 3H_2O$, 49.4% C, 5.9% H, 16.1% N; found 48.9% C, 5.8% H, 16.4% N.]

Procedures

Direct method. To a 25-ml volumetric flask, containing a sample or standard solution with 0.5—2.5 μg of magnesium, add 0.5 ml of 0.05% PNH solution and 1.25 ml of 0.6 M ammonia solution, and dilute the mixture to the mark with distilled water. Measure the fluorescence intensity (λ_{ex} 395 nm, λ_{em} 480 nm) against a reagent blank prepared in a similar manner without magnesium.

Extraction method. To 0.5—3.5 ml of sample or standard solution containing 0.5—2.5 μg of magnesium in a separating funnel, add 0.2 ml of 0.05% PNH solution, 0.25 ml of 0.6 M ammonia solution and 1 ml of 1 M sodium perchlorate, and dilute to 5 ml with distilled water. Extract the mixture with 20 ml of isobutanol by shaking for 3 min. Allow the phases to separate, transfer the organic layer to a 25-ml flask, and dilute to the mark with ethanol. Measure the fluorescence intensity (λ_{ex} 395 nm, λ_{em} 480 nm) after 1 h against a reagent blank prepared in a similar manner without magnesium. The measured solution contains 20—100 ng Mg ml^{-1} for the calibration graph.

RESULTS AND DISCUSSION

Properties of the reagent

The infrared spectra of PNH in KBr disks were obtained at 20°C, and the bands were assigned to the stretching vibrations of hydroxyl (3480 cm^{-1}), N—H (3000—3200 cm^{-1}), C=O (1670 cm^{-1}), C=C and N=C in the rings (1610 cm^{-1}), CONH (1575 cm^{-1}), C=N (1300 cm^{-1}) and phenolic hydroxyl (1170 cm^{-1}). The presence of water in the reagent molecule was proved by i.r. spectroscopy with a temperature-programmed cell. Increase of temperature caused the i.r. spectra to show slight variations in some stretching vibrations, which are possibly due to hydrogen bonding between water and PNH, and a sharp decrease of the OH band of water (3480 cm^{-1}) in the temperature range 90—120°C (Fig. 1). This "thermogram" allows the conclusion that water is removed at 90—120°C.

The reagent is very soluble in ethanol and dimethylformamide (40 g l^{-1}). The solubilities in methanol, acetone, isoamyl alcohol and water are 11.8, 8.6, 5.9 and 2.0 g l^{-1}, respectively.

A 5.6×10^{-4} M PNH solution in 4% ethanol shows an absorption maximum at 300 nm (pH 5.8). In acidic medium, the absorbance decreases and there is a bathochromic shift; in alkaline medium, there is also a bathochromic shift but a new absorption band appears at 400 nm. These absorption spectra remained stable for at least 6 h.

A simultaneous potentiometric/photometric method was used to determine the ionization constants in 22% ethanolic solution; the average pK values found were 4.6 ± 0.1 and 8.0 ± 0.1. These values were determined by the Stenstrom and Goldsmith procedure [19]. The first pK value probably corresponds to the protonated pyridine nitrogens and the second to the hydroxyl group. The reagent spectra showed important shifts when oxidizing agents (e.g., persulfate and metaperiodate) and reducing agents (e.g., ascorbic acid) were added in acidic and alkaline media in 15:1 ratios to PNH. PNH is resistant to hydrolysis of the =C=N— groups at any pH.

The reactions of the reagents with 46 inorganic ions at various pH values were investigated. Only the titanium(IV)—PNH complex formed in acidic media has any analytical interest for spectrophotometry (Table 1).

Fluorimetric aspects of PNH

Reagent solutions show a green fluorescence in the pH range 4.0—8.5 and exhibit maximum fluorescence intensity at pH 6.5—7.5 (λ_{ex} 395 nm, λ_{em} 480 nm). The reagent does not fluoresce in sodium hydroxide solutions at pH >8.5, but shows a yellow fluorescence (λ_{ex} 300 nm, λ_{em} 380 nm) in ammoniacal buffers (Fig. 2). The fluorescence intensity of the reagent solutions remained constant for 8 h under these conditions.

A potentiometric/fluorimetric method was used to determine the ionization constant in water—ethanol medium (24:1). The average pK values found, by the method of Bridges et al. [20], were 5.5 and 8.4; these values are similar to those found spectrophotometrically.

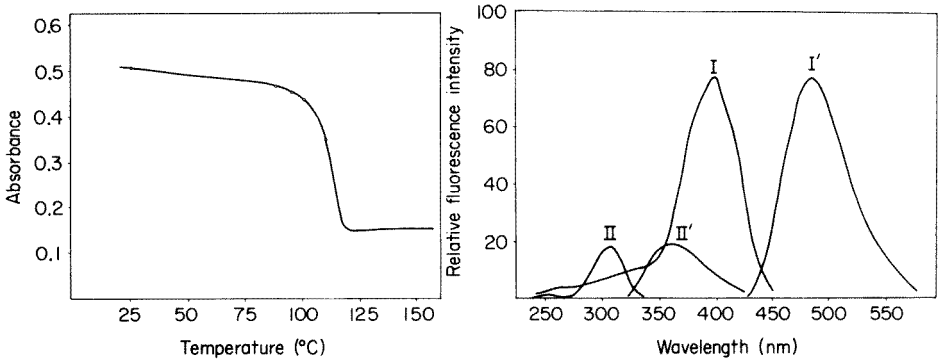

Fig. 1. Effect of temperature on the absorbance of the OH band at 3480 cm^{-1}.

Fig. 2. Fluorescence spectra of 6×10^{-5} M PNH solutions. (I) Excitation spectrum (λ_{em} = 480 nm) for acetate buffer solution pH 5.0; (I') emission spectrum (λ_{ex} = 395 nm) for acetate buffer solution pH 5.0. (II) Excitation spectrum (λ_{em} = 365 nm) for ammonia—ammonium chloride buffer solution pH 10.0; (II') emission spectrum (λ_{ex} = 300 nm) for ammonia—ammonium chloride buffer solution pH 10.0. The spectra are uncorrected (sensitivity, 0.3).

The fluorescent reactions of the reagent with 46 inorganic ions at various pH values were investigated. The salient results (Table 2) indicate that only the Mg(II) and Zn(II) complexes have interesting fluorescent reactions.

Spectrofluorimetric study of magnesium—PNH—amine systems

The excitation spectrum of magnesium with PNH in ammonia—ammonium chloride buffer shows two bands at 320 nm and 395 nm (λ_{em} 480 nm), and emission spectrum one band at 480 nm (λ_{ex} 395 nm) (Fig. 3). Both spectra show a slight instability probably because of the quenching effect of the chloride ions. In sodium or potassium hydroxide solutions, magnesium does not form a fluorescent complex with PNH, unless ammonia or an amine (e.g., ethylenediamine or pyridine) is present, so that ternary complex formation becomes possible. The reagent itself does not fluoresce significantly

TABLE 1

Spectrophotometric characteristics of PNH complexes in solution

Metal ion	pH	λ_{max} (nm)	Molar absorptivity ($\times 10^3$ l mol^{-1} cm^{-1})
Cu(II)	3.3	400	7.3
Fe(II)	4.6	380	4.0
Fe(III)	3.3	395	8.7
Ni(II)	4.6	425	7.2
Zr(IV)	3.3	410	3.6
Ti(IV)	2.3	410	8.0

TABLE 2

Fluorimetric characteristics of PNH complexes in pH 10 solution

Metal ion	λ_{ex} (nm)	λ_{em} (nm)	Intensity (%)
Zn(II)	420	490	100
Mg(II)	395	480	90
Mn(II)	400	480	17
Pd(II)	420	490	14

at these wavelengths in such media. The excitation and emission spectra of the ternary magnesium—PNH complex in 3×10^{-2} M ammonia solution remain stable for at least 3 h. Increasing concentrations of ethanol and decreasing temperatures increase the fluorescence intensity. With 4% ethanol in the mixture at 20 ± 0.1°C, good analytical results can be obtained. The order of addition of the reagents does not affect the complex formation.

The linear calibration graphs obtained for 0.5—2.5 μg of magnesium showed the greatest sensitivity with reagent concentrations in the range 3.0—6.0 $\times 10^{-5}$ M. Relative decreases in the fluorescence intensity were observed for higher and lower reagent concentrations.

Stoichiometry of the complex. The stoichiometry of the magnesium(II)—PNH—amine complex was evaluated by the continuous variations and molar ratio methods. The former method was applied to determine the Mg(II):PNH ratio with a constant excess of amine (ethylenediamine or ammonia) and varying concentrations of magnesium and PNH. The ratio found was 1:1 (Fig. 4).

The Mg(II):amine ratio was evaluated by the molar ratio method; the concentration of PNH was kept constant and in excess. As a change in the amine concentration would affect the pH, the amine concentration (ammonia, ethylenediamine or pyridine) was kept constant and the magnesium concentration was varied. The Mg(II):amine ratio was found to be 1:1 in all cases. With the same method, the PNH:amine ratio was determined in the

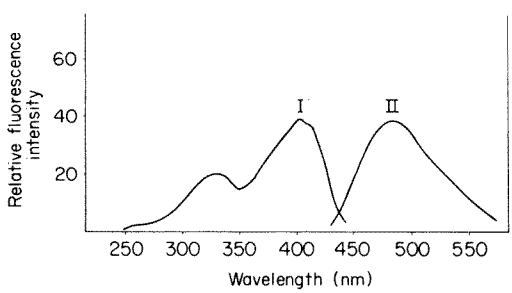

Fig. 3. Fluorescence spectra of the magnesium complex in ammonia—ammonium chloride buffer solution pH 10.0. (I) Excitation spectrum (λ_{em} = 480 nm); (II) emission spectrum (λ_{ex} = 395 nm). The spectra are uncorrected (sensitivity, 0.3).

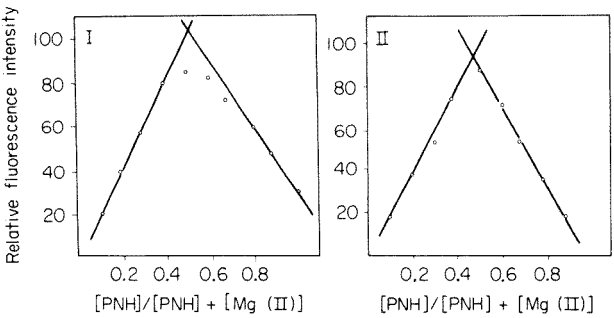

Fig. 4. Continuous variations method for the PNH—Mg(II) ratio with 5×10^{-5} M PNH and 5×10^{-5} M magnesium sulfate solutions. (I) with 10^{-3} M ethylenediamine present; (II) with 10^{-3} M ammonia present.

presence of a constant excess of magnesium(II); here the PNH concentration was changed and the amine concentration kept constant to avoid large pH variations. The ratio found was 1:1.

This study indicated that the stoichiometry for the different mixed complexes Mg(II)—PNH—amine is 1:1:1. The reagent probably acts as a terdentate ligand, the amine taking the fourth coordinated bond of the magnesium(II) ion.

Extraction of the complex. When an ammoniacal solution of magnesium with PNH is shaken with isobutanol, the complex can be extracted quickly and completely. The optimum volume ratio of the organic to aqueous phases is 4:1.

The optimum volume of 0.6 M ammonia solution is 0.25 ml. This provides a pH of about 10; the tolerable pH range for full development of the fluorescence is 9.8—10.2. The optimum reagent concentration is 0.2 ml of 0.05% (w/v) PNH solution. After 1 h, the fluorescence intensity of the complex remains stable for at least 2 h. Sodium perchlorate (0.1 g) acts as a salting-out reagent.

Spectrofluorimetric determination of magnesium

Direct method. There is a linear relation between the emitted fluorescence intensity and the magnesium(II) concentration between 20 and 100 ng Mg ml^{-1} in the final solution. When the recommended procedure was applied to two series of 10 samples (50 and 100 ng ml^{-1}) the relative standard deviations (P = 0.05) on the method were found to be ±1.8 and ±1.3%, respectively. When this direct method is applied, interferences are numerous.

Extraction method. The calibration graphs were linear over the same range of magnesium concentration as in the direct method, and the relative standard deviations at the 50 and 100 ng ml^{-1} levels were ±1.5 and ±1.4%, respectively (n = 10). The extraction procedure improves remarkably the selectivity of the method. The tolerance limits of different species in the magnesium determination are listed in Table 3. Magnesium can be determined

TABLE 3

Tolerance limits in the determination of 0.5 μg of magnesium(II) in 10 ml of solution

Amount added (μg/5 ml)	Species tolerated
10	Hg(II), In(III), Na, K, Ba, V(V), Hg(I), W(VI), U(VI), Be, Pb, Ga, Ti(IV), Cd, Mo(VI), Sn(II), Bi(III), Cl^-, F^-, I^-, BrO_3^-, IO_3^-, SO_3^{2-}, SCN^-, CN^-, SO_4^{2-}, citrate, tartrate
8	Ca, Fe(III)
5	Al, Mn(II), Zr(IV), PO_4^{3-}, EDTA
0.5	Co(II), Cu(II), Fe(II)

in the presence of a 16-fold amount of calcium, which is of interest because calcium is an important interference in many determinations of magnesium. The most serious interferences are from zinc(II) and nickel(II) that interfere at equal concentrations with magnesium (Table 2).

REFERENCES

1 D. Pérez Bendito and M. Valcárcel, Afinidad, 366 (1980) 123.
2 S. Rubio, A. Gómez Hens, M. Valcárcel, An. Quím., in press.
3 M. Gallego, Ph. D. Thesis, Univ. of Córdoba, 1980.
4 D. Luque, Ph. D. Thesis, Univ. of Sevilla, 1976.
5 R. A. Passwater, Guide to Fluorescence Literature, Plenum, Data Division, New York, Vol. 1 (1967), Vol. 2 (1970), Vol. 3 (1974).
6 R. M. Dagnall, R. Smith and T. S. West, Analyst, 92 (1967) 20.
7 S. Watanabe, W. Frantz and D. Trottier, Anal. Biochem., 5 (1963) 345.
8 S. Watanabe, T. Trosper, M. Lyun and L. Eveson, J. Biochem. (Tokyo), 54 (1963) 17.
9 D. P. Shcherbov, R. N. Plotnikova and T. N. Skvortsova, Prom. Khim. Reakt. Osobo Chist. Veshchestv, 8 (1967) 166.
10 D. Schachter, J. Lab. Clin. Med., 58 (1961) 495.
11 R. E. Thiers, Standard Methods of Clinical Chemistry, Vol. 5, p. 131. Academic Press, New York, 1965.
12 V. Petrovsky, Collect. Czech. Chem. Commun., 32(7) (1967) 2656; Fresenius Z. Anal. Chem., 230 (1967) 355.
13 B. Klein and M. Oklander, Clin. Chem., 13 (1967) 26.
14 F. D. Snell, Photometric and Fluorimetric Methods of Analysis, Vol. 2, 1938, J. Wiley, New York, 1978.
15 R. Olsen and H. Diehl, Anal. Chem., 35 (1963) 1142.
16 H. Diehl, R. Olsen, G. I. Spielholtz and R. Jensen, Anal. Chem., 35 (1963) 1144.
17 M. Breen and R. T. Marshall, J. Lab. Clin. Med., 68(4) (1966) 701.
18 R. A. Swanson, D. Hovland and L. O. Fine, Soil Sci., 102(4) (1966) 244.
19 W. Stenstrom and N. Goldsmith, J. Phys. Chem., 30 (1926) 1683.
20 J. W. Bridges, D. S. Davies and R. T. Williams, Biochem. J., 98 (1966) 451.

Analytica Chimica Acta, 130 (1981) 81—91
Elsevier Scientific Publishing Company, Amsterdam — Printed in The Netherlands

DETERMINATION OF BIODEGRADED LIGNIN BY ULTRAVIOLET SPECTROPHOTOMETRY

H. JANSHEKAR, C. BROWN and A. FIECHTER*

Chair of Microbiology, Swiss Federal Institute of Technology, ETH-Hönggerberg, CH 8093 Zürich (Switzerland)

(Received 11th March 1981)

SUMMARY

The characteristic absorption bands of lignin in the ultraviolet range of the spectrum are used for the determination of residual free lignin in broth cultures. The effects of medium composition, pH, biomass, metabolite production and some lignin-related aromatic compounds are reported.

Lignin together with cellulose and hemicellulose is one of the major constituents of the tissues of woody plants being decomposed in the soil. It is a highly branched, irregular three-dimensional organic polymer containing many types of chemical linkage between its phenyl propanoid units. Raw material and energy shortage on the one hand, and mounting environmental pollution on the other hand, have led to a growing interest in the potential use of micro-organisms for the bioconversion of plant residues or lignin-containing industrial waste. The study of lignin biodegradation requires an accurate method of measuring lignin concentration during delignification of broth. At present, there is no definitive method on which assays of biodegradation can be based. This is because in comparison to the biodegradation of other biopolymers, such as proteins, carbohydrates and lipids, etc., the biodegradation of lignin involves several changes in its molecular structure which cannot be detected by a single chemical method.

Many methods have been suggested for the determination of lignin in plant materials [1]. Lignin may be determined directly or indirectly. In direct methods such as those based on mineral acid or alkali, lignin is isolated directly or after dissolution and measured as an insoluble residue. In indirect methods such as the methoxyl or Metha's colorimetric methods, a characteristic group or a characteristic chemical reaction of lignin is assayed. Polysaccharides, pectins, proteins, fats, waxes, resins, tannins, colouring matter, and other organic and inorganic compounds not derived from lignin can interfere with these lignin determinations. Therefore, the above-mentioned methods of lignin determination have been subjected to many modifications [2]. So far, however, attention has been concentrated on the measurement of the lignin content of plant materials and pulps.

For the determination of lignin in a biological system, there are several factors that must be considered, including medium constituents, the presence of biomass, the nature of the organism under investigation, the pH of the medium required for growth, etc. The isolated lignin used in microbial culture is often very finely divided and cannot be filtered easily. Separation of lignin from growing mycelial pellets presents a further problem, and in addition not all of the lignin present may be found in an insoluble form. Therefore, dry weight techniques cannot be accurate.

In the work described here, the effects of microbial growth were investigated and a method of sample preparation was developed that allows the characteristic u.v. spectrum of lignin to be used in measuring the concentration of free lignin in a biological system.

EXPERIMENTAL

Lignins and organisms

The lignins used in this study were of four types each of which was extracted by a different method: cold dioxane—hydrochloric acid lignin [3]; hot dioxane—hydrochloric acid lignin [4]; alkali lignin isolated by treatment with 1% sodium hydroxide at 121°C for 1 h; and commercially available Kraft pine lignin polymer (Indulin AT; Westvaco Co., Charleston, SC).

The air-dried straw used for lignin isolation was ground to pass a screen of about 24 mesh.

The following organisms which are quoted as having lignocellulosic activity were studied [5—8]: *Nocardia autotrophica* (DSM 43099), *Nocardia opaca* (DSM 43002), *Nocardia asteroides* (DSM 43003), *Pseudomonas putida* (DSM 50906), *Trichoderma reesei* (QM 9414), *Chaetomium cellulolyticum* (ATCC 32319), *Sporotrichum pulverulentum* (ATCC 24725).

Solutions and procedure

Lignin was added to the following basal medium used for cultivation of micro-organisms. The medium contained per l of distilled water: K_2HPO_4, 1.60 g; KH_2PO_4, 0.50 g; $(NH_4)_2SO_4$, 1.25 g; NH_4NO_3, 1.00 g; $MgSO_4 \cdot 7H_2O$, 0.50 g; NaCl, 0.25 g; $FeCl_3 \cdot 6H_2O$, 25 mg; $CaCl_2$, 10 mg; yeast extract (Difco), 0.10 g. A nitrogen-limited medium also used was identical to that above with the exception that the nitrogen-containing salts were present at one-tenth of the above-mentioned masses.

For lignin determination homogenized samples were mixed with equal volumes of dioxane for u.v. spectrophotometry. For mycelial cultures the samples were then sonicated for 10 s. The solution was then allowed to stand overnight at room temperature. After centrifugation (5000 rpm, 10 min), 0.15 ml of the supernatant liquid was mixed with 1.85 ml of a solution of dioxane/water (1:1 v/v). The absorbance of the resulting solution was read at 281 nm in a cell with a 1-cm light path against a dioxane/water (1:1 v/v) reference.

Some organisms may produce metabolites which could interfere with the absorption spectrum of lignin. In this case the culture may be purified by the following method. A portion (35 ml) of a homogenized culture is transferred to a centrifuge tube and its pH is reduced to 3 with hydrochloric acid. The solution is left to stand overnight. It is then centrifuged and the residue is washed twice with distilled water at pH 3; centrifugation is at 20000 rpm for 30 min. The first supernatant liquid may be assayed to check for lignin soluble at pH 3. To the residue remaining after centrifugation are added 1 ml of distilled water and 7 ml of dioxane. The solution is sonicated and then allowed to stand overnight at room temperature. The volume is adjusted to 10 ml with distilled water and then the solution is centrifuged (5000 rpm, 10 min). An aliquot (1 ml) of the resulting supernatant liquid is added to 6 ml of a dioxane—water solution (4.66 ml/10 ml H_2O), and 0.15 ml of this solution is further diluted as mentioned above.

The reference solutions of lignin must be treated in the same manner as samples.

Cultures were homogenized in a kinetic high-frequency apparatus; a model B12 sonifer (Branson Sonic Power Co., Danbury) was used for sonication.

RESULTS

Lignin solutions gave characteristic absorption bands in the ultraviolet range indicating that they possess identical basic structures (Fig. 1). The absorption decreases from a maximum below 240 nm to a minimum at about 260 nm; the next maximum at 281 nm is followed by a gradual decrease towards the visible range of the spectrum. The acidolysis lignins (curves A and B) show another but lower peak at 315 nm.

Although there are many conflicting interpretations [9], the band at 281 nm is possibly due to the unsubstituted *m*-position in the benzene ring, and the band near 310 nm to a carbonyl bond or an ethylene type double bond in conjunction with a benzene nucleus. It has also been reported that within the guaiacyl groups of the lignin polymer, the partly etherified hydroxyl groups may be responsible for the absorption maximum at about 281 nm [2]. Although the differently isolated lignins showed the same characteristic absorption band at 281 nm, the intensity of absorption varied (Fig. 1). The absorbance at 281 nm (and at 315 nm for acidolysis lignins) was found to follow Beer's law with all lignins investigated during this study. Calibration curves illustrating the relationship between absorbance and concentration for cold dioxane—hydrochloric acid lignin are presented in Fig. 2.

Table 1 shows the specific absorptivity of the examined lignins at 281 nm. Different lignins have different absorptivities. The choice of the reference substance should be made accordingly. Deviations arise from pipetting of samples and solvents, but more important contributing factors are the degree of homogeneity of the lignin suspension, and the uniformity of the lignin

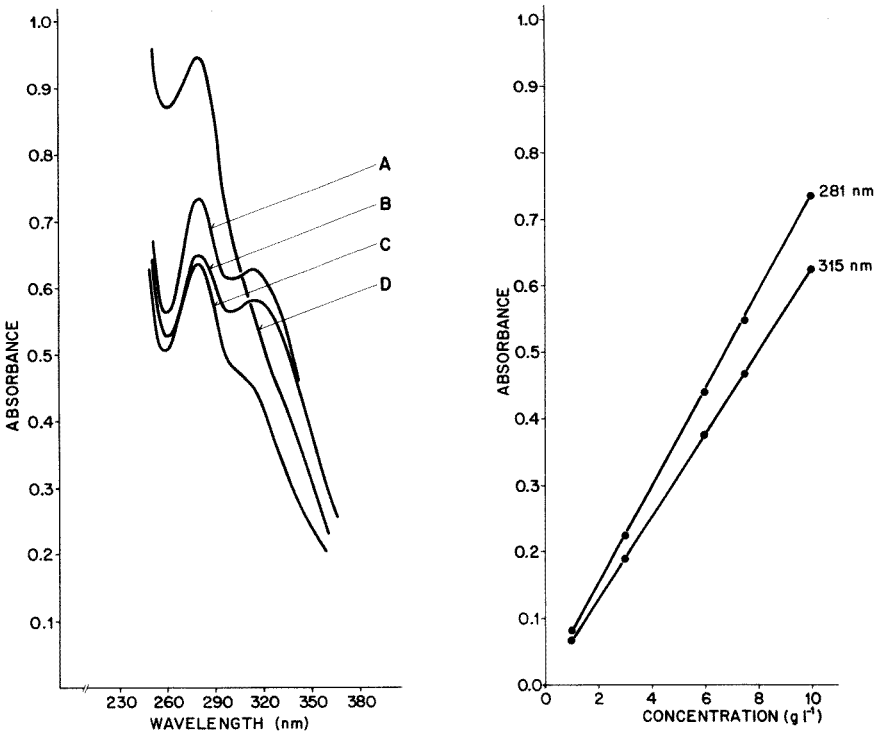

Fig. 1. Absorption spectra for different lignins: (A) cold dioxane—hydrochloric acid lignin; (B) hot dioxane—hydrochloric acid lignin; (C) alkali lignin; (D) indulin AT. Lignin concentration in original samples was 1 g l^{-1}.

Fig. 2. Calibration curves showing the Beer's Law relationship. The abscissa presents the lignin concentration in the original solutions (see Experimental).

TABLE 1

Specific absorptivities at 281 nm for lignins extracted differently
(The absorptivities are the mean value of 15 samples taken from a 1 g l^{-1} lignin solution)

Lignins	Absorptivity ± standard deviation ($l\ g^{-1}\ cm^{-1}$)
Cold dioxane—hydrochloric acid	19.3 ± 0.21
Hot dioxane—hydrochloric acid	16.9 ± 0.21
Sodium hydroxide	16.6 ± 0.21
Indulin AT	24.8 ± 0.21

particles in the medium from which the samples are taken. Lignin can be bound by the hyphae of some organisms and become entrapped in the fungal pellets as they are formed. Erroneous lignin measurements may also be due to surface adsorption by the mycelia. Table 2 shows the effect of homo-

TABLE 2

Effect of homogenization and sonication of the culture on measurement of degraded alkali lignin
(*Sporotrichum pulverulentum* was grown in standing nitrogen-limited cultures under pure oxygen at 38°C for 14 days. The lignin content was measured as described and was compared to that of an uninoculated but similarly treated culture. Values are the per cent of degraded lignin.)

No homogenization or sonication	Homogenization only	Homogenization and sonication
42—59	32—33	22—25

genization and sonication during assays of alkali lignin degraded by *Sp. pulverulentum*. It can be seen that homogenization alone of the culture cannot release all the entrapped or adsorbed lignin. Sonication should be done in the solvent (dioxane—water).

Effects of medium composition

The composition of a culture medium may influence the lignin determination. The following factors may be involved.

Mineral salts and trace elements which are necessary for the metabolic activity of micro-organisms can affect the assay. As is shown in Fig. 3, when the basal medium concentration is increased above the level indicated in the text, the absorbance of the solution increases in the wavelength range examined and can cause erroneous results. If an increase in medium concen-

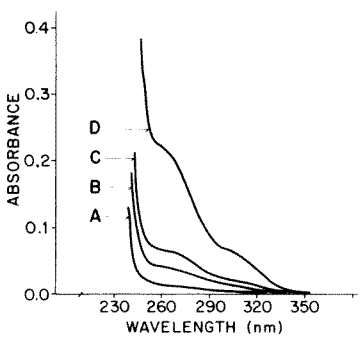

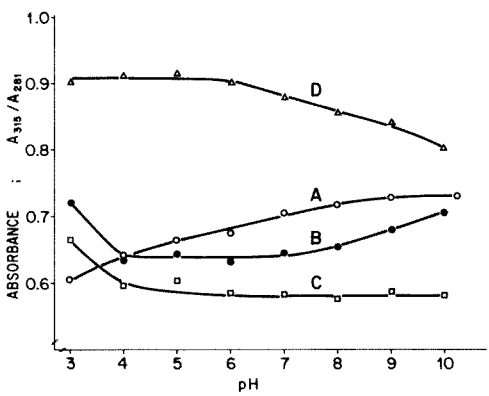

Fig. 3. Absorption spectra of basal medium at different concentrations: (A) composition of the medium as under Solutions; (B, C, and D) 2, 3.25, and 12.5 times more concentrated, respectively.

Fig. 4. Variation in absorbance of lignin with pH: (A) absorbance of alkali lignin at 281 nm; (B, C) absorbance of cold dioxane—hydrochloric acid lignin at 281 and 315 nm, respectively; (D) relative absorptivity (A 315/A 281).

tration is required, the lignin content of samples should be compared with an uninoculated sample of identical medium concentration and the assay should by preceded by purification as already described.

Proteinaceous materials may be present in the fluid phase of the samples; these can be either of extracellular origin or the result of cell rupture and disintegration. Additionally, the medium may contain carbohydrates to serve as a growth substrate supporting lignin metabolism. Lignin itself may contain some impurities, e.g., from incomplete removal of extractants with organic solvents. Extraction of wood with organic solvents should remove a broad spectrum of extraneous components such as polysaccharides, pectins, fats, waxes and resins. Some impurities may arise from the condensation of intermediate products with lignin such as furfuraldehyde which may be formed during lignin extraction. The effects of such compounds on lignin absorptivity are shown in Table 3. Addition of these compounds to the medium did not change the position of the maximum in the absorption band. Considering the standard deviation of the absorptivity of lignin, it can be concluded that carbohydrates, pectin, uronic acid, saturated fatty acids and protein in the tested concentrations do not affect the lignin measurement. The effects of unsaturated fatty acids, resin acid and yeast extract at low concentration may be negligible. Tannic acid and furfural cause severe interference with the lignin determination. However, furfural can be reduced by the treatment of lignin with hot water, if necessary.

TABLE 3

The effect of different compounds on the absorptivity of lignin
(The compounds were added to a medium containing 1 g l^{-1} dioxane—acid extracted lignin. The absorbance was measured at 281 nm after treatment of the samples as described in the text. The standard deviation for the absorptivity of lignin standard solution is ±0.21 l g^{-1} cm^{-1}.)

Compound	Amount added (g l^{-1})	Change in absorptivity (l g^{-1} cm^{-1})	Compound	Amount added (g l^{-1})	Change in absorptivity (l g^{-1} cm^{-1})
Glucose	1	+0.03	Linoleic acid	0.25	+0.90
Maltose	1	—0.13	Galacturonic acid	0.25	—0.21
Fructose	1	+0.18	Lauric acid	0.25	+0.05
Galactose	1	+0.08	Abietic acid	0.25	+0.77
Mannose	1	+0.11	Furfural	0.25	+49.57
Xylan	1	+0.11	Benzaldehyde	0.25	+1.60
Avicel-cellulose	1	+0.12	Bovine albumin	0.25	+0.20
Starch	1	—0.14		1	+0.14
Urea	1	—0.03		5	+0.17
Pectin	0.25	+0.19	Yeast extract	0.25	+0.62
Tannic acid	0.25	+13.87			

Effect of pH

As a result of the metabolic activity of the cells, the pH of the culture may change. The effect of the pH of the samples on the absorbance observed with alkali and dioxane—acid lignin is shown in Fig. 4. For alkali lignin, the absorbance increases steadily as the pH is increased from 3 to 9. For dioxane—acid lignin, the absorbances at 281 and 315 nm decrease between pH 3 and 4 and then remain unchanged up to pH 7. A further increase in the pH increased the absorbance at 281 nm whilst that at 315 nm was unaffected, causing a decrease in relative absorbance (A_{315}/A_{281}). Thus it may be necessary to adjust the pH of the samples prior to lignin determination if the pH of the culture changes to any great degree.

Effects of cellular growth

Addition of solvent (dioxane) to the samples may affect the cell wall, causing dissolution and the introduction into the solution of cell matter that influences the absorption band of lignin. This was investigated by the addition of different organisms to the standard lignin solution. The results are shown in Table 4. A low concentration of cells (0.5 g l^{-1}) caused little or no interference. However, the higher cell concentration (1.5 g l^{-1}) of some of the organisms caused an increase in the observed absorptivity of lignin at 281 nm. For example, the presence of 1.5 g l^{-1} *Ch. cellulolyticum* in a sample caused an overestimation of about 7% in lignin concentration.

Additional interference may be caused by the presence of metabolites. Metabolic compounds formed during the period of cultivation or originating from the inoculum may absorb light in the range used for lignin determination. These extracellular compounds cannot be modified. Their nature depends on many factors including the organism, culture condition, composition of growth medium, age of the culture, etc. As an example, Fig. 5 shows how

TABLE 4

The effect of different organisms on the absorptivity of lignin
(Two different quantities of freeze-dried cells (0.5 and 1.5 g l^{-1}) were added to a medium containing 1 g l^{-1} dioxane—acid extracted lignin. The absorbance was measured at 281 nm after treatment of the samples as mentioned in the text. Standard deviation for absorptivity of lignin standard solution is ±0.21 l g^{-1} cm^{-1}.)

Organism	Change in absorptivity (l g^{-1} cm^{-1})	
	0.5 g l^{-1}	1.5 g l^{-1}
Ch. cellulolyticum	+0.08	+1.28
S. pulverulentum	+0.03	+1.01
T. reesei	+0.35	+1.15
P. putida	+0.13	+0.67
N. asteroides	0.00	+0.59
N. opaca	—0.19	+0.05
N. autotrophica	—0.16	+0.13

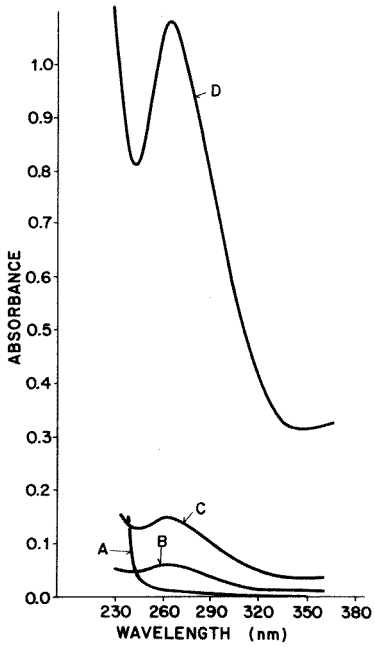

Fig. 5. Absorption spectra of basal medium after addition of supernatant liquid from a fungal culture. *T. reesei* was grown in medium no. 65, taken from the DSM catalogue (1977). After centrifugation of the culture, the supernatant liquid was added to the basal medium and the samples were treated as for lignin determination. Curves A—D represent 0, 5, 10, and 100% (v/v) addition, respectively.

significantly the spectrum of the medium can be influenced by addition of supernatant liquid from an already grown culture of *T. reesei*. Fortunately, microbial metabolites are usually water-soluble and can be separated by purification as already described.

Some aromatic compounds may be derived from the microbial degradation of lignin. Since the microbial depolymerization of lignin is a relatively new subject and the biopathways involved are almost unknown, it is not yet possible to predict which compounds could be formed as intermediates or products. However, so far, some compounds like vanillic, ferullic, syringic, *p*-hydroxybenzoic, *p*-hydroxycoumaric acids, vanillin, coniferaldehyde, syringaldehyde, and others have been isolated from the cultures [10]. Some authors believe that the low-molecular-weight intermediates do not accumulate in the culture and suggest a successive breakdown of lignin from terminals rather than extensive depolymerization and formation of low-molecular-weight intermediates [11]. Table 5 shows the absorptivity of some lignin-related aromatic compounds. The spectra of some of these compounds showed several peaks in the u.v. range. Only those peaks near the maximum absorbance band of lignin are considered here. Vanillin and pyrocatechol have the same maximum band as lignin (281 nm). All of these

TABLE 5

The maximum absorptivities (in l g^{-1} cm^{-1}) and corresponding wavelengths (in nm) of different lignin-related aromatic compounds in water at pH 3 and in 1:1 dioxane—water

Compound	Water pH 3		Dioxane—Water		Compound	Water pH 3		Dioxane—water	
	λ	Abs.	λ	Abs.		λ	Abs.	λ	Abs.
p-Coumaric acid	309	—[a]	312	155.8	4-Hydroxy-benzoic acid	259	137.4	258	119.0
Sinapinic acid	321	—[a]	318	76.2					
Syringic acid	275	59.8	277	61.8	Vanillin	279	82.6	281	85.4
Vanillic acid	260	67.6	263	94.0		309	73.0		
	293	35.0	292	50.2	Coniferyl alcohol	267	—[a]	268	83.8
Benzoic acid	276	10.2	250	15.2					
					Hydroquinone	291	29.6	295	27.2
					Pyrocatechol	277	29.0	281	32.6

[a]Not completely soluble.

compounds when present in the culture can cause overestimation of lignin concentration. However, if such compounds were present in the culture, it would be in trace quantities, and they can be washed and separated from the lignin by purification as already described. These compounds could then be detected and identified in the supernatant liquid knowing their absorptivities.

DISCUSSION

Table 6 compares the extent of the lignin degradation measured by the permanganate [12]. Acetyl bromide [1], and the proposed dioxane method. According to the recommendations for the first two methods, the sample size had to be optimized in each case and was not the same for the different methods. The sulfuric acid method as used for materials high in proteins [1] was also tried but could not be successfully completed because of the difficulties arising during the filtration of lignin solutions. Solubilization of the

TABLE 6

A comparison of the extent of lignin degradation measured by different methods (Lignin, organism and culture conditions were the same as in Table 2. Values are in per cent degraded lignin.)

Permanganate method	Acetyl bromide method	Dioxane method	
		Without purification	With purification
6—13	(—26) —64	22—25	41—43

culture in a 4 M solution of sodium hydroxide and absorbance measurements at 280 nm as described by Jungschaffer [13] indicated negative degradation showing the predominant effect of interfering substances. As shown in Table 6, the permanganate method has good repeatability but gives much lower results than the dioxane method. This may be because not only lignin but also other medium constituents such as metabolites and cell matter, are oxidized by potassium permanganate and affect the results. Enormous variation was observed between the results obtained by the acetyl bromide method. This happened in spite of taking precautions for the probable water contamination, the freshness of the digestion mixture, the grade of acetic acid used, and the time between dilution and measurement of absorbance which have been found to affect the reproducibility of the method [14]. In the dioxane method, besides the interfering effects of metabolites, which could explain the difference between the results obtained from the samples without and with preceding purification, some of the lignin could also be solubilized as a result of microbial attack showing a higher percentage of degradation for washed samples.

Dioxane is a solvent that does not contain chemically reactive groups. It is colourless, has no strong absorption bands of its own, and transmits the major portion (90—100%) of the incident radiation at 280—310 nm; it is completely miscible with water. It dissolves lignin completely and the absorbance maximum of the solution at 281 nm is not influenced by carbohydrates. These properties make dioxane an appropriate solvent in lignin determinations. Advantages of the method are that only small amounts of sample (35 mg of lignin or less) are needed, and that the total free lignin is determined spectrophotometrically in one step rather than as the sum of Klason and soluble lignin. The method is not time-consuming and shows good reproducibility. In the absence of background absorbance by interfering substances, the presence of as little as 4 mg l^{-1} can be determined. Carbohydrates and proteins show no appreciable absorption and their presence does not interfere with the absorption spectrum of lignin. The interference by basal media, cell materials, metabolites, and cell compounds present in the culture and soluble in dioxane—water can be eliminated by a washing step with water at pH 3 prior to the application of dioxane—water solvent. For lignin-related aromatic compounds like *p*-coumaric acid, sinapinic acid, coniferyl alcohol, etc., which, similar to lignin, are soluble in dioxane—water but insoluble in water at pH 3, other appropriate washing solutions or pretreatment methods should be used for their prior elimination from the lignin.

The decrease in absorbance at 281 nm in the spectrum of lignin as a result of microbial attack can only be attributed to cleavage of the aromatic ring structures within the polymer. Those lignin reactions such as dimethoxylation or metabolism of the side-chains in which the basic structural chromophores responsible for absorption at 281 nm are not involved, cannot be detected by this method.

This work was supported by a grant from Swiss Federal Institute of Technology, Zürich. The authors express their thanks to Mr. T. Haltmeier for valuable discussions during the work.

REFERENCES

1 B. L. Browning, Methods of Wood Chemistry, Vol. 2, J. Wiley, New York, 1967, pp. 785—798.
2 F. E. Brauns and D. A. Brauns, The Chemistry of Lignin, Academic Press, New York, 1960, p. 127 and 199.
3 E. Odier and B. Monties, Ann. Microbiol, Inst. Pasteur, 129A (1978) 361.
4 E. Odier and B. Monties, C. R. Acad. Sci. Paris, Ser. D, 284 (1977) 2175.
5 K. Haider, J. Trojanowski and V. Sundman, Arch. Microbiol., 119 (1978) 103.
6 M. Mandels, R. Andreotti and C. Roche, Biotechnol. Bioeng. Symp. No. 6. (1976) 21.
7 M. Moo-Young, D. S. Chahal and D. Vlach, Biotechnol. Bioeng., 20 (1978) 107.
8 K.-E. Eriksson, Biotechnol. Bioeng., 20 (1978) 317.
9 K. V. Sarkanen and C. H. Ludwig, Lignins, Occurrence, Formation, Structure and Reactions, Wiley—Interscience, New York, 1971, p. 241.
10 M. Kuwahara, in T. K. Kirk, T. Higuchi and H.-M. Chang (Eds.), Lignin Biodegradation, Microbiology, Chemistry, and Potential Applications, Vol. 2, CRC Press, FL, 1980, p. 127.
11 H. Kawakami, in T. K. Kirk, T. Higuchi and H.-M. Chang (Eds.), Lignin Biodegradation, Microbiology, Chemistry, and Potential Applications, Vol. 2, CRC Press, FL, 1980, p. 103.
12 TAPPI Official Standard, 1976, T236 0S-76.
13 G. Jungschaffer, Ph. D. Thesis, TU Graz, Austria, p. 83.
14 J. D. Van Zyl, Wood Sci. Technol., 12 (1978) 251.

Analytica Chimica Acta, 130 (1981) 93—102
Elsevier Scientific Publishing Company, Amsterdam — Printed in The Netherlands

DETERMINATION OF CARBONATE IN THE PRESENCE OF HYDROXIDE

Part 2. Evidence For the Existence of A Novel Species From First-Derivative Potentiometric Titration Curves

A. K. COVINGTON*, (the late) R. A. ROBINSON and M. SARBAR

Department of Physical Chemistry, University of Newcastle, Newcastle upon Tyne NE1 7RU (Gt. Britain)

(Received 2nd April 1981)

SUMMARY

An additional maximum has been detected in the differential potentiometric titration of mixtures of sodium hydroxide and sodium carbonate with hydrochloric acid using pH-responsive glass electrodes. This maximum is not detected under the following conditions: if ethanol (mol fraction >0.2) or *t*-butanol (mol fraction >0.1) is added; when the temperature is raised above 55°C; when hydrogen gas is bubbled through the solution; if a hydrogen gas electrode is used instead of the glass electrode; when carbonic anhydrase is added. The additional feature is ascribed to a new species $HCO_3^- \cdot H_2CO_3^-$ formed in solutions by a slow reaction.

In the previous paper [1], it was shown that the differential potentiometric titration curve of a mixture of hydroxide and carbonate should contain three maxima, corresponding to the conversions $OH^- \rightarrow H_2O$, $CO_3^{2-} \rightarrow HCO_3^-$ and $HCO_3^- \rightarrow H_2CO_3$ ($H_2O + CO_2$). However, at certain proportions of CO_3^{2-}/OH^-, an extra maximum was discernible between those corresponding to the latter two conversions. This paper is concerned with the characterisation and identification of the origin of this extra maximum.

EXPERIMENTAL

Titrations were carried out in a water-jacketed cylindrical vessel of 25-ml volume. The vessel was thermostatted by circulating water at a rate of 1.4 l min^{-1} from a thermostat controlled by a Tempunit (Techne, Cambridge) Type Temcon B. The top of the vessel was sealed with a lid fitted with an O-ring; the lid contained ports allowing the fitting of glass and reference electrodes, thermometer, nitrogen gas entry tube, and titrant entry tube. The solution in the vessel was stirred by means of a teflon-covered iron bar and magnetic stirrer.

A Mettler titrimeter (Zurich, Switzerland), comprised of the modular units, 10-ml burette (DV10) with conversion and control units (DK11 and

0003—2670/81/0000—0000/$02.50

DK12) and electrometer (DK10), was used to display the differential titration curves (dE/dV) on the recorder (GA10).

A variety of glass electrodes was used, including Radiometer (Copenhagen) Types 202B and 202C, Electronic Instruments Ltd. (Chertsey) Type 331070030, Beckman (Glenrothes, Fife) Type AS2LC, Pye-Ingold (Cambridge) Type 104023092, and Jenaer Glaswerk (Mainz) Type N65. Some of these are combination electrodes but others were used in conjunction with a Radiometer Type K401 saturated KCl, calomel electrode. Some titrations were also carried out with associated measurements of CO_2 concentration by means of a Radiometer carbon dioxide electrode Type PS1-904-123.

Sodium hydroxide was a carbonate-free solution (BDH, Poole). Hydrochloric acid was prepared from BDH AVS ampoules. Sodium and potassium carbonate were analytical reagent grade. Tetramethylammonium hydroxide was 25% (v/v) solution from BDH and tetramethylammonium carbonate was prepared from it by saturation with carbon dioxide [2]. Alcohols were the best available grade, deuterium oxide was Norske Hydro 99.9%, and deuterium chloride was from BDH. Bovine carbonic anhydrase was obtained from Sigma Chemical Co.

RESULTS

Figure 1 shows the results of extending to lower carbonate/hydroxide mole ratios, the differential titrations with 0.25 mol l^{-1} HCl shown in Fig. 11 of the previous paper [1]. Identical titrations were obtained if the cation present was sodium or potassium. However, the titration of 20% tetramethylammonium carbonate/hydroxide is shown in the inset to Fig. 1, where it can be seen that the additional maximum is less apparent than in the presence of alkali metal cations and both the first and second maxima

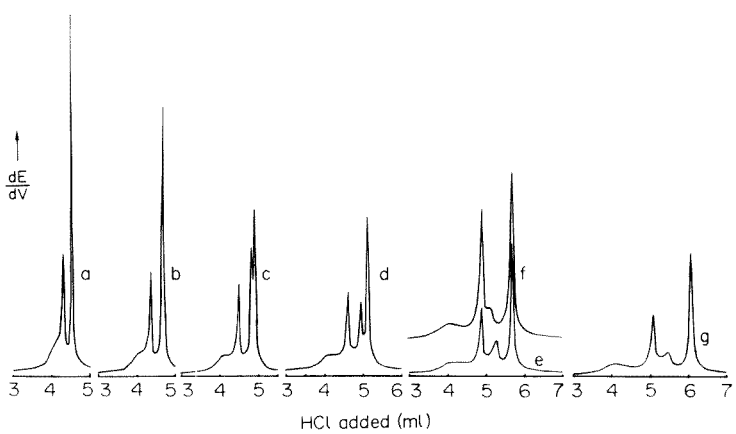

Fig. 1. Titration of 0.1 mol l^{-1} NaOH + Na_2CO_3 solutions with 0.25 mol l^{-1} HCl at various CO_3^{2-}/OH^- mole percentages: (a) 5%; (b) 7.5%; (c) 10%; (d) 12.5%; (e) 20%; (f) 20% $(Me_4N)_2CO_3$ + Me_4NOH; (g) 25%.

are greater in height. The results from titrations in the presence of different mole ratios of Na^+/NMe_4^+ are shown in Fig. 2 at 20% carbonate/hydroxide ratio.

The additional maximum is not present (Fig. 3) if, instead of passing nitrogen over the surface of the solution during the titration, it is bubbled through the solution, which, of course, drives the carbon dioxide liberated in the titration out of the solution. It is therefore not surprising that use of the hydrogen gas electrode also does not show the extra maximum since bubbling of hydrogen gas to saturate the solution also achieves this. It may

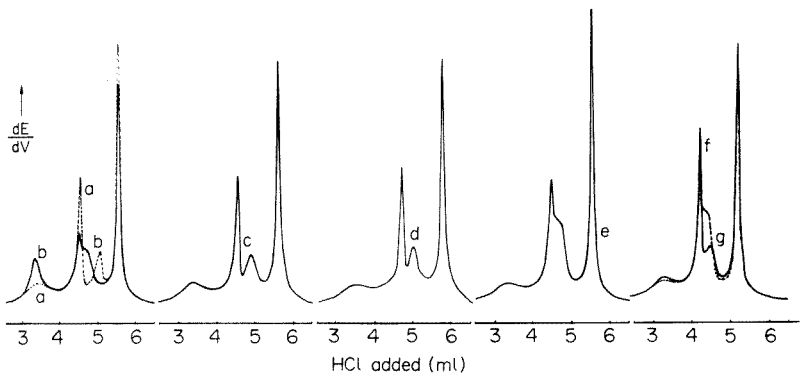

Fig. 2. Titration of various hydroxide solutions at 20 mol % CO_3^{2-}/OH^-: (a) NaOH + Na_2CO_3; (b) NaOH + Na_2CO_3 + NaCl (4.5 mol l^{-1}); (c) NaOH + Na_2CO_3 + Me_4NCl ($[Na^+]$ = 0.2 $[Me_4N^+]$); (d) NaOH + Na_2CO_3 + Me_4NCl ($[Na^+]$ = 0.02 $[Me_4N^+]$); (e) NaOH + Na_2CO_3 + Me_4NCl ($[Na^+]$ = 0.0125 $[Me_4N^+]$); (f) Me_4NOH + $Me_4N_2CO_3$; (g) Me_4NOH + $Me_4N_2CO_3$ + Me_4NCl (4.5 mol l^{-1}).

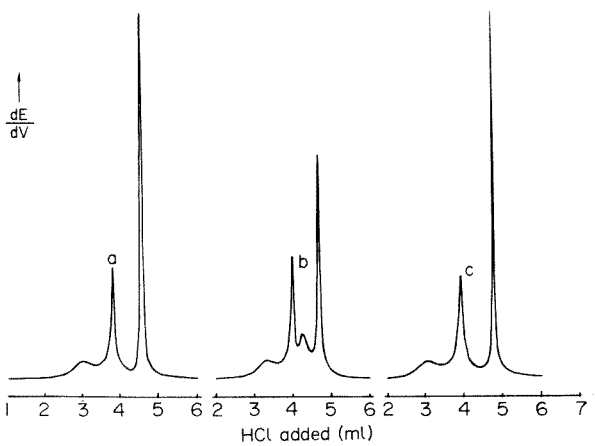

Fig. 3. Titration of 0.1 mol l^{-1} NaOH + Na_2CO_3 (20 mol % CO_3^{2-}/OH^-) with 0.25 mol l^{-1} HCl: (a) with glass electrode after bubbling nitrogen gas through the solution for 90 min; (b) with glass electrode and gas passing over the solution; (c) with platinised platinum hydrogen gas electrode.

be noted that the height of the third maximum ($HCO_3^- \rightarrow CO_2 + H_2O$) is thereby increased (Fig. 3). The results obtained (Fig. 1) are independent of the glass electrode used, provided that it is adequately conditioned before use. Figure 4 shows results for successive titrations with a previously unused glass electrode. The third titration shows the additional maximum most clearly and this is probably related to the speed of response which is greater for a properly conditioned glass electrode. The results are independent of the type of reference electrode used.

The volume scale of the recorder curves can be expanded by titration with less concentrated acid. Figure 5 shows the results of titrating carbonate/

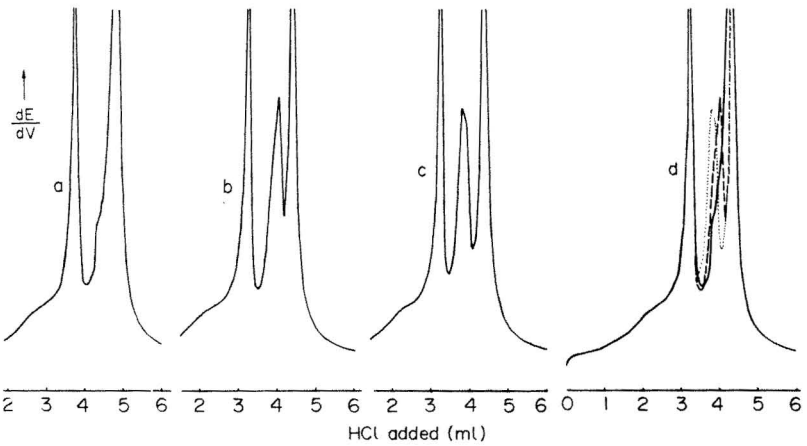

Fig. 4. Titration of 0.1 mol l^{-1} NaOH + Na_2CO_3 (5 mol % CO_3^{2-}/OH^-) with 0.05 mol l^{-1} HCl using a new Radiometer 202C glass electrode after conditioning for 10 h in 0.1 mol l^{-1} HCl, then 3 h at pH 4: (a) first; (b) second; (c) third; (d) superposed curves.

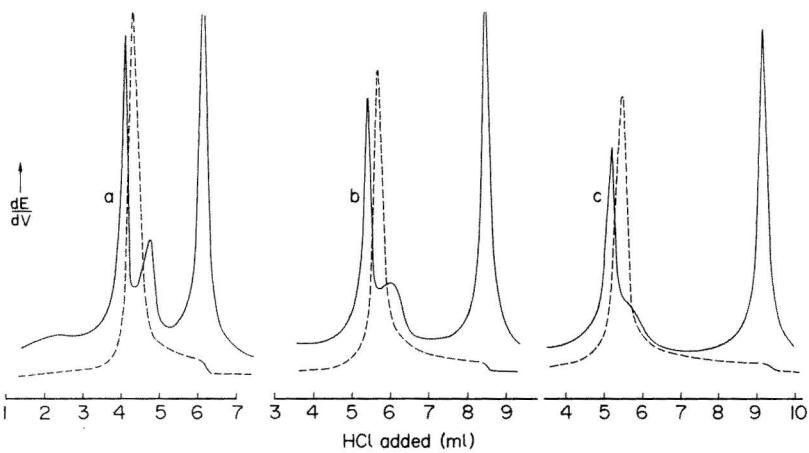

Fig. 5. Titration of 0.1 mol l^{-1} NaOH + Na_2CO_3 at various CO_3^{2-}/OH^- mol % with 0.05 mol l^{-1} HCl: (a) 10%; (b) 15%; (c) 20%; (—) glass electrode; (---) CO_2-gas electrode.

hydroxide mixtures in the range 10—15 mole % with 0.05 mol l^{-1} hydrochloric acid. It should be noted that in both Fig. 1 and Fig. 5 the position of the extra maximum with respect to the second ($CO_3^{2-} \rightarrow HCO_3^-$) remains constant with change in CO_3^{2-}/OH^- percentage. However, at the same CO_3^{2-}/OH^- percentage, the position of the extra maximum is not the same in the titrations with the two concentrations of hydrochloric acid. Also shown in Fig. 5 are the differential titration curves obtained when a carbon dioxide gas electrode was used. The maximum in these curves coincides with the minimum between the second and the extra maximum in the glass electrode titration curves. A point of inflexion occurs corresponding to the maximum for the conversion $HCO_3^- \rightarrow H_2CO_3$. At higher temperatures, the CO_2 electrode maximum moves closer to the second maximum ($CO_3^{2-} \rightarrow HCO_3^-$) in the pH titration.

Figure 6 shows the effect of varying the temperature of the titration between 5 and 65°C for a 5 mol % carbonate/hydroxide solution. The additional maximum moves from close to that for $HCO_3^- \rightarrow CO_2 + H_2O$ at 5°C, to a central position at 25°C and, diminishing in height, apparently disappears into the second ($CO_3^{2-} \rightarrow HCO_3^-$) above 55°C.

The extra maximum was also found when the entire titration of NaOH/Na_2CO_3 was carried out with DCl in D_2O at 5 and 25°C. As in light water, it was not present at above 55°C. Other additions to the titrations were investigated. Addition of various amounts of ethanol in the mole fraction range 0.02—0.20 produced marked effects on the differential titration curves, as shown in Fig. 7. Use of the higher acid concentration (0.25 mol l^{-1} HCl) minimises the change in solvent composition during the titration. With mole fractions of ethanol in the range 0.13—0.19, the extra feature disappears. A bonus finding is to be noted from Figs. 2 and 7, i.e., that the first maximum

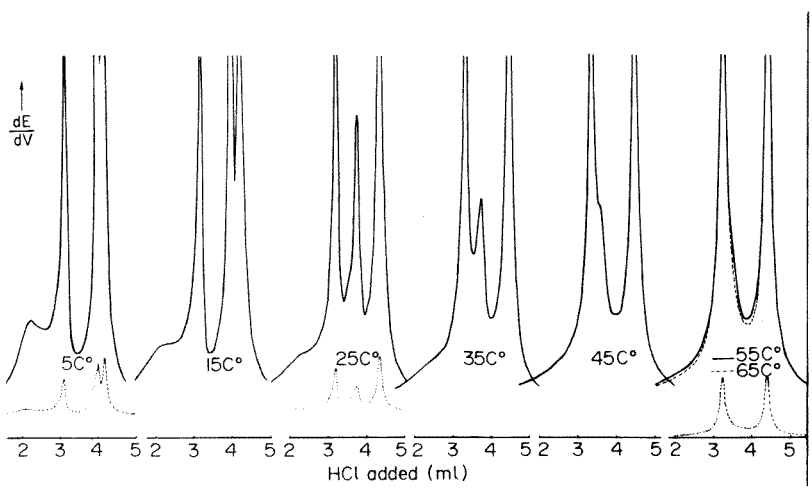

Fig. 6. Titration of 0.1 mol l^{-1} NaOH + Na_2CO_3 (5 mol % CO_3^{2-}/OH^-) with 0.05 mol l^{-1} HCl at 5—65°C. Insets: full curves.

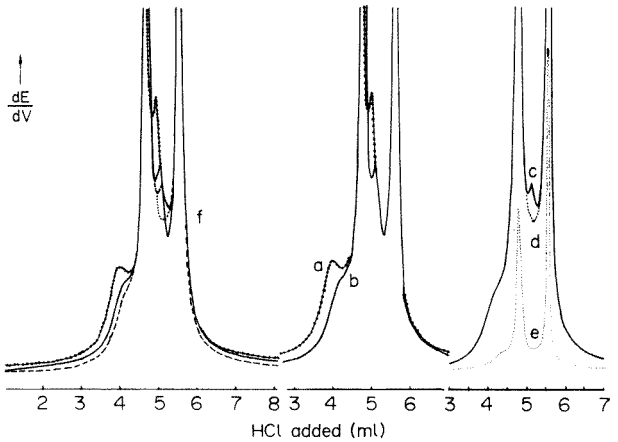

Fig. 7. Titration of 0.1 mol l^{-1} NaOH + Na_2CO_3 (20 mol % CO_3^{2-}/OH^-) with 0.25 mol l^{-1} HCl in presence of ethanol at different mole fractions: (a) 0.02; (b) 0.1; (c) 0.13; (d) 0.19; (e) as (d), full curve; (f) superposition a—d.

($OH^- \rightarrow H_2O$) is developed by the addition of either sodium chloride or ethanol, which may be a useful analytical aid. Addition of *t*-butanol, but at lower mole fraction (about 0.1), also removes the extra maximum, as shown in Fig. 8. A small quantity of carbonic anhydrase added to the titration also causes the removal of the extra feature, as shown in Fig. 9. In Fig. 10 are shown the results of titrations in which the same carbonate/hydroxide ratios were used as in Fig. 1 but at constant carbonate instead of constant hydroxide concentration. The new feature becomes less distinguishable as the amount of hydroxide added is diminished.

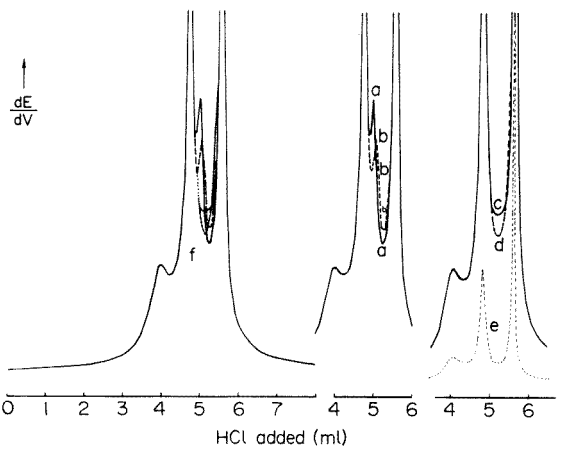

Fig. 8. As Fig. 7, but in presence of *t*-butanol at different mole fractions: (a) 0.02; (b) 0.045; (c) 0.112; (d) 0.126; (e) as (d), full curve; (f) superposition a—d.

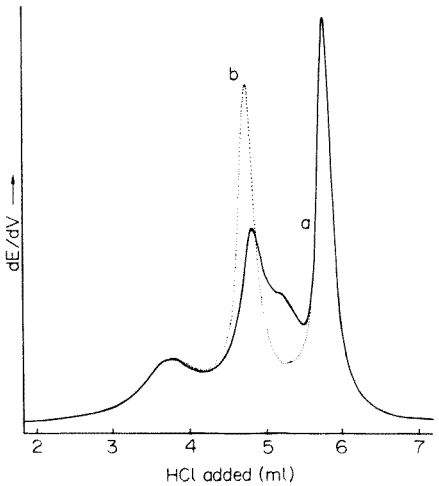

Fig. 9. Effect of bovine carbonic anhydrase on titration curves: (a) titration of 25 ml of 0.04 mol l^{-1} NaOH + 0.008 mol l^{-1} Na_2CO_3; (b) as (a), but with addition of 1 mg of carbonic anhydrase.

DISCUSSION

Kern [3] and Edsall [4] have reviewed the equilibrium and kinetic properties of the aqueous carbon dioxide system. Valuable summaries are also given in Gmelin [5] and in Stumm and Morgan [6]. Of particular interest in the present connection are the facts that only a small proportion of dissolved carbon dioxide exists in the form of carbonic acid, H_2CO_3, such that $K_0 = [H_2CO_3]/[CO_2] = 1.5 \times 10^{-3}$, and that the reaction

$$CO_2 + H_2O \rightarrow H_2CO_3 \quad (k_f = 0.03\ s^{-1}) \qquad (1)$$

is not fast so that equilibrium for the pH range 6—8 in this system is reached [3] with a half-life of slightly less than 20 s. (Note that values [3] in the seventh column of Kern's table 1 are incorrect and should be multiplied by ln 2.) Also relevant is that the solubility of CO_2 in water, which is 0.03 mol l^{-1} at 25°C, decreases with increase in temperature, and is greater in ethanol [4].

The new feature in the differential potentiometric titration curves which occurs at pH 6.5 is not related to the solubility of CO_2, because in all the experiments the amount of carbonate was insufficient for the solution volume to reach saturation with CO_2 gas at that stage in the titration. When reaction (1) is combined with the very fast reaction

$$H_2CO_3 + OH^- \rightarrow HCO_3^- + H_2O \qquad (2)$$

then $-d\,[CO_2]/dt = -d\,[OH^-]/dt = 2 \times 10^{-4}$ mol l^{-1} s^{-1} at this pH. This may be compared with the slowest rate of increase in hydrogen ion concentration in the titrations, which was 4×10^{-5} mol l^{-1} s^{-1}. The titrations are about five

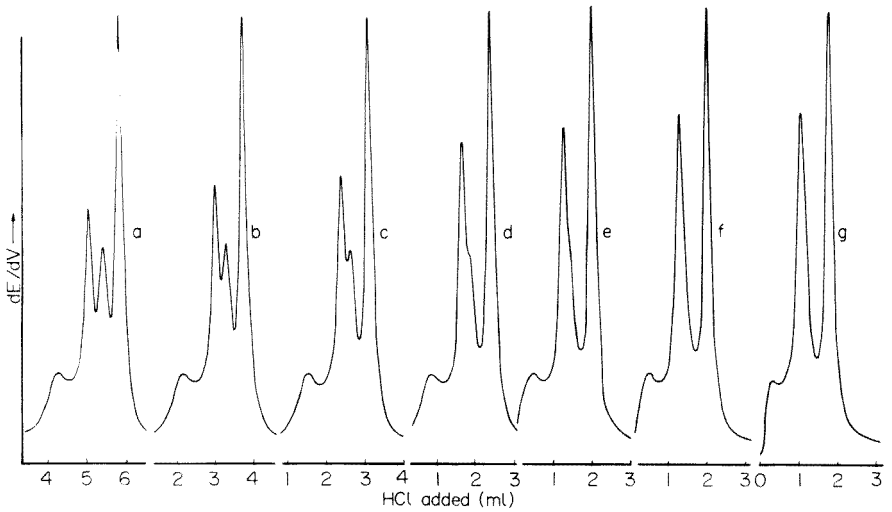

Fig. 10. Titration of 0.01 mol l^{-1} Na_2CO_3 (25 ml) containing various amounts of NaOH at different mole percentages with 0.25 mol l^{-1} HCl: (a) 20%; (b) 40%; (c) 60%; (d) 125%; (e) 200%; (f) 400%; (g) no NaOH added.

times slower but a slight effect of stirring on the position of the extra maximum but not the others suggests a slight influence of kinetic factors. The effect of slow kinetics in the system was examined by computer simulation methods [7]. It may be noted that the position of the extra maximum in relation to the others was changed by the use of more dilute acidic titrant. This is because the rate of increase of hydrogen ion concentration is different, but the position of the extra maximum becomes the same if the rate of addition of the dilute acid is increased by a factor of five. For the same acid concentration the effect of increasing the rate of hydrogen ion addition is apparently to increase the amount of species responsible for the extra maximum.

Addition of ethanol or *t*-butanol will reduce the hydroxide ion concentration, and in tetramethylammonium hydroxide of the same stoichiometric concentration as sodium hydroxide, the effective hydroxide concentration may be lower. In the presence of these reagents, the position of the extra maximum is changed or the maximum disappears with sufficient addition of reagent.

Increasing the temperature of the titration results in the extra feature moving nearer to the second expected maximum in the titration curve and finally disappearing above 50°C with the second maximum becoming sharper. Lowering the temperature has the effect of moving the extra maximum towards the third expected maximum. This can be explained by the fact that the dehydration of carbonic acid is slow at low temperatures and that the solubility of carbon dioxide is high, whereas its concentration at high temperatures is low. Increasing the rate of addition of acid titrant has exactly the same effect as decreasing the temperature.

All the evidence suggests that the novel feature is a property of the titrated solution which is detected by glass electrodes. Similar results were obtained when other hydrogen ion-responsive electrodes were used, such as the rhodium/rhodium oxide electrode [8] and the quinhydrone electrode, but not the hydrogen gas electrode because of the effect of hydrogen gas sweeping carbon dioxide out of the solution. The position of the extra maximum between the carbonate and hydrogen carbonate equivalence points suggests that the new feature is due to the protonation of a novel species with pK intermediate between carbonate and hydrogen carbonate such as $HCO_3 \cdot H_2CO_3^-$. Further experiments are required to confirm this and will be reported in a later paper describing the titration of carbonic acid solutions [9]. The hypothesis of the formation of the species $HCO_3 \cdot H_2CO_3^-$ has been confirmed [9] by computer-calculated titration curves. However, it may be noted that both Kern [3] and Edsall [4] drew attention to inconsistencies in some of the kinetic data reported by different techniques for the dehydration reaction, the reverse of eqn. (1), in neutral and dilute acid solutions. Koefoed and Engel [10] studied the acid catalysis for the hydration process and could only explain their results by invoking catalysis by a new species which they concluded could be trimeric carbonic acid. It is interesting to note that the solid hydrate $Na_2CO_3 \cdot NaHCO_3 \cdot 2H_2O$ exists as the mineral trona and is a byproduct of the ammonia soda process known as sodium sesquicarbonate whose crystal structure has been determined [11].

As far as is known, differential titration curves using the carbon dioxide gas electrode have not been presented before. The maximum in the curve which appears just after the carbonate equivalence point can be predicted by considerations similar to those employed in Part 1 [1]. It can be shown that

$$\mathrm{d}\ln[CO_2]/\mathrm{d}x = [K_0K_1\ (h + 2K_2)/\sum]\ \mathrm{d}\ln h/\mathrm{d}x$$

where h is the hydrogen ion concentration, and $\Sigma = h^2 + hK_1 + K_1K_2$, with K_1 and K_2 being the first and second dissociation constants of carbonic acid. Hence, by the method described in Part 1, the theoretical titration curve can be calculated and compared with the experimental curve. A feature at pH 11 in the theoretical curve is not seen experimentally because the carbon dioxide concentration level is below the detection limit of the electrode. The position of the main carbon dioxide maximum (Fig. 5) is between the additional maximum and the first carbonate maximum. As the temperature is increased, the two become closer. This may be due to increased speed of response of the gas electrode at higher temperatures; this point will be considered further in a discussion of the use of the electrode in titration of carbonic acid solutions with alkali [9]. The maximum in the gas electrode curve becomes less sharp with increasing temperature because of the loss of carbon dioxide from solution.

Finally the effect of the addition of carbonic anhydrase on the observation of the novel species must be mentioned. It is shown elsewhere [7] that slow

kinetics of hydration—dehydration cannot lead to the presence of additional maxima in the titration curves, therefore it follows that the removal of the feature by the addition of the enzyme must be due to the influence of the enzyme on the formation kinetics of the new species.

Addendum

The following typographical errors in Part 1 may be noted: eqns. (8—11) should have Ka not Ka terms. Two lines above eqn. (12) the second term inside the braces should read (h/K_2) not (h/K_1). Two lines above eqn. (14), $b = a_1 (1 + 2k)x$.

The authors thank the Royal Society for a grant for the purchase of the Mettler titrator, and the Medical Research Council for a grant in support of minor apparatus and running costs. One of us (M.S.) thanks the University of Tabriz, for the award of a scholarship.

REFERENCES

1 A. K. Covington, R. A. Robinson and M. Sarbar, Anal. Chim. Acta, 100 (1978) 367.
2 A. K. Covington and M. I. A. Ferra, Anal. Chem., 49 (1977) 1363.
3 D. M. Kern, J. Chem. Educ., 37 (1960) 14.
4 J. T. Edsall, N.A.S.A. Spec. Rep. No. 188, pp. 15–20, 1969.
5 R. J. Meyer (Ed.), Gmelin Handbuch der anorganischen Chemie, Carbon, 8th edn.. Vol. C3, Verlag Chemie, Weinheim, 1973.
6 W. Stumm and J. J. Morgan, Aquatic Chemistry, J. Wiley, New York, 1970, Ch. 4.
7 A. K. Covington, R. N. Goldberg and M. Sarbar, Anal. Chim. Acta, 130 (1981) 103.
8 A. K. Covington and D. G. Jones, unpublished, 1977.
9 A. K. Covington and M. Sarbar, in preparation.
10 J. Koefoed and K. Engel, Acta Chem. Scand., 15 (1961) 1319.
11 C. J. Brown, H. S. Peiser and A. Turner-Jones, Acta Crystallogr., 2 (1949) 167.

Analytica Chimica Acta, 130 (1981) 103—109
Elsevier Scientific Publishing Company, Amsterdam — Printed in The Netherlands

COMPUTER SIMULATION OF TITRATION CURVES WITH APPLICATION TO AQUEOUS CARBONATE SOLUTIONS

A. K. COVINGTON*, R. N. GOLDBERG** and M. SARBAR
Department of Physical Chemistry, University of Newcastle upon Tyne, Newcastle upon Tyne NE1 7RU (Gt. Britain)

(Received 2nd April 1981)

SUMMARY

A computer simulation calculation is used to generate theoretical acid—base titration curves for aqueous carbonate solutions. The calculation allows for the time delay in the conversion of aqueous CO_2 to H_2CO_3 and permits the calculation of concentrations of the species in solution and their time derivatives during the course of a titration. Detailed calculations, which include the effect of the time delay, show that the existence of a peak in the differential titration curve corresponds to the protonation of a species in solution, and that no extra peaks are produced as a result of the time delay. The calculations also show that the pK values obtained from such titrations are not affected by the time delay, and that a systematic error may be incurred when such titrations are used for analytical purposes when the rate of addition of titrant is too rapid.

Titration curves are customarily used for examining the nature, number of species, and amount of substance present in a solution and are therefore a valuable tool for analytical and thermodynamic measurements. In a study of aqueous carbonate solutions [1], the questions arose as to whether an extra, previously unobserved, peak in the differential titration curve, could be accounted for by the slow kinetics of transformation of $CO_2(aq)$ to $H_2CO_3(aq)$, and whether in the analysis of solutions containing carbon dioxide this kinetic effect introduced a systematic error in the determination of the end-point(s) in the titration curve. In order to answer these questions, equilibrium and kinetic rate constant data were used to perform a computer simulation of the titration curve. The calculation techniques described below provide a generalization of the mathematical analysis presented earlier [2] and were applied to this specific problem.

COMPUTATIONAL PROCEDURE

The equilibrium case

The situation where there are no kinetic complications is designated here as the "equilibrium" case. An aqueous solution having a volume of 1 dm^3

**On secondment during 1980 from: National Bureau of Standards, Washington, DC 20234, U.S.A.

and initially containing α mol of CO_2 derived species and n_{HCl} mol of hydrochloric acid is considered. Sodium hydroxide is added to this solution at a rate dn_{NaOH}/dt. It is assumed that the amount and concentration of the sodium hydroxide solution is such that the total volume of the system remains constant; this makes it possible to take concentrations, indicated as quantities in square brackets, equal to the number of moles of a given species present in the solution. The relevant equilibria and their equilibrium constants are

$$CO_2 + H_2O \rightleftharpoons H_2CO_3 \qquad (K_o) \qquad (1)$$

$$H_2CO_3 \rightleftharpoons H^+ + HCO_3^- \qquad (K_A) \qquad (2)$$

$$HCO_3^- \rightleftharpoons H^+ + CO_3^{2-} \qquad (K_B) \qquad (3)$$

$$H_2O \rightleftharpoons H^+ + OH^- \qquad (K_w) \qquad (4)$$

Throughout it is understood that all species are in aqueous solution unless indicated otherwise. Application of the condition of electroneutrality requires that

$$n_{H^+} + n_{Na^+} = n_{Cl^-} + n_{OH^-} + 2n_{CO_3^{2-}} + n_{HCO_3^-} \qquad (5)$$

Because α is the total amount of CO_2-derived species present in the system

$$\alpha = n_{CO_2} + n_{H_2CO_3} + n_{HCO_3^-} + n_{CO_3^{2-}} \qquad (6)$$

Substitution of expressions for the equilibrium constants K_o, K_A and K_B into eqn. (6) and rearrangement yields

$$\alpha = [CO_3^{2-}]\{([H^+]^2/K_oK_AK_B) + ([H^+]^2/K_AK_B) + ([H^+]/K_B) + 1\} = [CO_3^{2-}]\beta \qquad (7)$$

where β is defined as the quantity in braces in eqn. (7).

The concentrations of species can be represented in terms of β by

$$[CO_3^{2-}] = \alpha\beta^{-1}; [HCO_3^-] = [H^+]\alpha\beta^{-1}/K_B; [H_2CO_3] = [H^+]^2\alpha\beta^{-1}/K_AK_B;$$

$$[CO_2] = [H^+]^2\alpha\beta^{-1}/K_oK_AK_B; [OH^-] = K_w/[H^+]$$

Substitution of these equalities into eqn. (5) yields, after rearrangement,

$$\beta\{[H^+]^2 + n_{NaOH}[H^+] - n_{HCl}[H^+] - K_w\} - ([H^+]^2\alpha/K_B) - 2\alpha[H^+] = 0 \qquad (8)$$

Because n_{NaOH}, n_{HCl}, the quantity α, and the equilibrium constants K_o, K_A, K_B, and K_w are known, eqn. (8) can be solved for $[H^+]$ numerically by using the method of successive approximations. The "equilibrium" case corresponds to the real case when the rate of interconversion of all of the species, in particular CO_2 to H_2CO_3, is much faster than the rate at which the titration is done either in the laboratory or on the computer.

The non-equilibrium case

In order to deal with a time delay in process (1), α^* is defined here as the total accessible carbonate: $\alpha^* = [H_2CO_3] + [HCO_3^-] + [CO_3^{2-}]$. The rate of transformation between these three carbonate species is assumed to be instantaneous. Following a similar procedure as before, an expression is developed for β^* in terms of the fundamental equilibrium constants

$$\alpha^* = [CO_3^{2-}]\{([H^+]^2/K_AK_B) + ([H^+]/K_B) + 1\} = [CO_3^{2-}](\beta^*) \quad (9)$$

where β^* is defined as the quantity in braces in eqn. (9) by analogy with the equilibrium case represented in eqn. (7). As in the previous section, the concentrations of CO_3^{2-}, HCO_3^-, H_2CO_3 and H^+ present in the system can be calculated. Application of the condition of electroneutrality yields

$$\beta^*\{[H^+]^2 + n_{NaOH}[H^+] - n_{HCl}[H^+] - K_w\} - ([H^+]^2\alpha^*/K_B) - 2[H^+]\alpha^* = 0 \quad (10)$$

which is the same as eqn. (8) with β for β^* and α for α^*. It does not appear to be possible to solve eqn. (10) in closed form for $[H^+]$, particularly when $[H_2CO_3]$ is a function of time. Thus it is necessary to resort to numerical solutions in which the interconversion of CO_2 to H_2CO_3 is allowed for according to

$$d[H_2CO_3]/dt = k_f[CO_2] - k_r[H_2CO_3] \quad (11)$$

where k_f and k_r are, respectively, the forward and reverse rate constants for process (1). Thus, knowledge of the equilibrium and rate constants permits solution for the concentrations of the various species present as a function of time by means of a simulation calculation.

Numerical aspects

The algorithm used is outlined in Fig. 1; the program, written in IBM H Extended FORTRAN [3], is available from the authors on request. Equations (8) and (10) are solved by an iterative procedure (CO5ABF) obtainable from a library of numerical analysis programs [4]. For this purpose, the expressions in eqns. (8) and (10) are declared as "EXTERNAL" variables in the computer program.

In doing these calculations, the following values were used for the equilibrium and kinetic rate constants: $K_o = 1.5 \times 10^{-3}$ [5], $K_A = 3.0 \times 10^{-4}$ mol dm^{-3} [5], $K_B = 4.7 \times 10^{-11}$ mol dm^{-3} [6], $K_w = 1.0 \times 10^{-14}$ mol dm^{-3} [7], $k_f = 0.03$ s^{-1} [5] and $k_r = 20.0$ s^{-1} [5].

A value of $dt \approx \Delta t = 0.1$ s was found to yield numerically reliable results consistent with a reasonably rapid computation rate. The calculation was done using double precision arithmetic to minimize machine-rounding errors.

Utility of the calculation and some underlying assumptions

It is clear that the analysis outlined above permits the calculation of the concentrations of all species as well as their time derivatives. What is calcu-

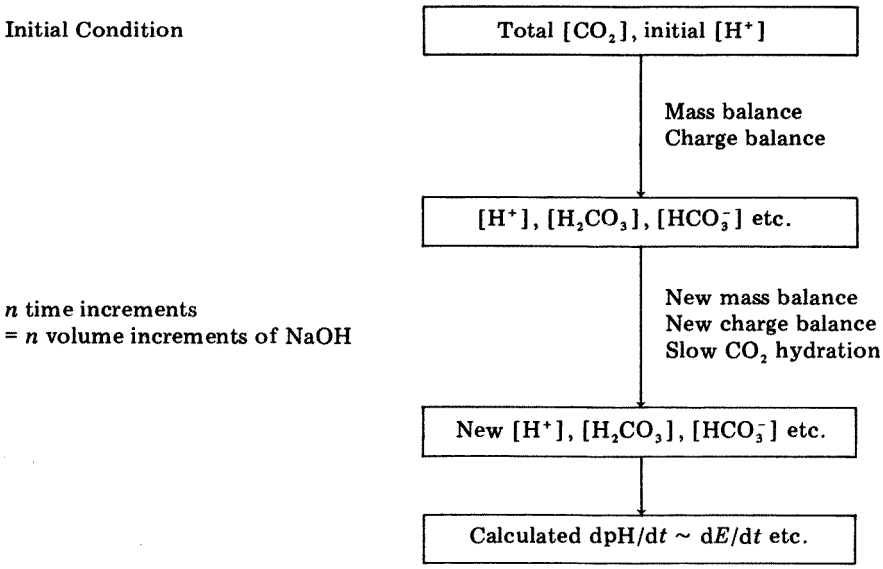

Fig. 1. Flow chart of computer simulation of titration curves with slow kinetics.

lated in practice depends upon the information desired; typically this is a comparison with the experimental curve. Modern instrumentation can display derivative data and this was allowed for in the computer program used.

Experimentally, a glass electrode, which is responsive to hydrogen ion, and a calomel reference electrode, are placed in the solution of interest. The assumption is made that this arrangement is sensitive to the concentration of the hydrogen ion only. This assumption depends upon activity coefficient and liquid junction effects on the measured electromotive force being minimal in comparison with the effect discussed above. If electrodes responsive to species other than the hydrogen ion were available, then the concentration of these species would become the quantities of particular interest.

Earlier it was assumed that there was no volume change on the addition of titrant to the solution. This assumption will not affect the total number of moles of any given species present in the system, but it will affect the calculated concentrations. This could easily be accommodated in a modification to the program. This effect, however, will not invalidate the results obtained from the calculations when it is derivative quantities that are examined in determining end-points of titrations or in determining the relevant species which must be accounted for in describing the behaviour of a solution.

RESULTS

Figures 2 and 3 show the results of calculations involving the addition of sodium hydroxide at a rate of 1.0×10^{-6} mol s^{-1} to a solution initially con-

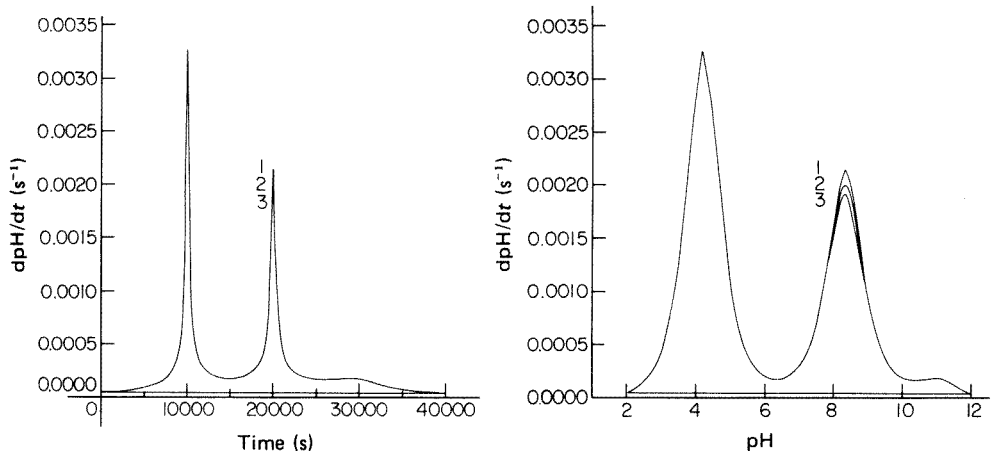

Fig. 2. Calculated values of dpH/dt (s^{-1}) as a function of time (s) for the titration of 0.01 mol of CO_2 and 0.01 mol of HCl with NaOH at a rate of 1.0×10^{-6} mol s^{-1}. The thermodynamic and kinetic rate constants given in the text were used to calculate curve 2. Curve 1 was obtained by removing all time delays in the interconversion of CO_2 to H_2CO_3. Curve 3 was obtained by setting $k_f = 0.015$ s^{-1} and $k_r = 10.0$ s^{-1}.

Fig. 3. Calculated values of dpH/dt (s^{-1}) as a function of pH. Curves 1—3 were obtained in the same way as the respective curves shown in Fig. 2.

taining 0.01 mol dm^{-3} CO_2 and 0.01 mol dm^{-3} HCl. This rate of addition and the concentrations of CO_2 and HCl were selected because they were similar to the quantities used in the practical work [1]. Also, in practice, it is the electromotive force of the cell which is measured directly, and, since the pH is proportional to the e.m.f. (E), dpH/dt ~ dE/dt. In Fig. 2 the quantity dpH/dt is plotted as a function of time and in Fig. 3 the quantity dpH/dt is plotted as a function of the pH of the solution. A step time of 0.1 was used. These figures each contain three separate curves. The curves labelled 2 were produced by using the equilibrium and kinetic rate constants given earlier. This curve thus corresponds to the computer simulation of the "real" case. To produce the curves labelled 1, all time delays in the interconversion of CO_2 to H_2CO_3 were removed, and to produce the curves labelled 3 the interconversion of CO_2 to H_2CO_3 was slowed down by setting k_f equal to 0.015 s^{-1} and k_r equal to 10.0 s^{-1}, which keeps K_o equal to its thermodynamic value of 1.5×10^{-3}. Thus, the curve labelled 1 relates to the hypothetical case where there is no time delay in the interconversion of CO_2 to H_2CO_3, and the curve labelled 3 relates to the case when there is an even longer time delay in the CO_2 to H_2CO_3 interconversion than in the "real" case.

The following points may be noted: the first peak corresponds to the conversion of HCl to NaCl and H_2O, the second peak corresponds to the conversion of CO_3^{2-} to HCO_3^-, and the third peak corresponds to the conversion of HCO_3^- to H_2O and CO_2. Examination of these figures makes it possible to answer one of the questions raised earlier. Specifically, for this

rate of addition of sodium hydroxide, the use of such titration curves for analytical purposes will not be subject to systematic errors caused by the time delay of conversion of CO_2 to H_2CO_3. If, however, the CO_2 could not be converted by any mechanism to H_2CO_3, there would be no second and third peaks present.

Such titration curves may also be used to obtain pK values corresponding to the acid ionization constants. Thus, the minima in Fig. 3 at pH 6.3 and 10.3 correspond to the appropriate pK values for the carbonate system. The value pK = 6.3 corresponds to a value of $-\log K_A/(1 + 1/K_o)$, which since $K_o \ll 1$, is very nearly equal to $-\log K_o K_A$; the value of pK = 10.3 corresponds to a value of $-\log K_B$. (The quantities $K_A/(1 + K_o)$ and K_B are frequently designated as K_1 and K_2, respectively, in much of the literature on carbonate systems.) Clearly, independent values of K_o and K_A cannot be obtained from such experiments. The results of the computer simulation calculations indicate that the measurement of these thermodynamic equilibrium constants by use of potentiometric titration at the indicated rate of addition of sodium hydroxide is not affected by the kinetic delays due to the interconversion of CO_2 to H_2CO_3. In the simulation calculations, the direct reaction of hydroxide ions with CO_2 was neglected because, in the region of pH 4—8, the concentration of hydroxide is negligible in comparison to the other quantities of interest.

If, however, a calculation similar to the previous one is done with a much faster rate of addition of sodium hydroxide to the solution, a systematic

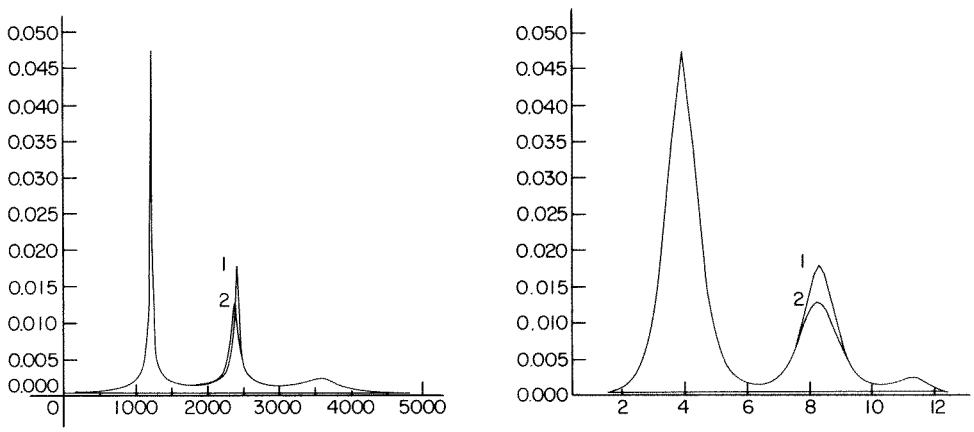

Fig. 4. Calculated values of dpH/dt (s^{-1}) as a function of time (s) for NaOH added at a rate of 2.5×10^{-5} mol s^{-1} to a solution containing 0.03 mol of HCl and 0.03 mol of CO_2. Curve 2 was calculated using the thermodynamic and kinetic rate constants given in the text. Curve 1 was obtained by removing all time delays in the interconversion of CO_2 to H_2CO_3.

Fig. 5. Calculated values of dpH/dt (s^{-1}) as a function of pH. Curves 1 and 2 were obtained in the same way as the respective curves shown in Fig. 4.

error is incurred. For example, at a rate of 2.5×10^{-5} mol s^{-1}, the middle peaks are wrongly located (see Figs. 4 and 5). The systematic error in an analysis performed under such conditions would be about 1.3%. At higher rates of addition (2.5×10^{-4} mol s^{-1}), this systematic error becomes very significant (16%), but becomes negligible (less than 0.1%) for rates of addition less than 1.0×10^{-5} mol s^{-1}. The values of the minima in the curve used to obtain pK values are not affected by the rate of addition of sodium hydroxide. Calculations were also done for rates of addition as slow as 1.0×10^{-7} mol s^{-1}; under such conditions, even the differences in the heights of the middle peaks became negligible.

It is also seen that the kinetic delay does not lead to any extra peaks in the titration curves. The observation of an extra peak in titration curves of this type is discussed elsewhere [1].

One of us (R.N.G.) acknowledges support by the U.S. Department of Energy and the Office of Standard Reference Data of the National Bureau of Standards. Another (M.S.) acknowledges support by the University of Tabriz, Iran.

REFERENCES

1 A. K. Covington, R. A. Robinson and M. Sarbar, Anal. Chim. Acta, 130 (1981) 93.
2 A. K. Covington, R. A. Robinson and M. Sarbar, Anal. Chim. Acta, 100 (1978) 367.
3 IBM System/360 and System/370 FORTRAN IV Language, IBM Corporation, New York, 1974.
4 NAG FORTRAN Library Manual, Mark 7 edn., NAG Central Office, Oxford, 1978.
5 D. M. Kern, J. Chem. Educ., 37 (1960) 14.
6 J. T. Edsall, N.A.S.A. Spec. Publ. 188, pp. 15—27, 1969.
7 H. S. Harned and B. B. Owen, The Physical Chemistry of Electrolytic Solutions, 3rd edn., Reinhold, New York, 1958.

Analytica Chimica Acta, 130 (1981) 111—132
Elsevier Scientific Publishing Company, Amsterdam — Printed in The Netherlands

POLAROGRAPHIC ANALYSIS OF CORTICOSTEROIDS
Part 6. Mechanism of Polarographic Electroreduction of Some Δ^4-3-Ketosteroids and $\Delta^{1,4}$-3-Ketosteroids

H. S. DE BOER

Duphar BU, POB 2, 1380AA Weesp (The Netherlands)

W. J. VAN OORT*

Department of Analytical Pharmacy, Faculty of Pharmacy, State University Utrecht, Catharijnesingel 60, 3511 GH, Utrecht (The Netherlands)

P. ZUMAN

Department of Chemistry, Clarkson College of Technology, Potsdam, NY 13676 (U.S.A.)

(Received 31st March 1981)

SUMMARY

Prednisolone and dexamethasone give waves in d.c. and normal pulse polarography and peaks in differential pulse polarography which correspond to a one-electron uptake. The transfer of the first electron is reversible and at pH <7 (i_1) is preceded or at pH >7 (i_3) is followed by a proton transfer. Protonation occurs on the carbonyl group and pinacol is formed. At pH >7, wave i_3 is followed by wave i_4 which involves transfer of another proton and electron on the carbonyl group and yields the unsaturated alcohol. At pH <3, the radical formed in the first electron uptake is further protonated and is reduced in wave i_{1+2}. In tetramethylammonium hydroxide solution, reduction of the side chains on C-17 occurs at more negative potentials. Reduction of testosterone and hydrocortisone follows a similar mechanism (A)—(G), but the second electron uptake in wave i_4 at pH >7 is not observed.

In Part 1 of this series [1] the potentials of peaks obtained by differential pulse polarography corresponding to the reduction of 3-ketosteroids bearing one or two conjugated ethylenic bonds in methanolic or aqueous dimethylformamide (DMF) solutions were compared. Such comparison indicated the potential ranges in which the Δ^4-3-keto group, the $\Delta^{1,4}$-3-keto group, the 20-keto group, and the halogen are separately reduced.

It is the aim of the present publication to contribute to better understanding of the individual steps in the reduction of α,β-unsaturated steroids. As in numerous other cases, d.c. polarography offered the most straightforward information concerning the nature of individual electrochemical and chemical steps involved. Such information was complemented by data obtained by normal and differential pulse polarography, linear sweep and cyclic voltammetry, controlled potential electrolysis and coulometry. As model substances, the corticosteroids chosen were hydrocortisone (II),

prednisolone (III), and dexamethasone (IV). For comparison, the behavior of testosterone (I) was included.

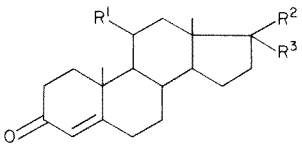

I $R^1 = H$, $R^2 = OH$, $R^3 = H$
II $R^1 = OH$, $R^2 = COCH_2OH$
$R^3 = OH$

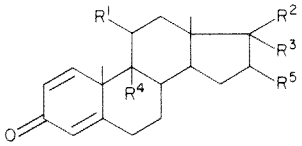

III $R^1 = OH$, $R^2 = OH$,
$R^3 = COCH_2OH$, $R^4 = H$
$R^5 = H$
IV $R^1 = OH$, $R^2 = OH$, $R^3 = COCH_2OH$,
$R^4 = F$, $R^5 = CH_3$

Early studies of the polarography of Δ^4-3-ketosteroids indicated reduction of protonated and unprotonated forms [2] depending on the pH of the solution, and transfer of one electron in the first step [3—5]. The pre-protonation of the α,β-unsaturated ketones has been ridiculed [5, 6], but more recent spectrophotometric studies [7, 8] have indicated the protonation of Δ^4- and $\Delta^{1,4}$-3-ketosteroids with pK_{BH^+} values varying between —4.7 and —2.3. Appearance of polarographic waves of the protonated form even at pH 8 is made possible by fast protonation, particularly when this process occurs [9] at the surface of the mercury electrode as a "surface reaction". Moreover, studies of 2-cyclohexanone [10, 11] showed a dependence of the limiting currents on pH similar to that reported [2] for Δ^4-3-ketosteroids. This behavior was also interpreted [10, 11] by pre-protonation. Attribution of spectra and the two one-electron waves of androst-4-ene-3,6,17-trione observed in DMF solutions [12] to reduction of the keto and enol forms is doubtful.

For $\Delta^{1,4}$-3-ketosteroids, one-electron transfer in the first step and occurrence of a second wave at pH >6.3 was reported [4] for prednisone and in unbuffered media containing tetrabutylammonium ions for cortisone and hydrocortisone. The more negative wave was ascribed [4] to the reduction of the side-chain in position 20, because its half-wave potential was similar to that of dihydroxyacetone. For androst-1,4-diene-3,17-dione and androst-1,4,6-triene-3,17-dione in unbuffered media containing 50% DMF, a one-electron reduction was reported [13].

Most other studies dealing with α,β-unsaturated 3-keto-steroids have been restricted either to a description of d.c. polarographic waves [14, 15] or to analytical applications of d.c. [16—23] and differential pulse [24—26] polarographic waves.

EXPERIMENTAL

Apparatus

The polarographic curves were recorded on a Bruker E310 modular electrochemical system, a PAR (Princeton Applied Research) model 174

polarograph, both of which were equipped with a drop timer and a Houston model 2000 X-Y recorder, and on a Metrohm Polarecord E506 equipped with a polarographic stand E505.

Linear sweep polarographic and cyclic voltammetric curves were obtained with the Bruker polarograph, equipped with a Tektronix 5103 N oscilloscope.

A water-jacketed 10-ml polarographic cell (Metrohm EA880-T-5) was employed with a dropping mercury electrode, a Metrohm EA436 Ag/AgCl/saturated KCl reference electrode and a platinum wire auxilliary electrode. The potential of the reference electrode was —50 mV versus a saturated calomel electrode when the bridge was filled with 0.03 M tetramethylammonium hydroxide in methanol. The cell was kept at 20 ± 0.5°C.

Controlled potential electrolysis at the dropping mercury electrode was done with a PAR model 364 polarograph equipped with a model 303 SMDE (static mercury drop electrode) and a Houston model 2000 X-Y recorder. The SMDE was used in the large drops mode. Coulometric measurements at the mercury pool were done with a Metrohm E524 coulostat and a Metrohm E525 integrator.

The pH values were measured with a Radiometer PHM64 research pH meter, equipped with an Ingold LOT-401 combined glass/reference electrode, calibrated in aqueous buffers. Because of alkaline error, the glass electrode was not used for determination of hydrogen ion activity in lithium hydroxide solutions. Because acidity functions are not available for lithium hydroxide solutions containing 50% methanol, and because acidity function values of lithium hydroxide solutions will differ only a little from these values for sodium hydroxide solutions [27], values of acidity function J_- for aqueous sodium hydroxide solutions [28—30] were used.

Chemicals

Hydrocortisone, prednisolone and dexamethasone (Nogepha, Alkmaar, The Netherlands) and testosterone (Merck) were preparations satisfying the requirements of the Dutch Pharmacopoeia [31] and were used without further purification.

The solvents and materials for the supporting electrolytes were methanol (Nanograde; Mallinckrodt), methanol (zur Analyse, Merck) and tetramethylammonium hydroxide (10% aqueous solution; zur Polarographie, Merck). The other reagents were of analytical-reagent grade.

The composition of the buffers used is listed in Table 1. Lithium hydroxide solutions were used for the alkaline media, as the waves of steroids were overlapped by the reduction current of sodium or potassium ions.

Procedures

All investigations were carried out in solutions containing 50% (v/v) methanol, prepared by mixing an aqueous buffer or other supporting electrolyte with an equal volume of methanol. The "pH" values of such solutions

TABLE 1

Composition of buffers

Buffer type		[Na^+] (mol dm^{-3})	[K^+]	[Cl^-]	pH	"pH" (in 50% methanol)
Acetate buffers						
[CH_3COOH]	[CH_3COO^-]					
1.0	0.1	0.1			3.8	4.6
0.3	0.1	0.1			4.2	5.1
0.1	0.1	0.1			4.8	5.5
0.03	0.1	0.1			5.3	6.5
Phosphate buffers						
[H_3PO_4]	[$H_2PO_4^-$]					
0.1	0.001	0.001	0.1	0.1	2.2	3.1
0.03	0.001	0.001	0.1	0.1	2.4	3.5
0.01	0.001	0.001	0.1	0.1	2.9	4.0
[$H_2PO_4^-$]	[OH^-]					
0.05	0.004	0.054			5.9	7.0
0.05	0.010	0.060			6.4	7.5
0.05	0.022	0.072			6.7	7.8
0.05	0.037	0.087			7.4	8.6
0.05	0.045	0.095			7.9	9.1
[HPO_4^{2-}]	[OH^-]					
0.05	0.004	0.104			11.0	11.4
0.05	0.011	0.111			11.5	11.8
0.05	0.170	0.270			12.0	12.2
Borate buffers						
[H^+]	[$B_4O_7^{2-}$]					
0.018	0.0125	0.025	0.1	0.118	8.2	8.6
0.009	0.0125	0.025	0.1	0.109	8.6	9.1
[$B_4O_7^{2-}$]	[OH^-]					
0.0125	0.004	0.029	0.1	0.1	9.1	9.5
0.0125	0.015	0.040	0.1	0.1	9.7	10.1
0.0125	0.021	0.046	0.1	0.1	10.2	10.6
Ammonia buffers						
[NH_4^+]	[NH_3]					
0.1	0.001		0.1	0.2	8.3	8.0
0.03	0.001		0.1	0.13	8.8	8.5
0.01	0.001		0.1	0.11	9.3	8.8
0.003	0.001		0.1	0.103	9.8	9.3
0.001	0.001		0.1	0.101	10.1	9.7

(Table 1) were measured by glass electrode, standardized in 50% methanol [32]. The methanolic buffer solution (10 ml) was deaerated by bubbling nitrogen and the polarographic curve was recorded. Then 100 μl of the freshly prepared stock solution of steroid in methanol was added, so as to achieve a final concentration of 2×10^{-4} M steroid, and the polarographic curve was recorded again, after an additional deaeration for 1 min, using a

controlled drop-time of 3 s and a scan rate of 2 mV s^{-1}. To reduce the hysteresis of the recording system, for accurate measurements of half-wave potentials, a scan rate of 0.2 mV s^{-1} was used. Under such conditions, the difference of half-wave potentials obtained from current—voltage curves recorded from positive to negative and from negative to positive potentials was less than ±4 mV.

Differential pulse polarographic curves were recorded for the same solutions at a scan rate of 2 mV s^{-1} and pulse amplitude of 100 mV, with a drop-time of 2 s. Similar compositions of the studied solutions were used in linear sweep voltammetry, where the effect of the scan rate was studied, and in cyclic voltammetry, where the potential was scanned as follows

	"pH" 6.5	"pH" 10.1
testosterone, hydrocortisone	−1.25 → −1.85 → −1.25	−1.5 → −2.0 → −1.5
prednisolone, dexamethasone	−1.0 → −1.9 → −1.0	−1.3 → −2.0 → −1.3

Current—voltage curves in 0.03 M $N(CH_3)_4OH$ in methanol were also recorded using a hanging mercury drop electrode and a scan rate of 2 mV s^{-1}.

Controlled potential electrolysis was examined for a mercury pool electrode and for a DME as the working electrode. For the electrolysis with the pool electrode (area about 25 cm^2), 20 ml of the 0.03 M $N(CH_3)_4OH$ solution in methanol was used, the solution was stirred vigorously, and the potential was controlled by a potentiostat. For the electrolysis at a DME, 2.5 ml of a mixture of equal volumes of methanol and a phosphate buffer pH 7.0 containing 2×10^{-4} M steroid was placed in a small cell. Stirring was done simply by the falling mercury drops, and the potential was applied from a polarograph controlled manually. To determine the pinacols formed after complete electrolysis, a 1.5-fold excess of sodium periodate was added and the mixture was refluxed for 1 h. Decrease of the periodate concentration was followed by differential pulse polarography, as periodate yields peaks at potentials more positive than those of the steroids studied [33].

RESULTS

D.c. polarography of testosterone and hydrocortisone

In acidic solutions containing 50% methanol, reduction of Δ^4-3-keto-steroids (enones) occurs in a single two-electron step (i_{1+2}). With increasing pH the height of this wave decreases (Fig. 1, Table 2). The plot of the limiting current as a function of "pH" (Fig. 2) has the shape of a dissociation curve of a monobasic acid with an inflection point (pK'_D) at "pH" about 3.7. At "pH" about 5 the wave-height (denoted here as i_1) reaches the value corresponding to a one-electron reduction and remains unchanged up to "pH" about 7. Further increase in pH results in a decrease in the height of wave i_1 and its replacement by wave i_3, the total height remaining constant. Both the plots of the decrease of wave i_1 and increase in wave i_3 have a shape of a dissociation curve of a monobasic acid with an inflection point (pK'_A)

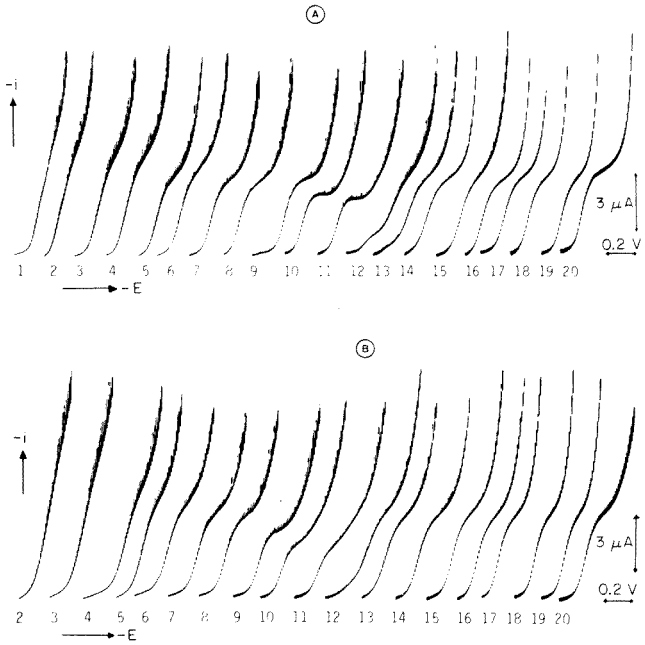

Fig. 1. D.c. polarographic curves of 2×10^{-4} M testosterone (A) and hydrocortisone (B) in buffer solutions containing 50% methanol of "pH" (1) 2.4; (2) 3.1; (3) 3.5; (4) 4.0; (5) 4.6; (6) 5.1; (7) 5.5; (8) 6.2; (9) 7.0; (10) 7.5; (11) 7.8; (12) 8.6; (13) 9.1; (14) 9.5; (15) 10.1; (16) 10.6; (17) 11.4; (18) 11.8; (19) 12.2; (20) 13.6. For buffer composition see Tables 1 and 2.

at "pH" 8.3 for testosterone and 7.8 for hydrocortisone. The height of wave i_3 remains constant up to "pH" 14 (Fig. 2). The ratio of $i_1 : i_3$ in the "pH" range between 7 and 9 is independent of buffer composition. At "pH" 8 the ratio was the same in phosphate as in borate buffers.

In a methanolic solution containing 0.03 M $N(CH_3)_4OH$, testosterone shows only a gradual increase in current at potentials more negative than about −1.9 V, whereas hydrocortisone shows another two-electron wave (i_5) at about −2.05 V.

The numbers of electrons transferred in individual steps (Table 3) were determined by comparison of wave-heights at "pH" 8.6 with those of equimolar solutions of benzophenone and 1,4-naphthoquinone (used as internal standards), comparison of wave-heights in 0.03 M $N(CH_3)_4OH$, and by large-scale coulometry in the same solution. The similarity of the results obtained with mercury electrodes with renewed and unrenewed surface reflects the fact that current—voltage curves of all four steroids in methanolic 0.03 M $N(CH_3)_4OH$ solution obtained with a DME and a hanging mercury drop electrode resemble each other closely.

The waves i_1 at "pH" 6 and i_3 at "pH" 11 are diffusion-controlled, as proved by linear dependence on steroid concentration and on the square

TABLE 2

Effect of pH on half-wave potential (V) and limiting current (μA) for testosterone and hydrocortisone at concentrations of 2×10^{-4} M

Curve[a]	"pH"[b]	Testosterone						Hydrocortisone					
		$-E_{1+2}$	$-E_1$	$-E_3$	i_{1+2}	i_1	i_3	$-E_{1+2}$	$-E_1$	$-E_3$	i_{1+2}	i_1	i_3
1	2.4 Z	1.08			0.46			—			—		
2	3.1 P	1.135			0.45			—			—		
3	3.5 P	1.165			0.425			1.19			0.455		
4	4.0 P	1.20			0.39			1.235			0.365		
5	4.6 Ac	1.25			0.315			1.27			0.335		
6	5.1 Ac		1.27			0.295			1.30			0.335	
7	5.5 Ac		1.31			0.30			1.34			0.32	
8	6.2 Ac		1.35			0.305			1.37			0.31	
9	7.0 P		1.415			0.31			1.43	—		0.265	0.035
10	7.5 P		1.44	—		0.27	0.03		1.45	—		0.21	0.09
11	7.8 P		1.45	—		0.26	0.04		1.455	1.65		0.18	0.135
12	8.6 P		1.495	1.63		0.04	0.25		—	1.61		0.06	0.255
	9.1 P		1.50	1.63		0.03	0.26			1.61			0.30
	8.6 B		1.47	1.615		0.045	0.255		—	1.60		0.03	0.30
13	9.1 B		—	1.61		0.015	0.29			1.59			0.30
14	9.5 B			1.605			0.30			1.605			0.315
15	10.1 B			1.62			0.285			1.62			0.315
16	10.6 B			1.63			0.30			1.64			0.31
17	11.4 P			1.66			0.305			1.675			0.31
18	11.8 P			1.68			0.305			1.695			0.30
19	12.2 P			1.695			0.30			1.71			0.30
20	13.6 Y			1.71			0.315			1.715			0.31
	14.5 X			1.705			0.315			1.705			0.325
	8.0 Am		1.47		0.36				1.48			0.38	
	8.5 Am		1.495		0.33				1.51			0.35	
	8.8 Am		1.525		0.32				1.54			0.33	
	9.3 Am		1.56		0.31				1.57			0.32	
	9.7 Am		1.57		0.30				1.59			0.31	

[a]Related to Fig. 1. [b]Ac, acetate buffer; Am, ammonia buffer; B, borate buffer; P, phosphate buffer; X, 1.0 M LiOH; Y, 0.1 M LiOH; Z, 0.01 M H_2SO_4.

root of mercury pressure. When the height of wave i_1 at "pH" 8.6 is only about 20% of its height at "pH" 6, the current is kinetic.

The half-wave potentials of wave i_{1+2} and i_1 are shifted to more negative values by 68 mV/pH unit for testosterone and by 66 mV/pH unit for hydrocortisone and become pH-independent at "pH" = pK'_A (8.3 for testosterone and 7.8 for hydrocortisone) (Fig. 3). The half-wave potential of wave i_3 is

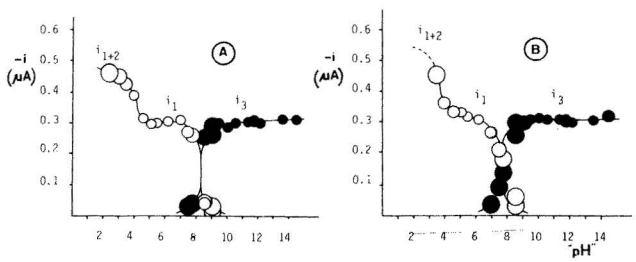

Fig. 2. Dependence of d.c. polarographic limiting currents of 2×10^{-4} M solutions of (A) testosterone and (B) hydrocortisone on "pH" in buffers containing 50% methanol.

TABLE 3

Comparison of the values of electrons transferred in wave i_3 measured by coulometry at a mercury pool and d.c. polarography

Coulometry in 0.03 M $N(CH_3)_4OH$/methanol					D.c. polarography					
					"pH" 8.6/50% methanol		0.03 M $N(CH_3)_4OH$/methanol			
Steroid	i_3	$(i_3 + i_4)$	i_5	$(i_3 + i_4 + i_5)$	i_3	$(i_3 + i_4)$	i_3	$(i_3 + i_4)$	i_5	$(i_3 + i_4 +$
Testosterone	1.0[a]	—	—	—	0.9	—	1.0	—	—	—
Hydrocortisone	1.0[a]	—	2.1[b]	3.7[c]	1.1	—	1.0	—	2.5	3.5
Prednisolone	1.0[d]	1.6[a]	2.1[b]	3.7[c]	1.0	1.8	1.0	2.0	2.0	4.0
Dexamethasone	1.0[e]	1.6[a]	2.2[b]	3.5[c]	1.0	2.0	—	—	—	—

[a]—1.74 V. [b]—2.0 V after a complete pre-electrolysis at the potential of the limiting current of wave i_3 or i_4, if present. [c]—2.0 V without pre-electrolysis. [d]—1.6 V. [e]—1.55 V.

practically pH-independent. The smaller variations shown are presumably due not to pH variations but to cation effects, and reflect the fact that cation kind and concentration in these buffers was not kept strictly constant. In solutions of lithium hydroxide in 50% methanol, where small cation effects are expected, the variations in half-wave potentials are negligible.

No separation of waves i_1 and i_3 could have been observed in ammonia—ammonium chloride buffers (Table 2). This is caused by the shift of the half-wave potentials of wave i_3 to more positive values in the presence of ammonium ions (by about 0.1 V in the presence of 0.1 M NH_4Cl), causing waves i_1 and i_3 to overlap. Change in the value of $dE_{1/2}/d$ pH in these buffers nevertheless indicates that the same change in the electroactive species at pH 7—9 occurs in ammonia—ammonium chloride buffers as occurs in other buffers.

A shift of the half-wave potential of i_3 to more positive values with increasing cation concentration was observed for cations other than the ammonium ion mentioned above. Thus an increase in sodium ion concentration from 0.1 to 1.1 M resulting from addition of sodium chloride to a

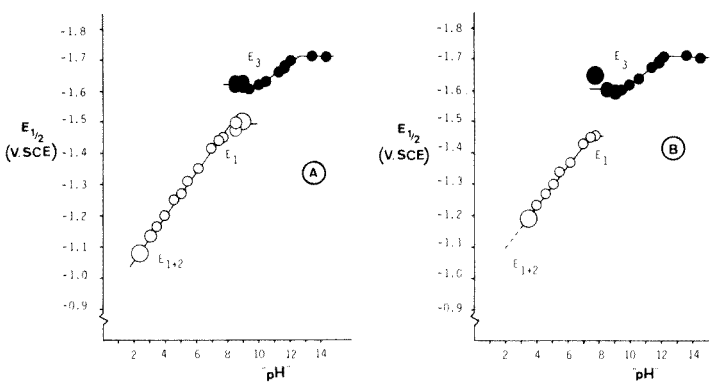

Fig. 3. Dependence of d.c. polarographic half-wave potentials of 2×10^{-4} M solution of (A) testosterone and (B) hydrocortisone on "pH" in buffers containing 50% methanol.

phosphate buffer "pH" 11.4 causes a shift of wave i_3 of hydrocortisone by 55 mV to more positive potentials. A similar increase in concentration of potassium ions resulted in a shift of only 30 mV, whereas addition of cesium ion caused a shift of only 15 mV.

Controlled potential electrolysis at the DME at a potential corresponding to the limiting current of wave i_3 of hydrocortisone quantitatively yielded the pinacol, as proved by a Malaprade reaction with periodate followed polarographically [33].

Pulse polarography of testosterone and hydrocortisone

The dependence of the peak heights obtained by differential pulse polarography (d.p.p.) and the limiting currents obtained by normal pulse polarography (n.p.p.) on pH (Fig. 4), as well as the pH-dependence of the characteristic potentials (Fig. 5) obtained by pulse polarographic techniques resembled closely the plots obtained by d.c. polarography (Figs. 2 and 3). Nevertheless, some small quantitative differences were observed. Thus the "pH" of the inflection point of the decrease in peak i_{p1} and increase in peak i_{p3} (pK'_A) in d.p.p. was 8.0 for testosterone and 7.5 for hydrocortisone. The height of the d.p.p. peak i_{p3} at "pH" 10 was somewhat smaller than that of the peak i_{p1} at "pH" 6 for both compounds; for n.p.p. this was observed only for testosterone, whereas for hydrocortisone the height of limiting currents i_{pl1} at "pH" 6 and i_{pl3} at "pH" 10 were approximately equal.

Also the slopes of the dE_{p1}/d pH plots obtained by d.p.p. (70 mV/pH for both steroids) and n.p.p. (72 mV/pH for testosterone, but 66 mV/pH for hydrocortisone) were slightly higher than those found for d.c. polarographic

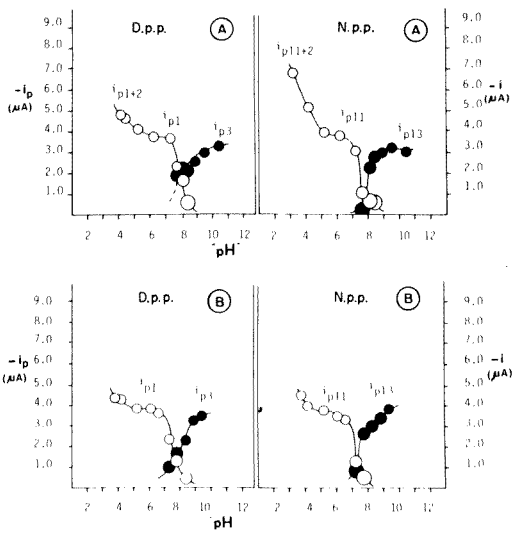

Fig. 4. Dependence of peak current in d.p.p. and limiting current in n.p.p. for 2×10^{-4} M solutions of (A) testosterone and (B) hydrocortisone, on "pH" in buffers containing 50% methanol.

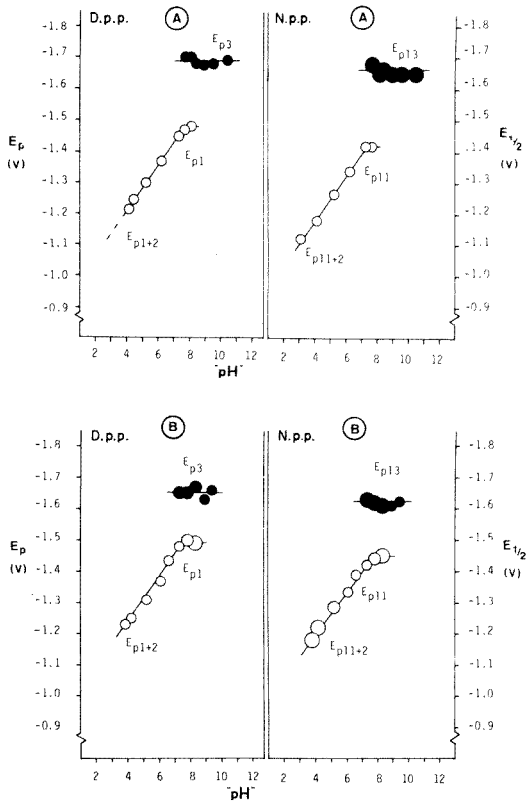

Fig. 5. Dependence of peak potential in d.p.p. and half-wave potential in n.p.p. for 2×10^{-4} M solutions of (A) testosterone and (B) hydrocortisone on "pH" in buffers containing 50% methanol.

$dE_{1/2}/d$ pH values. Potentials of peak i_{p3} and wave i_{p13} were practically pH-independent (Fig. 5) and less affected by cation effects than the d.c. wave i_3.

D.c. polarography of prednisolone and dexamethasone

The reduction pattern of the dienones studied resembles the reduction of enones in its main features (Fig. 6). As for enones, the reduction of the dienones in strongly acidic media occurs in a single two-electron wave (i_{1+2}, Fig. 7), the height of which decreases with increasing pH. The plot of the height of wave i_{1+2} as a function of pH has the shape of the dissociation curve of a monobasic acid with inflection point (pK'_D) at "pH" 5.5 for dexamethasone and "pH" 5.0 for prednisolone. At pH 6—7, a one-electron wave i_1 is observed, which is replaced at pH $\geqslant$8 by wave i_3. Replacement of wave i_1 by wave i_3 is best seen from changes in the slopes of the $E_{1/2}$—pH plots (Fig. 8, Table 4).

The dienones differ from the enones in that wave i_3 is accompanied by another one-electron wave i_4 (Figs. 6, 7; Table 4). The half-wave potential of

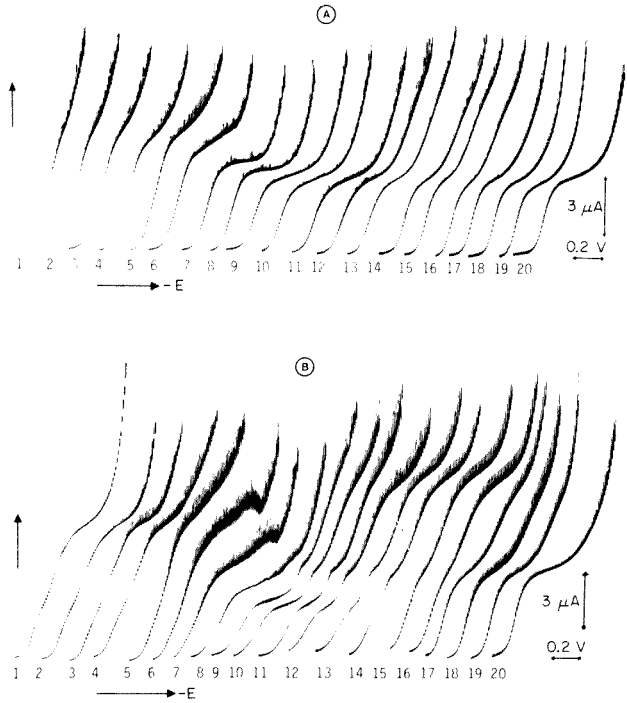

Fig. 6. D.c. polarographic curves of 2×10^{-4} M prednisolone (A) and dexamethasone (B) in buffer solutions containing 50% methanol at "pH" (1) 2.4; (2) 3.1; (3) 3.5; (4) 4.0; (5) 4.6; (6) 5.1; (7) 5.5; (8) 6.2; (9) 7.0; (10) 7.5; (11) 7.8; (12) 8.6; (13) 9.1; (14) 9.5; (15) 10.1; (16) 10.6; (17) 11.4; (18) 11.8; (19) 12.2; (20) 13.6. For buffer composition see Tables 4 and 1.

this wave i_4 remains pH-independent up to "pH" 10.3 for prednisolone and "pH" 10.8 for dexamethasone, but is shifted towards more negative potentials at higher pH values. Another difference observed for dienones is that the half-wave potentials of wave i_3 remain pH-dependent up to "pH" 11.8 (Fig. 8). The slopes of the $E_{1/2}$—pH plots are also slightly different: the slopes of waves i_{1+2} and i_1 are 62 mV/pH for prednisolone and 67 mV/pH for dexamethasone. The wave i_3 from "pH" 8—11 is shifted by 50 mV/pH for prednisolone and by 40 mV/pH for dexamethasone. The waves i_3 and i_4 at "pH" 10

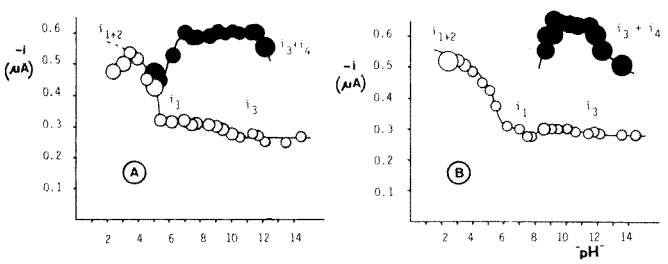

Fig. 7. Dependence of d.c. polarographic limiting currents of 2×10^{-4} M solutions of (A) prednisolone and (B) dexamethasone on "pH" in buffers containing 50% methanol.

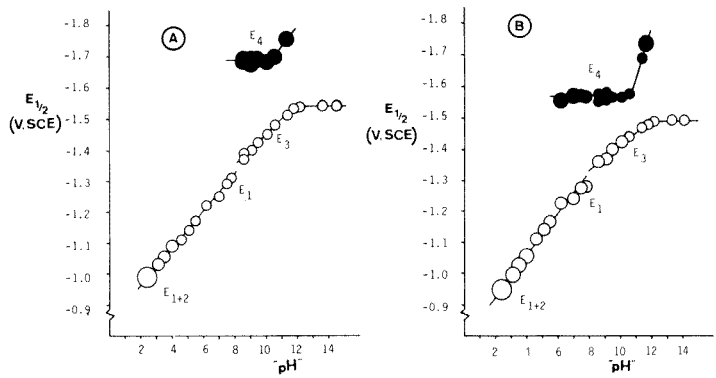

Fig. 8. Dependence of d.c. polarographic half-wave potentials of 2×10^{-4} M solutions of (A) prednisolone and (B) dexamethasone on "pH" in buffers containing 50% methanol.

are diffusion-controlled, as proved by linear dependence on the steroid concentration and on the square root of mercury pressure. Like hydrocortisone, prednisolone and dexamethasone in methanolic solution containing 0.05 M $N(CH_3)_4OH$ yield another two-electron wave (i_5) at about −2.0 V (Table 3).

Increasing concentration of sodium ions (from 0.1 to 1.1 M) added to a phosphate buffer of "pH" 11.4 results in a positive shift of the half-wave potential of wave i_3 by 50 mV and of wave i_4 by 115 mV. Similar increase in concentration of K^+ causes a shift of 30 mV for i_3 and 170 mV for i_4, whereas an increase in Cs^+ concentration causes a shift of 130 mV for i_3 and about 200 mV for i_4. In the presence of cesium ions, the shift of wave i_4 results in merging of i_3 and i_4 (Fig. 9). Ammonium ions have a similar effect on the shift of the half-wave potential of wave i_4 to more positive potentials. At "pH" 4.6—5.5, a wave of catalytic hydrogen evolution was observed for the polarographic curves of dexamethasone (Fig. 6). The wave i_1 of dexamethasone at pH 6—8 is complicated by an adsorption post-wave (Fig. 6, curves 8—13). Adsorption of dexamethasone at the DME was proved by electrocapillary curves.

Pulse polarography of prednisolone and dexamethasone

Dependence of the peak heights in pulse polarography on pH for the first wave i_{p1+2}, i_{p1}, and i_{p3} for prednisolone (Fig. 10A) closely resembles the pH dependence of these waves obtained by d.c. polarography (Fig. 7A) over the range in which it was studied. Peaks i_{p1+2} decreased, to be replaced at "pH" 6 by peak i_{p1}. The polarographic dissociation curve had an inflection point (pK'_D) at about "pH" 5.0. At "pH" $\geqslant$8.5, peak i_{p1} was replaced by peak i_{p3}.

The shifts of the peak potentials with pH (Fig. 11A) for prednisolone resembled strongly those obtained for the d.c. half-wave potentials (Fig. 7A). The slope of the pH-dependence of the potential of peaks i_{p1+2} and i_{p1} was 67 mV/pH unit and that of i_{p3} was 45 mV/pH unit. The limiting currents of waves i_{pl1+2}, i_{pl1} and i_{pl3} obtained for prednisolone by normal pulse polarography followed a similar pattern of pH-dependence as in d.c.p. and d.p.p.

TABLE 4

Effect of pH on half-wave potential (V) and limiting current (μA) for prednisolone and dexamethasone at concentrations of 2×10^{-4} M

Curve[a]	"pH"[b]	Prednisolone						Dexamethasone					
		$-E_{1+2}$	$-E_3$	$-E_4$	i_{1+2}	i_3	$i_3 + i_4$	$-E_{1+2}$	$-E_3$	$-E_4$	i_{1+2}	i_3	$i_3 + i_4$
1	2.4 Z	0.99			0.515			0.95			0.475		
2	3.1 P	1.03			0.52			0.995			0.500		
3	3.5 P	1.055			0.505			1.025			0.535		
4	4.0 P	1.09			0.485			1.055			0.515		
5	4.6 Ac	1.11			0.45			1.11			0.45		
6	5.1 Ac	1.14			0.425			1.14			0.425		0.485
7	5.5 Ac	1.17			0.375			1.165			0.32	$i_1 + i_4$	0.45
8	6.2 Ac	1.22			0.31			1.225		1.555	0.315		0.525
9	7.0 P	1.25	E_1		0.30	i_1		1.24	E_1	1.57	0.32	i_1	0.60
10	7.5 P	1.29			0.275			1.275		1.57	0.305		0.585
11	7.8 P	1.31			0.275			1.28		1.565	0.31		0.585
12	8.6 P		1.37	1.69		0.30	0.55		1.36	1.575		0.305	0.59
	9.1 P		1.40	1.69		0.30	0.60		1.37	1.58		0.30	0.60
	8.6 B		1.39	1.68		0.30	0.60		1.36	1.55		0.305	0.595
13	9.1 B		1.40	1.67		0.30	0.65		1.37	1.555		0.305	0.605
14	9.5 B		1.425	1.69		0.30	0.64		1.40	1.565		0.29	0.595
15	10.1 B		1.45	1.68		0.30	0.635		1.425	1.565		0.275	0.605
16	10.6 B		1.48	1.695		0.29	0.64		1.44	1.575		0.265	0.60
17	11.4 P		1.51	1.75		0.285	0.63		1.47	1.69		0.275	0.60
18	11.8 P		1.53	—		0.29	0.60		1.48	1.74		0.27	0.60
19	12.2 P		1.535	—		0.285	0.55		1.49	—		0.25	0.55
20	13.6 Y		1.535	—		0.285	0.50		1.49			0.245	
	14.5 X		1.535			0.29			1.49			0.28	
	8.0 Am		1.315			0.295			1.32	1.51		0.35	0.75
	8.5 Am		1.345			0.29			1.33	1.53		0.35	0.75
	8.8 Am		1.375			0.30			1.37	1.55		0.34	0.735
	9.3 Am		1.41			0.30			1.40	1.56		0.33	0.71
	9.7 Am		1.43			0.30			1.41	1.56		0.315	0.66

[a]Related to Fig. 6. [b]See footnote to Table 2.

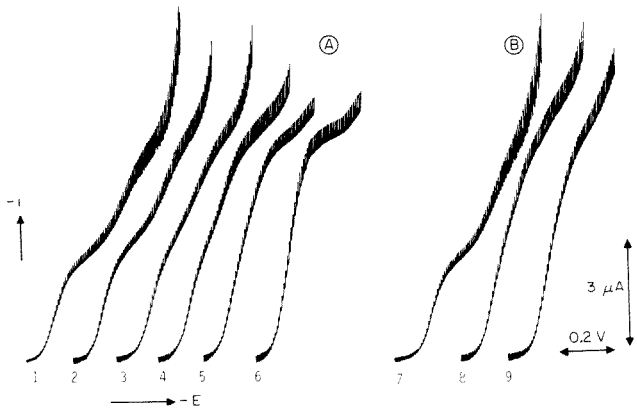

Fig. 9. (A) Polarographic curves of 2×10^{-4} M dexamethasone in a phosphate buffer containing 50% methanol "pH" 11.4 (1) and after addition of alkali metal salts: (2) 0.1 M NaCl; (3) 1.0 M NaCl; (4) 0.1 M KCl; (5) 1.0 M KCl; (6) 0.1 M CsCl. (B) Polarographic curves of 2×10^{-4} M prednisolone in borate buffer containing 50% methanol "pH" 10.6 (7) and after addition of (8) 0.1 M CsCl; (9) and 1.0 M CsCl.

The shifts of half-wave potentials of the waves of prednisolone (Fig. 11A) obtained with n.p.p. were similar to those obtained by d.c.p. and d.p.p., with slopes of 72 mV/pH unit for waves i_{pl1+2} and i_{pl1}, and of 35 mV/pH unit for wave i_{pl3}. No peak or wave corresponding to the d.c. wave i_4 was observed by either d.p.p. or n.p.p. in buffered solutions. In 0.03 M $N(CH_3)_4OH$ in methanol, the peak i_{p4} obtained by d.p.p. was much smaller than peaks i_{p3} and i_{p5} (Fig. 12).

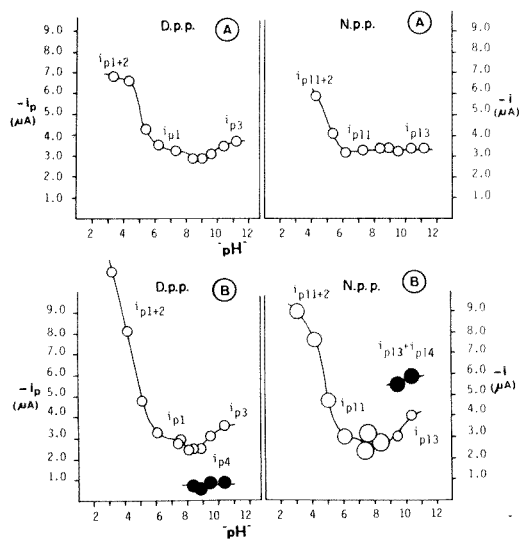

Fig. 10. Dependence of peak current in d.p.p. and limiting current in n.p.p. on "pH" in 2×10^{-4} M solutions of (A) prednisolone and (B) dexamethasone in buffers containing 50% methanol.

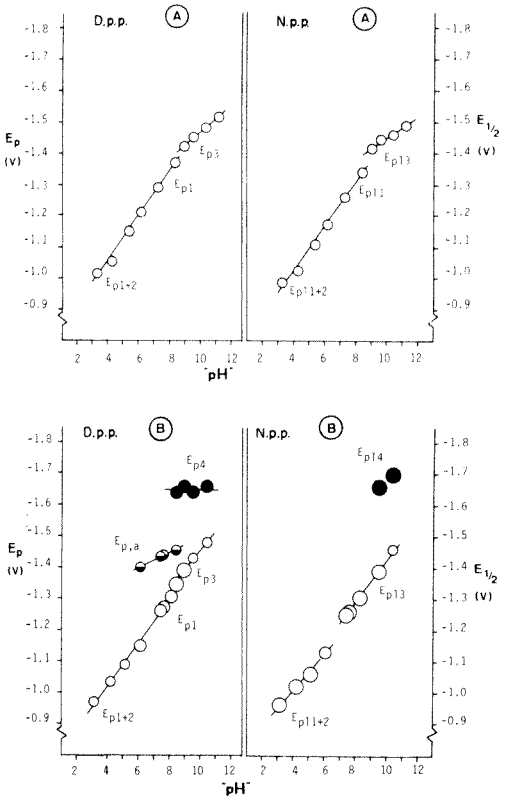

Fig. 11. Dependence of peak potential in d.p.p. and half-wave potential in n.p.p. in 2×10^{-4} M solutions of (A) prednisolone and (B) dexamethasone on "pH" in buffers containing 50% methanol.

For dexamethasone, the presence of peaks i_{p1+2}, i_{p1} and i_{p3} in d.p.p. and waves i_{p11+2}, i_{p11} and i_{p13} in n.p.p. resembled the behavior in d.c. polarography (Fig. 10B). All these peaks were accompanied by adsorption pre- or post-waves at "pH" <9 and at "pH" <5 by a catalytic wave. Essential differences were the total height corresponding to the process i_{1+2} in strongly acidic media and the potentials corresponding to the wave i_3. Thus in acidic media, the peak i_{p1+2} and the wave i_{p11+2} reach a height about 3 times larger than the current at "pH" 8, probably because of catalytic hydrogen evolution. The half-wave potential of wave i_{p13} as well as the peak potential of peak i_{p3} change definitely with pH. The slope of the pH-dependence of peaks i_{p1+2} and i_{p1} was 70 mV/pH unit and of peak i_{p3} 60 mV/pH unit. In n.p.p. the observed values were 58 mV/pH unit for wave i_{p11+2} and 85 mV/pH unit for wave i_{p13}. This might be due to complications by adsorptive phenomena.

The differential pulse peak i_{p4} was only about 25% of the peak i_{p3} at "pH" 9, whereas i_{p14} in n.p.p. had a height similar to the height of i_{p13}. The peak potential of peak i_{p4} in d.p.p. was practically independent of pH. Because of

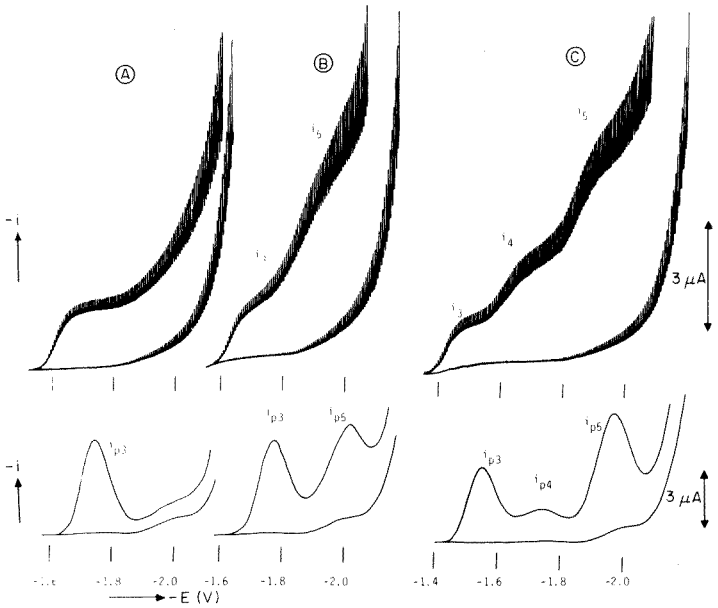

Fig. 12. D.c. (above) and d.p. (below) polarographic curves of 10^{-4} M solutions of (A) testosterone, (B) hydrocortisone, and (C) prednisolone in 0.03 M tetramethylammonium hydroxide in methanol.

complications caused by adsorption waves, the half-wave potentials of wave i_{pl4} in n.p.p. could be measured only at two pH values.

Linear sweep and cyclic voltammetry

Linear sweep voltammetric curves were recorded with varying scan rates (v). The dependence of the values of peak potentials (E_p) for waves i_1 and i_3 of hydrocortisone and prednisolone on the logarithm of the scan rate was linear over a wide pH range. The slope of this linear dependence, i.e. $dE_p/d\log v$ changed with pH from a value of about 30 mV per tenfold change in v at pH smaller than about 11 to a value approaching 20 mV per tenfold change in v in more alkaline media (Fig. 13).

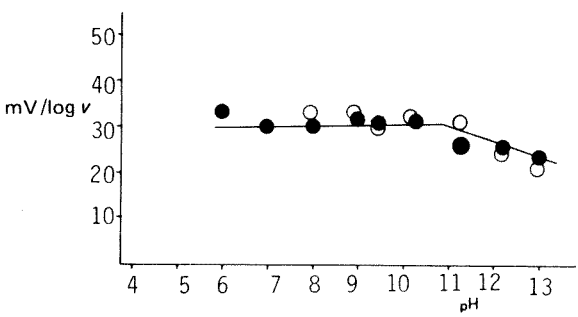

Fig. 13. Dependence of the slope ($dE_p/d\log v$) of the plot of peak potential against logarithm of the scan rate in linear sweep polarography on pH for 10^{-4} M hydrocortisone (○) and 10^{-4} M prednisolone (●) in buffers containing 50% methanol.

Cyclic voltammograms recorded at a scan rate of 20 V s^{-1} at "pH" 6.5 and 10.1 showed a small oxidation peak in the potential range of the first electron transfer (corresponding to wave i_1 or i_3). In the potential range of the second electron uptake (corresponding to wave i_4) in the solutions of prednisolone or dexamethasone, no oxidation peak was observed.

DISCUSSION

In the first part of this series [1], the observations [4, 18, 34—36] that in Δ^4-3-ketosteroids and $\Delta^{1,4}$-3-ketosteroids, reduction of the COCH=CH group occurs in the first wave of enones and first two waves of dienones, were generalized and confirmed.

It was also confirmed that the reduction potentials became more positive with increased size of the conjugated system. The wave (i_5) at —2.0 V was attributed to the reduction of the C-17 side chain. This reduction process is practically unaffected by reductions occurring in ring A, as can be seen by comparison particularly of the differential pulse polarographic peaks i_{p5} of hydrocortisone (Fig. 12) and prednisolone. These peaks resemble each other in spite of the fact that the preceding process involves only one electron for hydrocortisone but two electrons for prednisolone. Wave i_5 thus does not correspond to a consecutive reduction of the same grouping reduced in waves i_3 (and i_4), but to an independent reduction process involving another reactive center. Such processes have been observed [37] for molecules having the two reactive centers separated by a system which does not readily transmit substituent effects. Groups in ring A and ring D of the steroid molecule evidently fulfill such a condition. This enables further discussion to be restricted to processes occurring in the most positive waves i_{1+2}, i_1, i_3 (and i_4).

The fundamental problem involved in the reduction of ring A in Δ^4- and $\Delta^{1,4}$-3-ketosteroids is the question whether the two-electron reduction results in a formation of an unsaturated alcohol or whether hydrogenation of an ethylenic bond occurs. Similarly, for the first one-electron step, distinction should be made between formation of a pinacol in a carbonyl—carbonyl coupling, a β—β coupling or a β-carbonyl coupling [38] under the conditions of polarographic electrolysis. Solution of this problem has implications not only for the analytical use of polarographic curves, but also for electrosynthesis, as it has been proved that the mechanism of this process follows a similar pattern at the DME and mercury electrodes with unrenewed surface such as hanging mercury drop or mercury pool electrode [39, 40]. This distinguishes the α,β-unsaturated ketosteroids from straight-chain α,β-unsaturated ketones (such as chalcone [41]) and aldehydes (such as cinnamaldehyde [42] and acrolein [43]).

α,β-Unsaturated ketones are considered [44—46] to be a single electroactive group to which the electron is transferred in a particular molecular orbital. From this point of view, conception of the site of electron attack is meaningless, and the nature of the products formed in electrolysis is

governed by the site of protonation [41—43, 47—49]. Such protonation can occur either before or after an electron transfer. Protonation of the parent compound or of radical anion formed in the first electron uptake on the carbonyl group leads to a formation of an unsaturated alcohol, and protonation on the ethylenic bond leads to hydrogenation of this bond. This site of protonation, using a given type of electrode, depends on the structure of the compound, the solvent and the proton donors involved.

For straight-chain α,β-unsaturated ketones an early study [50] reported formation of saturated ketones indicating protonation and reduction of the ethylenic bond. All studies at the DME [38, 41, 47, 49] and the majority of studies of such reductions on other electrodes [38] indicate a similar reaction path. Reported exceptions involve reductions at mercury pool electrodes of 1-phenyl-2-butenone [51] (for which a formation of 2.5% of the unsaturated alcohol was reported), of chalcone [48] (for which yields of chalcol were not reported), and of 1,5-diphenyl-2,4-pentadienone [52] (even if the experimental evidence for the formation of 1,5-diphenyl-5-hydroxy-1,3-pentadione is inconclusive and no yield was reported). For cyclohex-2-enone [10, 11] and 2,5-cyclohexadienones [53, 54], no attention has been paid to the two-electron reduction products.

For the dienones studied, the experimental evidence available indicates that the compounds involved are protonated on the carbonyl group and that an unsaturated alcohol results. This conclusion follows from the fact that wave i_4 corresponds to a one-electron uptake. If in the process of the two-electron reduction one ethylenic bond were hydrogenated, an α,β-unsaturated ketone (enone) would be formed. This species would be reduced at the potential of wave i_4 so that the total height of wave i_4 would correspond to a two-electron transfer. Independent proof for the preferred protonation at the carbonyl group is the formation of the pinacol in the first one-electron step discussed below.

The results obtained by d.c. and pulse polarographic methods together with the linear sweep and cyclic voltammetry data can be rationalized when the following mechanism (where only ring A is shown) is considered

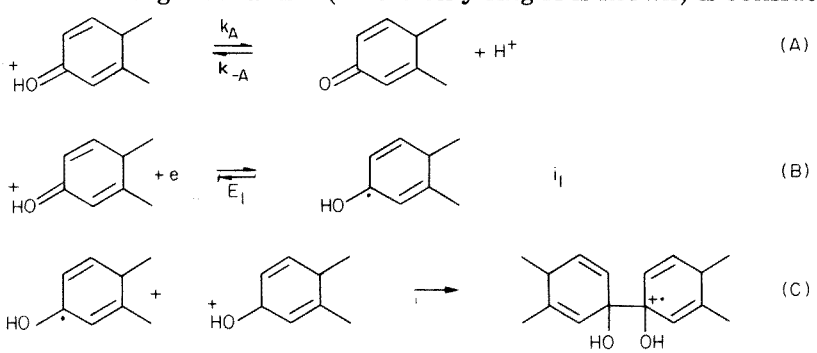

with the following stabilization of the radical cation by a second electron uptake

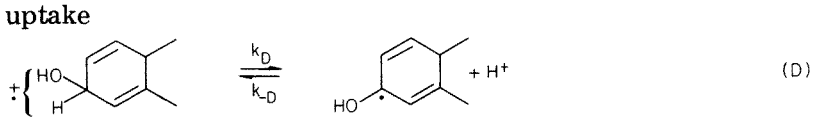

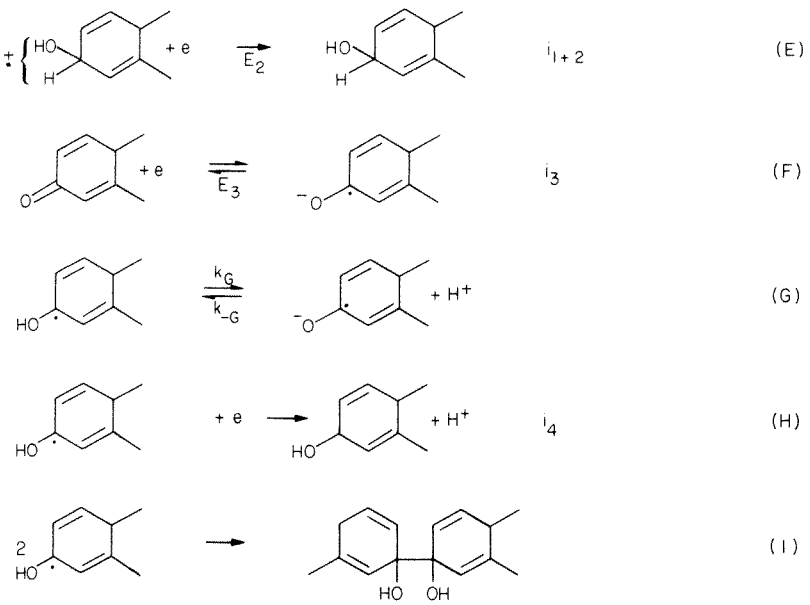

Protonation of α,β-unsaturated ketosteroids in sulfuric acid solutions has been proved [7, 8]. The involvement of the protonated form in the electroreduction of these compounds even at pH 7 is caused by the fact that electrolytic currents are governed by kinetic rather than thermodynamic control. As long as the rate of protonation with constant k_{-A} is sufficiently fast to convert all ketosteroid to the more easily reducible protonated form, the height of wave i_1 does not decrease below the value corresponding to a one-electron transfer. At pH >7 the rate of protonation with constant k_{-A} decreases, the height of wave i_1 decreases and this wave is replaced by wave i_3. Large difference between the value of pK_1 determined spectrophotometrically [7, 8] and the "pH" corresponding to the inflection point of the decrease of i_1 indicates that protonation with constant k_{-A} occurs as a heterogeneous process at the electrode surface [55].

As long as the protonation of the radical in (D) is fast, a two-electron transfer occurs in wave i_{1+2} involving steps (A) through (E), as potential E_2 is similar to or more positive than potential E_1. Decrease in the rate of protonation with rate constant k_{-D} with increasing pH results in a decrease in current i_{1+2}, until it reaches the value corresponding to a one-electron step and steps (A) and (B) are followed. The half-wave potentials of waves i_{1+2} and i_1 follow a single linear plot for E_{1+2} and E_1 (Fig. 8), indicating that step (B) remains a potential-determining step even for wave i_{1+2}.

At "pH" >8.5, reduction of the unprotonated form of the steroid (F) occurs. Even when waves i_1 and i_3 are not well separated, this change in the nature of the electroactive species can be deduced from the change in the slope of the E—pH plots, particularly for data obtained with pulse polarography (Fig. 11).

Further indication of the change in the process is the occurrence of wave i_4 in this pH range. Analogy with the behavior of enones where waves i_1 and i_3 are better separated can also be accepted as circumstantial evidence. Dependence of the half-wave potential of wave i_3 can be ascribed to the acid—base equilibrium (G) following a reversible one-electron uptake. Competition from a Michael addition of the hydroxide ion to the radical anion and from the cation effects cannot be excluded. Effects of the nature and concentration of the cation of the supporting electrolyte can be due either to a change in the double-layer structure or alternatively cations might form reducible ketyles as shown in (J)—(L)

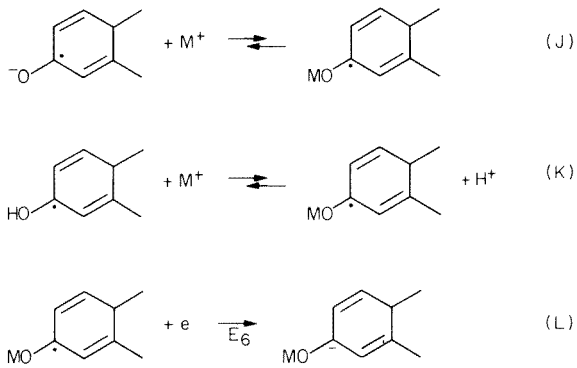

followed by the reaction of the anion with hydrogen ions. Shifts in potentials of waves i_3 and i_4 are then due to the fact that potential E_6 is more positive than potential E_4, as was observed in the reduction of other metal ketyls [56].

Protonation of the radical anion in reaction (G) is also responsible for the change in slope of the E—pH plot for wave i_4 (Fig. 8). The "pH" of the intersection of the two linear portions gives approximate value of "pK_G", being about 10.3 for prednisolone and 10.8 for dexamethasone.

The observed slope of 30 mV for the E_p—log v plot indicates [57, 58] a dimerization reaction in which radical is coupled to a parent molecule (C). Changes in the slope (Fig. 13) occur at pH >11. This pH is larger than pK'_A, but the difference can be due to differences in the conditions in polarography and linear sweep methods. If such an assumption is correct, then (I) is the process corresponding to the 20 mV slope. When analogous criteria developed [59, 60] for d.c. polarographic waves were applied [11] to the waves of cyclohex-2-enone, a reversible electron transfer followed by dimerization was also postulated. Nevertheless, the value of $dE_{1/2}/d\log c$ = 20 mV indicated radical—radical interaction even at pH 3.3.

The majority of α,β-unsaturated ketones [61, 62] undergoes β—β coupling because of the preferential protonation on ethylenic carbons. The present results obtained on the micro scale for both enones and dienones show the formation of pinacol in agreement with earlier studies [3, 4]. This further confirms the preferred protonation on the carbonyl group. Pinacol formation was also assumed for the product of the one-electron reduction of cyclohex-2-enone [11] and reported for the reduction of 2,5-cyclohexadienone [53].

Reduction of the enones studied can be described by the same scheme (A)—(G) as that for the dienones. Independence of the characteristic potential of wave i_3, clearly evident for the values obtained by pulse polarography (Fig. 5), indicates that equilibrium (G) is shifted to the right in the whole range of pH studied. As the radical anion formed in reaction (F) is not protonated, it cannot be reduced in wave i_4. Thus wave i_4 is absent on the current—voltage curves of the enones. The gradual increase of limiting current observed for testosterone at potentials more negative than about −1.9 V (Fig. 12) and indicated by the value of n = 3.7 (instead of 3.0) at the limiting current of wave i_5 in methanolic 0.03 M $N(CH_3)_4OH$, can be attributed to a slow reduction of the radical anion formed in (F).

Quantitative differences between the "pH" values of the inflection points of the dependences of limiting currents on "pH" and between the slopes of the dependences of characteristic potentials on pH obtained by d.c. and pulse polarographic methods can be attributed to the difference in time-interval ("window") in which measurement is carried out. Conversion of the electro-inactive to the electroactive species in reactions like those with rate constants k_{-A}, k_{-D} and k_{-G} will produce different amounts of the electroactive species during the 3 s involved in d.c. polarography and the 17 ms that is needed for the measurement in d.p.p.

The preference for protonation on the carbonyl group for α,β-unsaturated ketosteroids and other alicyclic compounds, when compared with preferred protonation on the ethylenic bond in straight-chain unsaturated ketones, can be abscribed to steric factors, but this seems to be somewhat doubtful in view of the small size of the proton. More plausible seems the assumption that such alicyclic ketones are oriented or adsorbed at the electrode surface in such a way that only certain sites are accessible to protonation. In the case of dexamethasone, adsorption at the electrode surface is particularly strong and results in formation of adsorption waves (Fig. 6).

REFERENCES

1 H. S. de Boer, J. den Hartigh, H. J. L. L. Ploegmakers and W. J. van Oort, Anal. Chim. Acta, 102 (1978) 141.
2 P. Zuman, J. Tenygl and M. Březina, Collect. Czech. Chem. Commun., 19 (1954) 46.
3 H. Lund, Acta Chem. Scand., 11 (1951) 283.
4 P. Kabasakalian and J. McGlotten, J. Am. Chem. Soc., 78 (1956) 5032.
5 P. Kabasakalian and J. McGlotten, J. Electrochem. Soc., 105 (1958) 261.
6 P. Zuman, J. Electrochem. Soc., 105 (1958) 758.
7 R. I. Zalewski and G. E. Dunn, Can. J. Chem., 48 (1970) 2538.
8 M. A. Smoczkiewicz and R. I. Zalewski, Steroids, 12 (1968) 391.
9 S. G. Mairanovskii, Catalytic and Kinetic Waves in Polarography, Plenum, New York, 1968, p. 128.
10 T. S. Ivcher, E. N. Zilberman and E. M. Perepletchikova, Zh. Fiz. Khim., 39 (1965) 749.
11 E. J. Denney and B. Mooney, J. Chem. Soc., (1968) 1410.
12 N. Shinriki and T. Nambara, Yakugaku Zasshi, 91 (1971) 611.
13 N. Shinriki and T. Nambara, Yakugaku Zasshi, 91 (1971) 6.
14 O. Hrdý, Česk. Farm., 11 (1962) 192.
15 Y. Asahi, Takeda Kenkyushu Nempo, 18 (1959) 17.

16 J. Eisenbrand and H. Picher, Z. Physiol. Chem., 260 (1939) 83.
17 J. K. Wolfe, E. B. Hershberg and L. F. Fieser, J. Biol. Chem., 136 (1940) 653.
18 A. I. Cohen, Anal. Chem., 35 (1963) 128.
19 J. L. Spahr and A. M. Knevel, J. Pharm. Sci., 55 (1966) 1020.
20 H. P. Deys and J. A. C. van Pinxteren, Pharm. Weekbl., 93 (1958) 760.
21 O. Hrdý, Česk. Farm., 11 (1962) 255.
22 P. Kabasakalian, S. DeLorenzo and J. McGlotten, Anal. Chem., 28 (1956) 1669.
23 P. Ekwall, T. Lundsten and L. Sjöblom, Acta Chem. Scand., 5 (1951) 1383.
24 R. N. Yadav and F. W. Teare, J. Pharm. Sci., 67 (1978) 436.
25 E. Jacobsen and B. Korvald, Anal. Chim. Acta, 99 (1978) 255.
26 M. J. Heasman and A. J. Wood, J. Pharm. Pharmacol., 23 (1971) 1765.
27 K. V. Nahabedian, 1973, private communication.
28 W. J. Bover and P. Zuman, J. Am. Chem. Soc., 95 (1973) 2531.
29 T. J. M. Pouw and P. Zuman, J. Org. Chem., 41 (1976) 1641.
30 T. J. M. Pouw, W. J. Bover and P. Zuman, in W. F. Furter (Ed.), Thermodynamic Behavior of Electrolytes in Mixed Solvents, Adv. Chem. Ser., 155 (1976) 343.
31 Nederlandse Farmacopee, 8th edn., Staatsuitgeverij, s'-Gravenhage, 1978.
32 M. Paabo, R. A. Robinson and R. G. Bates, J. Am. Chem. Soc., 87 (1965) 415.
33 P. Zuman and J. Krupička, Collect. Czech. Chem. Commun., 23 (1958) 598.
34 D. M. Robertson, Biochem. J., 61 (1955) 681.
35 O. Hrdý, Collect. Czech. Chem. Commun., 27 (1962) 2447.
36 P. Zuman, Talanta, 12 (1965) 1337.
37 P. Zuman, Fresenius Z. Anal. Chem., 224 (1967) 374.
38 D. H. Evans, Carbonyl Compounds, in A. J. Bard and H. Lund (Eds.), Encyclopedia of Electrochemistry of the Elements, Vol. XII, M. Dekker, New York, 1978, pp. 1—259.
39 P. Zuman, J. Polarogr. Soc., 13 (1967) 53.
40 P. Zuman, Relation Between Micro and Macro Phenomena, in M. Baizer (Ed.), Organic Electrochemistry, M. Dekker, New York, 1973, p. 155.
41 A. Ryvolová-Kejharová and P. Zuman, J. Electroanal. Chem., 21 (1969) 197.
42 D. Barnes and P. Zuman, Trans. Faraday Soc., 65 (1969) 1668, 1681.
43 J. Spritzer and P. Zuman, J. Electroanal. Chem., in press.
44 P. Zuman, Chem. Listy, 48 (1954) 94.
45 P. Zuman, Substituent Effects in Organic Polarography, Plenum, New York, 1967, p. 8.
46 P. Zuman, Fortschr. Chem. Forsch., 12 (1969) 1 (p. 63).
47 P. Zuman and J. Michl, Nature, 192 (1961) 655.
48 V. N. Nikulin, N. M. Kargina and Yu. M. Kargin, Zh. Obshch. Khim., 43 (1973) 2712.
49 P. Zuman and L. Spritzer, J. Electroanal. Chem., 69 (1976) 433.
50 R. Pasternack, Helv. Chim. Acta, 31 (1948) 753.
51 M. A. Michel, P. Martinet, G. Mousset and J. Simonet, C. R. Acad. Sci. Paris, 274 Ser. C (1972) 470.
52 Yu. M. Kargin, V. A. Latypova-Kondranina, N. M. Kargina and S. F. Pivovarova, Zh. Obshch. Khim., 48 (1978) 2746.
53 A. Mazzenga, D. Lomnitz, J. Villeges and C. J. Polowczyk, Tetrahedron Lett., (1969) 1665.
54 D. Rasuleva, A. A. Volodkin, V. V. Ershov, A. I. Prokofev and S. P. Solodovnikov, Izv. Akad. Nauk SSSR, Ser. Khim., (1970) 1659.
55 S. G. Majranovskij and L. I. Lishcheta, Collect. Czech. Chem. Commun., 25 (1960) 3025.
56 M. Ashworth, Collect. Czech. Chem. Commun., 13 (1948) 229.
57 C. P. Andrieux, L. Nadjo and J. M. Savéant, J. Electroanal. Chem., 26 (1970) 147.
58 C. P. Andrieux, L. Nadjo and J. M. Savéant, J. Electroanal. Chem., 42 (1973) 223.
59 J. Koutecký and V. Hanuš, Collect. Czech. Chem. Commun., 20 (1955) 124.
60 S. G. Mairanovskii, Izv. Akad. Nauk USSR, Otd. Khim. Nauk, (1961) 2140.
61 M. M. Baizer and J. P. Petrovich, Adv. Phys. Org. Chem. (A. Streitwieser, Ed.), 7 (1970) 189.
62 K. W. Bowers, R. W. Giese, J. Grimshaw, H. O. House, N. H. Kolodny, K.-H. Kronberger and D. K. Roe, J. Am. Chem. Soc., 92 (1970) 2783.

Analytica Chimica Acta, 130 (1981) 133—140
Elsevier Scientific Publishing Company, Amsterdam — Printed in The Netherlands

POLAROGRAPHIC INVESTIGATION OF THE STABILITY OF TIN(II) SOLUTIONS IN THE PRESENCE OF SOME STABILIZING AGENTS

STEFAN GŁODOWSKI and ZENON KUBLIK*
Department of Chemistry, University of Warsaw, 02093 Warsaw, Pasteura 1 (Poland)
(Received 31st March 1981)

SUMMARY

The stability of acidic tin(II) solutions was investigated polarographically in the presence of substances with mild antioxidant properties. The best stabilizing action is exerted by pyrogallol, hydrazine or phenolsulphonic acid. In methanolic solutions containing perchloric acid, the stability improves whereas chloride ions hasten the oxidation of tin(II). It is shown that the enhanced stability is due neither to complexation of tin(II) nor to reduction of oxygen by the antioxidants used. The fact that some of the reagents tested exert a powerful stabilizing action even in very small concentrations supports an earlier suggestion that the reaction between tin(II) and oxygen is a chain reaction which is inhibited by the stabilizer.

Solutions of tin(II) are readily oxidized by atmospheric oxidation and there is no sure way as yet of improving effectively the stability of such solutions. For analytical purposes, it is usually recommended to prepare and store tin(II) solutions under an inert atmosphere [1] or to generate tin(II) ions coulometrically in the deaerated solution under test [2]. According to Fano and Zanotti [3] and Metzger et al. [4], tin(II) is less stable in aqueous solutions than in methanolic solutions. To stabilize tin(II) in tin-plating solutions, the sulphonated phenols are often used [5]. Some improvement in the stability of tin(II) solutions is also attained in the presence of Bandrowski's base [6].

It seemed that the stability of tin(II) solutions might be improved by the addition of certain substances with mild reducing properties, such as hydrazine, hydroxylamine, hypophosphorous acid, ascorbic acid or certain *o*-diphenols. Some of these substances have been used as antioxidants [7, 8] or for the removal of oxygen from solutions [9]. The main purpose of the investigations described in this paper was to compare the stability of tin(II) solutions in the presence of such antioxidants. Polarography was used to monitor the changes in concentration of tin(II) in the solutions.

0003—2670/81/0000—0000/$02.50

EXPERIMENTAL

The polarographic curves were recorded with a Radelkis OH-105 polarograph with a three-electrode arrangement. The auxiliary electrode consisted of a bright platinum sheet with a surface area of 2 cm^2 and the reference electrode was a saturated calomel electrode, to which all the measured potentials are referred. The dropping mercury electrode had the characteristics $m = 1.55$ mg s^{-1} and $t = 5$ s at $h = 91$ cm. Most experiments were done at ambient room temperature (18—22°C). For quantitative work, a thermostatted, circulated water bath was used to maintain the temperature at 20 ± 0.1°C. Prior to recording the curves, the solutions were deaerated by a stream of hydrogen.

All inorganic chemicals, as well as pyrogallol (Mallinckrodt or Koch-Light), tiron (Fluka), and ascorbic acid (Polfa), were of analytical grade and were used as received. *p*-Phenolsulphonic acid (Fluka) was of technical grade and contained 65% phenolsulphonic acids, 2% free sulphuric acid and 2% phenol, and water. Bandrowski's base was prepared by oxidation of *p*-phenylenediamine in ammoniacal solution [10]. A tin(II) solution (10^{-2} mol l^{-1}) was prepared by dissolution of an appropriate amount of tin(II) oxide in deaerated 2 mol l^{-1} sulphuric acid solution. This stock solution was stored under hydrogen and was used for no longer than 3 days. More dilute solutions were prepared fresh daily and were also stored under hydrogen. According to Baes and Mesmer [11], tin(II) hydrolyses in solutions only at pH $\geqslant$1.5; to exclude such hydrolytic interferences, the pH of the working solutions was kept below 1.5. Standard tin(IV) solutions were prepared by dissolution of tin metal in 4 mol l^{-1} sulphuric acid in the presence of hydrogen peroxide. Water used to prepare solutions was distilled first in a metal apparatus and then twice in a quartz still.

RESULTS

Preliminary experiments

Prior to the investigation of the stability of tin(II) species, it was necessary to establish the extent to which the tin(II) reduction and oxidation waves are affected by the presence of the tin(IV) species that may appear by oxidation of tin(II), by the presence of the added antioxidants, and by the presence of dissolved oxygen. Accordingly, the polarographic behaviour of fresh tin(II) and tin(IV) species was compared in deaerated solutions in the absence and presence of the antioxidants tested. In order to establish whether or not the changes in the tin(II) oxidation wave can be ascribed to the presence of dissolved oxygen, the oxygen wave was recorded for each supporting electrolyte separately. Several typical curves obtained in these experiments are presented in Fig. 1. Some data concerning the $E_{1/2}$ values are presented in Table 1. Among the substances tested as antioxidants, only Bandrowski's base gave a cathodic wave prior to the reduction wave of tin(II) under the present

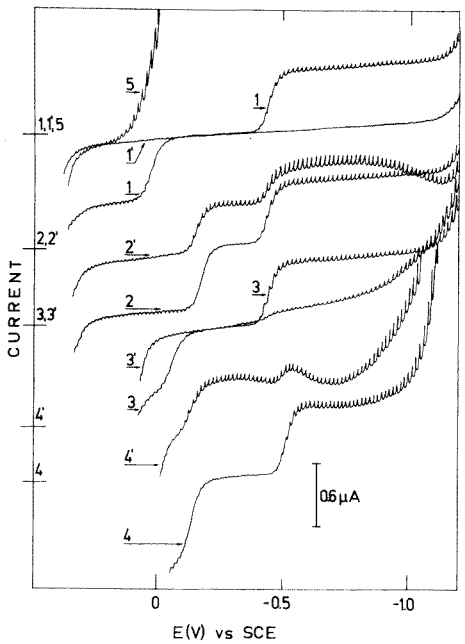

Fig. 1. Polarographic curves obtained for (1—4) 10^{-4} mol l^{-1} Sn(II); (1'—4') 10^{-4} mol l^{-1} Sn(IV). Supporting electrolytes: (1,1') 0.1 mol l^{-1} $HClO_4$ in water; (2,2') 0.1 mol l^{-1} $HClO_4$ + 0.01 mol l^{-1} pyrogallol; (3,3') 0.1 mol l^{-1} HCl in water; (4,4') 0.1 mol l^{-1} HCl in methanol. (5) Initial portion of oxygen wave recorded in aqueous 0.1 mol l^{-1} $HClO_4$ solution.

experimental conditions. The occurrence of this wave led to some trouble in the measurement of the tin waves and, therefore, the influence of this base on the stability of tin(II) solutions was not investigated further. In the presence of phenolsulphonic acid, the background current increased but this did not affect the shape of tin(II) waves if the concentration of tin(II) was higher than 1×10^{-4} mol l^{-1}.

In 0.1 mol l^{-1} perchloric acid solution, tin(II) gave two waves (curve 1). The cathodic wave was reversible whereas the anodic wave was not entirely reversible. The results obtained here are consistent with the earlier polarographic results of Schaap et al. [12]. Under the same conditions, tin(IV) gave no wave (curve 1'). The behaviour of tin(II) and tin(IV) did not change essentially when the polarographic curves were recorded in aqueous perchloric acid solutions containing hydrazine, hydroxylamine, ascorbic acid or phenolsulphonic acid. Similar curves were also obtained in methanolic solution containing perchloric acid. The position of the cathodic wave obtained for tin(II) in the presence of pyrogallol (curve 2) remained essentially unaltered whereas the anodic wave shifted towards more negative potentials with simultaneous improvement of reversibility. Tin(IV) was converted by pyrogallol to the electroactive form giving two reduction waves (curve 2').

TABLE 1

The variations in tin(II) concentration after storage of the solution open to air
(The percentages given are relative to the height of the wave measured for fresh tin(II) solutions. Tin(II) concentration, 2×10^{-4} mol l^{-1}. Unless otherwise stated, the concentrations of acids and stabilizing agents were 0.1 mol l^{-1}.)

Composition of solutions	$E_{1/2}^{cath}$ (V vs. SCE)	Current relative to fresh solutions (%) after		
		2 h	24 h	2 weeks
Aqueous solutions				
$HClO_4$	−0.42	15	0	
$HClO_4$ + $NaClO_4$	−0.42	65	0	
$HClO_4$ + $NaClO_4$[a]	−0.42	10	0	
$HClO_4$[a]	−0.45	0		
$HClO_4$ + HCl	−0.44	0		
$HClO_4$ + NaF	−0.47	6	0	
HCl	−0.44	0		
$HClO_4$ + $N_2H_4 \cdot 2HCl$	−0.46	95	83	65
$HClO_4$ + $N_2H_4 \cdot 2HCl$ + $NaClO_4$	−0.46	97	91	87
$HClO_4$ + $NH_2OH \cdot HCl$	−0.45	80	45	
$HClO_4$ + $NaClO_4$ + ascorbic acid	−0.42	40	15	
$HClO_4$ + $NaClO_4$ + NaH_2PO_2	−0.48	0		
$HClO_4$ + pyrogallol[b]	−0.42	91	89	87
$HClO_4$ + pyrogallol[b] + $NaClO_4$	−0.42	90	89	87
$HClO_4$ + tiron[b]	−0.42	67	29	0
$HClO_4$ + phenolsulphonic acid	−0.44	93	87	74
Methanolic solutions				
$HClO_4$	−0.37	85	10	
HCl	−0.51	0		
NaCl	−0.48	0		

[a]1 mol l^{-1}. [b]0.01 mol l^{-1}.

The first wave was reversible whereas the second wave, occurring at the potential of the reduction of tin(II), was less well developed. The minimum occurring on the limiting current of this wave was observed and investigated earlier by Bard [13].

In 0.1 mol l^{-1} hydrochloric acid solution, both tin(II) waves shifted slightly towards more negative potentials. Simultaneously, the final rise of the mercury dissolution current shifted more distinctly in the same direction and so the more anodic wave for tin(II) became ill-defined. Comparison of curves 3′ and 1′ shows that tin(IV) is reduced in 0.1 mol l^{-1} hydrochloric acid solution in a drawn-out wave beginning at the reduction potential of tin(II). The addition of hydrazine, hydroxylamine, ascorbic acid or hypophosphorous acid to 0.1 mol l^{-1} hydrochloric acid solution did not affect the behaviour of tin(II) and tin(IV) species, whereas the addition of pyrogallol gave a tin(IV) reduction wave similar to curve 2′.

Curves 4 and 4′ were obtained for tin(IV) and tin(II) species in methanolic

solutions containing 0.1 mol l^{-1} HCl. The curves obtained under these conditions for tin(II) differed only slightly from curve 3 obtained in aqueous solution. Yet tin(IV) was reduced in methanolic solution more easily than in aqueous solution though the second wave exhibited a minimum under such conditions.

Investigation of the stability of tin(II) solutions

A comparison of curve 5, which is the initial portion of the reduction wave of dissolved oxygen, and the more positive portion of the tin(II) curves shows that the decay in the height of the anodic tin(II) wave can be followed even in the presence of dissolved oxygen provided that the final rise of the anodic current is sufficiently positive. Such a situation was observed in aqueous phenolsulphonic acid solutions, in perchloric acid solutions with and without addition of pyrogallol, hydrazine, hydroxylamine, ascorbic acid or hypophosphorous acid, as well as in methanolic perchloric acid solution. Figure 2 shows the diffusion current—time curves recorded at a constant potential more positive than the potential of the oxygen wave. It is evident that the procedure described permits the variations of tin(II) concentrations to be monitored quite easily without removal of oxygen.

In the presence of chloride ions, the final rise of the anodic current shifted markedly towards more negative potentials whereas the position of the oxygen wave remained practically unaltered. Under such conditions, the procedure described above could not be applied, and monitoring the variations in the height of tin waves required prior removal of oxygen from the solution. At sufficiently low chloride ion concentrations, where the anodic wave of tin(II) exhibited a limiting current plateau (curve 3), the variations in tin(II) concentration were determined by measurement of the height of the anodic wave. At higher chloride ion concentrations, the anodic current plateau disappeared and then the variations in tin(II) concentration could be

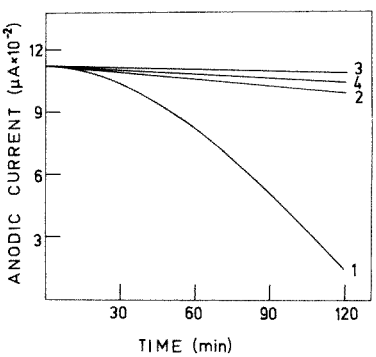

Fig. 2. Time dependence of the anodic limiting current of tin(II) recorded in the presence of oxygen for 2 × 10^{-4} mol l^{-1} tin(II) at potentials: (1—3) 0.2 V; (4) 0.3 V. Supporting electrolytes: (1) 0.1 mol l^{-1} $HClO_4$ in water; (2) 0.1 mol l^{-1} $HClO_4$ + 0.01 mol l^{-1} pyrogallol; (3) 0.1 mol l^{-1} $HClO_4$ + 0.1 mol l^{-1} phenolsulphonic acid; (4) 0.1 mol l^{-1} $HClO_4$ in methanol.

monitored by measurement of the height of the cathodic wave against the residual current line. However, this procedure gave only approximate data, particularly when significant amounts of tin(II) were converted to tin(IV).

Table 1 presents the quantitative data obtained for different solutions stored open to the air for 2 h, 24 h and 2 weeks. The data presented indicate that in aqueous perchloric acid solutions tin(II) was more stable than in hydrochloric acid solution. The presence of fluoride ions improved the stability only slightly compared to the results obtained for chloride solutions. The presence of an inert salt at moderate concentration (0.1 mol l^{-1}) improved the stability of tin(II) solutions somewhat, but with a large amount of sodium perchlorate the stability decreased again. Neither increases nor decreases in the acidity improved the stability of the tin(II) species. No essential improvement in the stability was observed in methanolic solutions containing chloride ions whereas in the presence of perchloric acid the stability of tin(II) increased markedly. Among the antioxidants investigated, only hypophosphorous acid showed no positive action. The best stabilizing actions were exerted by phenolsulphonic acid, hydrazine and pyrogallol.

The influence of variations in concentration of pyrogallol, hydrazine and phenolsulphonic acid on the stability of tin(II) solutions is shown in Table 2. It should be remembered that, in the absence of stabilizing agents, storage of solutions for 24 h open to air gave complete oxidation of tin(II). The data presented in Table 2 show that these antioxidants have a stabilizing action even when present at concentrations lower than that of tin(II). Below concentrations of 10^{-4} mol l^{-1}, the stabilizing action of phenolsulphonic acid and hydrazine deteriorates but pyrogallol had a positive effect even at concentrations as low as 10^{-6} mol l^{-1}. After 24 h of storage of such a solution open to the air, 75% of the tin(II) remained unoxidized. It should be stressed that samples of pyrogallol from different sources exerted much the same stabilizing action. It is evident that the stabilizing agents play the role of inhibitor for the reaction between tin(II) and oxygen.

TABLE 2

Variations in tin(II) concentration after storage of the solution open to air. (2×10^{-4} mol l^{-1} Sn(II) in 0.1 mol l^{-1} $HClO_4$ plus appropriate antioxidant. The percentages given are relative to the height of the tin(II) wave measured for fresh tin(II) solution.)

Antioxidant concentration (mol l^{-1})	Current relative to fresh solutions (%) after					
	24 h	1 week	24 h	1 week	24 h	1 week
	Pyrogallol		Phenolsulphonic acid		Hydrazine	
10^{-1}	84	60	96	62	100	90
10^{-2}	92	90	96	60	96	68
10^{-3}	90	86	92	54	96	74
10^{-4}	98	75	80	26	96	76
10^{-5}	98	72	58	5	18	0

The reproducibility of the results obtained for fresh solutions prepared under hydrogen was good. For example, for 5 measurements of fresh solutions containing 0.1 mol l^{-1} $HClO_4$ and 2×10^{-4} mol l^{-1} Sn(II), the standard deviation was 2%. Similar reproducibility was obtained for solutions aged for periods ~48 h in the presence of hydrazine, hydroxylamine or pyrogallol. In contrast, the reproducibility of results obtained after short storage periods in the absence of stabilizing agents was distinctly poorer; e.g. the standard deviation obtained for 9 successive determinations of tin(II) in 0.1 mol l^{-1} $HClO_4$ solution after 45 min of storage open to air was 20%.

The behaviour of the oxygen wave in the presence of stabilizing agents

In order to establish whether or not the enhanced stability of tin(II) was due to removal or tying-up of dissolved oxygen, the first oxygen wave was investigated in the presence of the stabilizing agents. These experiments showed that in perchloric acid solution containing hydrazine, hydroxylamine, pyrogallol or phenolsulphonic acid, the height of the first oxygen wave remained unaltered for periods as long as 24 h. In the presence of ascorbic acid, the height of the oxygen wave decreased slowly but this effect was insufficient to be regarded as responsible for the enhanced stability of tin(II); after 90 min of storage, the limiting current of oxygen decreased by only 5%.

An investigation of the shape of the first oxygen wave also did little to clarify the origin of the stabilizing action. The shape and position of this wave were unaltered in the presence of all the stabilizing substances used except phenolsulphonic acid. In the latter case, the wave shifted slightly towards negative potentials and its slope was more drawn out. However, this effect does not provide convincing evidence for phenolsulphonic acid tying-up the oxygen. Similar behaviour was observed in perchloric acid solution in the presence of Triton X-100. It is, therefore, possible that the change of position and shape of the wave was not caused by phenolsulphonic acid but by the surface-active contaminants present in the technical-grade reagent used.

DISCUSSION

The results described above show that polarography is a convenient technique for determinations of the stability of tin(II) solutions. In the absence of chloride ions, the stability of tin(II) can be established even in the presence of dissolved oxygen. In certain cases, the method proposed makes it possible to estimate not only the decay of the tin(II) concentration but also the increase of the tin(IV) concentration. Determinations of this type are important for proper monitoring of tin plating baths [14]. In accordance with literature data [1, 15], phenolsulphonic acid was found to exert a significant stabilizing action on tin(II) solutions. In addition, it was found that the stabilizing action was exerted by hydrazine or pyrogallol to the same or an even greater extent.

In contrast to the literature data, the results of the present work show that tin(II) is not stabilized either by hypophosphorous acid, as claimed by Fainberg and Tal [8], or by methanolic hydrochloric acid solution, as claimed by Fano and Zanotti [3]. However, a distinct stabilization of tin(II) species was observed in methanolic solution containing perchloric acid.

The nature of the stabilizing action is not completely clear. The above studies show that the enhanced stability is not caused by reduction or tying-up of dissolved oxygen, by reduction of tin(IV), or by complexation of tin(II). The latter conclusion follows from the virtually unaltered values of the $E_{1/2}$ values given in Table 1. It should be noted that similar conclusions regarding tin(II) and phenolsulphonic acid were reached by Meibuhr [16]. The fact that in some cases the stabilizing action was exerted even at very low concentrations of the stabilizing agents supports an opinion given earlier [6] that oxidation of tin(II) by dissolved oxygen proceeds according to a chain mechanism. The stabilizing agents may be considered simply as inhibitors facilitating the chain-breaking process.

REFERENCES

1 Z. G. Szabo and E. Sugar, Anal. Chim. Acta, 6 (1952) 293.
2 A. J. Bard, Anal. Chem., 32 (1960) 623.
3 V. Fano and L. Zanotti, Microchem. J., 18 (1973) 345.
4 L. Metzger, G. G. Willems and R. Neeb, Fresenius Z. Anal. Chem., 288 (1977) 35.
5 J. A. McCarthy, Plating, 47 (1960) 805.
6 E. H. Baker, J. Appl. Chem., 1953, 323.
7 I. E. Davidson and W. F. Smyth, Anal. Chem., 49 (1977) 1195.
8 S. J. Fainberg and E. M. Tal, Zavod. Lab., 11 (1945) 631.
9 T. M. Florence and Y. Farrar, J. Electroanal. Chem., 41 (1973) 127.
10 E. Bandrowski, Ber. Dtsch. Chem. Ges., 1894, 480.
11 C. F. Baes and R. E. Mesmer, The Hydrolysis of Cations, J. Wiley, New York, 1976, p. 349.
12 W. B. Schaap, J. A. Davis and W. H. Nebergall, J. Am. Chem. Soc., 76 (1954) 5226.
13 A. J. Bard, Anal. Chem., 34 (1962) 266.
14 A. Jaklewicz, Chem. Anal. (Warsaw), 20 (1975) 817.
15 S. Meibuhr and P. R. Carter, Electrochem. Technol., 2 (1964) 267.
16 S. G. Meibuhr, Electrochim. Acta, 13 (1968) 831.

Analytica Chimica Acta, 130 (1981) 141—147
Elsevier Scientific Publishing Company, Amsterdam — Printed in The Netherlands

DETERMINATION OF NANOGRAM QUANTITIES OF MERCURY IN WATER WITH A GOLD-PLATED PIEZOELECTRIC CRYSTAL DETECTOR

MAT H. HO and GEORGE G. GUILBAULT*
Department of Chemistry, University of New Orleans, New Orleans, LA 70122 (U.S.A.)
EUGENE P. SCHEIDE
Environmetrics, Inc., 1567 North Warson Road, St. Louis, MO 63132 (U.S.A.)
(Received 3rd April 1981)

SUMMARY

The use of a gold-coated piezoelectric crystal, coupled with a direct reduction technique, is described for the determination of mercury in water. The linear range is 5—100 ng with a sensitivity of 1.78 Hz ng^{-1} of mercury. Reversibility of the detector is achieved by thermal desorption at 170°C. The effect of carrier gas flow rate, sample size and detector cell configuration on the sensitivity are discussed.

Mercury is a health hazard because of the strong bonds formed by it with sulfur atoms in the body. This formation interferes with the functions and the synthesis of both enzymes and proteins. Mercury is also concentrated in the brain, liver and other organs and is a cumulative poison [1]. The important toxicological effect of mercury species in water is reflected in the extensive research on mercury determinations, about which many papers have been published in recent years. Cold-vapor atomic absorption spectrometry, which is based on the procedure of Hatch and Ott [2], has received greatest attention and is being widely used because of its sensitivity; mercury species in the aqueous sample are reduced to the elemental state by a reducing agent such as hydroxylamine or tin(II) chloride and the resulting mercury vapor is measured at 253.7 nm. However, this method is not specific, and other species which absorb at the same wavelength, such as sulfur dioxide, nitrogen dioxide, ammonia and hydrocarbons can interfere [1]. The loss of mercury activity during sample storage, which has been reported by many investigators [3, 4], may create problems when nanogram quantities of mercury need to be determined. As a way to solve these problems, a selective, sensitive and portable gold-coated piezoelectric crystal detector capable of field use for determining mercury in water has been developed.

The principle of the piezoelectric crystal detector is that the frequency of an oscillating crystal is decreased by deposition of a small mass of material on its surface. Sauerbrey [5] and Stockbridge [6] developed an equation describing the linear relationship between mass added to the crystal surface

and the change in the resonant frequency of that crystal. This linear relationship enables a piezoelectric crystal to be used as a sorption analytical detector. Gaseous or vapor samples are reversibly adsorbed by the coating of the crystal, thereby changing the mass on the crystal. As a result, the change of frequency is indicative of the sample concentrations. Several analytical applications have been based on this principle [7—13]. A hand calculator-sized piezoelectric crystal detector has already been demonstrated as a potential tool for environmental pollution analysis [9], and a detector for mercury in air based on a gold-coated piezoelectric crystal has been reported [10].

The ability of gold to adsorb and amalgamate mercury is well known and this principle has frequently been used to collect mercury for subsequent determination by atomic absorption [14]. In this paper, the use of a gold-coated piezoelectric crystal, coupled with a direct reduction technique, is described for the determination of nanogram quantities of mercury in water.

EXPERIMENTAL

Apparatus

Figure 1 shows a schematic diagram of the experimental set-up. Nitrogen was used as carrier gas and the flow rate was checked and controlled by means of a calibrated flow meter and flow controller, respectively. The flow rate was kept at 200 ml min^{-1}. The reduction vessel was a pyrex bottle with a ground 29/42 neck; this vessel was closed with a 29/42 male joint which was modified to have a fritted gas distribution tube, an outlet and an injection port. The reducing agent was introduced into the vessel by a syringe through the septum of the injection port. A drying tube, 8 cm in length and 1.7 cm in diameter, filled with anhydrous magnesium perchlorate, was used to prevent water vapor from entering the detector cell. All the tubing lines were made of glass or teflon and all the connectors were of tygon tubing.

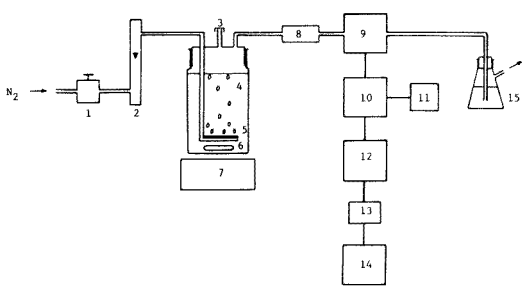

Fig. 1. Experimental set-up: (1) flow controller; (2) flow-meter; (3) septum for injection of $SnCl_2$; (4) Hg^{2+} sample solution; (5) glass frit; (6) stirring bar; (7) magnetic stirrer; (8) $Mg(ClO_4)_2$ drying tube; (9) crystal and detector cell; (10) oscillator; (11) power supply; (12) frequency counter; (13) digital-to-analog converter; (14) recorder; (15) $KMnO_4$ and H_2SO_4 trap solution.

The detector consisted of a gold-coated piezoelectric crystal, the detector cell, an oscillator, a frequency counter and a recorder. The crystals used were 15.0 MHz, HC6/U holder, AT-cut quartz plates, resonating in the thickness shear mode. Each crystal consisted of a vacuum-deposited gold electrode located on the center of each side of the quartz plate. The crystals were obtained from International Crystal Mfg., Co., Oklahoma City, OK. The oscillator (International Crystal Mfg., Co., Model OT-14) which drove the crystal at its fundamental resonant frequency, was powered by a regulated power supply. The applied voltage was kept constant at 9 V d.c. The frequency output from the oscillator was measured by a frequency counter (Heath Schlumberger, Model SM-4100) which was modified by a digital-to-analog converter so that the frequency could be recorded. For field use, the portable detector, which is operated on batteries and has solid-state display of the readout, has been described previously [9].

Detector cells. The crystal was housed in the detector cell. Several cell configurations were investigated in order to optimize the collection efficiency of mercury on the gold electrode surfaces of the crystal. These configurations are shown in Fig. 2. In design A, the sample stream is focused and impinged on the center of one side of the crystal and comes out at the other side. In design B, the crystal is placed in line and parallel with the sample stream. The most efficient arrangement is shown in design C. The entering sample stream was split into two equal streams, each passing through a 5-mm diameter glass tube and impinging on the center of the electrodes. Mercury flows directly and perpendicularly onto both sides of the crystal and hence gives the greatest sensitivity.

Reagents

Standard mercury solutions. A stock solution of mercury(II) (1 mg ml^{-1}) was prepared by dissolving pure mercury(II) chloride in 1 M nitric acid and

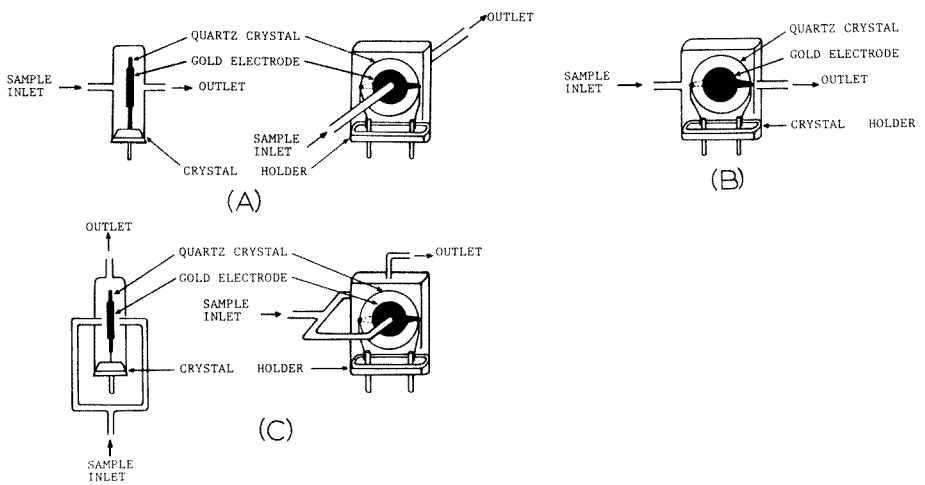

Fig. 2. Details of detector cell designs.

diluting to appropriate volume with double-distilled, deionized water. Mercury(II) chloride (Merck) was dried in a desiccator for 24 h before weighing. Working standards were prepared daily by suitable dilution in 1 M nitric acid.

Reducing solution. A 15% tin(II) chloride solution in 2 M hydrochloric acid was prepared fresh daily and purged for several minutes with nitrogen to remove any free mercury before use. All chemicals were reagent grade and used without further purification. All glassware was soaked in a nitric acid—permanganate solution, washed with concentrated hydrochloric acid and finally rinsed with distilled water.

Procedure

Since the sensitivity of the detector was affected by the flow rate of carrier gas, it had to be controlled carefully. For this purpose, the reducing vessel was filled with 105 ml of double-distilled, deionized water and nitrogen was passed through. The flow rate was monitored and adjusted by a calibrated flow meter and a flow controller, respectively. Nitrogen was then by-passed, the vessel was emptied and 100 ml of standard sample was introduced. A portion (5 ml) of 15% tin(II) chloride was injected into the vessel through the septum of the injection port. The solution was stirred for 30 s and nitrogen was passed through the solution to sweep mercury onto the gold electrode of the crystal. After the frequency reading became stable, the gas flow was turned off and the vessel was emptied for the next measurement. The response was the difference of frequency before the purging gas was turned on and the maximum frequency reached before the gas flow was turned off.

RESULTS AND DISCUSSION

Mercury species in the aqueous sample are reduced to elemental mercury by tin(II) chloride. The mercury vapor produced is volatilized from solution and, adsorbed on the surface of gold electrode, causes an increase in the mass of the crystal, therefore decreasing the frequency. The change of frequency, which is monitored by a frequency counter, is proportional to the amount of mercury.

Since the collection efficiency of mercury on a gold-coated electrode is a function of the surface composition, the gold electrode should be fresh for the best collection efficiency. A commercially available gold-plated crystal was placed in an oven at 170°C and hot nitrogen was passed over for 1 h to flush off any contaminants. A second crystal had a fresh gold film evaporated onto the nickel electrode using our conventional vacuum system. These two crystals gave the same collection efficiency and therefore the commercially available gold-coated electrode crystals were used in this study, after heat-cleaning.

The sensitivity, or the collection efficiency, of the gold electrode, depends not only on the surface contamination but also on the configuration of the

TABLE 1

The effect of the detector cell configurations on the response for 20 ng of Hg at a flow rate of 200 ml min^{-1}

Configuration	A	B	C
Frequency response (Hz)[a]	20	12	35

[a]Average value of five measurements.

detector cell. Table 1 shows the frequency response to 20 ng of mercury given by three different types of detector cell (see Fig. 2). Design C is about three times more sensitive than design B. These results show that the design C is the most sensitive because it provides the best contact between the gold coating and the sample stream.

The effect of flow rate of carrier gas was also studied. There are two important factors that should be considered in optimizing the flow rate for the greatest sensitivity: first, the efficiency of the diffusion of mercury out of the solution into a small volume of carrier gas to provide a concentrated mercury stream, and second, the efficiency of the collection of mercury on the surface of the gold electrode. For the best removal of mercury from the solution in the reducing vessel, a high flow rate is needed. However, at high flow rates the collection efficiency of mercury is decreased because of incomplete adsorption; at 200 ml min^{-1} the collection efficiency is 15% lower than that at 90 ml min^{-1} [13]. If the flow rate of carrier gas is less than 100 ml min^{-1}, however, the removal of mercury from the solution is too slow, less sensitivity is obtained, and more time is required for completion of the determination. As a way to solve these problems, the diameter of the entrance tubing of the detector cell was increased, thus decreasing the velocity of the gas flow. This allowed a high flow rate of sample to be achieved with optimum collection efficiency on the gold electrode. Also the solution in the reducing vessel was stirred to increase the rate of volatilization. For a 5-mm diameter entrance to the detector cell, the optimum flow rate was found to be 200 ml min^{-1} as shown in Fig. 3.

The amount of mercury adsorbed on the surface of gold before saturation depends on the surface area of the gold. Figure 4 shows that saturation began at 175 Hz. For a 15-MHz crystal with an electrode area of 0.1 cm^2, the mass sensitivity was about 5175 Hz μg^{-1} calculated from Sauerbrey's equation. For 100 ng of mercury in the standard solution, the frequency change was 175 Hz which corresponded to about 34 ng of mercury collected. The collection efficiency is therefore about 34% assuming that all of the mercury is volatilized from the solution. The linear range of the detector is from 5—100 ng. Increasing the surface area of the gold electrode would increase the linear range of the detector, but the mass sensitivity would decrease because the mass sensitivity of the crystal is inversely proportional to the electrode area. The detector responds to mass rather than to concentration and a larger volume of sample, giving a larger mass of mercury, would increase the

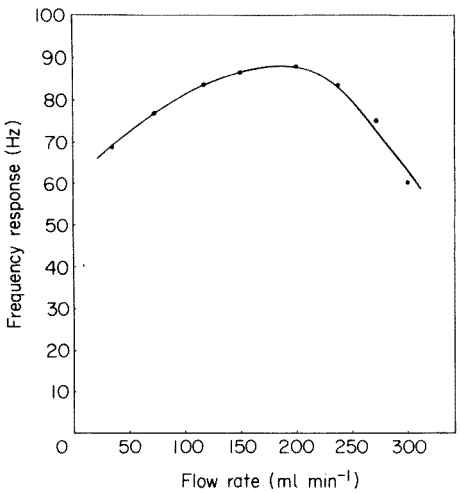

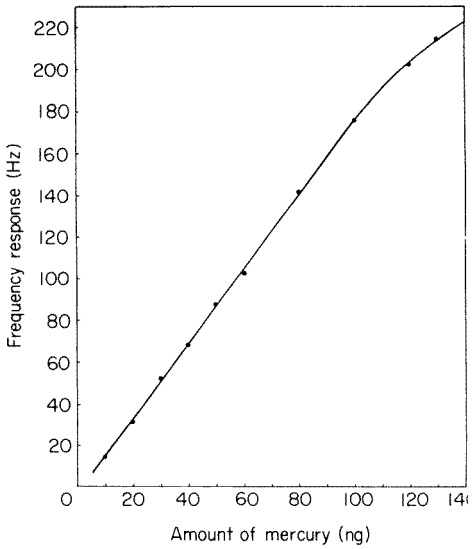

Fig. 3. Effect of carrier gas flow rate on sensitivity for 50 ng of Hg in 100 ml of sample.

Fig. 4. Response of the detector to mercury for 100-ml samples with a flow rate of 200 ml min^{-1}.

sensitivity. Large volumes of sample would, however, require a higher flow rate of purge gas and make the collection of mercury on the gold electrode less efficient. This problem might be solved by collecting mercury from the solution with a gold-coated collector, releasing the mercury from the collector by heating and sweeping with carrier gas into detector cell.

The reversibility of the detector is achieved by thermal desorption. After the measurement, the crystal was heated to 170°C and hot purified air or nitrogen was passed through for several minutes. Mercury was desorbed and the surface of gold electrode was thus regenerated. As a result, the frequency returned to the original base-line and the next measurement could be made. The desorption temperature should not be over 170°C because of the low-melting soldered electrical connections. If hard, temperature-stable soldered connections are used, the temperature can be raised for faster desorption. For the best results, the crystal should be desorbed after each measurement.

Figure 4 shows the frequency responses of the detector for different amounts of mercury. From this calibration plot, the sensitivity of the detector is 1.78 Hz ng^{-1}. The relative standard deviation is about 7%. Gold is a highly selective adsorber for mercury [15] and detection is free of interferences usually observed in the cold-vapor atomic absorption technique.

The lifetime of the detector is shown in Table 2. After 60 adsorption—desorption cycles the crystal demonstrated essentially the same frequency response for 50 ng of mercury.

TABLE 2

Lifetime of the detector for adsorption—desorption cycles involving 50 ng of mercury

No. of cycles	1	10	50	60
Frequency response (Hz)	88	89	84	86

Conclusion

The gold-coated piezoelectric crystal detector is not only a selective and sensitive detector but also is simple and provides an inexpensive method for determination of mercury in water. The detector is free of the interferences observed in cold-vapor atomic absorption. The detector can be made portable, low power is required, so that it can be operated on batteries suitable for field use, and its operation requires little skill. This technique is not restricted to the determination of mercury in water but may be applicable to other systems such as the determination of mercury in biological samples.

The authors gratefully acknowledge the financial support of the Army Research Office (Grant No. DAAG-77-G-0266) in carrying out this research project.

REFERENCES

1 M. Katz (Ed.), Methods of Air Sampling and Analysis, 2nd edn., American Public Health Association, Washington DC, 1977, pp. 926—931.
2 W. R. Hatch and W. L. Ott, Anal. Chem., 40 (1968) 2085.
3 C. Feldman, Anal. Chem., 46 (1974) 99.
4 I. Sanemasa, T. Deguchi, K. Urata, J. Tomooka and H. Nagai, Anal. Chim. Acta, 87 (1976) 479.
5 G. Sauerbrey, Z. Phys., 155 (1959) 206.
6 D. Stockbridge, Vac. Microbalance Tech., 5 (1966) 193.
7 J. Hlavay and G. G. Guilbault, Anal. Chem., 49 (1977) 1890.
8 M. H. Ho, G. G. Guilbault and B. Rietz, Anal. Chem., 52 (1980) 1489.
9 E. P. Scheide and R. B. J. Warner, Am. Ind. Hyg. Assoc. J., 39 (1978) 745.
10 E. P. Scheide and J. K. Taylor, Environ. Sci. Technol., 8 (1974) 1087.
11 Y. Tomita, M. H. Ho and G. G. Guilbault, Anal. Chem., 51 (1979) 1475.
12 T. E. Edmonds and T. S. West, Anal. Chim. Acta, 117 (1980) 147.
13 M. H. Ho and G. G. Guilbault, Anal. Chem., in press.
14 Z. Yoshida and K. Motojima, Anal. Chim. Acta, 106 (1979) 405.
15 P. J. Murphy, Anal. Chem., 51 (1979) 1599.

Analytica Chimica Acta, 130 (1981) 149—156
Elsevier Scientific Publishing Company, Amsterdam — Printed in The Netherlands

PRECONCENTRATION OF INORGANIC MERCURY WITH AN ANION-EXCHANGE RESIN AND DIRECT REDUCTION—AERATION MEASUREMENTS BY COLD-VAPOUR ATOMIC ABSORPTION SPECTROMETRY

I. SANEMASA*, E. TAKAGI, T. DEGUCHI and H. NAGAI

Department of Chemistry, Faculty of Science, Kumamoto University, Kurokami-machi 2-39-1, Kumamoto 860 (Japan)

(Received 20th March 1981)

SUMMARY

Inorganic mercury ions (5—50 ng l^{-1}) present in natural waters (500 ml) are concentrated on anion-exchange resin (0.2 g; chloride form) in a batchwise operation. The resin is filtered off and introduced into a bubbler containing tin(II) solution. The adsorbed mercury ions are reduced to the metal and vaporized with a stream of air in a closed system. Satisfactory recoveries are obtained for sea waters made 0.1 M in nitric acid, and for river and spring waters also made 0.1 M in nitric acid or 0.01 M in ammonium thiocyanate. The method preconcentrates traces of inorganic mercury ions by an order of magnitude, and is also effective in preventing mercury loss during sample storage.

There are three main problems encountered in the determination of mercury in natural water samples: mercury contents are generally too small to measure directly by conventional atomic absorption spectrometry (a.a.s.); water samples collected and stored in containers are subject to mercury losses by adsorption, volatilization, complexation, etc.; and mercury occurs in inorganic and organic forms, so that it may be necessary to determine them totally or separately.

Many procedures have been developed for preconcentrating mercury in water. The most prevalent one is a gas-stripping (purge and trap) procedure which is essentially based on the reduction—aeration method by Kimura and Miller [1]. Dithizone-coated polystyrene beads [2], 2-mercaptobenzothiazole-coated silica gel [3], macroreticular styrene-divinylbenzene copolymer beads [4], and chelating resins [5, 6] have recently been used for collecting inorganic and organic mercury by column operation. A weakly basic cellulose anion exchanger has also been used in thiocyanate media for selective separation of mercury from other metal ions [7]. A strongly basic anion-exchange resin seems to be undesirable because mercury ions are difficult to elute from the resin [8—10]. Becknell et al. [11] have eliminated the elution process by making use of neutron activation analysis.

Various methods have been published for preventing mercury losses. The most common is to keep mercury ions in their higher oxidation state by treating the sample solution with H_2SO_4—$KMnO_4$ [12] or HNO_3—$K_2Cr_2O_7$

0003—2670/81/0000—0000/$02.50

[13]. The use of ligands such as iodide, cyanide [14], and cystine [15] has also been reported. It has been shown [16, 17] that water samples treated with HNO_3—NaCl or HNO_3—NH_4SCN exhibit no mercury loss during long storage; this is probably due to the formation of stable mercury(II) complexes with chloride or thiocyanate ions, which prevent the adsorption of mercury on the container wall and particulates.

It is known that mercury ions are strongly adsorbed on anion-exchange resins from chloride or thiocyanate media. The resin would be useful as a simple concentration agent if the mercury ions could be almost completely removed from the resin without any elution process. From this standpoint, an investigation was made to establish whether a direct reduction—aeration technique is applicable to mercury ions adsorbed on the anion-exchange resin.

EXPERIMENTAL

Reagents

All the chemicals used were reagent grade except nitric acid, which was SuperSpecial grade. Stock solutions of nitric acid (2 M), sodium chloride (1 M), and ammonium thiocyanate (1 M) were prepared as described previously [17]. Stock solution of mercury(II) (1000 mg l^{-1}) and intermediate standard solutions were prepared, from which working standard solutions (5 and 50 $\mu g\ l^{-1}$) were freshly prepared by appropriate dilution. A commercially available anion-exchange resin (Dowex 1-X8, Cl^--form, 100—200 mesh) was used without further treatment.

Procedures

A Hitachi Model 508 atomic absorption spectrometer was used to measure mercury by the cold-vapour technique. In a cylindrical gas bubbler (300 ml; 50 mm i.d., 15 cm long) were placed suitable amounts of sulphuric acid (1 + 1) and tin(II) chloride (10% w/v in 1 M HCl) solutions (see below) and distilled water to make the total volume 30 ml. The mixture was aerated in an open system to remove any mercury arising from the reagents. All subsequent measurements were carried out in a closed system. A circulating pump, which was combined with the system, was operated at a constant flow rate of 1.5 l min^{-1}.

Mercury ions in natural water samples were determined in the following ways.

River and spring waters (standard addition method). Ten 1-l polyethylene bottles were prepared. Of these, five were used for portions of the sample to be analyzed and the other five for redistilled water. Into each bottle, 470-ml portions of sample or redistilled water were poured, followed by 25 ml of 2 M HNO_3 and 5 ml of 1 M NH_4SCN. Standard mercury solution (5 $\mu g\ l^{-1}$; 0, 1, 2, 3 or 4 ml) was added to pairs of sample and distilled water bottles. The mixtures were allowed to stand for 1 day with occasional agitation.

A 0.2-g portion of resin was then added to each mixture and the bottles were vigorously shaken mechanically for 1—2 h. The contents of each were filtered through membrane filters (0.45 μm porosity) with suction. The resin on the filter was transferred to the gas bubbler, in which 4 ml of the sulphuric acid and 8 ml of the tin(II) solution have previously been placed, with the aid of a small portion of redistilled water. The circulating pump was turned on and the atomic absorption of mercury vapour was recorded as a function of time at 254 nm. The maximum steady peak was observed about 6 min after aeration began. The peak heights from the sample and the redistilled water were plotted against the amount of standard mercury solution added, and the amount of mercury determined by conventional standard addition calculations.

Instead of the standard addition method, the conventional calibration method can also be used. Again, in this case, redistilled water treated in the same way as the sample should be analyzed in order to correct for blank values.

Sea water (calibration method). Into each 1-l polyethylene bottle, a 475-ml portion of sea water was poured, and 25 ml of 2 M HNO_3 was added, either on board ship or in the laboratory (in the latter case, the addition of acid should be made within 5 days of sampling). The contents were allowed to stand for 1 week with occasional agitation, then a 0.2-g portion of the resin was added, and vigorously shaken mechanically for 1—2 h. The resin was separated as above, added to the gas bubbler, in which 2 ml of the sulphuric acid and 2 ml of the tin(II) solution had previously been placed, and the atomic absorption of the mercury vapour was measured as described above. After the absorption had been measured, all the mercury vapour in the system was removed by operating the circulating pump in an open system. The system was closed again and, in the presence of the resin in the gas bubbler, 0.1—0.5 ml of mercury standard solution (50 μg l^{-1}) was added. Calibration curves were prepared from a sequence of standards analyzed in this way. Corrections for mercury blanks were made using samples which were unacidified upon sampling, allowed to stand for 5 days thereafter, and then acidified by adding 25 ml of 2 M HNO_3 just before the addition of the resin. The values of mercury obtained under these conditions were taken to be the blank values.

Measurement of the distribution coefficient of mercury(II) ions

The anion-exchange resin (Cl^--form) was stirred with redistilled water and the fines were decanted. The air-dried resin (0.200 g) was added to each 100-ml polyethylene bottle in which 50-ml portions of solutions of various HNO_3—NaCl or HNO_3—NH_4SCN concentrations had previously been placed. Known amounts of mercury(II) (50 μg for HNO_3—NaCl and 500 μg for HNO_3—NH_4SCN) were added to the mixtures. The contents were mechanically shaken for 30 min and allowed to stand for a while, and appropriate aliquots of the supernatant solutions were analyzed by a.a.s. The amount of mercury

taken up by the resin was determined by material balance. Distribution coefficients were calculated from the equation K_d = (μg of Hg/g of resin)/(μg of Hg/ml of solution).

RESULTS AND DISCUSSION

Distribution coefficient measurements

The coefficients measured are shown in Table 1. If more than 95% uptake of mercury is required by 0.2 g of resin in a single batch equilibrium from 500 ml of solution, the K_d value must be larger than 4.8×10^4. The conditions, HNO_3 (0.1 M)—NaCl (0.1—0.5 M) and HNO_3 (0.1 M)—NH_4SCN (0.01 M), which were found to be effective both for preventing mercury loss and for recovering mercury once "lost" [17], satisfy this requirement.

Recovery of mercury ions adsorbed on the resin by reduction—aeration

The initial investigations were undertaken with small volumes (25 ml) of solution spiked with 125 ng of mercury(II) and 0.2 g of resin, to see whether mercury ions adsorbed on the resin can be liberated as vapour by the reduction—aeration method. The resin samples were collected from solutions treated to be HNO_3 (0.1 M)—NaCl (0.5 M) or HNO_3 (0.1 M)—NH_4SCN (0.01 M). The use of 2 ml each of the sulphuric acid and tin(II) chloride solution gave quantitative recoveries of mercury in the former case, while it failed to generate any mercury vapour in the experiments involving HNO_3—NH_4SCN. Typical results for the latter medium are shown in Table 2. The use of 4 ml of sulphuric acid and 8 ml of tin(II) chloride solution or more is necessary to give quantitative recoveries from the resin collected from solutions containing thiocyanate.

Recoveries of mercury from 500 ml of redistilled water at various HNO_3—NaCl and HNO_3—NH_4SCN concentrations are shown in Table 3. Recoveries from 1-l portions of solution were incomplete (the data are not shown). In view of the distribution coefficients listed in Table 1, quantitative recoveries from 1-l samples would be expected when thiocyanate is present. The reason

TABLE 1

Distribution coefficients of mercury between anion-exchange resin (Cl^--form) and solutions containing various concentrations of nitric acid

Concentration of NaCl or NH_4SCN	Distribution coefficient			
	0.001 M HNO_3	0.01 M HNO_3	0.1 M HNO_3	0.5 M HNO_3
—	3.7×10^4	3.2×10^4	2.2×10^3	1.2×10^2
0.1 M NaCl	7.0×10^4	5.9×10^4	4.9×10^4	4.9×10^3
0.5 M NaCl	4.1×10^4	6.2×10^4	5.0×10^4	7.9×10^3
0.01 M NH_4SCN	—	4.0×10^5	8.4×10^5	6.1×10^4

TABLE 2

Effect of amount of reductant and aeration time on recovery of mercury from the resin after adsorption from 0.1 M HNO_3—0.01 M NH_4SCN

Vol. added to bubbler (ml)		Mercury recovery (%)	Aeration time (min)
H_2SO_4 (1 + 1)	$SnCl_2$ (10%)		
2	2	—[a]	30
4	4	87	33
4	8	97	6
10	20	98	6

[a]No measurable absorbance observed in a 30-min aeration.

for this discrepancy is not clear at present, but insufficient mixing of the resin with the whole solution may be partly responsible, because the liquid almost completely fills the 1-l polyethylene bottle, making mixing difficult.

Determination of mercury ions in river and spring waters

Mercury ions present in river and spring waters were determined by making the sample solutions 0.1 M in nitric acid and 0.01 M in ammonium thiocyanate. The results are shown in Table 4. Samples for runs 1—4 were treated with nitric acid and thiocyanate as early as possible and the final determinations were done within 1 week after sample collection. Samples for runs 5 and 6 were stored in 1-l polyethylene bottles for 1 week before treatment; analyses were completed 3 days after this treatment. The blank values were considerably lowered in the latter two runs, probably because the stock nitric acid and thiocyanate solutions used were freshly prepared.

TABLE 3

Recoveries of mercury from resins collected from redistilled water with various HNO_3—NaCl and HNO_3—NH_4SCN concentrations[a]

HNO_3 (M)	NaCl (M)	NH_4SCN (M)	Recovery (%)			
			Amount of Hg added (ng)			
			5	10	15	20
0.1	0.1	—	95	94	96	96
	0.5	—	95	95	95	96
0.01	0.1	—	95	98	98	96
	0.5	—	96	94	96	97
0.1	—	0.05	84	85	84	83
	—	0.01	98	99	99	99
	—	0.002	94	92	93	93

[a]Recoveries were corrected for mercury blanks. For resins collected from HNO_3—NaCl, 2 ml each of H_2SO_4 (1 + 1) and $SnCl_2$ (10%) solutions were used, while for those collected from HNO_3—NH_4SCN solutions, 4 ml of H_2SO_4 and 8 ml of $SnCl_2$ solutions were used.

TABLE 4

Determination of mercury in river and spring waters[a]

Run	River water[b]			Spring water[c]		
	Found (ng)	Blank (ng)	Conc. (ng l^{-1})	Found (ng)	Blank (ng)	Conc. (ng l^{-1})
1	11.4	8.6	6.0	14.4	11.2	6.8
2	13.0	11.0	4.3	11.8	9.8	4.3
3	11.8	9.5	4.9	12.0	10.0	4.3
4	13.0	10.5	5.3	14.0	11.3	5.7
5	3.3	0.8	5.3			
6	4.8	2.0	6.0			

[a]Experimental conditions: 0.1 M HNO_3—0.01 M NH_4SCN, 470 ml of sample, total volume 500 ml, 0.2 g of resin. [b]Shirakawa river in Kumamoto City. [c]Hakemiya Spring in Kumamoto City.

The results for a typical run are shown in Fig. 1, from which mercury in the sample of run 1 (spring water) was determined. The upper and the middle calibration lines correspond to those prepared by the standard addition method for the sample and for redistilled water, respectively; the bottom line is a conventional calibration line. It can be seen from Fig. 1 that the method of standard additions is not necessary for the determination of mercury in these natural waters.

Determination of mercury ions in sea water

All the results (Table 5) were based on the conventional calibration method. The treatment of samples I, II and III was as follows: sample I had previously been stored in 1-l polyethylene bottles for 5 days after sampling without any treatment, and acidified just before preconcentration; sample II was acidified immediately after sampling and the determination was completed 2—3 days afterwards; sample III had been stored in 1-l polyethylene bottles for 5 days without any treatment, acidified, and measured 1 week later. The value obtained for sample I was used to correct for mercury blanks, which may arise from the nitric acid and the resin, because all the mercury ions naturally present in sample I can be considered to be "lost" during the 5-day storage under non-acidified conditions [16]. The mercury concentrations in samples II and III are fairly similar.

Cleaning of sample containers

The cleaning of the 1-l polyethylene bottles consisted of two processes. First, the bottles were scrubbed with detergent and water, stored overnight in 1 M HNO_3, and rinsed with distilled water. Next, the bottles were 80—90% filled with HNO_3—NaCl (both 0.1 M) solution, a 0.2-g portion of resin was added to each, and they were mechanically shaken for 2—3 h. The bottles were emptied, and the HNO_3—NaCl—resin treatment was repeated

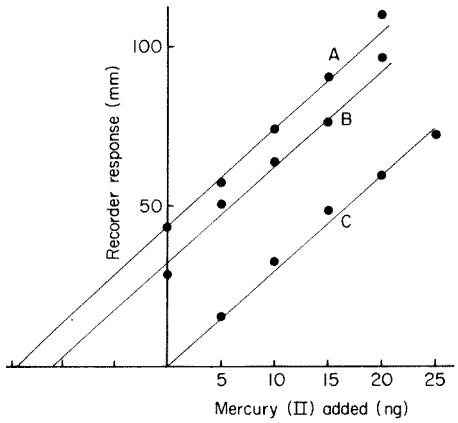

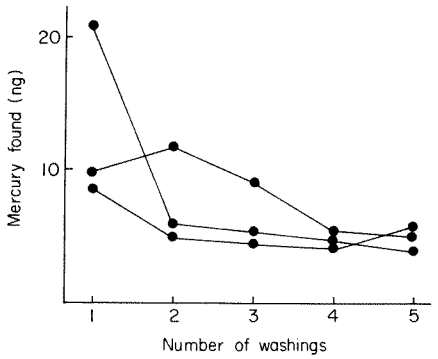

Fig. 1. Calibration graphs: (A) standard addition for run 1 (spring water) in Table 1; (B) standard addition for redistilled water; (C) conventional calibration.

Fig. 2. Effect of washing polyethylene containers with anion-exchange resin in HNO_3—NaCl (both 0.1 M).

at least three times. The mercury content of the resin obtained after each operation was measured. The results are shown in Fig. 2 as a function of the number of washing operations. As can be seen, irrespective of differences in the initial mercury content, the amount of mercury found after three washing operations was constant at about 5 ng, which might arise from contamination from the wash solution and resin. This degree of cleaning was considered satisfactory.

Other parameters affecting the method

Recoveries and blank mercury values were investigated by changing the amount of resin added in the range 0.2—0.5 g. Recoveries were not affected, and the blank values arising from the resin itself were calculated to be $\leqslant 1$ ng

TABLE 5

Determination of mercury in sea waters[a]

Run	Amount of Hg found (ng)		
	Sample I	Sample II	Sample III
1	6.3	11.1	14.0
2	6.8	14.7	15.3
3	5.3	13.5	14.2
4	5.7	—	13.5
5	6.4	—	—
Mean	6.1	13.1 (14.7)[b]	14.3 (17.3)[b]

[a]Samples taken from Shimabara Bay, Kyushu Island. [b]Concentration (ng l^{-1}) in sea water.

per 0.1 g of the resin. At the beginning of this study, resin in the thiocyanate form was used for recovery of mercury from the solutions conditioned with nitric acid and thiocyanate. However, the thiocyanate-form resin, into which the chloride form had been converted in advance by passing 1 M NH_4SCN, exhibited a very large mercury blank. Furthermore, purification of the chloride form of the resin by washing with 1 M HCl led only to an increased mercury blank. Accordingly, the commercially available resin was used without any pretreatment or conditioning. Most of the blank mercury probably arises from the reagents (HNO_3, NaCl, and NH_4SCN): though quantitative data were not obtained, the blank values depend not only on the storage period of these reagents, but also on the frequencies of removing the solution from their stock bottles during storage. Each stock solution, especially ammonium thiocyanate, should not be stored for more than 10 days.

The recovery of mercury from the resin collected from sample solution was found to be considerably affected by the shape of the gas bubbler. Early in this study, a 300-ml round-bottomed flask was used as the reduction—aeration bottle. The recoveries were unsatisfactory (ca. 80%). The cylindrical gas bubbler used here gave good recoveries, probably because of its greater bubbling efficiency. Finally, it should be mentioned that the temperature of the solution in the gas bubbler affects the time required to attain the maximum atomic absorption of mercury. Most of the measurements in this study were done at room temperature (ca. 20°C). The reduction—aeration of mercury from the resin should not be done below 10°C, otherwise an unfavorably long time will be needed to liberate the mercury vapour.

REFERENCES

1 Y. Kimura and V. L. Miller, Anal. Chim. Acta, 27 (1962) 325.
2 A. G. Howard and M. H. Arbab-Zavar, Talanta, 26 (1979) 895.
3 K. Terada, K. Morimoto and T. Kiba, Bull. Chem. Soc. Jpn., 53 (1980) 1605.
4 A. Sugii, N. Ogawa and H. Imamura, Talanta, 26 (1979) 941.
5 E. Yamagami, S. Tateishi and A. Hashimoto, Analyst, 105 (1980) 491.
6 K. Minagawa, Y. Takizawa and I. Kifune, Anal. Chim. Acta, 115 (1980) 103.
7 R. Kuroda, T. Kiriyama and K. Ishida, Anal. Chim. Acta, 40 (1968) 305.
8 F. Ichikawa, S. Uruno and H. Imai, Bull. Chem. Soc. Jpn., 34 (1961) 952.
9 A. K. Majumdar and B. K. Mitra, Fresenius Z. Anal. Chem., 208 (1965) 1.
10 H. D. Livingston, H. Smith and N. Stojanovic, Talanta, 14 (1967) 505.
11 D. E. Becknell, R. H. Marsh and W. Allie, Jr., Anal. Chem., 43 (1971) 1230.
12 S. H. Omang, Anal. Chim. Acta, 53 (1971) 415.
13 C. Feldman, Anal. Chem., 46 (1974) 99.
14 S. Shimomura, Y. Nishihara and Y. Tanase, Jpn. Anal., 18 (1969) 1072.
15 Y. Dokiya, S. Yamazaki and K. Fuwa, Environ. Lett., 7 (1974) 67.
16 I. Sanemasa, T. Deguchi, K. Urata, J. Tomooka and H. Nagai, Anal. Chim. Acta, 87 (1976) 479.
17 I. Sanemasa, T. Deguchi, K. Urata, J. Tomooka and H. Nagai, Anal. Chim. Acta, 94 (1977) 421.

Analytica Chimica Acta, 130 (1981) 157—166
Elsevier Scientific Publishing Company, Amsterdam — Printed in The Netherlands

SIMULTANEOUS DETERMINATION OF TRACE METALS IN SEWAGE AND SEWAGE EFFLUENTS BY INDUCTIVELY COUPLED ARGON PLASMA ATOMIC EMISSION SPECTROMETRY

M. M. MOSELHY* and P. N. VIJAN

Laboratory Services Branch, Ministry of the Environment, P.O. Box 213, Rexdale, Ontario, M9W 5L1 (Canada)

(Received 2nd June 1980)

SUMMARY

Inductively coupled plasma excitation sources are adapted for the simultaneous determination of multiple elements in sewage and sewage effluents by atomic emission detection. Digestion with aqua regia in test tubes is recommended for sample preparation. A typical comparison of lead in sewage by atomic emission (x) and atomic absorption (y) gave a least-squares fit of $x = 0.98\ y + 0.03$ with a standard error of 0.5 mg l^{-1} and a correlation coefficient of 0.996. More complete comparison data by the atomic emission and absorption techniques are presented for other elements.

The increasing use of sewage sludge of farmland [1] combined with the nutritional and toxic effects of metal ions makes it highly desirable to have effective methods for the determination of multiple elements in sewage sludge. Because atomic absorption spectrometric (a.a.s.) methods have not proven completely satisfactory, recent developments in excitation sources and computerized spectrometric systems suggest [2] inductively coupled plasma atomic emission spectrometry (i.c.p.e.s.) as a promising alternative. While papers dealing with elemental determinations in environmental materials have been published, few deal specifically with a complex matrix such as sewage.

Existing methods of sample preparation [3, 4] although adequate, leave room for improvement in sample handling, manipulation, and efficiency of digestion in order to be compatible with i.c.p. measurement systems.

Corrondo et al. [5] determined some common heavy metals in sewages by injecting small volumes of undigested homogenized samples to the electrothermal atomizer of an atomic absorption spectrometer, using the method of standard additions. Their claims of speed, freedom from interferences, and adequate precision and accuracy were not supported. Ritter and Stevens [6] compared five procedures for digestion of dried sludges. Some other studies of the determination of metals in sewage samples have used similar a.a.s. techniques [7—9].

0003—2670/81/0000—0000/$02.50

An a.e.s. method based on d.c. arc excitation of dried samples is useful for the determination of 26 elements in waste waters and sludges [10]; the recoveries varied between 77 and 150%, and determinations in three samples required one man-day. Winefordner et al. [11] summed up advantages of a.e.s. over a.a.s. for multi-element determination.

The primary objectives of this study were to evaluate the current a.a.s. method for a large number of sewage samples, to incorporate improvements in sample digestion procedures, to adapt and apply a rapid i.c.p.e.s. technique to simultaneous multi-element determinations in sewage digests, and to compare the results obtained by the two methods.

EXPERIMENTAL

Instrumentation

The four instruments used in this study were two a.a.s. units and two i.c.p. systems. A Varian-Techtron model 1250 and a Perkin-Elmer model 5000 comprised the a.a.s. equipment. Each included provision for background correction. The instrumental parameters used were essentially those recommended in instruction manuals. A compromise burner height was set for all the metals and background correction was used for the determinations of zinc, lead, nickel, and cadmium at low concentrations. No significant broadband absorption effects were encountered at high concentrations.

A Jarrell-Ash 3.4-m Ebert convertible spectrograph multichannel spectrometer and a Jarrell-Ash Plasma AtomComp 750 were used. Both systems were equipped with i.c.p. units and were independently controlled by dedicated PDP-8 computers. The instrumental setup of the 3.4-m Ebert system, initially used in this study, has been described previously [2]. Data presentation was set up to print mg l^{-1} concentrations of aluminum, calcium, cadmium, cobalt, chromium, copper, iron, magnesium, manganese, molybdenum, nickel, lead, strontium, titanium, and zinc. Two-point standardization of the system with 1% nitric acid and 10 mg l^{-1} multi-element standards was used to set up gains and offsets prior to determinations. Compromise operating conditions and correction for interferences remained the same as previously reported. The Plasma AtomComp 750 was originally supplied with 20 analytical channels and a mercury channel for profiling purposes. Two analytical channels were added, one for titanium and the second for magnesium at 383.2 nm. The latter was used to determine high concentrations of magnesium to minimize self-reversal. The spectral line signals of cadmium, cobalt, chromium, manganese, molybdenum, nickel, lead, strontium, vanadium, and zinc were corrected for background variations using a computer-controlled automatic background corrector. The aluminum, calcium, iron, magnesium, and titanium line signals were not corrected for background. Other details of the system components such as i.c.p. source attachment, slit illumination arrangement, profiling of spectral lines, cali-

bration and standardization were essentially the same as described in the instrument manual. Because the software did not provide warning if the standardization gains and offsets departed from the initial values, these drifts were detected by processing control standards after each group of ten samples. Restandardization was done when required.

A Model MN-2500E Plasmatherm r.f. source with an incident power of 1.1 kW and a reflected power of <1% was used. A constant flow of sample solution was introduced into a cross-flow nebulizer (Jarrell-Ash) using a Gilson peristaltic pump. The plasma was sustained by an argon flow of 18 l min^{-1} as coolant and 1 l min^{-1} for nebulization. The viewing zone of the plasma was 14 mm above the r.f. coil. The integration times used were two 4-s periods on line and one 4-s period on background.

The individual spectral lines on both the Ebert and AtomComp spectrometers were selected by rotation of refractor plates positioned in front of each slit. Quartz refractor plates were used for the spectral range 170—230 nm, Corex was used for 230—380 nm, and glass was used for 350—780 nm. Spectral line fluxes were measured by 13-nm R427 Hamamatsu photomultiplier tubes with fused quartz windows for the spectral range 170—230 nm and by R300 tubes with u.v. glass windows for 230—500 nm.

Computer program for AtomComp

A computer program was developed for processing digested sewage samples with the Jarrell-Ash AtomComp. This program specified the operating channels, integration time, channels to be corrected for background, composition and levels of the standardization solutions, interference correction factors, affecting and affected channels, channels to be corrected for background variations, and the limits of concentration range for each element. The measurement channels were arranged in the computer program with the affecting elements specified first, followed by the low concentration components arranged in order of magnitude of their interference effects. The interference correction factors were calculated as described previously [2].

Table 1 shows the channels affected by iron, magnesium, and/or aluminum, spectral lines, and the calculated correction factors for the AtomComp system. Correction for interference from iron in zinc, aluminum, cadmium, manganese, copper, nickel, lead, and vanadium yielded acceptable results. The interference of the iron II 238.86-nm line with the cobalt II 238.89-nm line was too severe to be compensated by such correction. Relocation of the cobalt channel is necessary. The residual responses of various channels to different concentrations of magnesium following the application of correction factors were negligible except for iron, aluminum, and calcium. Aluminum and calcium exhibited a proportional increase in response with increasing magnesium concentration. This suggests the presence of aluminum, iron, and calcium as impurities in the added magnesium salt.

A set of standards containing matching concentrations of the elements of interest in sewage samples was used and the upper limit of calibration

TABLE 1

Correction factors used for the affected elements with the AtomComp system

Affecting element	Wavelength (nm)	Affected element	Wavelength (nm)	Correction factor
Fe(II)	238.2[a]	Zn(I)	213.9	0.0001
		Cd(II)	226.5	0.0001
		Co(II)	238.9	0.0060
		Mn(II)	257.6	0.0004
		Cu(I)	324.7	0.0015
		Ni(II)	231.6[a]	0.0003
		Pb(II)	220.4	0.0002
		V(II)	292.5	0.0002
Mg(II)	279.5	Al(I)	309.3	0.0060
Al(I)	309.3	Pb(II)	220.4	−0.0010

[a]Second order.

curves was terminated at 60 mg l^{-1} for trace and minor elements and 250 mg l^{-1} for major elements such as aluminum, calcium, iron, and magnesium. Because the content of alkali metals in sewage samples varies over a wide concentration range, accurate matrix matching of standards and sample solutions is difficult. Besides, the addition of potassium to calibration standards was found to be unnecessary. A reasonable agreement between the i.c.p. and a.a.s. values for most of these elements and acceptable quality control data tend to support this contention.

Effect of sulfuric acid

The effect of different acids on spectral line intensities produced by spark and plasma excitation of aerosols was reported earlier [2, 12]. The effect of sulfuric acid on line intensities was evaluated by the use of 10 mg l^{-1} multi-element standards containing, 0, 10, 20 and 30% (v/v) sulfuric acid. Sulfuric acid concentration beyond 5% caused a linear reduction in the intensity for all elements. A decrease in the nebulizer uptake rate was noticed with increasing sulfuric acid concentration. The use of a peristaltic pump to maintain the normal flow rate of the nebulizer restored the expected intensity for all elements except lead. The rapid reduction in lead concentration is primarily due to its precipitation as sulfates.

Pipetting precision

The precision of pipetting of the heterogeneous sewage samples was tested by weighing a number of 5-ml and 2-ml aliquots. Serological pipets, calibrated to the tip and having wide bores, were used with suction. Pipets were used to stir the samples to prevent suspended material from settling. The pipetting imprecision was 5% and 7% r.s.d. for 5-ml and 2-ml aliquots, respectively.

Reagents

All acids and reagents used were ACS grade. Stock standard solutions of each element (1000 mg l^{-1}) were prepared from high-purity metals and nitrates. Solutions used for standardization of the i.c.p. instrument were prepared by dilution of composite standards with 1 M nitric acid. Solution 1 contained 1 mg l^{-1} Cd, Co, Cr, and Mo, 10 mg l^{-1} Zn, Pb, Mn, Ni, and Cu, and 50 mg l^{-1} Fe, Al, Mg, and Ca. Solution 2 contained 1 mg l^{-1} V and Sr. Solution 3 contained 10 mg Ti l^{-1}.

Procedure

Aliquots (2 ml) of each sample were pipetted into numbered test tubes held in the aluminum blocks. Blanks and control solutions were included in each block. The loaded blocks were placed in a forced air oven (Thelco) to dry overnight at 90°C. The dried materials were digested in aqua regia: 4 ml of aqua regia was dispensed into each test tube, and the aluminum block was placed on a hot plate at 120°C. Samples were allowed to digest until brown fumes ceased to evolve and smooth boiling and refluxing ensued. A few drops of nitric acid were added to test tubes showing a dark residue. The volume in each test tube was reduced to approximately 2 ml by evaporation. The aluminum block was allowed to cool to room temperature and the content of each tube was diluted to 25 ml with distilled water. The acid concentration of the prepared solution was 1—1.3 M.

RESULTS AND DISCUSSION

Six typical sewage samples were selected for evaluation of the digestion procedure. Each set was composed of 16 test tubes, i.e. six pairs of duplicate samples, two control solutions, and two blanks. Eight such sets of solutions were prepared on different days. Duplicate samples were also digested with sulfuric—nitric and perchloric—nitric acid mixtures. Elements in the prepared sample solutions were quantified by i.c.p. and flame a.a.s.

Typical results for sixteen a.a.s. determinations in each of the digestion media yielded average concentrations (mg l^{-1}) ± pooled standard deviations of 0.47 ± 0.05 for zinc, 0.44 ± 0.66 for copper, 0.24 ± 0.036 for manganese, 0.15 ± 0.03 for lead, 0.5 ± 1.3 for iron, 9.48 ± 1.2 for aluminum, and 22.7 ± 2.6 for calcium. No significant difference exists at the 95% confidence level among the results obtained in different digestion media; the F test showed no significant difference at the 95% confidence level between within-run standard deviations for the digestion media and the pooled standard deviations for all runs. The data also indicate that the differences in anionic composition of the prepared solutions did not affect the results significantly. Beaker digestions are prone to contamination by Fe, Al, Ca, and Mg which are the major constituents of glass. For example, an average Al blank for beaker digestion was 0.5 mg l^{-1} as compared with 0.17 mg l^{-1} for test tube digestion. Results obtained for lead in H_2SO_4—HNO_3 digestions were ex-

cluded from the calculated averages owing to the precipitation of lead sulfate.

The i.c.p. results for manganese obtained by aqua regia digestion were on average 6.5% higher than the corresponding a.a.s. values. Digestions of the same samples with $HClO_4$—HNO_3 and H_2SO_4—HNO_3 yielded results that were 17.5% lower by i.c.p. The i.c.p. method was also used to compare Ni, Zn, Cr, Mg, Pb, and V concentrations in samples digested with aqua regia in test tubes and beakers. Comparison of the pooled metal concentrations in beakers with those in test tubes showed a slope of 0.84 ± 0.04, an intercept of 0.24 ± 0.3 mg l^{-1}, a standard error of 1.5 mg l^{-1}, a correlation coefficient of 0.997, and an overall recovery of 115%. The high recovery could be attributed to sample contamination from beaker, fume hood, and excessive volumes of acids used. The test tube procedure appears to be superior in convenience, ease of handling, relative freedom from extraneous contamination, and thoroughness of digestion with minimum use of acids. Although $HClO_4$—HNO_3 digestion might appear to be the best in terms of extractability of metals and solubility of their perchlorates, it is considered hazardous especially for treatment of samples rich in organic matter. In addition, $HClO_4$—HNO_3 digested samples tend to cause frequent clogging of nebulizers, probably owing to the precipitation of $KClO_4$. Based on these considerations, aqua regia digestion in test tubes was selected.

To ensure the validity of the final results, two blanks and two control solutions (A and B) were included in each set of samples to aid with quality control. Also, elemental contents of standards and verification solutions containing sixteen elements were quantified after every ten samples to maintain a check on the instrumental drift. The i.c.p.e.s. and a.a.s. results obtained on these solutions over a three month period of routine determinations were accumulated. This provided enough data to evaluate between-run precision and accuracy statistically. As shown in Table 2, results appear to be acceptable, although there is a slight bias towards the high concentration for i.c.p.e.s. Statistical evaluation of the i.c.p. and a.a.s. results obtained on control solutions A and B for the same period is also summarized in Table 2. The calculated accuracy and precision values represent the long-term analytical performance of both the i.c.p.—spectrometer and the a.a.s. systems. Similar "between-run" precision was obtained for i.c.p. results for the "verification" solution.

The importance of processing paired solutions of known concentrations (A and B) for routine quality control has been emphasized by King [13]. Long-term stability and the analytical performance of the instruments used here were assessed by interpretation and evaluation of results obtained on paired solutions. Figure 1 shows the A and B plots for nickel by a.a.s. and i.c.p. The radii of inner and outer circles are equal to twice the within and between-run standard deviations, respectively. The lines on the A + B plots represent control and warning limits, relative to the expected concentrations. Similar plots obtained for other ions were also useful indicators of systematic

TABLE 2

Typical results for selected samples and measurement methods
(All concentrations are in mg l^{-1})

Sample	Quality control A					Quality control B				
Method	I.c.p.			A.a.s.		I.c.p.			A.a.s.	
Element	Expected	Found[a]	S.d.	Found[a]	S.d.	Expected	Found[a]	S.d.	Found[a]	S.d.
Fe	2.0	2.07	0.17	1.97	0.16	4.0	3.88	0.31	3.89	0.17
Al	2.0	1.87	0.19	1.90	0.23	4.0	3.49	0.35	3.73	0.19
Ca	25.0	24.8	1.89	25.6	1.75	50.0	48.3	3.59	49.0	2.02
Zn	0.4	0.42	0.08	0.37	0.03	0.8	0.78	0.09	0.74	0.03
Cd	0.4	0.40	0.03	0.40	0.03	0.8	0.76	0.06	0.79	0.08
Co	0.5	0.47	0.04	0.46	0.06	1.0	0.89	0.08	0.94	0.06
Mg	10.0	9.77	0.85	10.4	0.57	20.0	18.7	1.52	20.8	2.44
Mn	0.4	0.39	0.03	0.41	0.04	0.8	0.74	0.06	0.08	0.04
Cr	0.5	0.48	0.04	0.47	0.04	1.0	0.91	0.07	0.94	0.07
Cu	0.4	0.41	0.07	0.40	0.05	0.8	0.74	0.10	0.77	0.03
Ni	1.0	1.01	0.08	0.94	0.09	2.0	1.91	0.15	1.88	0.08
Pb	0.5	0.51	0.06	0.50	0.06	1.0	0.98	0.08	0.98	0.07
Mo	0.2	0.21	0.02	0.20	0.02	0.4	0.40	0.03	0.39	0.04
Sr	0.2	0.20	0.02	0.23	0.03	0.4	0.40	0.05	0.46	0.05
Ti	—	—	—	—	—	—	—	—	—	—
V	0.2	0.18	0.02	0.19	0.04	0.4	0.36	0.03	0.39	0.05

[a]Average of 20.

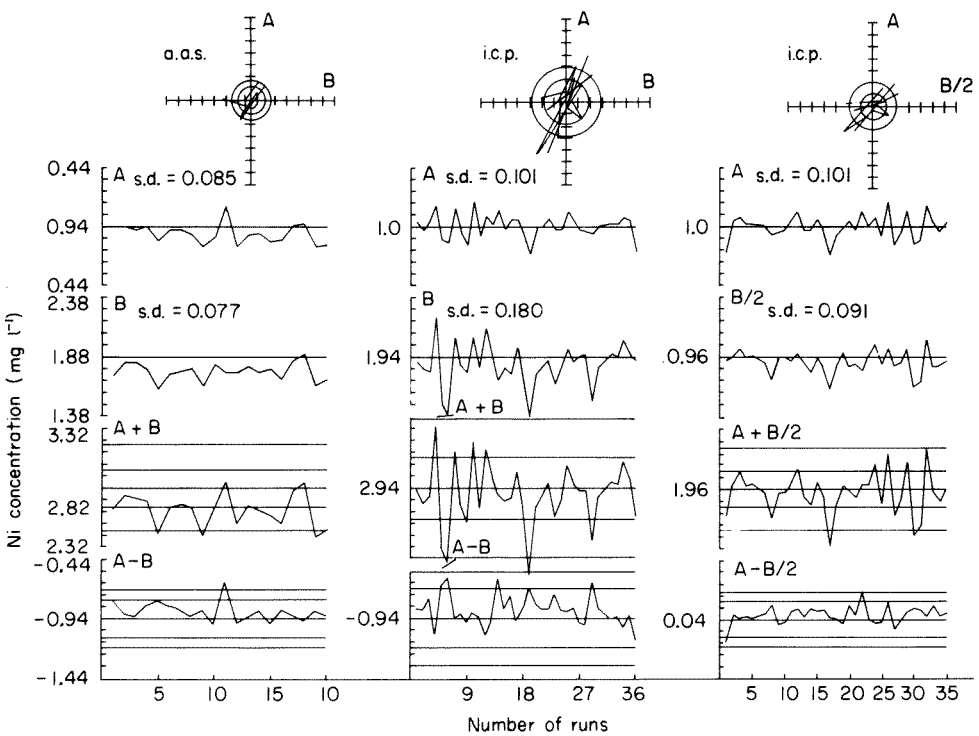

Fig. 1. Quality control plots for nickel by a.a.s. and i.c.p.e.s.

errors. The latter are related to the control of intercept and sensitivity (instruments offset and gain). Complete evaluation of A vs. B data requires that the standard deviations for both A and B be approximately equal. In the case of nickel by a.a.s., the fact that A − B is less variable than A + B suggests that while the slope is in control, some systematic error occurred related to the setting of the intercept. Within-run standard deviation is 0.057 for the concentration range 0—2 mg Ni l^{-1} whereas between-run standard deviation is significantly larger (0.081). In contrast, nickel by i.c.p. shows a strong dependence of standard deviation on concentration. The plot of A vs. B shows a great deal of systematic error which appears to be caused by day-to-day variation in sensitivity. The plot of A vs. B/2 suggests that if the slope could be controlled, the between-run standard deviation would drop from about 10% to 5%. The plot of A vs. B/2 for strontium showed a severe sensitivity drift over the period of study for a.a.s. while the i.c.p. showed the typical day-to-day random variations with only a very slight drift in sensitivity. The characteristics already described for the two instrumental systems with respect to Ni, Sr, and V were representative of all elements examined. Instrumental sensitivity rather than sample preparation is therefore responsible for the systematic errors. A similar pattern of possible systematic error in sensitivity control was observed for data obtained on the i.c.p.—Ebert system for cobalt.

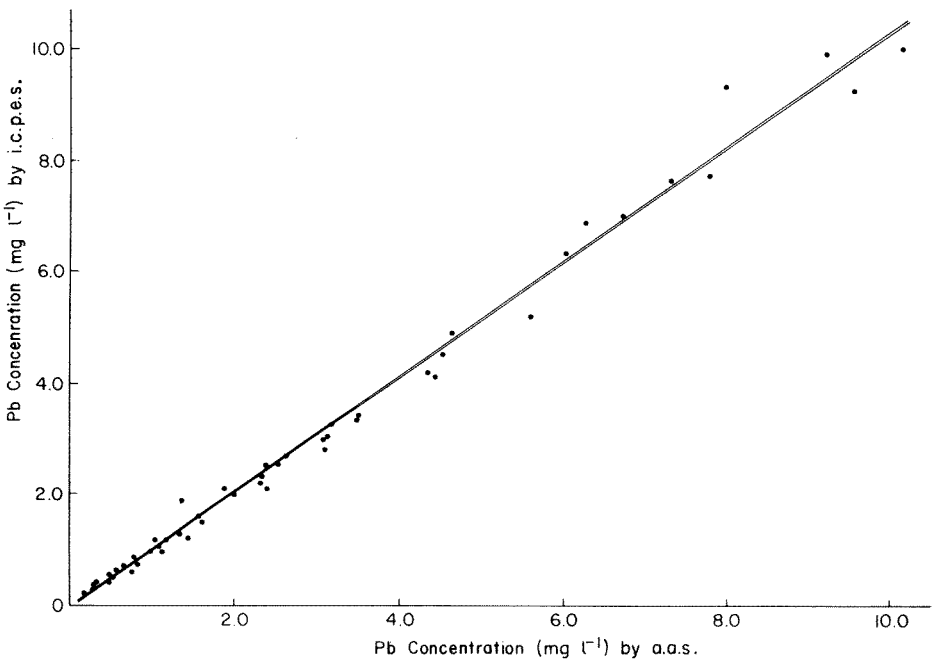

Fig. 2. Regression curves for lead in sewage by a.a.s. and i.c.p.e.s. $x = (0.975 \pm 0.05)y + (0.03 \pm 0.2)$ mg l^{-1} with $s_{xy} = 0.5$, $y = 0.996$.

TABLE 3

Relationship between a.a.s. and i.c.p.e.s. data

Element	n[a]	Conc. range (ml l^{-1})	Intercept (mg l^{-1})	S.d. of intercept (mg l^{-1})	Slope	S.d. of slope	r[a]	$S.e.$[a] (mg l^{-1})
Cr	57	0.05—10	−0.013	0.016	0.975	0.008	0.998	1.97
Pb	80	0.05—10	−0.015	0.024	1.017	0.010	0.996	2.38
Fe	18	0.10—20	−0.124	0.044	1.041	0.009	0.999	4.85
Fe	57	0.50—100	0.367	0.584	1.021	0.019	0.990	30.77
Ni	27	0.01—2	−0.017	0.006	1.005	0.009	0.999	0.68
Cu	70	0.08—16.5	−0.106	0.071	1.002	0.017	0.990	4.15
Zn	74	0.07—14	0.072	0.098	1.061	0.026	0.979	3.74
Cd	40	0.005—1	−0.012	0.007	1.109	0.036	0.979	0.20

[a]Number of determinations (n), correlation coefficient (r) and standard error ($s.e.$).

The results obtained for zinc in a set of samples by the i.c.p.—Ebert system and a.a.s. gave the slope, intercept, standard error, and correlation coefficient 1.04 ± 0.1, 0.03 ± 0.1 mg l^{-1}, 0.8 mg l^{-1}, and 0.96, respectively. Similarly, the i.c.p.—Ebert system vs. a.a.s. values for chromium were 1.083 ± 0.1, 0.011 ± 0.1 mg l^{-1}, 0.8 mg l^{-1}, and 0.999, compared to 1.053 ± 0.1, 0.013 ± 0.1 mg l^{-1}, 0.8 mg l^{-1} and 0.997 for the i.c.p.—AtomComp system vs. a.a.s. data. The i.c.p.—Ebert data tended to deviate from linearity below 1 mg l^{-1} suggesting the need for background correction at low concentrations. The i.c.p.—AtomComp data did not deviate. Correlation of the data obtained for nickel by i.c.p.—AtomComp and a.a.s. showed that the data were evenly distributed around the ideal line, but those for copper showed a slight bias towards higher a.a.s. results.

Differences in calibration of either system rather than difference in recovery could explain the bias. If the background correction of the two analytical systems is different, the data plotted on a log—log scale should curve away from the ideal line at the bottom end. If the sensitivities (slopes) of the analytical systems are different, however, the data plots should be parallel to, but not coincide with, the ideal line.

The regression curves for lead (Fig. 2) and the data presented in Table 3 exemplify the linear correlation between the i.c.p.—AtomComp and a.a.s. results obtained on aqua regia-digested sewage samples. The good fit of the data points indicates an adequate control of between-run precision and accuracy of the two analytical systems.

The authors thank the Laboratory Services Branch, Ontario Ministry of the Environment for encouragement and support.

REFERENCES

1 J. D. Cunningham, D. R. Keeney and J. A. Ryan, J. Environ. Qual., 4 (1975) 448.
2 M. M. Moselhy, D. Boomer, J. Bishop, P. Diosady and A. Howlett, Can. J. Spectrosc., 23(6) (1978) 186.

3 S. A. Katz, S. W. Jennis, T. Mount, R. E. Tout and A. Chatt, Abstract 323, 31st Pittsburgh Conference, Atlantic City, NJ, 1980.
4 Handbook of Analytical Methods for Environmental Samples, Laboratory Services Branch, Ministry of the Environment, Ontario, Canada, 1970.
5 M. J. T. Corrondo, R. Perry and J. N. Lester, Sci. Total Environ., 104 (1979) 1, 31.
6 C. J. Ritter and S. C. Stevens, At. Absorpt. Newsl., 17 (4) (1978) 70.
7 J. N. Lester, R. M. Harrison and R. Perry, Sci. Total Environ., 104 (1979) 13.
8 S. Stoveland, M. Astrue, J. N. Lester and R. Perry, Sci. Total Environ., 194 (1979) 25.
9 K. Y. Chen, C. S. Young, T. K. Jan and N. Rohatgi, J. Water Pollut. Control. Fed., 12 (1974).
10 D. H. Kampbell, 19xx, private communication.
11 J. D. Winefordner, J. J. Fitzgerald and N. Omenetto, Appl. Spectrosc., 29 (1975) 369.
12 M. M. Moselhy, Can. J. Spectrosc., 18 (5) (1973) 119.
13 D. E. King, US—NBS Special Publication, 402, Proc. 7th Material Research Symposium, 1 (1976) 141.

Analytica Chimica Acta, 130 (1981) 167—175
Elsevier Scientific Publishing Company, Amsterdam — Printed in The Netherlands

MULTI-ELEMENT ANALYSIS OF URINE BY ENERGY-DISPERSIVE X-RAY FLUORESCENCE SPECTROMETRY

L. VOS, H. ROBBERECHT, P. VAN DYCK and R. VAN GRIEKEN*
Department of Chemistry, University of Antwerp (UIA), B-2610 Wilrijk (Belgium)
(Received 24th April 1981)

SUMMARY

For multi-element analysis of human urine, 25-ml samples doped with yttrium as internal standard are evaporated gently and then ashed up to 460°C overnight. The residue is pelletized and analysed by energy-dispersive x-ray fluorescence. Acid addition to facilitate the digestion is not mandatory. Recoveries are nearly quantitative for traces of Fe, Ni, Cu, Zn and Sr, to a lesser extent for lead, but not for arsenic or selenium. The standard deviation per measurement is typically around 6%. The detection limits are such that some 10 elements can be determined simultaneously in normal urine, and possibly more in cases of importance to toxicology or industrial hygiene.

The role of trace elements in biological fluids and tissues is an area which continues to attract much attention. Urine is particularly important because its elemental composition reflects the performance of the kidneys in regulating the electrolyte and water metabolism of the body, and because it removes many superfluous and toxic substances from the body. Research in this field has shown that each mode of excretion deals specifically with certain waste products: e.g., urine removes the bulk of Na, Cl, F, P, As, K, Se, Rb, Ca, Mg, Co and Br, whereas the intestine eliminates most of the Mn, Cu and Zn [1—4]. Various studies have indicated correlations between particular elemental concentrations and specific medical disorders: e.g., excessive urinary zinc excretion followed by a zinc deficiency syndrome has been reported in association with a variety of diseases [5], and intravenous nutrition may lead to excessive urinary losses of metals bound to amino acids and peptides and so to trace element deficiencies [6]. The concentrations of trace elements in urine can also give indications about the quality of modern nutrition [7, 8], which can undoubtedly be correlated with environmental pollution, and are important in toxicology. Urine is also easy to collect and to handle. All these considerations indicate why so much attention is given to investigating the concentrations of the different trace elements in the urine of both normal healthy individuals, and pathological cases. The potential importance of interactions between different trace elements, e.g., copper and molybdenum or zinc and copper [9], emphasizes the advantages of employing a multi-element analytical technique wherever possible.

Up to now, most clinical studies on trace elements in urine have dealt with only one element or have involved only a few elements simultaneously. The multi-element capabilities of x-ray fluorescence spectrometry (x.r.f.) in its energy-dispersive version could increase significantly the information available from each sample. It is surprising that practically no analytical research has been done in this field. A major reason might be the limited sensitivity of direct x.r.f.: the process for multi-element analysis of urine thus relies on the preconcentration step necessary to bring the trace elements to detectable levels.

Only a few preconcentration methods have been reported in combination with x.r.f. for urine analysis. Most were for single elements: wet destruction and extraction for chromium determination [10]; wet destruction and co-precipitation for yttrium determination [11]; a modification of the Gutzeit test for arsenic determination [12]; evaporation onto cellulose for bromine measurements [13] or direct assays for bromine and iodine [14]. By pre-concentrating on a chelating resin, Agarwal et al. [15] determined Zn, Cu and Pb in urine and Kingston and Pella [16] measured nickel. Only one multi-element energy-dispersive x.r.f. method for urine seems to have been published: Nielsen and Kalkwarf [17] used evaporation, ashing of the residue and pelletizing. Therefore a further investigation of the possibilities of multi-element trace analysis of urine by x.r.f. seemed worthwhile.

In the study reported here, the possibilities of using a chelating filter were first examined for preconcentrating the trace elements from the urine, and then the ashing procedure was optimized, further evaluated and applied.

EXPERIMENTAL

Equipment and spectrum analysis

The energy-dispersive x.r.f. apparatus used consists of a Siemens Kristalloflex 2 high-voltage generator and a Kevex 0810 subsystem. This subsystem includes a W-anode x-ray tube, various secondary targets (Ti was used for the low-energy region (P, S, Cl), and Mo for the high-energy region) with appropriate filters and a 16-position sample turntable. The characteristic x-rays are collimated at an angle of 90° relative to the exciting beam and measured by a nitrogen-cooled Si(Li) detector. After pulse pile-up, rejection and amplification, the pulses are stored in a Northern Econ II 4096-channel analyzer and recorded on a Northern NS-408 F magnetic tape unit for off-line computer evaluation with a PDP 11/45 unit.

The net intensities of the characteristic peaks in the spectrum were evaluated by means of a computer routine [18, 19] based on a non-linear least-squares fit that corrects accurately for deviations from the Gaussian peak shape and for variations in resolution and energy calibration. All the samples were measured together with a zirconium or nickel reference wire [20] positioned in front of the sample, which serves as a calibration for variation in the x-ray tube output and for dead-time correction. The mass of

the sample, the absorption correction and the concentration of the different elements are calculated by an iterative computer routine [21] based on the intensities of the characteristic peaks and the intensities and ratio of the coherent and the incoherent scatter peaks. A series of commercially available thin-film standards was used for calibration.

Sample preparation and analytical procedure

The sample preparation procedure that was finally selected involves gently ashing 25-ml urine samples overnight in an automatic Tecator wet destruction unit; the program involves heating at 130°C (2 h), 150°C (1 h), 250°C (1 h), 350°C (1 h), 400°C (1 h) and 460°C (3 h). After cooling, the residue is transferred to an agate grinding unit for homogenizing. (The contamination from this unit has been shown to be relatively insignificant [22].) Between two thin Mylar foils (Somar Labs., New York) the powder is then pressed into a pellet at 7000 kg cm^{-2} with a Beckmann 00-25 press. The pellet of about 60 mg cm^{-2} thickness is fixed onto a Mylar foil in a teflon ring which fits into the x.r.f. target holder. (The use of thinner pellets or lower pressures leads to brittle samples, while at higher pressure the Mylar foils are damaged.) The x.r.f. measurement is usually carried out during 3000 s.

RESULTS AND DISCUSSION

In a first approach, a chemical preconcentration step was tested for trace metal enrichments from urine; the DEN filters [23, 24] used are cellulose filters onto which diethylenetriamine has been introduced as a chelating functional group. The results obtained for natural waters with DEN filters have been very promising. Yet it appeared that substances with complexing amino functions, present in the urine, formed stronger complexes with the trace elements than did the DEN filter. When the urine was first decomposed with nitric acid and neutralized with sodium hydroxide, the blank level was too high. When the acid was previously evaporated, the scatter of those results was prohibitively high. Therefore this approach was abandoned after a number of experiments.

Nielson and Kalkwarf [17] described a method in which they first dried the sample under an i.r. lamp and then partially mineralized the residue on a hot place or in a muffle oven. With such equipment however, the drying and digesting conditions were not very reproducible, and further optimization seemed warranted. To dry and mineralize the sample, a 20-position Tecator Digestion System 20 was used. This system includes a control unit that is programmable in twelve steps; for each step one can adjust the temperature from 50 to 470°C and the time from 1 min to 24 h.

In energy-dispersive x.r.f. the detection limits are roughly inversely proportional to the target mass. Urine contains significant amounts of organic material, e.g. creatinine (0.7 g l^{-1}), which can be destroyed at higher temperatures. Heating the urine residue thus leads to smaller target thickness,

and so more advantageous x.r.f. detection limits. Without any decomposition step, the urine residue is also very hygroscopic and difficult to handle. However, heating involves an important risk of trace metal volatilization. In order to choose the optimal ashing temperature, a thermogravimetric ashing curve for the urine residue was recorded (Fig. 1). Since a significant weight loss was observed just below 460°C, and since most authors do not report elemental losses below 500°C (except for, e.g., Hg, Se, As), the maximum ashing temperature was set at 460°C.

The results of the x.r.f. measurements on the urine residue can be transformed to concentrations relative to the original wet urine sample, either by weighing the final residue obtained from a certain urine volume and dividing the x.r.f. results, as elemental weight fraction in the residue, by the urine volume-to-residue weight ratio, or by applying an internal standard method. In the latter case, yttrium can be advantageously added to the urine samples, e.g. 2 mg of yttrium per litre of urine. This element is present at extremely low levels in normal urine and it can be measured sensitively by x.r.f. with Mo excitation. The preconcentration factor is then obtained by dividing the measured yttrium concentration in the urine residue pellet by the original yttrium concentration in the liquid urine. Table 1 summarizes the results of measurements using both the direct and internal standard approach. There is no significant difference in the concentrations calculated in either way. The second method with the internal standard is clearly more precise than the method based on weighing. This is obviously because the latter method corrects automatically for uncertainties in the positioning of the pellet in the x.r.f. apparatus and for variable pellet thickness.

Possible losses of elements by volatilization were investigated by adding various standards to the urine. The results are summarized in Table 2. For

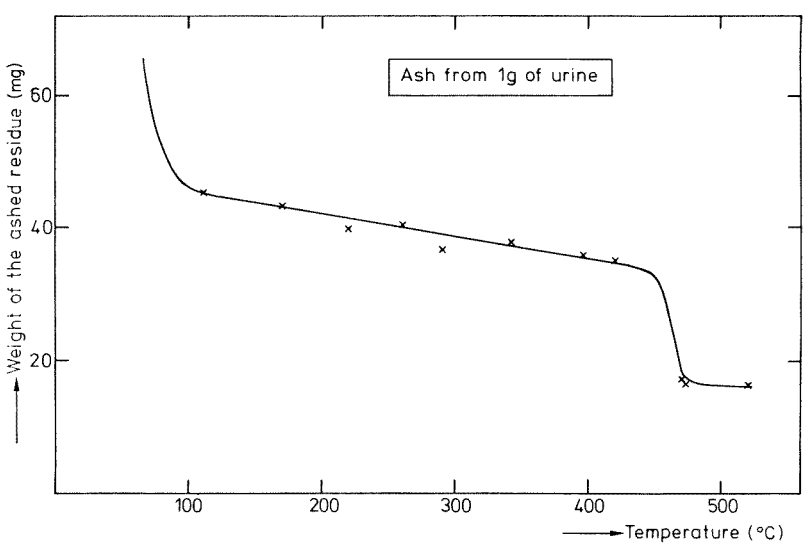

Fig. 1. Weight of the residue from 1 g of urine as a function of the heating temperature.

TABLE 1

Comparison of the two methods of calculating the preconcentration factor involving either weighing the urine residue or addition of an yttrium internal standard (All results involve 5 replicate determinations)

Element	Residue weighing		Internal standard	
	Concn. ($mg\ l^{-1}$)	S.d.[a] (%)	Concn. ($mg\ l^{-1}$)	S.d.[a] (%)
Cl	4620	13	4190	7
K	3520	10	3190	4
Ca	180	16	170	11
Fe	0.12	16	0.11	10
Ni	0.04	18	0.04	10
Cu	0.07	13	0.06	6
Zn	0.89	17	0.81	8
Br	5.02	8	4.55	1
Rb	2.48	6	2.26	3
Sr	0.21	10	0.19	4
Average s.d. (%)		12.7		6.5

[a]Standard deviation for a single measurement.

iron the recovery varies between 80 and 100% and the scatter in the results may correspond to the reproducibility on the x.r.f. determination. The recovery of nickel in the high concentration range is quantitative. The apparently lower recovery in the lower concentration range may be due to the fact that the detection limit is of the same order. Copper is recovered practically completely over the whole concentration range. In this high concentration range, the recovery of zinc is 70—90%. For strontium the recovery is complete. A level of 40 ppb lead is not detectable, but for high concentration the recovery lies between 50 and 74%. For arsenic the recovery was only around 30% and for selenium, added as H_2SeO_3, only 10% was recovered.

In the hope that addition of nitric acid would influence volatilization or adsorption losses, many experiments were repeated in 5% nitric acid solution. The results are included in Table 3. The recovery for Cl, Br and maybe Ca are lower than without acid addition while none of the other elements is affected by the acid medium. There is therefore no rationale in favour of addition of acid, which involves some contamination risk. Nielson and Kalkwarf [17] also found losses of P, Cl, Ca and Br on acid addition.

It can also be seen in Table 3 that when the urine sample is diluted five-fold with double-distilled water before the evaporation step, the results are exactly as expected, both with and without acid addition. Hence the recoveries are independent of elemental concentration variations within this range.

TABLE 2

Percentage recovery of some elements added to urine in different concentrations

Element	Recovery (%)[a] at different concentrations					
	0.04 ($mg\ l^{-1}$)	0.08 ($mg\ l^{-1}$)	0.12 ($mg\ l^{-1}$)	0.2 ($mg\ l^{-1}$)	0.4 ($mg\ l^{-1}$)	0.5 ($mg\ l^{-1}$)
Fe	N.a.[b]	N.a.	N.a.	100	97	80
Ni	60	90	87	95	95	100
Cu	95	80	80	97	99	104
Zn	N.a.	N.a.	N.a.	90	70	90
Sr	115	103	104	—	—	—
Pb	N.d.[c]	62	85	60	66	74

[a]Average of duplicate experiments. [b]Not added, because the natural levels are of the same order of magnitude or higher. [c]Not detectable with this method.

The standard addition results included in Table 3 confirm the data in Table 2, indicating nearly quantitative recoveries for Fe, Ni, Cu and Zn, and around 70% for lead. Again, as from Table 1, a standard deviation per measurement of about 6% can be inferred from the data in Table 3 that are well above the detection limits.

To check the reliability of the procedure, electrothermal atomic absorption spectrometry (a.a.s.) was applied to one urine sample. The a.a.s. results (in $mg\ l^{-1}$) were 2200 for K, 0.055 for Cu and 0.34 for Zn, with a 10—20% uncertainty, while the x.r.f. procedure yielded 2100 ± 200 for K, 0.04 ± 0.01 for Cu and 0.53 ± 0.06 for Zn as averages of five-fold measurements. A commercial lyophilized urine control specimen (Travenol) was analyzed by x.r.f. after dilution: the manufacturer lists concentrations of 0.044 mg Ni l^{-1}, 1.45 mg Zn l^{-1} and 0.18—0.22 mg Pb l^{-1}, and the x.r.f. results were 0.04 ± 0.01 mg Ni l^{-1}, 1.01 ± 0.12 mg Zn l^{-1} and 0.14 mg Pb l^{-1}. The somewhat low lead result is probably due to 30% volatility losses (see above). The discrepancies for zinc cannot be explained at present: but for K, Ni and Cu, the agreement is quite satisfactory.

The limits of detection of the proposed procedure, determined by blank effects and statistical background variations, are compared with normal elemental concentrations for urine in Table 4; selenium and arsenic are not listed, because of important volatilization uncertainties. In practice, spectral interferences will increase the detection limits, mainly for Ca, Rb and Pb, to some extent. Still, it is believed that the sensitivity of energy-dispersive x.r.f. is sufficient to determine some ten elements simultaneously in average urine residue ash. The average results obtained in this work fall within the published normal concentration ranges [25, 26].

TABLE 3

Influence of acid addition and elemental concentration on the recoveries from the evaporation residue after different treatments (Results are given in mg l^{-1} with the standard deviation for single measurements)

Element	Untreated urine (n = 8)	Diluted 5-fold urine[a] (n = 4)	Spiked urine[b] (n = 4)	Urine + 5% HNO_3 (n = 8)	Urine +5% HNO_3, 5-fold diluted[a] (n = 3)	Spiked urine[b] +5% HNO_3 (n = 4)
K	4200 ± 250	3900 ± 600	4100 ± 400	4050 ± 300	4300 ± 300	4500 ± 100
Ca	165 ± 15	130 ± 30	155 ± 25	120 ± 15	125 ± 5	145 ± 10
Fe	0.13 ± 0.07	0.14 ± 0.07	0.48 ± 0.03	0.14 ± 0.04	0.19 ± 0.10	0.52 ± 0.02
Ni	<0.02	<0.02	0.37 ± 0.08	<0.02	<0.02	0.38 ± 0.05
Cu	0.10 ± 0.01	0.15 ± 0.10	0.50 ± 0.06	0.08 ± 0.02	0.11 ± 0.01	0.58 ± 0.03
Zn	0.48 ± 0.06	0.43 ± 0.08	0.76 ± 0.08	0.44 ± 0.04	0.47 ± 0.09	0.98 ± 0.05
Se	<0.03[c]	<0.02	<0.02	0.03 ± 0.01[c]	<0.04	0.03 ± 0.01
Br	5.2 ± 0.1	4.1 ± 0.2	4.9 ± 0.3	0.35 ± 0.05	0.46 ± 0.16	0.77 ± 0.09
Rb	2.5 ± 0.1	2.3 ± 0.2	2.3 ± 0.2	2.4 ± 0.1	2.4 ± 0.3	2.4 ± 0.1
Sr	0.15 ± 0.01	0.14 ± 0.02	0.14 ± 0.01	0.15 ± 0.01	0.13 ± 0.01	0.15 ± 0.01
Pb	<0.06	<0.06	0.27 ± 0.04	<0.06	<0.06	0.32 ± 0.01

[a]Recalculated. [b]Spiked with 0.4 mg l^{-1} Fe, Ni, Cu, Zn, Pb. [c]To some of these samples 0.4 mg Se l^{-1} was added. The recoveries were 10% at most, for trimethylselenonium chloride and 30% for H_2SeO_3.

TABLE 4

The detection limits (in mg l^{-1}) of the proposed method and the normal elemental concentrations in urine

Element	Detection limit of the proposed x.r.f. procedure	Normal elemental concentration ranges according to		Average result of all measurements in this work[b]
		Cornelis et al. [25][a]	Iyengar et al. [26][a]	
Cl	6	3700—4800	2900—4300	3500
K	3	2300	1200—2000	2600
Ca	1	90—230	100—300	190
Fe	0.06	0.06—0.17	0.09—0.80	0.15
Ni	0.02	0.01	0.002—0.62	0.04
Cu	0.01	0.003—0.09	0.007—0.22	0.05
Zn	0.02	0.09—0.35	0.03—0.83	0.67
Br	0.01	2—5.3	2.5—4.7	3.4
Rb	0.01	0.7—1.6	0.7—1.6	1.7
Sr	0.01	0.10—0.24	0.07—0.26	0.19
Pb	0.06	0.02—0.12	0.007—0.08	<0.06

[a]The original values were given in amounts per day. These have been recalculated to mg l^{-1} assuming a 1.5-l excretion per day. [b]These values are the average of some 70 experiments on 6 urine samples, all taken from the same individual. Hence these values are not necessarily representative of average human urine.

Conclusion

The proposed procedure makes it possible to determine about ten elements in normal urine in a labour-saving and cost-efficient way. In cases of poisoning or pathological conditions, additional elements might show up. The method could therefore be attractive for clinical screening and diagnostic work. X-ray fluorescence is not commonly available as an analytical technique in clinical laboratories, however, although it is widely used in most industries. Accordingly, the proposed method might most easily find applications in the field of industrial hygiene.

One of us (H. R.) acknowledges financial support from the Belgian Ministry of Health via a research project on selenium impact in the environment. H. Claessens (Provinciaal Instituut voor Hygiëne, Antwerp) carried out the a.a.s. measurements.

REFERENCES

1 N. A. Schroeder and A. P. Nason, Clin. Chem., 17 (1971) 461.
2 H. J. M. Bowen, Trace Elements in Biochemistry, Academic Press, New York, 1966, p. 98.
3 L. S. Maynard and S. Fink, J. Clin. Invest., 35 (1956) 831.
4 G. C. Cotsias, Physiol. Rev., 38 (1953) 503.
5 R. I. Henkin, B. M. Pattern and D. A. Bronzert, Arch. Neurol., 32 (1975) 745.
6 J. B. Freeman, L. D. Stegink, P. D. Meyer, L. L. Fry and K. Den Besten, J. Surg. Res., 18 (1975) 463.
7 E. J. Underwood, Trace Elements in Human and Animal Nutrition, 3rd edn., Academic Press, New York, 1971.
8 W. Mertz and W. E. Cometzer, Newer Trace Elements in Nutrition, M. Dekker, New York, 1971.
9 L. H. Klevay, J. Clin. Chem., 28 (1974) 764.
10 K. Beyerman, Anal. Chim. Acta, 45 (1969) 51.
11 R. A. Long, Am. Ind. Hyg. Assoc. J., 33 (1972) 343.
12 J. C. Mathies, Appl. Spectra, 28 (1974) 165.
13 H. L. Boiteau, S. Gelot and M. Robin, Ann. Biol. Clin., 29 (1971) 163.
14 J. T. Purdham, O. P. Strausz and K. I. Strauss, Anal. Chem., 47 (1975) 2030.
15 M. Agarwal, R. B. Bennet, I. G. Stump and J. M. D'Auria, Anal. Chem., 47 (1975) 924.
16 H. Kingston and P. A. Pella, Anal. Chem., 53 (1981) 223.
17 K. K. Nielson and D. R. Kalkwarf, in P. A. Russell and A. E. Hutchins (Eds.), X-ray Techniques in Environmental and Occupational Health Analysis, Vol. XX, Ann Arbor, MI, 1975, p. 31.
18 P. Van Espen, H. Nullens and F. Adams, Nucl. Instrum. Methods, 142 (1977) 243.
19 P. Van Espen, H. Nullens and F. Adams, Nucl. Instrum. Methods, 145 (1977) 579.
20 P. Van Espen and F. Adams, Anal. Chem., 48 (1976) 1823.
21 P. M. Van Dyck and R. E. Van Grieken, Anal. Chem., 52 (1980) 1859.
22 R. Van Grieken, R. Van de Velde and H. Robberecht., Anal. Chim. Acta, 111 (1980) 137.
23 J. A. Smits and R. E. Van Grieken, Anal. Chem., 52 (1980) 1479.
24 J. Smits and R. Van Grieken, Int. J. Environ. Anal. Chem., 9 (1981) 62.
25 R. Cornelis, A. Speecke and J. Hoste, Anal. Chim. Acta, 78 (1975) 367.
26 G. V. Iyengar, W. E. Kollmer and H. J. M. Bowen, The Elemental Composition of Human Tissues and Body Fluids, Verlag Chemie, Weinheim, 1978, p. 127.

Analytica Chimica Acta, 130 (1981) 177—182
Elsevier Scientific Publishing Company, Amsterdam — Printed in The Netherlands

ZUR FLÜSSIG—FLÜSSIG-EXTRAKTION VON GALLIUM MIT ZWEIZÄHNIGEN CHELATBILDNERN

E. UHLEMANN* und W. MICKLER

Pädagogische Hochschule "Karl Liebknecht", DDR-1500 Potsdam (D.D.R.)

C. FISCHER

Akademie der Wissenschaften der DDR, Zentralinstitut für Festkörperphysik und Werkstofforschung, DDR-8027 Dresden (D.D.R.)

(Eingegangen den 12. März 1981)

SUMMARY

(Liquid—liquid extraction of gallium with bidentate ligands)

The extraction of gallium with bidentate ligands such as β-diketones, 4-benzoylpyrazol-5-ones, N-benzoylhydroxylamines and 8-quinolinols, as well as some analogous thio derivatives in the pH region 1—12 in the presence of tartrate is reported. Extractions were monitored radiometrically. Equilibration times and pH of half-extraction are used to characterize the extractants. For the extraction of gallium from highly alkaline solutions, only 7-alkyl-8-quinolinols are suitable.

ZUSAMMENFASSUNG

Auf radiometrischem Wege wurde die Extraktion von Gallium mit zweizähnigen Chelatbildnern aus den Gruppen der β-Diketone, 4-Benzoylpyrazol-5-one, N-Benzoylhydroxylamine und Chinolin-8-ol sowie entsprechender. Thioderivate im pH-Bereich 1—12 bei Gegenwart von Tartrat untersucht. Die Charakterisierung der Extraktionsmittel erfolgte nach der Geschwindigkeit der Gleichgewichtseinstellung und den pH-Werten der Halb-Extraktion. Für die Galliumextraktion aus hochalkalischen Lösungen erwiesen sich lediglich 7-Alkylchinolin-8-ol als geeignet.

Über die Möglichkeiten zur Extraktion von Gallium aus alkalischer Lösung liegen bisher nur wenige Informationen vor [1, 2], meist tritt im alkalischen Bereich ein rapider Abfall der Extraktionsausbeute ein. Extraktionsmittel, die die Extraktion auch aus stark alkalischer Lösung gestatten, sind aber für die Gewinnung von Gallium aus Laugen des Bayer-Prozesses von großer Bedeutung. Es wurde daher eine Reihe zweizähniger Chelatbildner über den gesamten pH-Bereich und in stark alkalischer Lösung für ihre Eignung zur Galliumextraktion überprüft. Nach Angaben aus der Literatur bieten sich dafür vor allem β-Diketone [3—6], N-Benzoylhydroxylamine [3—5, 7—9], Chinolin-8-ol [3—5, 10—12] und alkylierte Brenzcatechine [1] an. Auch Acylpyrazolone erwiesen sich für die Galliumextraktion geeignet [13]. Aus

diesen Gruppen wurden die folgenden Substanzen untersucht: Dibenzoylmethan, Thiodibenzoylmethan [14], *p*-Heptylbenzoyltrifluoraceton, 1-Phenyl-3-methyl-4-benzoylpyrazol-5-on [15], 1-Phenyl-3-methyl-4-thiobenzoylpyrazol-5-on [16], 1-Phenyl-3-methyl-4-benzoylpyrazol-5-thion [17], N-Benzoyl-N-phenylhydroxylamin, N-Thiobenzoyl-N-phenylhydroxylamin [18], Chinolin-8-ol, 2-Methylchinolin-8-ol, 5-Nonanoylchinolin-8-ol [19], 7-Nonanoylchinolin-8-ol [19], 5-Nonylchinolin-8-ol, 7-Nonylchinolin-8-ol, 7-[α-(*o*-Carbomethoxyanilino)benzyl] chinolin-8-ol (CMAB—Oxin) [20].

EXPERIMENTELLES

Extraktionsmittel und Meßlösungen

Die verwendeten Extraktionsmittel wurden nach Literaturangaben synthetisiert oder stellten Handelsprodukte dar. 5- und 7-Nonylchinolin-8-ol sind durch Kishner-Wolff-Reduktion der entsprechenden Nonanoylchinolin-8-ol zugänglich. 5-Nonylchinolin-8-ol: Fp. 59—60°C (Hexan); Hydrochlorid Fp. 175—80°C; Analyse ber. (gef.) 70,2 (69,5) % C; 8,5 (8,2) % H; 4,55 (4,5) % N; 11,5 (11,6) % Cl. 7-Nonylchinolin-8-ol: Hydrochlorid Fp. 130—145°C; Analyse ber. (gef.) 70,2 (70,1) % C; 8,5 (8,3) % H; 4,55 (4,7) % N; 11,5 (11,4) % Cl.

Als Gallium-Standardlösung diente eine 10^{-4} M $Ga(NO_3)_3$-Lösung in 0,1 M $NaClO_4$, die zur Unterdrückung von Hydrolyseeffekten 5×10^{-4} M an Kaliumtartrat war. Die Einstellung der pH-Werte erfolgte durch Zusatz von 1 M $HClO_4$, 0,1 M $HClO_4$, bzw. 0,1 M NaOH sowie 0,01 M NaOH.

Die Extraktionsmittelkonzentration betrug 10^{-2} M, als Verdünnungsmittel wurde Chloroform eingesetzt.

Zur Untersuchung der Galliumextraktion bei dem Bayer-Prozeß angenäherten Bedingungen diente eine Lösung von 122 g $Al(OH)_3$ und 0,570 g Ga_2O_3 in 1 l 5 M NaOH. Die organische Phase war 0,1 bis 0,4 M an Extraktionsmittel, gelöst in Benzen/Decanol (Volumenverhältnis 90:10) bzw. Benzen/Hexanol (Volumenverhältnis 50:50).

Durchführung der Verteilungsmessungen

Die Bestimmung der Verteilungskoeffizienten wurde auf radiometrischem Wege vorgenommen. Es kam das Radionuklid ^{72}Ga mit der Halbwertszeit t = 14,1 h zum Einsatz. Die spezifische Aktivität betrug 25 Ci g^{-1}. Als Strahlungsdetektor diente ein NaJ (Tl)-Bohrlochszintillator, als Strahlungsmeßgerät ein Einkanalzählmeßgerät 220-24 (VEB RFT Meßelektronik Dresden, DDR) mit automatischer Nulleffektskorrektur. Gearbeitet wurde nach der Methode der Indikatoranalyse. Die Impulszahl der Ausgangslösung war bei allen Untersuchungen auf etwa 200 000 pro min und ml eingestellt. Zur Dosierung diente der Multi-Dosimat E415 (Metrom Herisau, Schweiz) mit zugehörigen Wechseleinheiten. Die Phasenmischung erfolgte in einer Überkopfschüttelmaschine in Schütteltrichtern.

Zur pH-Messung wurde der pH-Meßverstärker MV87 (VEB Präcitronik

Dresden, DDR) mit dem Elektrodensystem aus Glaselektrode GA50N und Ag/AgCl-Elektrode SE20 (Forschungsinstitut Meinsberg, Dresden, DDR) benutzt.

Berechnung der Verteilungskonstanten

Zur Charakterisierung der untersuchten Extraktionsmittel diente der pH-Wert der Halbextraktion, $pH_{1/2}$. Man erhält ihn aus der Funktion $\log D = f(pH)$. Wegen der durch Tartratzusatz vorgenommenen Maskierung des Galliums wurde der experimentell ermittelte Verteilungskoeffizient nach

$$D = D_{exp.}\,(1 + \beta_1\, C_{Tart^{2-}} + \beta_2\, C^2_{Tart^{2-}})$$

$$C_{H_2Tart} = C_{Tart^{2-}}\,[1 + (C_{H^+}/K_{s_2}) + (C^2_{H^+}/K_{s_1}\,K_{s_2})]$$

korrigiert. Die Werte für β_2 [5] und $K_{s_{1,2}}$ [21] sind aus der angegebenen Literatur zugänglich, β_1 wurde abgeschätzt. Merklichen Einfluß gewinnen die Korrekturglieder auf die $pH_{1/2}$-Werte nur bei Extraktionsmitteln, die Gallium erst oberhalb pH 2,5 zu extrahieren beginnen.

ERGEBNISSE UND DISKUSSION

Für die ausgewählten Extraktionsmittel wurde zunächst die Zeitabhängigkeit der Gleichgewichtseinstellung des Extraktionsvorganges bestimmt. Dabei ergaben sich bemerkenswerte Unterschiede, die aber keine Beziehung zur Art des Extraktionsmittels erkennen lassen. Eine günstige Extraktionskinetik besitzen N-Benzoyl-N-phenylhydroxylamin, 1-Phenyl-3-methyl-4-benzoylpyrazol-5-on und -5-thion, Chinolin-8-ol, 2-Methylchinolin-8-ol und 5-Nonanoylchinolin-8-ol, während bei *p*-Heptylbenzoyltrifluoraceton, 1-Phenyl-3-methyl-4-thiobenzoylpyrazol-5-on, N-Thiobenzoyl-N-phenylhydroxylamin, 5- und 7-Nonylchinolin-8-ol und Kelex 100 bis zu 2 h zur Gleichgewichtseinstellung benötigt werden. Bei Dibenzoylmethan, Thiodibenzoylmethan und CMAB—Oxin dauert die Extraktion sogar länger als 2 h. Für ausgewählte Extraktionsmittel ist die Zeitabhängigkeit der Extraktion in Abb. 1 dargestellt. Zur Untersuchung der Extraktionsgeschwindigkeit wurde in jedem Fall ein pH-Gebiet mittlerer Extraktionsausbeute ausgewählt.

Die gewonnenen kinetischen Erkenntnisse stellen die Grundlage für die Ermittlung der Extraktionskurven dar. Einige Beispiele sind in den Abb. 2 und 3 dargestellt, und Tab. 1 gibt einen Überblick der daraus bestimmten $pH_{1/2}$-Werte. Von den untersuchten strukturanalogen Verbindungen erweisen sich solche mit Sauerstoffligatoren für die Galliumextraktion günstiger als analoge Thioverbindungen (vgl. Abb. 2). Dies entspricht den Eigenschaften des Galliumions nach dem Pearsonschen HSAB-Konzept. Mit Monothiodibenzoylmethan wird Gallium unter den gewählten Bedingungen überhaupt nicht extrahiert, weil ein Austausch mit dem Tartratkomplex nicht stattfindet. Bei Abwesenheit von Maskierungsmitteln verläuft die Extraktion auch in diesem Fall erfolgreich [6]. Ebenso ist unter den gewählten Bedingungen

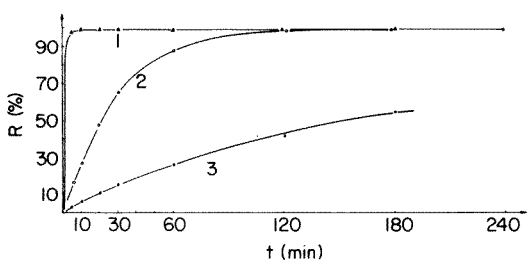

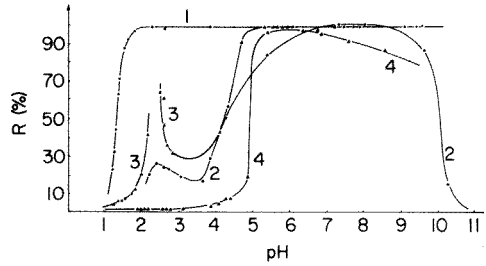

Abb. 1. Zeitabhängigkeit der Galliumextraktion mit (1) N-Benzoyl-N-phenylhydroxylamin (pH 4,05); (2) 5-Nonylchinolin-8-ol (pH 2,12); (3) CMAB-Oxin (pH 6,95). $C_{Ga^{3+}} = 10^{-4}$ mol l^{-1} in 0,1 M $NaClO_4$ + 5 × 10^{-4} M Kaliumtartrat, Extraktionsmittelkonzentration = 10^{-2} mol l^{-1}.

Abb. 2. Extraktion von Gallium mit (1) N-Benzoyl-N-phenylhydroxylamin; (2) N-Thiobenzoyl-N-phenylhydroxylamin; (3) 1-Phenyl-3-methyl-4-benzoylpyrazol-5-on; (4) 1-Phenyl-3-methyl-4-benzoylpyrazol-5-thion. $C_{Ga^{3+}} = 10^{-4}$ mol l^{-1} in 0,1 M $NaClO_4$ + 5 × 10^{-4} M Kaliumtartrat, Extraktionsmittelkonzentration = 10^{-2} mol l^{-1}.

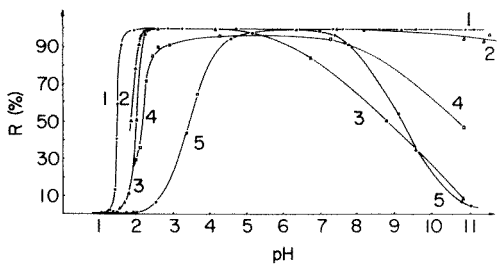

Abb. 3. Extraktion von Gallium mit (1) Chinolin-8-ol; (2) 5-Nonylchinolin-8-ol; (3) Kelex 100; (4) 5-Nonanoylchinolin-8-ol; (5) 2-Methylchinolin-8-ol.

TABELLE 1

$pH_{1/2}$-Werte für die Extraktion von Gallium bei Anwesenheit von Tartrat

Extraktionsmittel	$pH_{1/2}$
N-Benzoyl-N-phenylhydroxylamin	1,30
Chinolin-8-ol	1,50
5-Nonylchinolin-8-ol	1,80
Kelex 100	2,00
5-Nonanoylchinolin-8-ol	2,20
1-Phenyl-3-methyl-4-benzoylpyrazol-5-on	2,35 bzw. 5,00
2-Methylchinolin-8-ol	2,90
N-Thiobenzoyl-N-phenylhydroxylamin	3,40
1-Phenyl-3-methyl-4-benzoylpyrazol-5-thion	3,55
p-Heptylbenzoyltrifluoraceton	3,70

auch Dibenzoylmethan nicht für die Galliumextraktion geeignet. Nahezu quantitativ wird Gallium durch *p*-Heptylbenzoyltrifluoraceton bei pH 5,5—7 extrahiert. Oberhalb pH 10 sinkt auch hier die Extraktionsausbeute auf 0 ab.

Bemerkenswert ist das Auftreten eines kleinen Maximums bei pH 2,5 in den Extraktionskurven von 1-Phenyl-3-methyl-4-benzoylpyrazol-5-on und N-Thiobenzoyl-N-phenylhydroxylamin (Abb. 2).

Einen Überblick über den Verlauf der Galliumextraktion mit Chinolin-8-ol und einigen seiner Derivate gibt Abb. 3. Bemerkenswert ist hierbei, daß die Extraktion mit 2-Methylchinolin-8-ol erst bei deutlich höherem pH einsetzt als mit den anderen Verbindungen. Beim Chinolin-8-ol erfolgt die Extraktion unter Bedingungen, wo der Ligand größtenteils in protonierter Form vorliegt. Im Einklang damit ergibt sich aus den log D/pH-Darstellungen die Zahl der bei der Extraktion bzw. Komplexbildung freigesetzten Protonen für Chinolin-8-ol zu 5,78; im Erwartungsbereich liegende Werte wurden für 5-Nonyl-8-chinolinol (3,61), Kelex 100 (3,53), N-Benzoyl-N-phenyl-hydroxylamin (3,54), N-Thiobenzoyl-N-phenylhydroxylamin (2,72) und 5-Nonanoylchinolin-8-ol (2,48) gefunden. In anderen Fällen wird der erwartete Wert von 3 deutlich unterschritten, so daß bei der Extraktion mit Spezies zu rechnen ist, wie sie auch bei der Extraktion von Eisen(III)-chelaten nachgewiesen wurden [16, 18, 22].

Ausgehend von den Ergebnissen der Extraktionsuntersuchungen im pH-Bereich 1—12 wurden die verwendeten Extraktionsmittel auch für die Galliumextraktion aus stark alkalischen Lösungen, wie sie im Bauxitaufschluß des Bayer-Verfahrens anfallen, untersucht. Für diese Anwendung wird vorausgesetzt, daß trotz hoher Hydroxidionenkonzentration Verteilungskoeffizienten und Extraktionsgeschwindigkeit im günstigen Bereich bleiben. Auch muß das Extraktionsmittel eine ausreichende Alkalibeständigkeit aufweisen und darf keine schwerlöslichen Alkalisalze bilden. Durch diese Faktoren wird der Kreis möglicher Extraktionsmittel stark eingeengt. Zur Extraktion des Galliums aus der vorliegenden Aluminat-Matrix ist schließlich eine hohe Selektivität des Extraktionsmittels erforderlich.

Einen Überblick über die experimentell ermittelten Verteilungskoeffizienten gibt Tab. 2. Von den angeführten Extraktionsmitteln sind für die Extraktion von Gallium aus Bayer-Laugen ausschließlich 7-Alkyl- bzw. 7-Alkenylchinolin-8-ole geeignet. Zwischen den untersuchten 5- und 7-Nonylchinolin-8-olen besteht ein frappierender Unterschied, so daß Aussagen [2] über die Eignung aller möglichen Alkylderivate des Chinolin-8-ols nicht aufrecht zu halten sind. Obwohl 5-Nonylchinolin-8-ol für die Galliumextraktion bei hohen pH-Werten gut geeignet ist (Abb. 3), scheidet es für die Anwendung im Falle der Bayer-Laugen aus. CMAB-Oxin extrahiert Gallium in gewissem Umfang, die Rückextraktion ist jedoch kinetisch gehemmt. Im Gegensatz dazu erfolgt die Rückextraktion bei Kelex 100 und 7-Nonylchinolin-8-ol mit 1,5 M Schwefelsäure ohne Schwierigkeiten.

TABELLE 2

Verteilungskoeffizienten D_{Ga} für die Extraktion aus simulierter Bayer-Lauge (Konzentration des Extraktionsmittels 0,1 bis 0,4 M, gelöst in Benzen/Decanol)

Extraktionsmittel	D_{Ga}	
	10 min	120 min
Thiodibenzoylmethan	0,0004	0,013
p-Heptylbenzoyltrifluoraceton	0,0017	0,0013
1-Phenyl-3-methyl-4-thiobenzoyl-pyrazol-5-on	0,002	0,002
N-Benzoyl-N-phenylhydroxylamin	0,006	0,006
CMAB-Oxin	0,11	0,40
5-Nonylchinolin-8-ol	0,04	0,05
7-Nonylchinolin-8-ol	0,13	1,03
Kelex 100	0,15	1,05
	0,17 [2]	2,37 [2]

LITERATUR

1 Yu. I. Tarnopolski, V. S. Kuznezova und V. F. Borbat, Izv. Vyssh. Uchebn. Zaved. Khim. Khim. Tekhnol., 17 (1974) 754.
2 J. Helgorsky und A. Leveque, Franz. Pat. 7 424 263 (1976); BRD-Pat. 27 43475 (1978).
3 J. Stary, The Solvent Extraction of Metal Chelates, Pergamon, Oxford, 1964.
4 A. K. De, S. M. Khopkar und R. A. Chalmers, Solvent Extraction of Metals, Van Nostrand Reinhold, London, 1970.
5 J. Stary und E. Hladky, Anal. Chim. Acta, 28 (1963) 227.
6 B. N. Prabhu und S. M. Khopkar, Talanta, 25 (1978) 109.
7 F. Umland, Theorie und praktische Anwendung von Komplexbildnern, Akademische Verlagsgesellschaft, Frankfurt/M, 1971.
8 H. R. Das und S. C. Shome, Anal. Chim. Acta, 27 (1962) 545.
9 E. H. Spak und W. A. Sazjuk, Zh. Anal. Khim., 34 (1979) 350.
10 M. R. Gupta, H. R. Das und S. C. Shome, J. Inorg. Nucl. Chem., 34 (1972) 350.
11 F. Umland, Fresenius Z. Anal. Chem., 190 (1962) 186.
12 S. Lacroix, Fresenius Z. Anal. Chem., 130 (1949) 354.
13 M. Y. Mirza, Talanta, 25 (1978) 685.
14 E. Uhlemann und H. Müller, Angew. Chem., 77 (1965) 172.
15 B. S. Jensen, Acta Chem. Scand., 13 (1959) 1890.
16 E. Uhlemann, B. Maack und M. Raab, Anal. Chim. Acta, 116 (1980) 153.
17 G. Wilke, W. Bechmann und E. Uhlemann, Z. Anorg. Allg. Chem., 428 (1977) 277.
18 E. Uhlemann, B. Maack und M. Raab, Anal. Chim. Acta, 116 (1980) 403.
19 E. Uhlemann, W. Mickler, E. Ludwig und G. Klose, J. Prakt. Chem., im Druck.
20 F. Umland und K.-U. Meckenstock, Fresenius Z. Anal. Chem., 177 (1960) 244.
21 K. Rauscher, J. Voigt, I. Wilke und K.-Th. Wilke, Chemische Tabellen und Rechentafeln für die analytische Praxis, VEB Deutscher Verlag für Grundstoffindustrie, Leipzig, 1972.
22 D. S. Narajan, E. K. Ivanova und V. K. Peshkova, Vestn. Mosk. Univ. Khim., 1972, 707.

Analytica Chimica Acta, 130 (1981) 183—192
Elsevier Scientific Publishing Company, Amsterdam — Printed in The Netherlands

NEW SPECTROPHOTOMETRIC METHOD FOR DETERMINING THE STOICHIOMETRY AND EQUILIBRIUM CONSTANTS OF SOME REDOX REACTIONS

M. ROMÁN CEBA, J. A. MUÑOZ LEYVA[a] and J. J. BERZAS NEVADO*

Department of Analytical Chemistry, Faculty of Sciences, University of Extremadura, Badajoz (Spain)

(Received 2nd February 1981)

SUMMARY

A new spectrophotometric method is proposed for determining the stoichiometries of redox reactions; it can be used in many cases for determining the equilibrium constant of the reaction. The method is based on that of Holme and Langmyhr. Good results were obtained for several redox reactions involving iodate, bromate or periodate, and manganese(II) or some cyclohexanedione bisthiosemicarbazones.

Holme and Langmyhr [1] proposed a method for determining the stoichiometry of weak complexes of the type A_mB_n. A modification of this method permits the indices m and n to be calculated [2]. The present work describes the application of this method for calculating the stoichiometries of redox reactions. The method has been applied to the analytically useful redox reactions between 1,3-cyclohexanedione bisthiosemicarbazone monohydrochloride (CHDT · HCl) and iodate and bromate ions, between 5,5-dimethyl-1,3-cyclohexanedione bisthiosemicarbazone monohydrochloride (DyDT) and periodate, and between periodate and manganese(II).

THEORY

For a redox reaction $mA + nB \rightleftharpoons (m/x)A'_x + (n/y)B'_y$, in which the effect of the reaction medium is omitted for simplicity, the law of mass action gives

$$1/K = [A]^m [B]^n / [A'_x]^{m/x} [B'_y]^{n/y} \quad (1)$$

where K is the apparent equilibrium constant. If compounds A'_x and B'_y absorb radiation and Beer's law is obeyed then the absorbance E is given by

$$E = l\epsilon_1 [A'_x] + l\epsilon_2 [B'_y] \quad (2)$$

---

[a]Present address: Department of Analytical Chemistry, Faculty of Chemistry, University of Sevilla, Sevilla, Spain.

where ϵ_1 and ϵ_2 are the molar absorptivities of A'_x and B'_y, respectively, and l is the path length.

According to the specified redox reaction, $[A'_x]n/y = [B'_y]m/x$. Thus, eqn. (2) can be written as $E = l[A'_x](\epsilon_1 + \epsilon_2 nx/my)$. Therefore

$$[A'_x] = E/l(\epsilon_1 + \epsilon_2 nx/my) \tag{3}$$

At equilibrium, the concentrations of the reagents are

$$[A] = a - x[A'_x] \text{ and } [B] = b - y[B'_y] \tag{4}$$

where a and b are the initial concentrations of A and B. If the same value of a is maintained and b is increased, then the concentrations of A'_x and B'_y become $\lim_{b\to\infty}[A'_x] = a/x$ and $\lim_{b\to\infty}[B'_y] = na/my$; i.e., the greatest absorbance, E_o, that can be obtained will be $E_o = l\epsilon_1 a/x + l\epsilon_2 na/my$. By combining this expression and eqn. (3)

$$[A'_x] = aE/E_o x \tag{5}$$

This equation combined with eqns. (1), (2) and (4), gives

$$1/K = (a - aE/E_o)^m [B]^n/(aE/xE_o)^{m/x}(naE/myE_o)^{n/y}$$

which can also be written as follows

$$1/[B]^n = Ka^m(x/a)^{m/x}(m/n)^{n/y}(y/a)^{n/y}(1 - E/E_o)^m(E_o/E)^{m/x+n/y}$$

If $E_o/E = \alpha$, then by taking the mth root and rearranging

$$1/[B]^{n/m} = K^{1/m} a(x/a)^{1/x}(ym/an)^{n/my}\{\alpha^{(nx+my)/mxy} - \alpha^{[(nx+my)/mxy]-1}\}$$

By taking logarithms and multiplying by m/n

$$-\log [B] = \log [K^{1/n} a^{(mxy-my-nx)/nxy} x^{m/nx}(my/n)^{1/y}]$$
$$+ (m/n) \log \{\alpha^{(nx+my)/mxy} - \alpha^{[(nx+my)/mxy]-1}\} \tag{6}$$

where $[B] = b - na/m\alpha$.

This result is also obtained if only one of the compounds formed absorbs radiation. So, if A'_x is the only absorbing compound, $E = l\epsilon_1[A'_x]$. However, $E_o = l\epsilon_1 a/x$, which, combined with the previous expression, gives $[A'_x] = aE/E_o x$; this is the same as eqn. (5), and allows eqn. (6) to be obtained.

In order to analyse eqn. (6), several cases can be examined. When $x = y = 1$, then eqn. (6) becomes

$$-\log [B] = \log (K^{1/n} m/na) + (m/n) \log [\alpha^{(n/m)+1} - \alpha^{n/m}]$$

This is a linear equation whose independent variable is different for every value of n/m. Therefore, for $n/m = 1$, the variable must be $\log(\alpha^2 - \alpha)$ and the straight line has a slope $m/n = 1$. For $x \neq 1$ and $y \neq 1$, the intercepts on the ordinate and the variables differ from those for $x = y = 1$ but the slope is always the same. For any value of x and y, considering a given stoichiometry (i.e., n/m), eqn. (6) describes a group of parallel lines whose slope is m/n. This can be seen in Fig. 1, where several straight lines are plotted for different

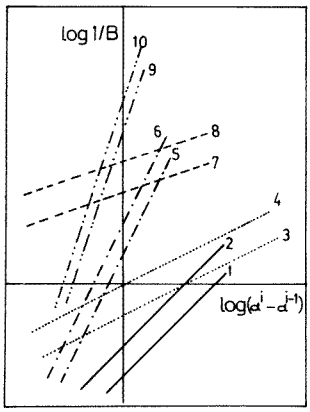

Fig. 1. Straight lines obtained by application of eqn. (6) for different values of n/m, x and y (for details see Table 1).

values for n/m, x and y. In order to make their plotting easier, the values u_1, u_2, u_3, etc. have been given for their intercepts at the ordinate. The correct values of these ordinate intercepts can be deduced from eqn. (6); they are given in Table 1.

In contrast, plotting the ordinate intercepts, u_i, against log a enables the values of x and y to be determined for each group of parallel lines with a given n/m value. In order to do this, the intercepts must be calculated for various values of a (without changing b) for the same ratio n/m. The straight line obtained by plotting u_i vs. log a has a different slope, depending on the values of x and y. If $n/m = 2$, then $u_i = \log [K^{1/2}a^{1/2-1/x-1/2y}x^{1/2x}(y/2)^{1/y}]$, i.e., $u_i = C + (1/2 - 1/x - 1/2y) \log a$. For given values of x and y, the slopes of these straight lines are listed in Table 2. For other values of n/m, similar results were obtained.

The results obtained by using incorrect values for n/m, x and y should also

TABLE 1

Intercepts and slopes for some solutions of eqn. (6) plotted in Fig. 1

Line	n/m	x	y	Intercept	Slope
1	1	1	1	$u_1 = \log (K_1/a)$	1
2	1	1	2	$u_2 = \log K_2(2/a)^{1/2}$	1
3	2	1	2	$u_3 = \log K_3^{1/2} a^{3/4}$	0.5
4	2	2	1	$u_4 = \log 0.59 (K_4/a)^{1/2}$	0.5
5	0.5	1	1	$u_5 = \log 2K_5/a$	2
6	0.5	2	2	$u_6 = \log 4K_6 a^{1/2}$	2
7	3	1	2	$u_7 = \log 0.58 K_7^{1/3} a^{-5/6}$	0.33
8	3	2	2	$u_8 = \log 0.92 (K_8/a)^{1/3}$	0.33
9	0.33	2	1	$u_9 = \log 8.48 K_9 a^{-1/2}$	3
10	0.33	2	2	$u_{10} = \log 6.93 aK_{10}$	3

TABLE 2

Slopes obtained by plotting log a against u_i in order to calculate x and y for $n/m = 1$ and $n/m = 2$

x	y	Slopes		x	y	Slopes	
		$n/m = 1$	$n/m = 2$			$n/m = 1$	$n/m = 2$
1	1	−1	−1/2	2	3	−1/6	1/12
1	2	−3/4	−1/4	3	1	−1/3	−1/6
1	3	−2/3	−1/6	3	2	−1/12	1/12
2	1	−1/2	−1/4	3	3	0	1/6
2	2	−1/4	0				

be considered. If $x = y = 1$, and the correct value of n/m is 1, but the incorrect values 0.33, 0.5, 2 and 3 are tested, then the lines plotted in Fig. 2 are obtained. The lines are nearly straight but the slopes do not coincide with the inverse of the stoichiometry tested, although in all cases they are close to the inverse of the correct stoichiometry. Similar results were obtained for other incorrect values of n/m, x and y; in all cases the lines were curved and the slopes were not the inverse of the stoichiometry tested, but were close to the inverse of the correct stoichiometry.

This shows that eqn. (6) can be used to establish the stoichiometries of redox reactions. Therefore when the correct values for n/m are used, irrespective of the values of x and y, straight lines of slopes n/m, i.e., the inverse of the tested stoichiometry, are obtained. If, however, the ratio n/m tested is incorrect, again irrespective of the values for x and y, the lines obtained are not straight and the slopes do not coincide with the inverse of the tested stoichiometry. Once the correct ratio n/m is known, it is possible to calculate x and y by plotting the value found for the intercept (for different values of the initial concentration of A, the same values of b and for the calculated ratio n/m) vs. log a. Straight lines of different slopes are obtained for each pair of values of x and y.

All these conclusions are applicable to redox reactions with small values of

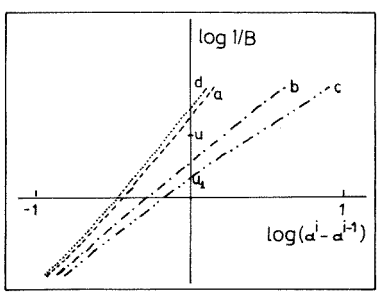

Fig. 2. Lines obtained by application of eqn. (6) for correct values of x and y and incorrect values for n/m: $x = y = 1$; n/m = (a) 0.33; (b) 0.5; (c) 2; (d) 3.

K, because the experiments can be done by fixing the concentration of A and changing the concentration of B, which is always bigger than that of A.

The method can also be applied to redox reactions with large values of K if the reaction is slow. If the reaction considered initially is slow, $K^* = [A'_x]^{m/x}[B'_y]^{n/y}/[A]^m[B]^n$ is not constant because the concentrations change with time, but at a given time some concentrations of A, B, A'_x and B'_y exist so that, independently of how they change during the reaction, they are always in the relation indicated by the stoichiometry; thus for given time, temperature and initial concentrations, the relation $[A'_x]^{m/x}[B'_y]^{n/y}/[A]^m[B]^n$ is constant. Therefore many of the arguments given above can be applied to slow redox reactions with large values of K, because there will be a certain time after the beginning of the reaction when K^* is small. In fact, in these cases only, it will be possible to establish n/m but not x and y; if the values of x and y are required, the concentrations must be changed and equilibrium must be reached.

EXPERIMENTAL AND RESULTS

In order to apply this method it is necessary to plot log (1/[B]) vs. log $(\alpha^i - \alpha^{i-1})$ where the value for i depends on the values given to n/m, x and y. If the value of log (1/[B]) is required, the values of b (which is the initial concentration of the reagent B, different for each sample) and the value of a (fixed initial concentration for the reagent A) are known. The ratio n/m is any value that is to be tested and α (i.e., E_o/E) is deduced from the experimental values of the absorbances, taking as E_o the value of the absorbance of the sample prepared with a large excess of B. The independent variable log $(\alpha^i - \alpha^{i-1})$ can be calculated from the values of E_o/E, by giving to the ratio n/m the value to be tested and putting $x = 1$ and $y = 1$ (which are the easiest to test and do not affect the calculation of the correct ratio n/m). A plot of log (1/[B]) vs. the suitable variable gives a straight line whose slope must be m/n. If the plot is not linear, the ratio n/m tested is incorrect and it is necessary to test another one. This does not mean that it is necessary to test as many ratios as possible, because the slope obtained is almost the inverse of the correct n/m ratio.

The method was applied to the calculation of n/m for the redox reactions between CHDT · HCl and iodate [3] and bromate [4], between DyDT and periodate [5] and between periodate and manganese(II) [6].

CHDT · HCl—iodate system

In this reaction, when an excess of CHDT · HCl is used, a yellow colour appears with an absorption maximum at 415 nm. If the concentrations are close to equimolar, the dark colour of iodine appears. Therefore, it was necessary to know the stoichiometry, employing CHDT · HCl in excess, particularly because these are the recommended conditions for the spectrophotometric determination of iodate.

In order to calculate the ratio n/m, several samples were prepared containing 2.28×10^{-5} M iodate, various concentrations of CHDT · HCl, 10 ml of anhydrous acetic acid and water to give 25 ml. After the samples had been heated for 10 min at 70°C and cooled, the absorbances were measured at 415 nm against demineralised water. Under the same conditions, a sample was prepared with a large excess of CHDT · HCl; the absorbance of this sample was taken to be E_o. For each CHDT · HCl concentration, three samples were prepared and the mean value of the absorbances taken. The results obtained are given in Table 3. Table 4 gives the abscissa and ordinate values for a number of ratios of n/m, which are plotted in Fig. 3. From these plots the values of the slopes were deduced; the results are shown in Table 5. Therefore the correct n/m ratio is 2, i.e., 1 mol of iodate reacts with 2 mol of CHDT · HCl.

TABLE 3

Experimental results used to calculate the stoichiometry of the iodate—CHDT · HCl reaction ($a = [IO_3^-] = 2.28 \times 10^{-5}$ M)

b = [CHDT · HCl] ($\times 10^{-4}$ M)	E	α	b = [CHDT · HCl] ($\times 10^{-4}$ M)	E	α
4.56	0.373	1.102	7.98	0.396	1.038
5.70	0.385	1.067	9.12	0.398	1.033
6.84	0.391	1.051	54.3	0.411[a]	—

[a]Taken as E_o.

TABLE 4

Abscissa and ordinate values used to calculate the stoichiometry of the iodate—CHDT · HCl reaction

n/m	1.5	2.0	2.5	3.0
$\log (b - na/m\alpha)^{-1}$	3.37	3.38	3.39	3.40
	3.27	3.28	3.29	3.30
	3.19	3.19	3.20	3.21
	3.12	3.12	3.13	3.13
	3.06	3.06	3.07	3.07
$\log (\alpha^i - \alpha^{i-1})$	−0.93	−0.91	−0.89	−0.86
	−1.13	−1.11	−1.10	−1.08
	−1.26	−1.25	−1.24	−1.23
	−1.40	−1.39	−1.38	−1.37
	−1.46	−1.46	−1.45	−1.44

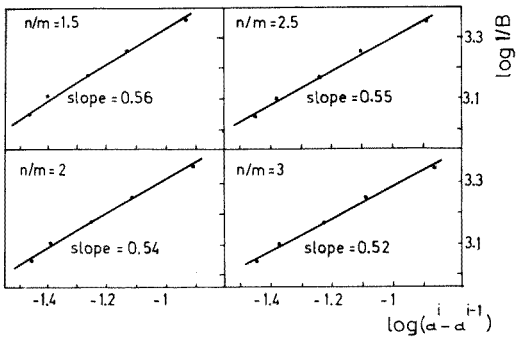

Fig. 3. Iodate—CHDT · HCl reaction. Various values of n/m tested.

TABLE 5

Experimental and theoretical values of the slopes used to calculate the stoichiometry of the iodate—CHDT · HCl reaction

n/m value tested	0.5	1.0	2.0	2.5	3.0
Slope obtained	0.64	0.58	0.54	0.53	0.52
Theoretical slope	2.00	1.00	0.50	0.40	0.33

CHDT · HCl—bromate system

Several samples were prepared containing 3.15×10^{-5} M bromate, various concentrations of CHDT · HCl, 12 ml of anhydrous acetic acid and water to give 25 ml. After the samples had been heated for 15 min at 70°C and cooled, the absorbances were measured at 415 nm against demineralised water. As before, a sample was prepared with an amount of CHDT · HCl greatly in excess, and its absorbance was taken to be E_o. The results obtained are shown in Table 6. Plotting these data for $n/m = 2$ gave a straight line of slope

TABLE 6

Data obtained for calculation of the stoichiometry of the bromate—CHDT · HCl reaction ($a = [BrO_3^-] = 3.15 \times 10^{-5}$ M; $n/m = 2$)

b = [CHDT · HCl] ($\times 10^{-3}$ M)	E	α	$\log(\alpha^3 - \alpha^2)$	$\log(b - na/m\alpha)^{-1}$
1.524	0.444	1.133	−0.77	2.83
1.778	0.451	1.115	−0.84	2.76
2.032	0.456	1.103	−0.90	2.70
2.286	0.468	1.075	−1.06	2.65
2.794	0.478	1.052	−1.24	2.56
3.302	0.483	1.041	−1.35	2.49
3.810	0.490	1.026	−1.57	2.43
6.096	0.503[a]	—	—	—

[a]Taken as E_o.

0.49, nearly the inverse of the ratio proposed. Therefore 1 mol of bromate reacts with 2 mol of CHDT · HCl.

The study was repeated for other concentrations of bromate, with the same concentration of CHDT · HCl, in order to establish the values of x and y. The compositions of the samples used and the results obtained are shown in Table 7. It is again confirmed that n/m is 2. In order to calculate x and y, the ordinate intercepts were plotted against log a for each group. The straight line obtained had a slope of —0.28. Inspection of Table 2 for n/m = 2 and for a slope close to —1/4 indicates that x = 1 and y = 2 or x = 2 and y = 1. Thus the reaction is $BrO_3^- + 2\ CHDT \cdot HCl \rightleftharpoons Br^+ + (CHDT \cdot HCl_{ox})_2$, because the alternative (x = 2, y = 1) is not chemically acceptable. The bromine cation would react further with the double bonds of the oxidized CHDT · HCl, displacing one proton.

When n/m, x and y are known, the expression for u_3 in Table 1 can be used to determine the value of the equilibrium constant. The values obtained

TABLE 7

Sample compositions and results obtained for determining x and y for the bromate—CHDT · HCl reaction (n/m = 2)

$a = [BrO_3^-]$ ($\times 10^{-5}$ M)	b ($\times 10^{-4}$ M)	E	log ($\alpha^3 - \alpha^2$)	Log 1/B	Slope	Intercept
	4.34	0.325	0.49	3.41		
	5.43	0.360	0.31	3.30		
3.90	6.52	0.390	0.15	3.22	0.52	3.26
	7.60	0.417	0.00	3.15		
	8.69	0.437	—0.11	3.09		
	54.30	0.612	—	—		
	4.34	0.274	0.44	3.40		
	5.43	0.300	0.27	3.30		
3.12	6.52	0.327	0.10	3.21	0.54	3.20
	7.60	0.348	—0.04	3.14		
	8.69	0.356	—0.09	3.08		
	54.30	0.501	—	—		
	4.34	0.222	0.35	3.39		
	5.43	0.246	0.15	3.29		
2.34	6.52	0.258	0.05	3.21	0.52	3.15
	7.60	0.280	—0.14	3.14		
	8.69	0.292	—0.24	3.08		
	54.30	0.387	—	—		
	4.34	0.152	0.24	3.38		
	5.43	0.169	0.02	3.28		
1.56	6.52	0.178	—0.10	3.20	0.48	3.145
	7.60	0.190	—0.26	3.12		
	8.69	0.200	—0.41	3.07		
	54.30	0.250	—	—		

for log K were 12.9, 13.1, 13.3, 13.7 and 13.1, with a mean value of 13.2 ± 0.2.

DyDT—periodate system

In this case the samples contained 2.10×10^{-5} M periodate, various concentrations of DyDT, 4 ml of trichloroacetic acid and demineralised water to give 25 ml. The absorbances were measured 30 min after preparation, at 415 nm against demineralised water. Again a sample with a large excess of DyDT was prepared, and its absorbance was considered as E_o. Table 8 shows the results obtained together with the concentrations of DyDT used and the data calculated for $n/m = 3$ (from a previous plot for $n/m = 1$, a slope close to 0.3 was obtained). A plot of these data gave a straight line of slope 0.32, showing that 1 mol of periodate reacts with 3 mol of DyDT.

In this case x and y cannot be determined because the reaction is not complete until 3 h after the reagents have been mixed.

Periodate—manganese(II) system

Several samples were prepared containing 2.0×10^{-4} M manganese(II), various concentrations of potassium periodate, 5 ml of sulphuric acid, 2.5 ml of phosphoric acid and water to give 50 ml. After the samples had been heated for 10 min at 90°C and cooled, the absorbances were measured at 522 nm against demineralised water. As before, a sample was prepared with a large excess of periodate, and the absorbance was taken as E_o. Table 9 shows the results obtained together with the concentrations of periodate used and the data calculated for $n/m = 2.5$. A plot of these data gave a straight line of slope 0.36, nearly the inverse of the ratio proposed [6], i.e., 2 mol of manganese(II) react with 5 mol of periodate. As n/m is known, and $x = y = 1$ in this case, the value obtained for log K is −3.5.

TABLE 8

Data obtained for calculation of the stoichiometry of the periodate—DyDT reaction ($a = [IO_4^-] = 2.10 \times 10^{-5}$ M; $n/m = 3$)

b = [DyDt] ($\times 10^{-5}$ M)	E	α	$\log(\alpha^4 - \alpha^3)$	$\log(b - na/m\alpha)^{-1}$
6.2	0.192	1.896	0.79	4.54
9.3	0.251	1.450	0.14	4.30
12.4	0.308	1.182	−0.52	4.15
15.5	0.324	1.123	−0.76	4.00
18.6	0.348	1.046	−1.28	3.90
24.8	0.356	1.022	−1.63	3.73
37.2	0.364[a]	—	—	—

[a]Taken as E_o.

TABLE 9

Data obtained for calculation of the stoichiometry of the manganese(II)—periodate reaction a = [Mn(II)] = 2.0×10^{-4} M; n/m = 2.5

$b = IO_4^-$ (M)	E	α	$\log(\alpha^{7/2} - \alpha^{5/2})$	$\log(b - na/m\alpha)^{-1}$
5×10^{-3}	0.380	1.168	−0.61	2.34
6×10^{-3}	0.401	1.107	−0.86	2.26
7×10^{-3}	0.412	1.078	−1.02	2.18
8×10^{-3}	0.421	1.055	−1.20	2.12
9×10^{-3}	0.428	1.037	−1.39	2.07
10×10^{-3}	0.432	1.028	−1.52	2.02
20×10^{-3}	0.444[a]	—	—	—

[a]Taken as E_o.

DISCUSSION

The results outlined above show the validity of eqn. (6) for the calculation of the stoichiometries of redox reactions, and agree with the results obtained by other methods, such as the continuous variations and mole ratio methods. The new method has an advantage in that the values of x and y and the stoichiometry can be determined in the presence of an excess of one of the reagents, as is usually proposed for spectrophotometric determinations. Also, in various cases the method permits the equilibrium constant of the redox reaction being studied to be calculated.

REFERENCES

1 A. Holme and F. J. Langmyhr, Anal. Chim. Acta, 36 (1966) 383.
2 J. C. J. Sánchez, J. A. M. Leyva and M. R. Ceba, Anal. Chim. Acta, 90 (1977) 223.
3 M. R. Ceba, J. A. M. Leyva and J. J. B. Nevado, An. Quim., 74 (1978) 1075.
4 M. R. Ceba, J. A. M. Leyva and J. J. B. Nevado, An. Quim., 74 (1978) 620.
5 M. C. Mochon, 1980, private communication.
6 G. Charlot, Colorimetric Determination of Elements, Elsevier, Amsterdam, 1964, p. 292.

Analytica Chimica Acta, 130 (1981) 193—197
Elsevier Scientific Publishing Company, Amsterdam — Printed in The Netherlands

Short Communication

AMPLIFICATION REACTIONS BY MULTIPLICATION WITH AN ION EXCHANGER IN AN INVERSION TUBE

HERBERT WEISZ* and BRIGITTE MOESTA
Institut für Analytische Chemie der Universität Freiburg, Freiburg i.Br. (W. Germany)
(Received 24th April 1981)

Summary. The problems of chemical amplification reactions are discussed and a definition of the term "chemical amplification" is offered. A simple arrangement is described for the amplification of hydrogen ions and calcium ions in the micromolar range using an ion exchanger in an invertible tube.

There are two ways of solving the problem of how to analyze very small samples: the usual one is to find a suitable method for handling such small quantities; the other is to magnify the tiny amount of substance to be determined (or its equivalent) by an amplification procedure. Such procedures have been known for a long time even if not always under this name. As early as 1933 Emich [1] discussed this problem and more recently other authors [2—12] have contributed. Definitions of the term "amplification" in analytical chemistry have been given by various authors [1, 3]. Some time ago, the following definition was proposed: "Amplification is an increase in the number of moles whereby the higher (amplified) mass (amount) to be measured or only detected is a function of the amount of the starting mass, but not a function of the reaction time" [11]. Consequently, the weighting effect in gravimetry, providing a better analytical factor, is not an amplification. Catalytic methods [13] giving a higher amount of reaction product, depending on the reaction time, are also not to be regarded as amplification according to the above definition. A procedure in which a standard amount a is added to the unknown amount x, the sum $(x + a)$ being determined and the added amount subtracted $(x + a - a)$, is certainly not an amplification method [14].

Amplification procedures can be classified as cyclic and noncyclic methods; cyclic methods are characterized by the fact that the reaction sequence is repeated and that after each cycle the starting substance is again present. Generally, noncyclic procedures can be converted to cyclic ones by regaining the amplifiable starting compound and repeating the reaction cycle. Amplifications can involve either multiplication or exponential systems. Thus in multiplication methods, $y = fnx$, whereas in exponential methods, $y = f^n x$ (where x is the starting amount (in mole), y is the amount after n cycles

(in mole) and f is the amplification factor). A typical example of an exponential method is the well-known amplification of iodide via iodate [15—17], where $y = 6^n x$.

Some years ago [9], a cyclic amplification procedure with the aid of ion exchangers was reported for the determination of hydrogen and sodium ions

$$\begin{matrix} M-H & Na^+ & M-H \\ & \rightleftharpoons & \\ M-Na & H^+ & M-Na \end{matrix} \qquad (M = \text{ion-exchange matrix})$$

A reasonably complete exchange of these ions is possible in both directions. For the amplification of sodium ions, several columns filled with the ion exchanger in the H^+-form are connected in series alternately with columns containing the ion exchanger in the Na^+-form; when the sample solution passes through the columns, sodium ions liberate an equivalent amount of H^+ ions from the first column, these then liberate sodium ions from the second column, etc. Finally, all columns in the Na^+-form are connected with each other, and the protons collected on them are eluted with sodium chloride solution and titrated with standard sodium hydroxide; this result is divided by the number of Na^+-columns. Recently [18] this method was applied to the determination of micromolar amounts of various metal ions (Ca, Mg, Al, Ca + Mg) and (with an anion exchanger), chloride and fluoride.

In this communication, a new and quite simple variation of the multiplication procedure with the aid of an ion exchanger is described, using an inversion tube (Fig. 1). For the amplification of protons or other cations, a cation exchanger in the Na^+-form is placed in one half of the tube and the same exchanger in the H^+-form is placed in the other half; the two different forms of the exchanger must be suitably separated so that they do not come in contact with each other, but the sample solution must have free access. If a defined amount of an acid is added to the half of the tube containing the ion exchanger in the Na^+-form, a certain amount of sodium ion is liberated. When the tube is inverted, the Na^+-containing solution permeates the ion exchanger in the H^+-form, thus liberating a certain amount of protons; after the next inversion, these protons react with the Na^+-exchanger, liberating sodium ions. After the cycle has been repeated several times, protons are accumulated on the ion exchanger in the Na^+-form; the protons are finally eluted with sodium chloride solution and titrated. It is not to be

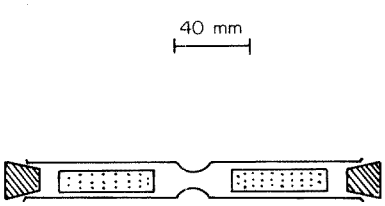

Fig. 1. The inversion tube.

expected that the various exchange reactions go to completion, but under identical conditions with the same number of cycles, finally a higher amount of acid should cause a higher consumption of standard alkali in the titration. Because this consumption proved to be sufficiently reproducible, determinations of protons, and of other cations such as calcium(II), are possible by extrapolation from a standard graph.

Experimental

A glass tube (180 mm long, 18 mm i.d.) is contracted centrally to about 9 mm i.d. (Fig. 1). Cation exchanger (Dowex 50W-X8, 20—50 mesh) is prepared in the H^+- and Na^+-forms. Bags made from nylon net (3 × 4.5 cm) are filled with about 7 g of the exchanger in a particular form, and suitably closed (glued or better sewn). To ensure complete conversion of the exchanger, the bag containing the Na^+-form is stirred or shaken for 2 h with 100 ml of saturated sodium chloride solution and then washed free from superfluous sodium chloride (electrical conductivity serves as monitor). The bag containing the ion exchanger in the H^+-form is washed several times with 20 ml of twice-distilled water until the consumption of 0.01 M sodium hydroxide (Tashiro indicator pH 5.4 [19]) is no higher than that for a 20-ml blank of twice-distilled water.

For the determination of protons, the bag with the Na^+-form exchanger is placed in one half of the tube and the tube is closed with a rubber stopper. The tube is inverted, 1 ml of the acidic sample and 4 ml of twice-distilled water are added, a stopwatch is started, and the tube is shaken 10 times. Then a bag containing the ion exchanger in the H^+-form is placed in the upper half of the tube which is likewise closed with a rubber stopper. After exactly 5 min, the tube is inverted so that the solution flows into the section containing the ion exchanger in the H^+-form. (To ensure free flow of solution, the tube must be thoroughly cleaned.) The tube is again shaken 10 times and after precisely 5 min, again inverted. This completes the first cycle (10 min). Reaction times longer than 5 min each would of course produce greater exchange, but would also increase the error because of the larger amount of ions (H^+ and Na^+) liberated from the exchanger itself. Subsequent cycles are carried out under exactly the same reaction conditions (time and number of mixings).

After the desired number of cycles, the bag with the ion exchanger (Na^+-form) is transferred to a beaker containing 100 ml of saturated sodium chloride solution, mixed several times and titrated with 0.01 M NaOH (Tashiro indicator, red—violet to gray).

Results

The ion exchange cannot be quantitative, but it is reproducible under controlled conditions of timing and shaking. Figure 2 shows the alkali consumption for the same amount of acid after different numbers of amplification cycles. In all cases, three identical samples were processed simul-

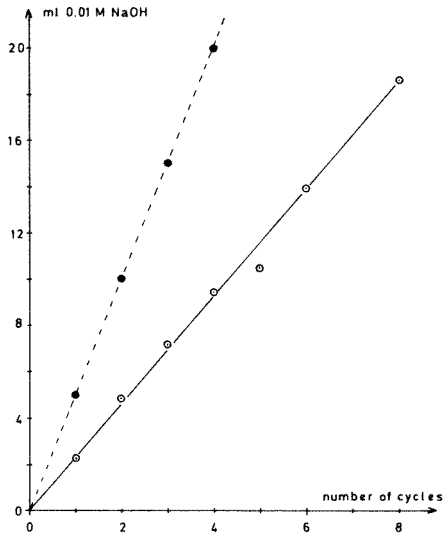

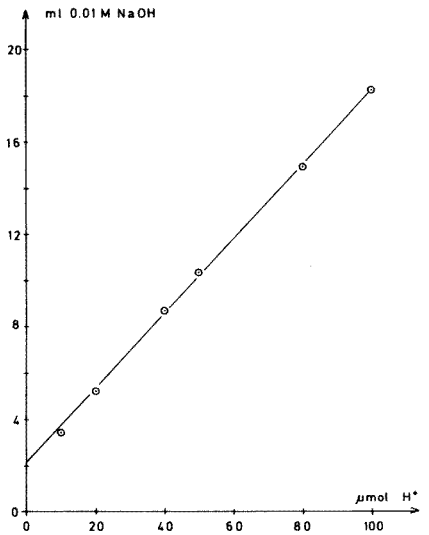

Fig. 2. Amplification of 50 μmol of H^+ depending on the number of cycles: (⊙) practical titration volumes; (•) theoretical titration volumes (100% ion exchange).

Fig. 3. Standard graph for the amplification of protons (5 cycles).

taneously and the titration results were averaged. For practical purposes, 5 cycles were always applied.

In order to determine unknown samples, a calibration graph must be prepared by using standard solutions of hydrochloric acid; Fig. 3 shows a typical graph, where the intersect with the ordinate represents the blank. Some results for various acid samples obtained from this graph are given in Table 1. The bags containing the ion exchanger in the H^+-form must be regenerated after each complete determination by stirring them for 15 min in 3 M HCl and then rinsing carefully with twice-distilled water.

TABLE 1

Determination of hydrogen or calcium ions with amplification (5 cycles)

Hydrogen ions					
Taken (μmol)	13.5	28.8	56.5	57.0	93.0
0.01 M NaOH required (ml)[a]	4.49	7.01	11.35	11.49	17.22
Found (μmol)	14.6	30.1	56.0	57.4	93.3
Calcium ions					
Taken (μmol)	8.8	12.5	16.8	39.5	47.5
Found (μmol)	8.5	12.2	15.2	40.0	47.2

[a]Average of three results.

Not only protons but also metal ions can be amplified, as was demonstrated for the example of calcium ions. Here, the sample solutions (or standards for the preparation of the calibration graph) are first added to the bag containing the ion exchanger in the H^+-form, and the liberated protons are multiplied as described above. It should be noted that the first step, i.e., exchange of calcium ions for protons, represents one cycle. The calibration graph is similar to that shown in Fig. 3. Some results for the determination of calcium are given in Table 1. The amplification of other cations and of anions (with an anion exchanger) should likewise be possible.

REFERENCES

1 F. Emich, Mikrochem., 13 (1933) 283.
2 H. Weisz and C. Tellgmann, Mikrochim. Acta (Wien), (1965) 258.
3 R. Belcher, Talanta, 15 (1968) 357; Proc. Soc. Anal. Chem., (1970) 61, and references therein.
4 H. Weisz and M. Gönner, Anal. Chim. Acta, 43 (1968) 235; Mikrochim. Acta (Wien), (1968) 355.
5 U. Fritsche, Mikrochim. Acta (Wien), (1969) 1322.
6 H. Weisz and U. Fritsche, Mikrochim. Acta (Wien), (1970) 638.
7 U. Fritsche and H. Weisz, Mikrochim. Acta (Wien), (1970) 1045.
8 H. Weisz, Mikrochim. Acta (Wien), (1970) 1057.
9 H. Weisz and U. Fritsche, Mikrochim. Acta (Wien), (1973) 361.
10 D. Klockow and G. Roenicke, Atmos. Environ., 7 (1973) 163.
11 U. Fritsche and H. Weisz, Mikrochim. Acta (Wien), (1974) 701.
12 R. Belcher, Talanta, 24 (1977) 533.
13 K. B. Yatsimirskii, Kinetic Methods of Analysis, Pergamon, Oxford, 1966.
14 M. H. Hashmi, K. A. Malik, N. A. Chughtai, I. Ahmad and A. U. Afzal, Mikrochim. Acta (Wien), (1970) 359.
15 L. W. Winkler, Z. Angew. Chem., 28 I (1915) 46; Fresenius Z. Anal. Chem., 39 (1900) 85.
16 T. Leipert, Mikrochemie, Pregl-Festschrift, (1929) 266.
17 P. Kainrath, Fresenius Z. Anal. Chem., 125 (1943) 1.
18 H. Weisz, S. Pantel and B. Moesta, Fresenius Z. Anal. Chem., 306 (1981) 106.
19 E. Bishop, Indicators, Pergamon, Oxford, 1972, p. 138.

Analytica Chimica Acta, 130 (1981) 199—201
Elsevier Scientific Publishing Company, Amsterdam — Printed in The Netherlands

Short Communication

A PHYSICALLY-COATED MERCURY FILM ELECTRODE FOR ANODIC STRIPPING VOLTAMMETRY

J. P. RILEY* and HONGKAN GU[a]

Department of Oceanography, The University of Liverpool, Liverpool (Gt. Britain)

(Received 1st April 1981)

Summary. The physically-coated Ag/AgHg/Hg film electrode described is easy to prepare and durable, and has excellent stability even when rapid stirring is used. It gives high sensitivity and provides well-defined voltammograms for zinc (1.8 ± 0.06 $\mu g\ l^{-1}$), cadmium (8.8 ± 0.6 ng l^{-1}) and lead (0.2 ± 0.008 $\mu g\ l^{-1}$) in 6-ml samples of sea water after a deposition time of 3 min.

Carbon electrodes electrochemically coated with mercury have been employed by many workers for the determination of trace elements in sea water by anodic stripping voltammetry [1, 2]. Unfortunately, the mercury film tends to be unstable (leading to changes in sensitivity) and it must be frequently renewed, which is time-consuming. A further cause of loss of sensitivity is contamination of the electrode surface by the adsorption which occurs if measurements are made in samples containing colloidal or suspended matter. Gu et al. [3, 4] attempted to overcome this problem by protecting the electrode with a membrane of alginic acid or calcium alginate. Using this electrode, they were able to determine lead (ca. 30 ng l^{-1}) with a precision of ±14% in samples of water from the China Sea containing such high concentrations of colloidal and suspended material that normal mercury film electrodes were useless. However, they found it was necessary to renew even this electrode daily.

The present communication describes a new physically coated Ag/AgHg/Hg film electrode developed from this electrode, which can be rapidly prepared and which is sufficiently stable to be used in the presence of colloidal material and at high stirring speeds.

Experimental

Mercury film electrode. The electrode is constructed with silver wire protruding from a glass tube and attached to a copper rod. The operative part consists of a 3-cm length of silver wire (1.6-mm diameter) which is hermetically sealed into the end of a glass tube with a short piece of tightly-fitting

[a]On leave from Institute of Oceanology, Academia Sinica, Tsingtao, People's Republic of China.

silicone rubber tubing after being attached to a copper rod to provide electrical contact. The length of silver wire protruding from the electrode body is 2 cm, and the connecting copper rod protrudes beyond the top of the glass tube. To prepare the electrode, the silver wire is rubbed with fine sandpaper, then dipped momentarily in 7 M nitric acid (electronic grade) and washed with distilled water when it appears silvery white. While it is still immersed in water, it is rubbed lengthwise on a hanging mercury drop (triply distilled mercury) which gives it a mirror-like appearance. The prepared electrode must be kept in water when not in use. Normally, electrodes coated in this way can be used daily for 1—2 weeks before they lose their shiny coating and must be recoated. Recoating is carried out in the same way, but omitting the nitric acid treatment. When this is done, any adsorbed impurities will be transferred to the top of the electrode from where they can be removed by wiping with a small piece of filter paper.

Anodic stripping voltammetry. A Southern Analytical pulse polarograph (Model A3100) was used in a 2-electrode pulse anodic stripping voltammetric mode for all work with the Ag/AgHg/Hg electrode. A silver reference electrode was used which functioned as the counter electrode as well.

Comparative data were obtained by using an ESA mercury-coated carbon electrode (area 4.0 cm^2) and an ESA (Model 2014) multiple anodic stripping analyzer.

Procedure. Place 6 ml of sea water in a 8.5 cm × 2.0 cm silica electrolysis tube, introduce the electrodes and, while stirring with a rapid current of nitrogen, plate the trace metal ions at a potential of —1.30 V vs. the silver reference electrode for a known period between 3 and 6 min. Turn off the nitrogen flow and after 15 s strip the plated metals by anodic stripping voltammetry using the polarograph in the pulse mode (voltage range —1.3 to —0.1 V, scan rate 5.5 mV s^{-1}, pulse height 5 mV, pulse integration 40—20 ms). After completion of the stripping, maintain the mercury electrode at —0.1 V for 2 min while stirring. The apparatus is then ready for measurements on the next sample. Carry out a blank in the same way using 6 ml of high-purity water. Standardize the method in a similar fashion by making standard additions of zinc, lead and cadmium equivalent to final concentrations of 1.0—10 μg Zn l^{-1}, 0.05—0.25 μg Pb l^{-1} and 0.01—0.25 μg Cd l^{-1}, respectively.

Results and discussion

Calibration curves prepared using known concentrations of zinc, cadmium and lead spiked in stripped sea water showed a good linear relationship between metal concentration and peak current (Fig. 1). However, with cadmium and lead, the extrapolated curve did not pass through the origin as has been found by other workers [2, 3], possibly because the water contained traces of catalysts [3, 5].

Replicate analyses (6) were carried out on a different sea water from the coastal Atlantic using a plating time of 6 min; a typical polarogram is shown in Fig. 2. The results showed the standard deviations to be ±0.06, ±0.0006 and

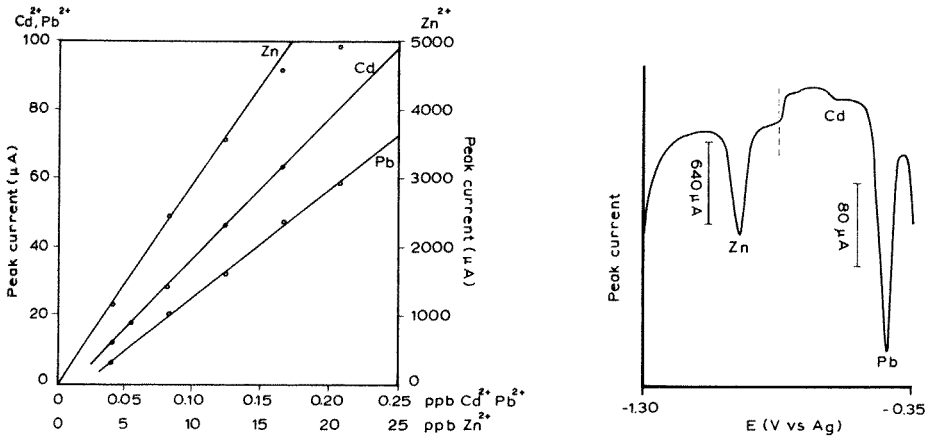

Fig. 1. Calibration graphs for standard additions of zinc, cadmium and lead to stripped sea water.

Fig. 2. Typical a.s.v. recording for coastal sea water containing 1.8 μg Zn l^{-1}, 0.009 μg Cd l^{-1} and 0.20 μg Pb l^{-1}.

±0.008 μg l^{-1} for zinc, cadmium and lead at average determined levels of 1.8, 0.0088 and 0.20 μg l^{-1}, respectively. The accuracy of the procedure was assessed by carrying out 6 replicate determinations on samples of stripped sea water which had been spiked with 4.2 μg Zn l^{-1}, 0.042 μg Cd l^{-1} and 0.042 μg Pb l^{-1}; the mean results and standard deviations obtained were 4.3 ± 0.15 μg Zn l^{-1}, 0.042 ± 0.0008 μg Cd l^{-1} and 0.041 ± 0.0008 μg Pb l^{-1}, so that satisfactory recoveries were achieved in each case. As a further check on the accuracy of the method, comparative determinations of cadmium in sea water were made by using the physically-coated electrode with a plating time of 6 min, and by using a chemically-coated mercury film electrode in a linear sweep a.s.v. technique with a plating time of 30 min. The mean results (n = 5) were 0.12 μg Cd l^{-1} by the recommended method and 0.11 μg Cd l^{-1} by the linear sweep technique; the standard deviation was 0.011 μg l^{-1} in each case. Excellent agreement was thus obtained between the two techniques, proving that the new electrode is suitable for use in the analysis of coastal and estuarine waters.

The authors thank Drs. Jon Hasle and Constantine van den Berg for helpful discussions.

REFERENCES

1 M. I. Abdullah, B. Reusch Berg and R. Klimek, Anal. Chim. Acta, 84 (1976) 307.
2 M. Whitfield, in J. P. Riley and G. Skirrow (Eds.), Chemical Oceanography, 2nd edn., Vol. 4, Academic Press, London, 1975.
3 Hongkan Gu and Mingxing Liu, Anal. Chem. (in Chinese), 1 (1973) 15; 2 (1974) 175.
4 Hongkan Gu, Mingxing Liu and Wanyou Bao, Scientia (in Chinese), 24 (1979) 208.
5 Hongkan Gu and Mingxing Liu, Stud. Mar. Sin. (in Chinese), 11 (1976) 25.

Analytica Chimica Acta, 130 (1981) 203—208
Elsevier Scientific Publishing Company, Amsterdam — Printed in The Netherlands

Short Communication

SOME ASPECTS OF ELECTROTHERMAL ATOMIZATION OF ELEMENTS FROM LARGE AMOUNTS OF INVOLATILE MATRICES

ZDENĚK SLOVÁK* and BOHUMIL DOČEKAL

Research Institute of Pure Chemicals, LACHEMA, Brno, CS-621 33 (Czechoslovakia)

(Received 3rd March 1981)

Summary. Non-volatile matrices which cannot diffuse into the graphite walls of an electrothermal atomizer (as obtained by direct sampling of solids, injection of solutions into tubes with pyrolytic coatings or with a hydrophobic film) make a "miniplatform" in the centre of the atomizing tube. A delay in the temperature increase of this platform at the beginning of the atomization step compared to that of the atomizer walls causes enhancement of the peak height sensitivity. This was proven by atomization of nanogram quantities of copper and iron from solutions of aluminium salts.

When impurities are determined in aluminium oxide powder by means of electrothermal atomic absorption spectrometry (a.a.s.), an increased peak-height sensitivity is obtained [1]. Higher sensitivities compared with aqueous solutions have also been obtained for injection of suspensions of ion-exchange resins [2]. This effect is probably caused by differences in temperatures of the analytes when they are placed immediately on the graphite tube surface (or soaked into the wall) or on a platform above it.

Experimental

Equipment and chemicals. Perkin-Elmer 4000 and 420 spectrometers with a model 56 recorder and HGA-74 furnace, standard graphite tubes and home-made pyrolytically-coated tubes [3] were used. In order to make a hydrophobic film in the centre of the tube, 20 μl of 1% (w/w) polystyrene solution in benzene was applied to the tube and dried for 20 s at 70°C before sample injection. Eppendorf pipettes (10—50 μl) were used for injections of solutions and suspensions.

Suspensions containing $\leqslant$10 mg of γ-Al_2O_3 per ml with known concentrations of chromium, copper, iron and lead were prepared as described earlier [1]. Standard solutions of copper and iron and solutions of $Al(NO_3)_3 \cdot 9H_2O$ (72 mg ml^{-1}), $NH_4Al(SO_4)_2 \cdot 12H_2O$ (90 mg ml^{-1}) and $AlCl_3 \cdot 6H_2O$ (48 mg ml^{-1}) were prepared in 0.01 M HNO_3 or HCl or in 0.005 M H_2SO_4. Laboratory chemicals of special purity were used for these experiments.

Procedure. Suspensions of 0.5 g of aluminium oxide were prepared in 50 ml of water in a teflon beaker by magnetic stirring. Portions of the steadily-stirred suspension or of solutions were injected into the furnace. The settings of the model 4000 spectrometer and HGA-74 graphite furnace are sum-

marised in Table 1. For measurements with the model 420 spectrometer, the conditions described previously [1] were used. All measurements were done with appropriate hollow-cathode lamps and with the automatic background correction.

Peak areas within the atomizing time for the model 420, or the integrated absorbances (A × s) for the model 4000 were displayed, and the characteristics of the peak shapes (Fig. 1) were determined from the chart recording using the highest chart speed of the recorder (160 mm min^{-1}). The reproducibility of this time measurement was ±75 ms (0.2 mm).

Results and discussion

The relative increases of the peak height, sensitivity in determinations of chromium, copper, iron and lead from aluminium oxide suspensions compared to pure solutions without aluminium using standard graphite tubes,

TABLE 1

Operating parameters for electrothermal a.a.s. with the Perkin-Elmer model 4000 spectrometer and HGA-74 furnace[a]

	Cu	Fe
Wavelength (nm)	324.7	372.0
Slit width (nm)[b]	0.7	0.2
Dry (°C, s)	100, 30	100, 30
Char (°C, s)	700, 10	500, 10
Atomize (°C, s)	2700, 10	2700, 10

[a]Argon in the miniflow mode (50 ml min^{-1}) was used as an inert gas. [b]Position "low".

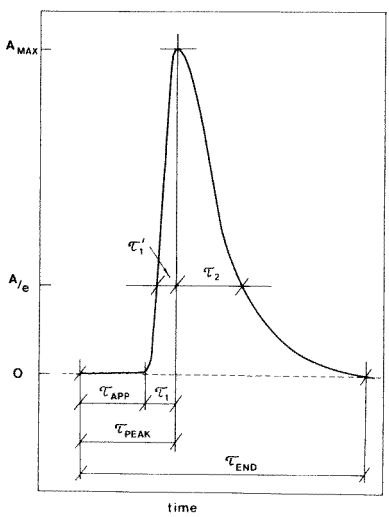

Fig. 1. Peak characteristics.

have already been summarised (see table 4 [1]); The difference in the time characteristics of the atomization of these elements from an aluminium oxide matrix injected as a suspension are given in Table 2 with respect to pure solutions of the analytes in 0.01 M HNO_3. The measurements were done with both standard and pyrolytically-coated tubes. Because of the slightly different heating rates of standard and pyrolytically-coated tubes [4], only results obtained with the same tube can be compared. The results in Table 2 were obtained with the same tube within one series of measurements, with alternating injections of an aluminium oxide suspension and a standard solution. The direct measurement of temperatures by means of an optical pyrometer is not suitable for this purpose, because practically the same radiation intensity from the tube wall is measured in all cases.

The melting point of α-Al_2O_3 is 2050—2100°C (b.p. 2900—3000°C), which is higher than the charring temperatures in the tube before the atomizing step. During the temperature increase in the atomization step, the matrix melts and begins to evaporate. The temperature of a sample which is placed on the surface of the tube is possibly lower than that of the graphite wall because of necessary heat-transfer process. This effect would be greater in smooth, pyrolytically-coated tubes. Indeed, the delays in the appearance times, τ_{app}, are 2—3 times greater when measured for pyrolytically-coated graphite tubes.

The peak times of elements with a high atomization temperature (Cr, Cu, Fe) are practically the same for injections of aluminium oxide suspensions or pure standard solutions into a given type of tube. The peak rise time, τ_1, is shorter in the case of a large amount of matrix. This "miniplatform" effect results from the temperature difference between the colder sample and the adjacent warmer tube wall [5, 6]. No condensation and re-evaporation of free atoms takes place, so that the peak rise time is shorter, the maximum atom concentration is higher and therefore the peak is also higher. Temperature profiles of analogous standard tubes have recently been published by Slavin et al. [7] in a paper dealing with the possibility of making an isothermal tube for electrothermal a.a.s.

TABLE 2

Time differences ($\tau_{suspension} - \tau_{solution}$) of the peak characteristics (given in seconds) (For symbols see Fig. 1)

	Cr		Cu		Fe		Pb	
	Stand.[a]	Pyro.[b]	Stand.	Pyro.	Stand.	Pyro.	Stand.	Pyro.
$\Delta\tau_{app}$	0.21	0.71	0.22	0.66	0.36	0.71	0.26	1.00
$\Delta\tau_{peak}$	−0.30	−0.11	−0.18	−0.07	−0.09	0.04	0.32	1.50
$\Delta\tau_1$	−0.51	−0.82	−0.40	−0.73	−0.45	−0.67	0.06	0.50
$\Delta\tau_1'$	−0.19	−0.52	−0.08	−0.15	−0.24	−0.47	−0.02	−0.03
$\Delta\tau_2$	−0.11	−0.23	0.11	0.15	−0.08	−0.52	−0.13	−0.03

[a]Standard tube. [b]Pyrolytically-coated tube.

Another possible explanation for the peak shifts might be the protection of the analyte in the colder matrix against contact with carbon, so that reduction of oxides occurs later. However, peak height enhancements were observed even with a carbon (coke) platform [2]. The differences in the position and shape of lead peaks compared with those of chromium, copper and iron are greater because of the low atomizing temperature of lead (appearance temperature 770°C, [8]) which atomizes by a reduction mechanism. It is possible that in this case the prevention of reduction plays the main role.

The miniplatform effect takes place also when relatively concentrated solutions of involatile matrices are injected, especially if the sample solution cannot diffuse into the tube walls (as in pyrolytically-coated tubes and probably all metal and glassy carbon devices). This was proved in experiments with aluminium salt solutions injected into standard and pyrolytically-coated graphite tubes and into tubes with a polystyrene film, which did not allow the sample solution to soak into the graphite during the drying stage. In Fig. 2 sensitivities (signal values for 1 ng of iron) are given for peak height and integrated absorbances for determination of iron, in the absence of aluminium and in the presence of 0.2 mg of aluminium oxide injected as aluminium nitrate or ammonium aluminium sulphate solutions. The enhancement of the peak height sensitivity compared with that for the pure analyte solutions in diluted acids is evident in all cases where a platform could form, that is in pyrolytically-coated tubes and in tubes with a polystyrene film. The peak area sensitivities are practically unchanged as assumed, because the physical miniplatform effect does not change the atomization mechanism.

The effects on the determination of copper are summarised in Fig. 3. In

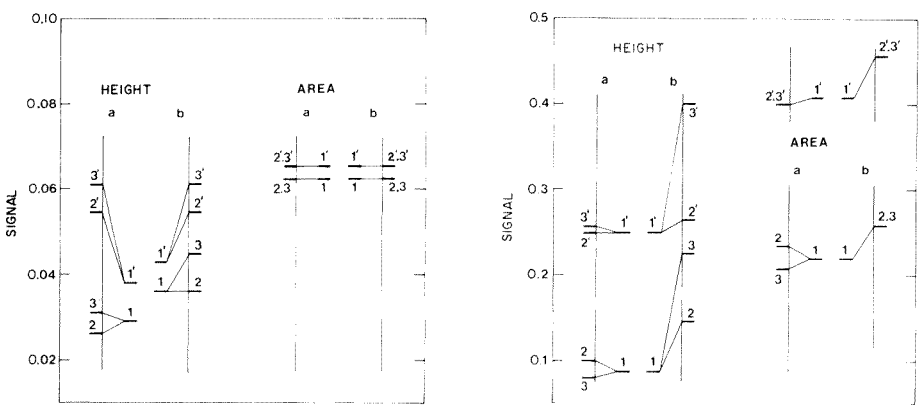

Fig. 2. Peak height (A) and peak area (A × s) signals for determination of 1 ng of iron: (a) without polystyrene film; (b) with polystyrene film; (1, 2, 3) for a standard tube; (1′, 2′, 3′) for a pyrolytically-coated tube; (1, 1′) standard solution without Al; (2, 2′) solution of $NH_4Al(SO_4)_2$; (3, 3′) solution of $Al(NO_3)_3$.

Fig. 3. Signal values for determination of 1 ng of copper. For symbols see Fig. 2.

this case there are some differences also in peak area sensitivities, but the miniplatform effect is undoubtedly the main reason for the observed changes in peak heights. In all cases where a platform was formed, shifts of τ_{app} to larger values were observed. However, an exact measurement of τ_{app} was not possible because of the curved shape of the start of a peak, probably because of the much finer agglomeration of the solid matrix compared with an injection of an aluminium oxide suspension. In contrast with the injection of aluminium oxide suspensions (Table 2), a slight shift of the peak time was observed in tubes with a hydrophobic film (Fig. 4), probably caused by the formation of a matrix skin with very bad contact with the tube wall. Various physical properties and forms of aluminium oxide platforms formed by aluminium sulphate or nitrate also explain the observed differences in peak height sensitivities.

In Fig. 4, the miniplatform effect is shown to depend on the amount of aluminium oxide (from $NH_4Al(SO_4)_2$) present in a standard tube. If some matrix is in direct contact with the tube and some is present as a "miniplatform" (e.g., 10—50 μg Al_2O_3 in a hydrophobic tube or >150 μg Al_2O_3 in a standard tube, Fig. 4), peak splitting can be observed. The injection of aluminium chloride into the tubes led in all cases to losses of copper (Fig. 4). Even a lower charring temperature could not substantially suppress this interference. However, the peak shapes and delays in appearance times were similar to those for other aluminium compounds; the losses of copper took place before an aluminium oxide platform was built.

It can be concluded that the atomization of elements from large amounts of matrices is characterized by a special physical interference, the "miniplatform" effect. Because of a temperature lag of the sample compared to the graphite wall (possibly combined with prevention of contact with the reducing carbon), the conditions of atomization are similar to those in isothermal atomization devices.

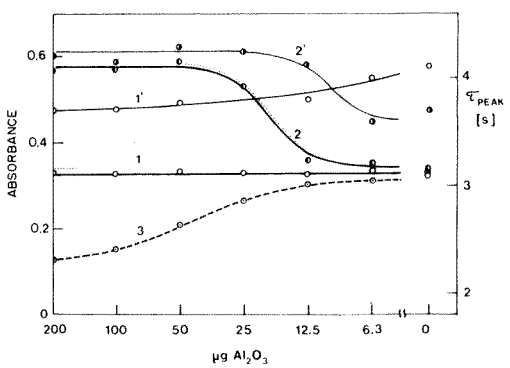

Fig. 4. Influence of aluminium matrix in the determination of 4 ng of copper: (1, 3) peak height, standard tube; (2) peak height, standard tube with polystyrene; (1', 2') τ_{peak} for (1) and (2); (1, 2) solutions of $NH_4Al(SO_4)_2$; (3) solutions of $AlCl_3$. Areas of peak splitting dotted.

REFERENCES

1 Z. Slovák and B. Dočekal, Anal. Chim. Acta, 129 (1981) 263.
2 Z. Slovák, Anal. Chim. Acta, 110 (1979) 301.
3 D. C. Manning, F. J. Fernandez and G. E. Peterson, A. A. Application Study No. 631, Perkin-Elmer, 1976.
4 R. E. Sturgeon and C. L. Chakrabarti, Prog. Anal. Atom. Spectrosc., 1 (1978) 5.
5 B. V. L'vov, Spectrochim. Acta, Part B, 33 (1978) 153.
6 W. Slavin and D. C. Manning, Anal. Chem., 51 (1979) 261.
7 W. Slavin, S. A. Myers and D. C. Manning, Anal. Chim. Acta, 117 (1980) 267.
8 R. E. Sturgeon, C. L. Chakrabarti and C. H. Langford, Anal. Chem., 48 (1976) 1792.

Analytica Chimica Acta, 130 (1981) 209—214
Elsevier Scientific Publishing Company, Amsterdam — Printed in The Netherlands

Short Communication

MATRIX MODIFICATION FOR THE DIRECT DETERMINATION OF CADMIUM IN URINE BY ELECTROTHERMAL ATOMIC ABSORPTION SPECTROMETRY

CARLOS BRUHN F.* and GLADYS NAVARRETE A.

Departamento de Análisis Instrumental, Facultad de Farmacia, Universidad de Concepción, P.O. Box 237, Concepción (Chile)

(Received 28th January 1981)

Summary. Matrix modification with ammonium nitrate, ammonium dihydrogen-phosphate and Triton X-100 proved suitable. Optimization of the graphite furnace parameters allowed cadmium to be quantified at 800°C. The response was 0.1 $\mu g\ l^{-1}$ for 1% absorption, and the relative standard deviation for consecutive determinations of a urine containing 1.5 μg Cd l^{-1} was 4%. Urinary cadmium levels of 0.4—1.8 $\mu g\ l^{-1}$ were found in five occupationally unexposed persons.

In the industrial environment, cadmium may be associated with chronic pathological conditions including emphysema, renal disfunction, liver damage, etc. [1, 2]. In addition, cadmium is widely distributed throughout the biosphere, and its environmental levels have become of concern in relation to nonindustrial exposure [3, 4]. Urinary cadmium concentrations adequately reflect body burden [5, 6] but determining the significance of urinary cadmium levels is made difficult by the problems of establishing a reliable normal range in this rather complex biological matrix. These problems have been discussed by Carmack and Evenson [7] and Legotte et al. [8].

The most widely used technique for cadmium determination at the parts per billion level in biological materials is electrothermal atomic absorption spectrometry (e.a.a.s.). Some procedures include extraction of cadmium from the high-salt background of urine, to eliminate matrix interferences [9, 10], but extractions are time-consuming and prone to losses or contamination. An alternative is matrix modification based on chemical changes before the measurement [11—13]. This communication reports a simple matrix modification procedure for cadmium determinations in urine; the urine is diluted with a mixture containing ammonium dihydrogenphosphate, ammonium nitrate, and a surfactant (Triton X-100). Ammonium dihydrogenphosphate allows charring at higher temperatures by reducing cadmium volatility through the increased thermal stability of cadmium phosphate. Ammonium nitrate is a well known ashing agent to reduce halide interferences [14]. Triton X-100 assists in the charring of organic matter at low temperatures [13] and in providing uniform surface tension in all urine samples.

Experimental

Apparatus. A Perkin-Elmer model 380 atomic absorption spectrometer equipped with a deuterium background corrector, a HGA-400 graphite furnace atomizer with temperature-controlled maximum power heating capability, a Beckman linear-log potentiometric recorder, and pyrolytic graphite tubes was used. The instrumental parameters used are given in Table 1.

All glassware was soaked in (1 + 1) nitric acid for 24 h, thoroughly rinsed with twice-distilled, deionized water and air-dried. Polyethylene vessels were cleaned similarly, but with (1 + 1) hydrochloric acid. Glassware and polyethylene vessels were filled with 1% (v/v) nitric acid and stored for 24 h. Cadmium standards prepared in 1% (v/v) nitric acid were used to evaluate each vessel by e.a.a.s.; only units free from cadmium were used.

Reagents and solution preparation. All reagents used were of analytical grade (Merck) except for Triton X-100 (Serva). Twice-distilled, deionized water was used throughout. Cadmium standard solutions were obtained by dilution from a 1000 μg ml^{-1} stock solution (cadmium metal in 1% (v/v) hydrochloric acid) with 1% (v/v) nitric acid and contained ammonium nitrate (0.063 M) ammonium dihydrogenphosphate (0.013 M) and Triton X.100 (0.01%). The matrix modifier solution was 2% (v/v) in nitric acid and contained ammonium nitrate (0.126 M), ammonium dihydrogenphosphate (0.026 M), and Triton X-100 (0.02%).

Procedures. Blank and working standard solutions were prepared daily by appropriate dilution in glass, and stored immediately in polyethylene containers. Unless otherwise noted, blanks and urine samples were mixed with an equal volume of the matrix modifier solution before measurement in the graphite furnace. Cadmium was quantified in urine samples from 5 occupationally unexposed persons one hour after sample collection in poly-

TABLE 1

Instrumental parameters for the determination of urinary cadmium

Wavelength (nm)	228.8	Sample volume (μl)	20[a]
Spectral bandwidth (nm)	0.7 (Alt)	Calibration mode	Concentration, peak height
Lamp current (mA)	4		
Nitrogen (ml min^{-1})[b]	310, internal	Integration time (s)	8
Graphite furnace sequence[c]			
	Temperature(°C)	Ramp time(s)	Hold time(s)
Dry	110	20	10
Char	380	30	15
Atomization	800	0[d]	8
Clean-out	2100	1	5

[a]Eppendorf pipettes with disposable plastic tips; the tips were soaked for 24 h in 20% (v/v) HNO_3 and rinsed several times with twice-distilled, deionized water before use. [b]Miniflow (35 ml min^{-1}) after 40(s) of charring. [c]Temperatures are final values. [d]Temperature-controlled maximum power heating mode.

ethylene containers. The samples were stored at 4°C and cadmium was redetermined after 24 h, without significant differences in results. A minimum of three measurements was performed on each standard and sample. Blank absorbances were subtracted using the auto-zero function of the spectrometer. The calibration curve was determined from the mean values of peak absorbances. The standard addition method was applied to each sample to compensate for matrix effects unaffected by the modifier solution. For each urine sample, at least three solutions were prepared in duplicate containing the sample (1 + 1) diluted with the matrix modification mixture, and cadmium standard additions of 0, 0.5 and 1.0 $\mu g\ l^{-1}$ mixed (1 + 1) with the matrix modification mixture.

Results and discussion

Charring and atomization temperatures. A suitable charring temperature for a urine pool was selected after a study of the minimum and maximum temperatures allowed; an atomization temperature of 900°C was used, as for aqueous cadmium standards. The minimum usable charring temperature was determined from a plot of this temperature vs. absorbance at 226.5 nm without background correction (Fig. 1). Comparison of curves (a) and (b) shows clearly that the presence of the matrix modification mixture significantly reduces the nonspecific absorption signal obtained with the same solution containing 1% (v/v) nitric acid only. This effect probably was due to the better ashing properties of the modified urine solution. The minimum charring temperature was 350°C. The maximum charring temperature was determined from a plot of relative absorbance at 228.8 nm with background correction vs. charring temperature (Fig. 2). It is clear that the matrix modifier (curve b) significantly improves the sensitivity. The maximum char-

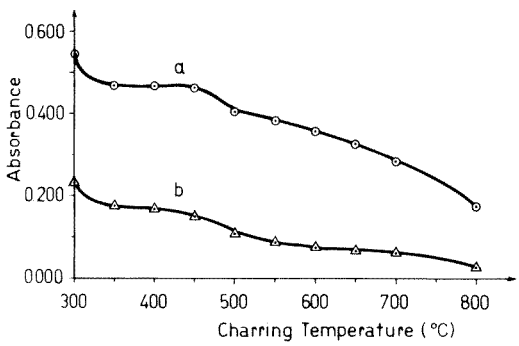

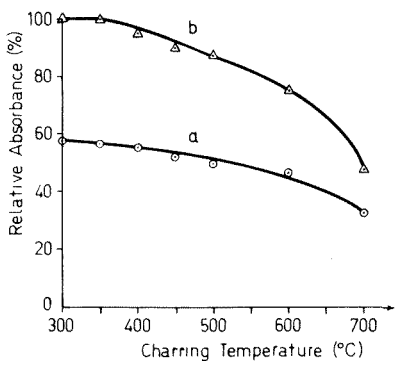

Fig. 1. Effect of charring temperature on non-specific background absorbance for urine (1 + 1 dilution + 2.0 μg Cd l^{-1}): (a) 1% (v/v) HNO_3; (b) 1% (v/v) HNO_3 + matrix modifier. Measurements at 226.5 nm without deuterium lamp.

Fig. 2. Effects of charring temperature on cadmium absorbance for urine (1 + 1 dilution + 2.0 μg Cd l^{-1}). Curves (a) and (b) as for Fig. 1. Measurements at 228.8 nm with deuterium lamp.

ring temperature allowed before significant cadmium losses occurred was 400°C. Therefore, a charring temperature of 380°C was selected as a compromise between the minimum and maximum temperatures allowed.

The atomization temperature was selected with the HGA-400 graphite furnace operating in the temperature-controlled maximum power heating mode; the tube was heated at 2000°C s^{-1} to the preselected temperature so that optimum atomization was achieved at lower temperatures compared to the voltage-controlled atomization mode. Figure 3 shows the results obtained for the spiked urine sample and for an aqueous standard. With the urine sample, optimum atomization in the temperature-controlled heating mode was reached at 800°C. In contrast, the cadmium standard solution required a temperature setting of 2100°C in the voltage-controlled mode to achieve maximum absorbance. The maximum power heating mode thus enables the graphite tube life to be prolonged.

Effects of phosphate. Phosphate in concentrations above 0.1 M has been reported to quench cadmium absorption in flame atomic absorption methods [15]. The dependence of cadmium absorbance on the content of ammonium dihydrogenphosphate in the matrix modifier was investigated. Cadmium solutions (2 $\mu g\ l^{-1}$) and blanks were prepared in the acidic matrix modification mixture containing variable ammonium dihydrogenphosphate concentrations in the 0—0.250 M range. The cadmium absorbance signal from these solutions showed a rapid increase as a function of dihydrogenphosphate concentration. The absorbance increased to about 1.8 times the original absorbance level up to a dihydrogenphosphate concentration of 0.013 M, and decreased slowly thereafter to reach the original level with the more concentrated solutions (0.200 M). The enhancement observed here is consistent with the increase in thermal stability and higher peak absorptions reported previously in a.a.s studies for cadmium and lead in phosphate matrix [16, 17]. With

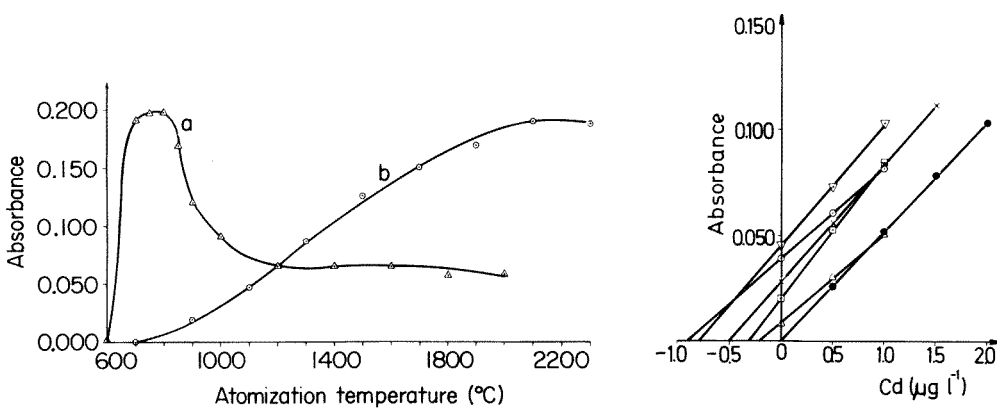

Fig. 3. Effect of the atomization temperature on cadmium absorbance. (a) Urine + 2.0 μg Cd l^{-1} + matrix modifier (temperature-controlled maximum power heating mode); (b) 2.0 μg Cd l^{-1} + matrix modifier (voltage-controlled atomization mode).

Fig. 4. Calibration curve for cadmium and the standard addition method with five urine samples. (•) Standards; (×, △, □, ○, ▽) samples 1—5 in Table 2.

TABLE 2

Urinary cadmium determination

Sample	1	2	3	4	5
Cd ($\mu g\ l^{-1}$) CC[a]	1.1	0.5	0.6	1.5	1.7
Cd ($\mu g\ l^{-1}$) SA[b]	1.0	0.4	0.6	1.8	1.6
Difference (%)	+10	+25	0	−17	+6

[a]Calibration curve. [b]Standard addition.

phosphate, the cadmium absorption peak was observed at 620°C compared to 470°C without phosphate, and the absorption peaks were larger and narrower.

Calibration curve and standard addition method. The calibration curve for cadmium standards prepared in 1% (v/v) nitric acid and the matrix modification mixture was found to be linear from 0 to 2.0 $\mu g\ l^{-1}$. The blank contribution from the matrix modification mixture consistently corresponded to 0.5 $\mu g\ l^{-1}$ as determined previously by the standard addition method in three replicates. Figure 4 shows a representative calibration curve and results for standard additions to five urine samples.

Because of the large variation in urine matrix composition between samples, the addition of the matrix modification mixture does not remove all interferences. Both the matrix modification and standard additions are required to make proper determination of cadmium in urine. To check the matrix influence of a urine sample on the method of standard additions, at least two different dilutions of the same sample were processed with good agreement in results. Table 2 shows a comparison of the results obtained with five urine samples from occupationally unexposed persons with both the calibration curve and the standard addition method. The observed cadmium levels (0.4—1.8 $\mu g\ l^{-1}$) are consistent with the values reported recently for cadmium levels in human urine samples [9, 18, 19].

Response, detection limit, and imprecision. The response for cadmium expressed as concentration required to produce 0.004 A was 0.1 $\mu g\ l^{-1}$ when a 20-μl sample aliquot was used. The detection limit estimated for a signal-to-background ratio of 2 was 0.1 $\mu g\ l^{-1}$ of the (1 + 1) diluted urine sample. Twelve replicate injections of a urine sample at a cadmium concentration of 1.5 $\mu g\ l^{-1}$ gave a relative standard deviation of 4%. This result is consistent with previous e.a.a.s. work [7, 10].

Analytical recovery. The results from the recovery test on 4 urine samples (Table 3) show that recoveries varied from 40 to 120%, with a mean recovery of 90 ± 37% when 0.5 $\mu g\ l^{-1}$ cadmium was added to each sample. These results are similar to previously reported e.a.a.s. data, both in range and precision. Compared to several extraction procedures, this method is advantageous in that it reduces sample preparation.

TABLE 3

Analytical recovery of cadmium added to urine

Cd in sample ($\mu g\ l^{-1}$)	1.0	0.4	0.6	1.8
Cd found ($\mu g\ l^{-1}$)[a]	1.6	1.0	1.0	2.0
Recovery (%)	120	120	80	40

[a]After addition of 0.5 μg Cd l^{-1}.

This work was supported partially by the Vicerrectoría de Investigación of the Universidad de Concepción (Proyecto 2.04.11). Concepción, Chile.

REFERENCES

1 R. L. Singhal, Z. Merali and P. D. Hrdina, Fed. Proc., 35 (1976) 75.
2 R. C. Schnell, Fed. Proc., 37 (1978) 28.
3 G. Kazantzis, Practitioner, 210 (1973) 482.
4 L. M. Friberg, M. Piscator, G. F. Nordberg and T. Kjellstrom, Cadmium in the Environment, 2nd edn., CRC Press, Cleveland, OH, 1974.
5 G. F. Nordberg, Environ. Physiol. Biochem., 2 (1972) 7.
6 K. Normiyama and H. Normiyama, in G. F. Nordberg (Ed.), Effects and Dose-Response Relationships of Toxic Metals, Elsevier, New York, 1976, p. 372.
7 G. D. Carmack and M. Evenson, Anal. Chem., 51 (1979) 907.
8 P. A. Legotte, W. C. Rosa and D. C. Sutton, Talanta, 27 (1980) 39.
9 T. Kjellstrom, B. Lind, L. Linnman and G. Nordberg, Environ. Res., 8 (1974) 92.
10 P. Allain and Y. Mauras, Clin. Chim. Acta, 91 (1979) 41.
11 R. D. Ediger, At. Absorpt. Newsl., 14 (1975) 127.
12 M. Cooksey and W. B. Barnett, At. Absorpt. Newsl., 18 (1979) 101.
13 H. J. Isaaq, Anal. Chem., 51 (1979) 657.
14 R. Ediger, G. Peterson and J. D. Kerber, At. Absorpt. Newsl., 13 (1974) 61.
15 P. Pulido, K. Fuwa and B. L. Vallee, Anal. Biochem., 14 (1966) 393.
16 E. J. Czobik and J. P. Matousek, Talanta, 24 (1977) 573.
17 S. Smith and R. Schleicher, in T. Y. Kometani (Ed.), Advances in Graphite Furnace Atomic Absorption Spectrometry, The Franklin Institute Press, Philadelphia, PA, 1978, p. 61.
18 D. E. Johnson, J. B. Tillery and R. J. Prevost, Environ. Health Perspect., 10 (1975) 151.
19 E. F. Perry, S. R. Koirtyohann and H. M. Perry, Jr., Clin. Chem., 21 (1975) 626.

Analytica Chimica Acta, 130 (1981) 215—220
Elsevier Scientific Publishing Company, Amsterdam — Printed in The Netherlands

Short Communication

DETERMINATION OF CARBON IN STAINLESS STEEL AND PLUTONIUM USING INFRARED DETECTION OF CARBON DIOXIDE

MAYNARD E. SMITH

Los Alamos National Laboratory, P.O. Box 1663, Los Alamos, NM 87545 (U.S.A.)

(Received 16th February 1981)

Summary. Carbon in stainless steel and plutonium metal in the 3—1000 ppm range is burned at 1300°C in a stream of purified oxygen and the carbon dioxide produced is quantified by integrating the signal from an infrared detector. The relative standard deviation is 10% or better. This method is approximately five times faster than the conventional manometric method and is equally accurate and precise. Use of a platinum resistance furnace makes the method more suitable for glove boxes or shielded enclosures than methods requiring inductively heated furnaces.

The presence of interstitial carbon is believed to affect the physical properties of metals and alloys. As stainless steels are sometimes used for the cladding of reactor fuels and other applications where prevention of failure is of utmost importance, determination of the carbon content is required. It is also required in characterizing plutonium metal and its compounds. Because in many cases only small samples are available, the manometric method reported by Smiley [1] for the determination of carbon in the ppm range has been used successfully for plutonium and other radioactive materials. The method, although reasonably precise, has several disadvantages. In addition to the well known drawbacks of manometric methods, the useful range is limited because the trap is inefficient at higher concentration levels, and the apparatus is not easily automated.

In the infrared method described below, the stainless steel samples enclosed in a tin capsule are burned at 1300°C in a stream of oxygen. The quantity of carbon dioxide produced by the combustion of carbon is measured by an infrared detector.

Experimental

Apparatus. A diagram of the apparatus is shown in Fig. 1. The metal plumbing consists of 6.35-mm copper tubing joined by hard solder connections. The Anarad Infrared Analyzer Model No. AR500R is equipped with a zero drift and span temperature compensation circuits, a carbon dioxide negative gas filter, and a barometric correction and linearizer circuit. A 914-mm path length provides adequate sensitivity. The linearizer was aligned at the factory using gases containing several different concentrations of carbon dioxide.

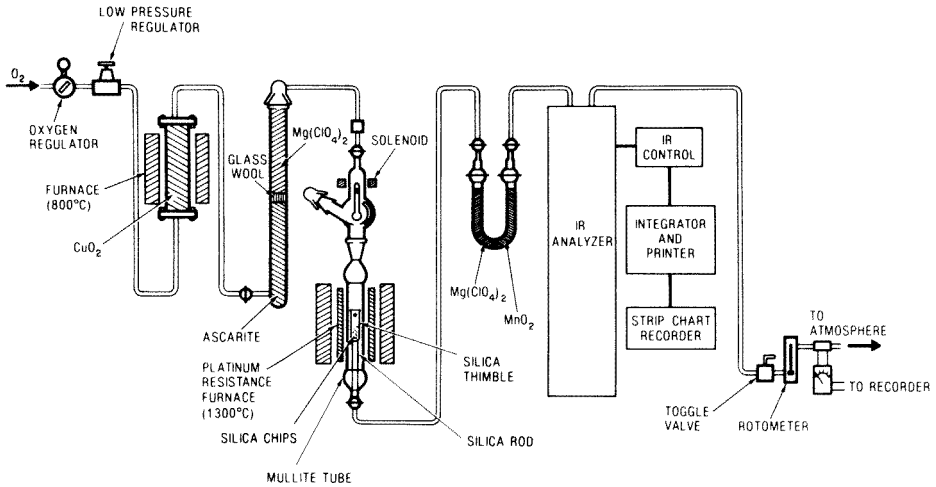

Fig. 1. Apparatus for the determination of carbon using an infrared detector.

Because the instrument was to be used here for the measurement of small quantities of carbon dioxide released from samples burned in a constant flow of oxygen, the linearizer had to be realigned using several standard reference materials with carbon concentrations in the desired range. Stainless steel samples obtained from the National Bureau of Standards (NBS) were used and alignment was done as recommended in the instrument manual. Linear relationships between the quantity of carbon released and the detector ouput increase the precision and simplify the calculations. Other than installing valves on the entrance and exit of the infrared reference cell, no further modification was necessary.

The platinum resistance furnace was made using a grooved alundum core (38-mm i.d., 150-mm long) with 1-mm platinum wire. This was inserted in another alundum core (58-mm i.d.) surrounded by a 40-mm thick layer of diatomaceous-earth insulation contained in a brass cylinder held in place by 13-mm thick top and bottom plates of asbestos. This arrangement facilitated replacement of the heating element when necessary. The furnace itself was supported on a metal tripod with a slit in the ring to permit easy removal of the furnace tube. The power supply for the heating element consisted of a 110 V variable transformer connected to a second transformer capable of delivering 50 V, 10 A maximum.

The furnace tube (Fig. 1), was aluminum silicate (mullite; 30-mm o.d., 350-mm long) with appropriate glass joints sealed to each end. Inside the tube, a silica thimble containing a few silica chips served to contain the tin oxide slag. The thimble was supported on a silica rod and two holes in the side of the thimble permitted a constant flow of oxygen through the tube. The tube was kept at 1300°C during sample runs but was lowered to 1000°C between series of samples to prolong the life of the heating element. As

many as 150 samples (100 mg) have been processed before replacement of the tube was necessary.

The sample dropper (Fig. 1) contained a plunger with a soft iron core which could be raised by activating a solenoid. This permitted samples to be loaded through the sidearm and retained until combustion was desired. A trap containing manganese dioxide and anhydrous magnesium perchlorate was connected to the exit of the furnace tube to retain sulfur oxides and water.

The span setting of the infrared detector depended on the capability of the integrator. With a span setting of 26 used for the 3—1000 ppm range, a voltage divider was required in the detector output to reduce the signal by a factor of 100. The integrator could then be used to measure the areas under the peaks produced and to print the result in arbitrary units. A strip chart recorder monitored the peak shape to indicate whether the sample had burned satisfactorily.

Controlled flow was achieved by regulating the oxygen to about 34 kPa before entering a low pressure regulator which pressurized the system at about 4.5 kPa. The flow was monitored by a thermo-electric flow meter connected to a strip chart recorder and measured by a "wet test meter."

Reagents. The oxygen was purified by passage through copper(II) oxide (wire form) at 800°C and then through ascarite and anhydrous magnesium perchlorate (both analytical grade). Tin capsules were obtained from the Leco Corporation (St. Joseph, MI 49085), and manganese dioxide (Sulsorbent) was obtained from the Burrell Co., Pittsburgh, PA).

Calibration. Standard curves were prepared by using nine NBS stainless steel reference materials with different carbon contents (29—900 ppm). Each sample was weighed to the nearest 0.1 mg and enclosed in a weighed tin capsule. Empty tin capsules were processed to determine the blank carbon content. The NBS certified values were then plotted versus the corrected peak area divided by the sample weight. The least-squares equation for the standard curve using all the data from the five individual curves (45 determinations) was C (ppm) = (32.22 ± 0.328) area mg^{-1} — 14.3 ± 5 with standard error of 18.85 and correlation coefficient of 0.997. The relative standard deviation for the slopes of the five standard curves processed individually was 2%. Because plutonium reference materials with certified carbon concentrations were not available, the same standard curve was used for the plutonium samples. If the method were automated, it might be advantageous to use measured injections of carbon dioxide to eliminate errors resulting from the carbon content of the tin capsules.

Sample preparation and procedure. After degreasing with a solvent if necessary, weigh the samples of stainless steel (small pieces, granular, or powder) and add to weighed tin capsules. Vary the sample size according to the expected concentration; weights of 100 mg are usually satisfactory for the 3—1000 ppm range. Fold the tin capsule to prevent leakage of the sample, manipulating carefully to avoid any contamination with carbon. It is not necessary to use tin capsules for plutonium metal samples.

With the reaction furnace temperature at 1300°C, adjust the oxygen flow rate through the system to the same as that used in calibration (240 ± 10 ml min^{-1}). Electronic circuits are permitted to stabilize (ca. 15 min) with gas flowing through the reference cell of the infrared detector. Then shut off the flow of gas with the reference cell at atmospheric pressure and disconnect the reference cell from the exiting gas. Adjust the barometric pressure compensator to the ambient pressure. Close the toggle valve to produce a positive pressure in the furnace tube and load the first sample through the side arm. Flush the cap with the gas flowing through the sample loader for a few seconds before replacing the cap. Open the toggle valve, adjust the span to the predetermined setting, and when the integrator indicates the base line to be stable, turn on the integrating switch and the chart drive. After the peak has been integrated and the area recorded, calculate the carbon concentration of the sample from the standard curve after correcting for the blank.

Results and discussion

Factors influencing the precision. Two critical parameters that affect the precision of the method are the flow rate and the span setting. The span setting is easily controlled by readjusting if necessary before each determination. The flow rate is more difficult to control. The time of passage of an increment of carbon dioxide through the cell of the detector affects the size of the peak area (Fig. 2). At flow rates less than 200 ml min^{-1}, the relationship between the flow rate and the peak area is nonlinear and the area increases greatly with a small change in flow rate. The combustion of the tin used to encapsulate the samples causes the flow rate to drop drastically (Fig. 3A). The flow nearly recovers before the released carbon dioxide reaches the detector. Combustion of an encapsulated stainless steel sample causes a small fluctuation as the flow begins to recover from the combustion of the tin capsule (Fig. 3B). Control of the flow rate by a low pressure regulator is adequate for maintaining a constant flow of gas through the system. Constant flow unaffected by progressive restriction by the combusted samples is maintained by the silica-thimble insert (Fig. 1), which permits the flow to remain constant until the slag formed by the molten tin oxide plugs the holes in the side of the thimble. At this point, a drastic reduction in flow occurs, leading to a large increase in peak width, and the reaction tube must be replaced.

Another important factor influencing the precision of the method is the heterogeneity of the carbon content of the tin capsules. The average carbon concentration per capsule in one batch was 35 ± 2.4 ppm for ten determinations. The limit of detection is approximately 3 ppm based on the criterion that a signal greater than twice the noise level can be measured.

Comparison between infrared method and manometric method. Data were obtained for carbon in stainless steel samples by using the combustion procedure described above but with the manometric method to measure the

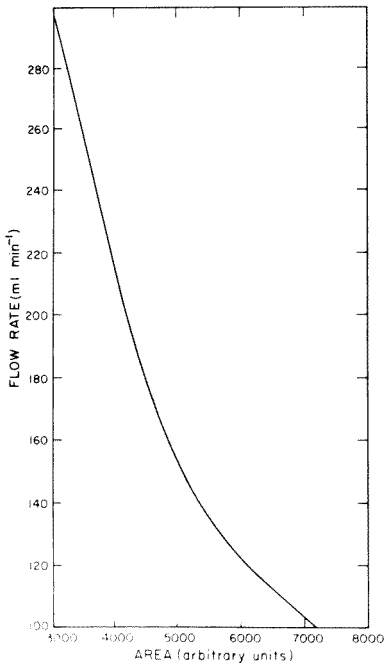

Fig. 2. Relationship of peak area to flow rate.

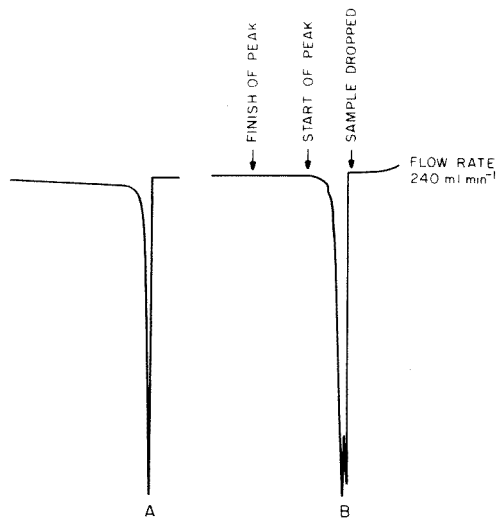

Fig. 3. Change in flow rate with sample combustion: (A) empty tin capsule; (B) tin capsule containing stainless steel sample.

carbon dioxide formed [1, 2]. The original version of the method traps the carbon dioxide in a capillary trap chilled with liquid nitrogen. When this method was used to determine the carbon in NBS stainless steel reference materials, consistently low results were obtained; these were attributed to incomplete trapping of the carbon dioxide. Calibration of the method was therefore changed to an empirical basis by constructing a correction curve based on the certified values for the NBS reference materials. Sample sizes ranged from approximately 100—200 mg depending on the expected carbon concentration of the sample. In both cases five determinations were made by each method on each of nine reference material samples. Summarizing the data, the least-squares regression lines for the infrared data (y_1) and the manometric data (y_2) were

$$y_1 = (0.997 \pm 0.013)\, x + (1.0 \pm 6) \text{ ppm}; S_{yx} = 11; r = 0.999$$

$$y_2 = (1.04 \pm 0.019)\, x - (6 \pm 9) \text{ ppm}; S_{yx} = 15; r = 0.999$$

where x is the SRM value, S_{yx} is the standard error, and r is the correlation coefficient. The pooled values of the standard deviations of the infrared and manometric methods were 7% and 5%, respectively, when the erroneous

results obtained by both methods for the steel containing least carbon (29 ppm) were excluded. The standard error is smaller with the infrared method. The precision of the two methods is essentially the same, the standard deviation of the infrared method is only slightly smaller, but the shorter processing time of the infrared method (approximately one-fifth that of the manometric method) and its ready adaptability to automation makes the infrared method more advantageous. Also, preliminary results indicate that the apparatus could be used for the determination of carbon in fluorine compounds using a method similar to that reported by Simmons and Randolph [3].

Results obtained by the two methods for the determination of carbon in 80—120 mg samples of two different plutonium metals were 96 ± 12 and 95 ± 12 ppm with infrared detection and 87 ± 24 and 75 ± 20 ppm with manometric detection. As standard reference materials for carbon in plutonium were not available, a reliable estimate of the accuracy is not possible. By pooling the standard deviations of the two methods, a value of 12% is obtained for the infrared measurements and a value of 22% for the manometric method indicating the infrared method is probably capable of better precision in the determination of carbon in plutonium samples.

Imprecise data reported above do not represent the exact precision of the method because of the inhomogeneity of the materials.

The use of a simple resistance furnace greatly facilitates the installation in enclosures used for processing radioactive material. The method as reported could be improved by automation using a more sophisticated integrating device or small computer and precise gas sampling valves for calibration.

The author thanks W. B. Hutchinson for assistance in processing the data, N. L. Koski and M. E. Quintana for assistance with the manometric method, and G. R. Waterbury for his valuable advice and for making this project possible.

REFERENCES

1 W. G. Smiley, Los Alamos National Laboratory Report (1950) LA-1128.
2 W. G. Smiley, Anal. Chem., 27 (1955) 1098.
3 R. E. Simmons and M. H. Randolph, Anal. Chem., 34 (1962) 1119.

Analytica Chimica Acta, 130 (1981) 221—226
Elsevier Scientific Publishing Company, Amsterdam — Printed in The Netherlands

Short Communication

THE USE OF EMPIRICAL MATHEMATICAL MODELS IN THE EXAMINATION OF HOMOGENEITY OF SOLIDS

A. PARCZEWSKI

Department of Analytical Chemistry, Jagiellonian University, ul. M. Karasia 3, 30-060 Kraków (Poland)

(Received 20th March 1981)

Summary. Experimental design theory is applied: the points to be analyzed on the sample surface are selected so that they form a pattern of rectangles, each of which is treated separately. When the points are arranged in rows and columns, the pattern can be described by factorials of the 2^2 or k^2 type. The results of determining a particular component at each point selected are used to calculate the regression coefficients in an empirical mathematical model; this approximates the dependence of the concentration of the component on the position on the surface within the rectangle. Such models are formulated for each area and the distribution of the component is approximated and finally mapped. Examples based on earlier results are given.

Two-dimensional variance analysis has been applied in the examination of homogeneity of solids and its advantages and disadvantages have been discussed by Danzer and Marx [1]. The method is especially useful when non-linear and interaction effects are not significant. Trends in inhomogeneity and concentration gradients can be detected and the procedural error estimated on the basis of the same experimental data. Danzer and Marx [1] took interaction contributions into account by using the method of Mandel [2].

In the present communication, the application of experimental design theory [3, 4] in examinations of homogeneity is suggested. The proposed method is simple and allows trends in inhomogeneity and concentration gradients to be visualized. The method is illustrated by examples based on experimental data given by Danzer and Marx [1] so that the two approaches can be compared easily.

Method

The examination of a surface (two-dimensional case) will be used to explain the method. The points to be analyzed are arranged in rows and columns as shown in Fig. 1A; other arrangements are also possible (see below). Thus the surface is divided into rectangles, e.g., A-1 is defined by points 1, 2, 3 and 4 forming its vertices. Each rectangle in the pattern shown in Fig. 1A is considered as a 2^2 factorial. Some component in the sample is determined at each point indicated in this pattern, and the results are arranged in rows and columns, correspondingly, as in the data arrangement in two-dimensional variance analysis.

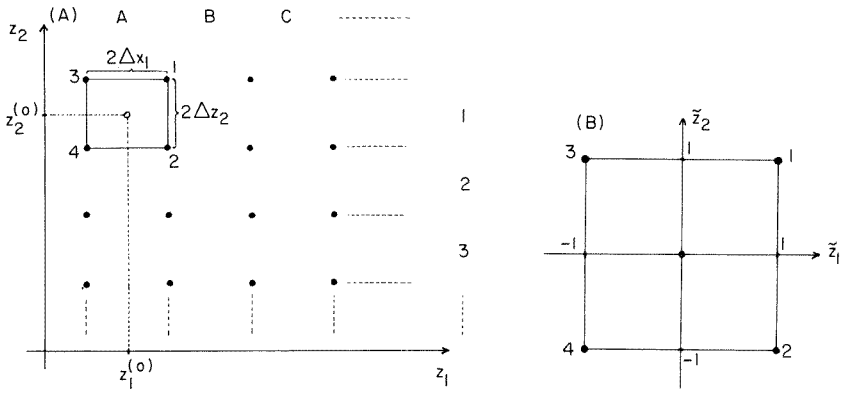

Fig. 1. (A) Regular arrangement of points; $z_1^{(o)}$ and $z_2^{(o)}$ are the coordinates of the center of rectangle or square A-1. (B) 2^2 factorial in a coordinate system $\tilde{z}_1$, $\tilde{z}_2$, corresponding to square A-1.

	A	B	C	.....	
1	x_{11}	x_{12}	x_{13}	x_{14}	x_{1c}
2	x_{21}	x_{22}	x_{23}	x_{24}	x_{2c}
	x_{31}	x_{32}	x_{33}	x_{34}	x_{3c}
.	.	.	.	.	.
.	.	.	.	.	.
.	x_{r1}	x_{r2}	x_{r3}	x_{r4}	x_{rc}

For example, the set of 4 results x_{12}, x_{22}, x_{11} and x_{21}, pertains to area A-1. These results enable the regression coefficients in the following model to be evaluated

$$\hat{x} = b_0 + b_1 z_1 + b_2 z_2 + b_{12} z_1 z_2 \qquad (1)$$

Model (1) approximates the relationship between the amount (concentration, measured signal, etc.) of the component and the position on the surface within area A-1. (In this case there is no degree of freedom for testing the adequacy of the model.) The same procedure is carried out for the other areas B-1, C-1, ..., A-2, B-2, C-2, ..., etc., and for each area a model $\hat{x}$ is formulated. The regression coefficients in a model $\hat{x}$ are easily calculated if standardized (coded, $\tilde{z}_1$ and $\tilde{z}_2$) instead of natural (z_1 and z_2) coordinates are used. Coordinates $\tilde{z}$ are defined by

$$\tilde{z}_i = (z_i - z_i^{(o)})/\Delta z_i \quad (\text{for } i = 1,2) \qquad (2)$$

where $z_i^{(o)}$ and Δz_i are explained in Fig. 1. Of course, the set of $z_i^{(o)}$ and $z_2^{(o)}$ is different for each area; this set of coordinates establishes the position of an area in the system (Fig. 1A). In Fig. 1B, area A-1 is described by the "local" coordinate system $\tilde{z}_1$, $\tilde{z}_2$. In Table 1 coordinates $\tilde{z}_1$ and $\tilde{z}_2$ of each vertex shown in Fig. 1B are presented, together with the corresponding result of the determination, x. The values of $\tilde{z}_1\tilde{z}_2$ are also given.

Model (1) can be expressed in coded variables $\tilde{z}_1$ and $\tilde{z}_2$ by

TABLE 1

2^2 factorial

Vertex	$\tilde{z}_1$	$\tilde{z}_2$	$\tilde{z}_1\tilde{z}_2$	x
1	1	1	1	x_{12}
2	1	−1	−1	x_{22}
3	−1	1	−1	x_{11}
4	−1	−1	1	x_{21}

$$\hat{x} = B_0 + B_1\tilde{z}_1 + B_2\tilde{z}_2 + B_{12}\tilde{z}_1\tilde{z}_2 \quad (3)$$

The regression coefficients B in eqn. (3) are calculated from the following formulae: $B_0 = (x_{12} + x_{22} + x_{11} + x_{21})/4$, $B_1 = (x_{12} + x_{22} - x_{11} - x_{21})/4$, $B_2 = (x_{12} - x_{22} + x_{11} - x_{21})/4$, and $B_{12} = (x_{12} - x_{22} - x_{11} + x_{21})/4$. It is obvious that coefficient B_1 is obtained by summing the results of the determinations multiplied by the corresponding coordinates $\tilde{z}_1$ presented in Table 1. The coefficients B_2 and B_{12} are obtained similarly. Once the coefficients B in eqn. (3) have been calculated, the coefficients b in model (1) can be obtained by inserting eqn. (2) into eqn. (3).

It follows from eqn. (3) that B_0 approximates the concentration x at the centre of a square; B_1 and B_2 express the dependence of x on the direction parallel to axes z_1 and z_2, though the gradient $\hat{x}$ depends also on the interaction term $B_{12}\tilde{z}_1\tilde{z}_2$. Actually, the components of the gradient $\hat{x}$ (eqn. 3) at a given point on the square surface are given by the formulae: $\partial\hat{x}/\partial\tilde{z}_1 = B_1 + B_{12}\tilde{z}_2$, and $\partial\hat{x}/\partial\tilde{z}_2 = B_2 + B_{12}\tilde{z}_1$. Then, gradient $\hat{x}$ is constant only if B_{12} is not significant. At each point on the surface, gradient $\hat{x}$ is perpendicular to the corresponding contour line (see below). At the centre of a square ($\tilde{z}_1 = \tilde{z}_2 = 0$) the components of gradient $\hat{x}$ equal B_1 and B_2, respectively; it should be noted that the standardized coordinates $\tilde{z}_1$, $\tilde{z}_2$ of the local coordinate system are considered.

Coefficients B in eqn. (3), corresponding to a square treated as a separate unit, are calculated independently from each other, and the error of each coefficient can be calculated from the formula $s_B = s_x/2$, where s_x is the standard error in the determination of x; s_x is estimated separately or from the results of replicate determinations at each point. The significance of coefficients B can be tested by Student's t test.

The arrangement of points in Fig. 1 can be divided into more complex units, e.g. 3^2 factorials (3 rows and 3 columns in a single square). More sophisticated models for $\hat{x}$ can then be applied [5] but, of course, the calculations become much more laborious; an example is given in Fig. 3B. Simplex plans or composite rotatable designs [3, 4] can also be used.

Once the regression coefficients in models $\hat{x}$ have been calculated, "contour" lines corresponding to constant values of x can be drawn, as shown in Figs. 2 and 3. In the preparation of these diagrams the distances between the points in rows and columns were assumed to be the same ($\Delta z_1 = \Delta z_2$). If this were not true, then eqn. (2) would have to be taken into account to obtain correct diagrams.

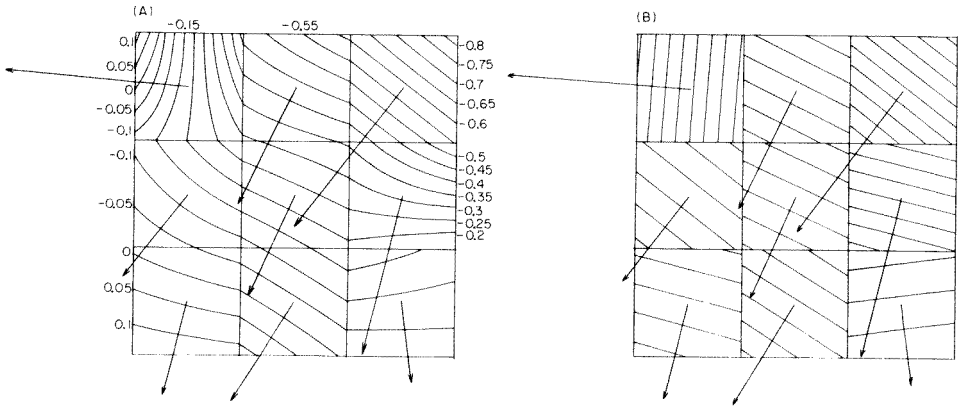

Fig. 2 (A) Distribution of boron with contour lines based on eqn. (3). (B) Simplified diagram of the distribution of boron.

Applications of the method

As mentioned above, the examples presented are based on the experimental data given by Danzer and Marx [1].

Distribution of boron on a surface. The results (in arbitrary units) of the emission spectrographic determination of boron at 16 points arranged regularly in 4 rows and 4 columns were as follows

	A	B	C	
1	+ 0.120	—0.469	—0.614	—0.821
2	—0.115	—0.290	—0.358	—0.555
3	—0.010	—0.080	—0.187	—0.135
	+0.140	+0.120	—0.010	—0.020

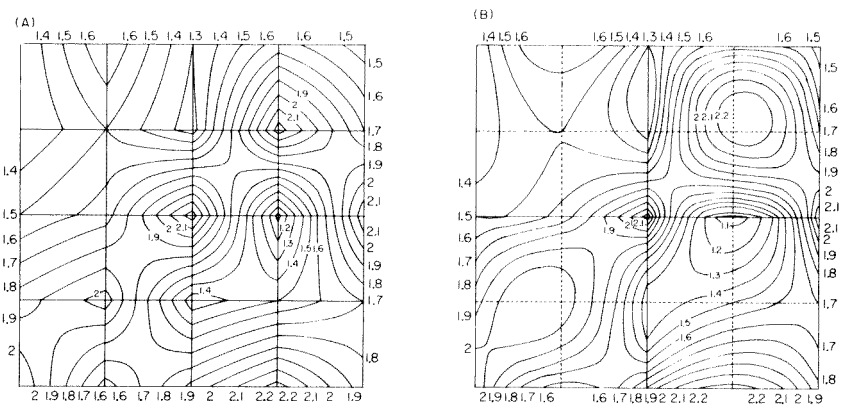

Fig. 3. (A) Distribution of manganese with the contour lines based on eqn. (3). (B) Improved diagram of the distribution of manganese.

The surface is partitioned into 9 squares; coefficients B in eqn. (3) were calculated for each square. For example, the parameters for square A-1 are $\hat{x} = -0.188_5 - 0.191\ \tilde{z}_1 + 0.014\ \tilde{z}_2 - 0.103_5\tilde{z}_1\tilde{z}_2$. The contour lines are shown in Fig. 2A along with the gradients at the centre of each square; for convenience the gradients have been enlarged 20 times. The lines in Fig. 2B correspond to eqn. (3) in which the interaction terms $B_{12}\tilde{z}_1\tilde{z}_2$ have been omitted. Figure 2A shows that boron is distributed unevenly over the surface. Gradients and contour lines show the direction in which the concentration of boron changes. The interaction terms seem to be not significant in this case; the contour lines are almost parallel, except in square A-1.

Distribution of manganese in steel. The results for the determination of manganese (%) presented below were used to calculate the coefficients B in eqn. (3) for each square:

	A	B	C	D	
1	1.30	1.70	1.30	1.65	1.45
2	1.30	1.50	1.25	2.25	1.70
3	1.50	1.65	2.25	1.07	2.20
4	1.85	2.05	1.33	1.50	1.70
	2.10	1.55	1.93	2.25	1.85

The corresponding contour lines are presented in Fig. 3A.

The arrangement presented above was also divided into four squares, each of which was a 3^2 factorial. In this case, the more sophisticated model $\hat{x}$ was applied [5]. The regression coefficients in the model corresponding to a square were calculated on the basis of 9 results. The contour lines obtained in this way are presented in Fig. 3B. It can be seen from Fig. 3 that the distribution of manganese is uneven; the manganese is segregated on the surface and the interaction effects are significant.

Discussion

The approach described above provides a general picture of the inhomogeneous distribution of a component; its simplicity, which is achieved by using a segmented approximation method with 2^2 factorials (or other plans) should be emphasized. Diagrams such as Figs. 2 and 3 are helpful for visualizing the distribution of a component and are easy to obtain, as indicated by the above examples. It should be pointed out, however, that when interactions are not significant, simplified diagrams such as Fig. 2B suffice to show trends in inhomogeneity, but when interactions are strong, as in Fig. 3, the simplifications are not advisable. The more sophisticated models based on 3^2 factorials lead to contour maps (e.g. Fig. 3B) similar to those based on 2^2 factorials (Fig. 3A), which are much more easily obtained. The differences between Fig. 3A and 3B are not very distinct because of the effect of experimental error on the contours. In general, the results obtained here agree with the conclusions reported by Danzer and Marx [1]; similar agreements was found for other examples not reported here.

It should be borne in mind that coefficients B in the models $\hat{x}$ corresponding to the different squares in a pattern are not independent. Adjacent squares have points in common, so that calculations of coefficients B corresponding to adjacent squares include some results common to both; the total number of calculated coefficients exceeds the number of points.

The methodology presented can, in principle, be applied to three-dimensional distributions. Three-factorial plans can be used, e.g., 2^3 factorials or rotatable designs, and $\hat{x}$ then includes three variables, z_1, z_2 and z_3.

The author is indebted to Prof. Dr. A. Rokosz for criticism of the manuscript.

REFERENCES

1 K. Danzer and G. Marx, Anal. Chim. Acta, 110 (1979) 145.
2 J. Mandel, J. Am. Stat. Assoc., 56 (1961) 878.
3 W. G. Cochran and G. M. Cox, Experimental Designs, J. Wiley, New York, 1950.
4 D. L. Massart, A. Dijkstra and L. Kaufman, Evaluation and Optimization of Laboratory Methods and Analytical Procedures, Elsevier, Amsterdam, 1978.
5 A. Parczewski and P. Kościelniak, Fresenius Z. Anal. Chem., 297 (1979) 148.

Vol. 130, No. 1

ACA announcements

ANNOUNCEMENTS OF MEETINGS

SYMPOSIUM ON "FOOD RESEARCH AND DATA ANALYSIS"

The above symposium will be held at the Voksenåsen Hotel, Oslo, Norway, on September 20–23, 1982. The symposium is intended to provide an interdisciplinary meeting ground for scientists interested in the development and use of computer aided analysis of multivariate food research data. Agronomists, microbiologists, chemists, technologists, statisticians, marketing people and psychologists with some experience in data analysis will be able to study the potential of more advanced analytic tools. Specialists in the fields of chemometrics, qualimetrics and psychometrics will have an opportunity to "shake hands".

The programme ranges from reviews of basic philosophy and available computer programmes to reports of practical results obtained by applying multivariate computer analysis to food research data. The oral contributions will be given so that food scientists without advanced knowledge in mathematics or computer science can understand.

All plenary lecturers are invited. Additional contributions are welcome and will be presented in a poster session. Lecture manuscripts and post abstracts will be published in symposium proceedings.

For further information contact: B. Eidstuen, P.O. Box 50, N-1432 Aas-NLH, Norway.

1982 WINTER CONFERENCE ON PLASMA SPECTROCHEMISTRY

The 1982 Winter Conference on Plasma Spectrochemistry, sponsored by the ICP Information Newsletter in cooperation with the Society for Applied Spectroscopy (Florida section) and the American Chemical Society (Tampa section of the Analytical Chemistry Division), will feature developments in atomic plasma spectrochemical analysis by inductively coupled plasma, d.c. plasma, and microwave plasma excitation sources. The meeting will convene on Monday, January 4 through Saturday, January 9, 1982, at the Orlando Hyatt Hotel in Kissimee, FL, U.S.A., adjacent to Walt Disney World.

Papers describing applications, fundamentals, and instrumental developments with atomic plasmas will be presented in lecture and poster sessions. General and special symposia organized and chaired by internationally recognized experts will include the following topics: 1) accuracy, precision, and optimization in plasmas; 2) applications to air, biologicals, chemicals, coal, food, metals, ores, plants, petroleum, soils, rocks, wastes, and water; 3) EPA plasma methods; 4) new instrumentation; 5) plasma detectors for chromatography; 6) plasma interferences and mechanisms; and 7) sample introduction methods. Roundtable discussion sessions will encourage an in-depth evaluation of these topics. Featured speakers will include: P.W.J.M. Boumans (Eindhoven), V.A. Fassel (Ames) and J.D. Winefordner (Gainesville).

A spectroscopic instrument exhibition and manufacturers' seminar program will complement the scheduled sessions. A plasma film festival and plasma photographic contest will also be held.

For information, contact: Dr. Ramon M. Barnes, Chairman, Department of Chemistry, GRC Towers, University of Massachusetts, Amherst, MA 01003, U.S.A.

CALENDAR OF FORTHCOMING MEETINGS

Sept. 4–8, 1981 Tokyo, Japan	**9th International Conference on Atomic Spectroscopy and 22nd Colloquium Spectroscopicum Internationale** Contact: The Japanese Society for Analytical Chemistry, 9th ICAS/22nd CSI, Gotanda Sanhaitsu, 26–2 Nishigotanda –chome, Shinagawa-ku, Tokyo 141, Japan.
Sept. 7–10, 1981 Guildford, Great Britain	**4th International Bioanalytical Forum** Contact: Dr. E. Reid, Wolfson Bioanalytical Unit, Robens Institute, University of Surrey, Guildford GU2 5XH, Great Britain.
Sept. 9–11, 1981 Coventry, Great Britain	**International Conference on Advances in Flow Measurement Techniques** Contact: Conference Organizer, BHRA Fluid Engineering, Cranfield, Bedford, Great Britain.

Sept. 10–11, 1981 Canterbury, Great Britain	**Symposium on "Concepts of Purity"** Contact: P.R.W. Baker, Dept. of Physical Chemistry, Wellcome Research Laboratories, Langley Court, Beckenham, Kent, Great Britain
Sept. 20-25, 1981 Philadelphia, PA, U.S.A.	**8th Annual Meeting of the Federation of Analytical Chemistry and Spectroscopy Societies (FACSS)** Contact: M.A. Kaiser, E.I. du Pont de Nemours & Co., Experimental Station E228/200, CR&D Department, Wilmington, DE 19898, U.S.A.
Sept. 21–24, 1981 Loughbourough, Great Britain	**Particle Size Analysis Conference** Contact: P.J. Lloyd, PSA 81 Conference, Particle Technology Group, Chemical Engineering Department, University of Technology, Loughborough, Leics. LE11 3TU, Great Britain. (Further details published in Vol. 120)
Sept. 28–Oct. 1, 1981 Barcelona, Spain	**16th International Symposium Advances in Chromatography** Contact: Dr. A. Zlatkis, Chemistry Department, University of Houston, Houston, TX 77004, U.S.A. Tel. (713) 749-2623. (Further details published in Vol. 222, No. 2)
Sept. 29–Oct. 2, 1981 Basle, Switzerland	**ILMAC 81; 8th International Exhibition of Laboratory, Chemical Engineering, Measurement and Automation Techniques in Chemistry** Contact: D. Gammeter, Secretariat ILMAC '81, Postfach, CH-4021 Basle, Switzerland. Tel. 061 26 20 20.
Oct. 27–29, 1981 London, Great Britain	**Petroanalysis 81** Contact: Miss I.A. McCann, Conference Officer, Institute of Petroleum, 61 New Cavendish Street, London W1M 8AR, Great Britain. (Tel: 01-636 1004, Telex 264380)
Nov. 23–25, 1981 Barcelona, Spain	**2nd International Congress on Analytical Techniques in Environmental Chemistry** Contact: Dr. Joan Albaigés, General Secretary, Plaza de Espana, Barcelona-4, Spain. Tel. 223 31 01.
Dec. 2–3, 1981 Paris, France	**Journées de Chromatographie en Phase Liquide** Contact: H. Colin, Laboratoire C.A.P., Ecole Polytechnique, Route de Saclay, 91128 Palaiseau Cedex, France.
Jan. 4–9, 1982 Orlando, FL, U.S.A.	**1982 Winter Conference on Plasma Spectrochemistry** Contact: 1982 Winter Conference, c/o ICP Information Newsletter, Chemistry GRC Towers, University of Massachusetts, Amherst, MA 01003, U.S.A. Tel. (413) 545-2294. (Further details published in Vol. 124, No. 2)
March 8–12, 1982 Atlantic City, NJ, U.S.A.	**1982 Pittsburgh Conference and Exhibition on Analytical Chemistry and Applied Spectroscopy** Contact: Mrs. Linda Briggs, Program Secretary, Pittsburgh Conference, Department J-057, 437 Donald Road, Pittsburgh, PA 15235, U.S.A.
March 28–April 2, 1982 Las Vegas, NV, U.S.A.	**National American Chemical Society Meeting** Contact: A.T. Winstead, American Chemical Society, 1155 Sixteenth Street, NW, Washington, DC 20036, U.S.A.
March 30–April 1, 1982 Birmingham, Great Britain	**Royal Society of Chemistry Annual Chemical Congress** Contact: Royal Society of Chemistry, Burlington House, London W1V 0BN, Great Britain.
April 5–8, 1982 Las Vegas, NV, U.S.A.	**International Symposium "Advances in Chromatography"** Contact: Prof. A. Zlatkis, Chemistry Department, University of Houston, Central Campus, 4800 Calhoun, Houston, TX 77004, U.S.A. Tel.: (713) 749-2623.
April 14–16, 1982 Amsterdam, The Netherlands	**12th Annual Symposium on the Analytical Chemistry of Pollutants** Contact: Prof. Dr. Roland W. Frei, The Free University, De Boelelaan 1083, 1081 HV Amsterdam, The Netherlands.

April 15–17, 1982 Tokyo, Japan	**International Symposium "Advances in Chromatography"** Contact: Prof. A. Zlatkis, Chemistry Department, University of Houston, Central Campus, 4800 Calhoun, Houston, TX 77004, U.S.A. Tel.: (713) 749-2623.
April 21–23, 1982 Neuherberg near Munich, G.F.R.	**Second International Workshop on Trace Element Analytical Chemistry in Medicine and Biology** Contact: Dr. P. Schramel, Gesellschaft fuer Strahlen- und Umweltforschung, Institut fuer Angewandte Physik, Physikalisch–Technische Abteilung, Ingolstaedter Landstrasse 1, D–8042 Neuherberg, G.F.R. (Further details published in Vol. 124, No. 2)
April 27–30, 1982 Munich, G.F.R.	**Biochemische Analytic Conference** Contact: Prof. I. Trautschold, Medizinische Hochschule Hannover, Karl-Wiechert-Allee 9, 3000 Hannover 61, G.F.R. (Further details published in Vol. 124, No. 2)
May 2–6, 1982 Interlaken, Switzerland	**2nd International Symposium on Instrumental TLC (HPTLC)** Contact: Dr. R.E. Kaiser, Institute for Chromatography, P.O. Box 1141, D-6702 Bad Dürkheim, G.F.R.
May 11–14, 1982 Ghent, Belgium	**4th International Symposium on Quantitative Mass Spectrometry in Life Sciences** Contact: Prof. A. De Leenheer, Symposium Chairman, Laboratoria voor Medische Biochemie en voor Klinische Analyse, De Pintelaan 135, B-9000 Ghent, Belgium.
June 6–12, 1982 Frankfurt, G.F.R.	**European Meeting on Chemical Engineering and ACHEMA Exhibition Congress 1982** Contact: DECHEMA P.O. Box 970146, D-6000 Frankfurt/M 97, G.F.R.
June 7–11, 1982 Philadelphia, PA, U.S.A.	**VI International Symposium on Column Liquid Chromatography** Contact: R.A. Barford, ERRC – SEA, U.S. Department of Agriculture, 600 Mermaid Lane, Philadelphia, PA 19118, U.S.A.
June 28–30, 1982 East Lansing, MI, U.S.A.	**35th American Chemical Society Annual Summer Symposium** Contact: A.I. Popov, Chemistry Department, Michigan State University, East Lansing, MI 48824, U.S.A.
July 11–16, 1982 Washington, DC, U.S.A.	**6th International Conference on Computers in Chemical Research and Education (ICCCRE)** Contact: Dr. Stephen R. Heller, Chairman, 6th ICCCRE, EPA, MIDSD, PM–218, 401 M Street, S.W., Washington, DC 20460, U.S.A. Tel. (202) 755–4938, Telex: 89–27–58. (Further details published in Vol. 126 and Vol. 133, No. 2)
Aug. 2–7, 1982 Pretoria, South Africa	**13th International Symposium on the Chemistry of Natural Products** Contact: The Symposium Secretariat – S.219, CSIR, P.O. Box 395, Pretoria, 0001 Republic of South Africa.
Aug. 11–13, 1982 Hameenlinna, Finland	**6th European Symposium on Polymer Spectroscopy (ESOPS 6)** Contact: Professor Johan Lindberg, Department of Wood and Polymer Chemistry, University of Helsinki, Meritullinkatu 1 A, SF 00170 Helsinki 17, Finland.
Aug. 15–21, 1982 Perth, Australia	**The 12th International Congress of Biochemistry** Contact: Brian Thorpe, Department of Biochemistry, Faculty of Science Australian National University, Canberra A.C.T. 2600, Australia.
Aug. 29–Sept. 4, 1982 Kyoto, Japan	**5th International Congress of Pesticide Chemistry** Contact: Rikagaku Kenyusho (The Institute of Physical and Chemical Research), 2–1 Hirosawa Wako-shi Saitama Pref. 351, Japan.
Aug. 30–Sept.3, 1982 Vienna, Austria	**9th International Mass Spectrometry Conference** Contact: Interconvention, P.O. Box 105, A - 1014 Vienna, Austria. (Further details published in Vol. 120)

Sept. 12–17, 1982 Kansas City, MO, U.S.A.	**National American Chemical Society Meeting** Contact: A.T. Winstead, American Chemical Society, 1155 Sixteenth Street, NW, Washington DC 20036, U.S.A.
Sept. 13–17, 1982 Petten, The Netherlands	**Practical Applications of Computers and Chemometrics in Analytical Chemistry** Contact: Dr. H.C. Smit, Laboratory for Analytical Chemistry, University of Amsterdam, Nieuwe Achtergracht 166, 1018 WV Amsterdam, The Netherlands.
Sept. 13–17, 1982 London, Great Britain	**14th International Symposium on Chromatography** Contact: The Executive Secretary, Chromatography Discussion Group, Trent Polytechnic, Burton Street, Nottingham, NG1 4BU, Great Britain.
Sept. 15–17, 1982 Petten, The Netherlands	**Chemometrics in Analytical Chemistry** Contact: Dr. H.C. Smit, Laboratory for Analytical Chemistry, University of Amsterdam, Nieuwe Achtergracht 166, 1018 WV Amsterdam, The Netherlands.
Sept. 19–24, 1982 Philadelphia, PA, U.S.A.	**9th National Meeting of the Federation of Analytical Chemistry and Spectroscopy Societies (FACSS)** Contact: Division of Analytical Chemistry, American Chemical Society, Department of Chemistry, Notre Dame, IN 46556, U.S.A.
Sept. 20–23, 1982 Oslo, Norway	**Food Research and Data Analysis** Contact: B. Eidstuen, P.O. Box 50, N-1432 Aas-NLH, Norway. Tel.: 47-2-94 08 60.
Sept. 22–25, 1981 Leipzig, G.D.R.	**Analytiktreffen 1981 – Strukturanalytische Methoden in der Stereochemie** Contact: Sektion Chemie der KMU Leipzig, Liebigstrasse 18, DDR – 7010 Leipzig, G.D.R.
July 17–23, 1983 Edinburgh, Great Britain	**SAC 83: Sixth International Conference on Analytical Chemistry** Contact: Miss P.E. Hutchinson, Royal Chemistry Society, Analytical Division, Burlington House, London W1V 0BN, Great Britain. Tel. 01–734 9971.
Aug. 28–Sept. 2, 1983 Amsterdam, The Netherlands	**9th International Symposium on Microchemical Techniques** Contact: Symposium Secretariat, c/o Municipal Congress Bureau, Oudezijds Achterburgwal 199, 1012 DK Amsterdam, The Netherlands. Tel: (020) 552 3459.

inued from outside of cover)

t Communications

in The Netherlands.

CONTENTS

(continued on inside page of cover)